

PN-ACM-314

SITE-SPECIFIC EARTHQUAKE HAZARD DETERMINATIONS IN CAPITAL CITIES IN THE SOUTH PACIFIC

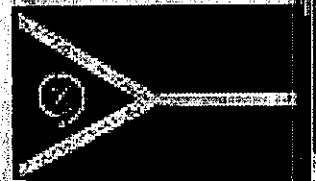
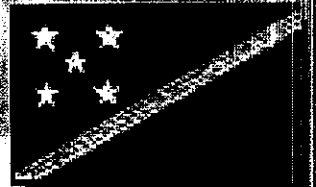
Compiled by

**Graham Shorten, Avi Shapira,
Marc Regnier, Geraldine Teakle,
Litea Biukoto, Monika Swamy
and Lasarus Vuetibau**

February 2001

SOPAC Technical Report 300

Second Edition



**SITE-SPECIFIC EARTHQUAKE HAZARD DETERMINATIONS IN
CAPITAL CITIES IN THE SOUTH PACIFIC**

Compiled by

Graham G. Shorten, Avi Shapira, Marc Regnier,
Geraldine Teakle, Litea Biukoto, Monika Swamy, and Lasarusa Vuetibau

February 2001

SOPAC Technical Report 300

Second Edition

Funding support for this project came primarily from the Government of the United States of America, with significant contributions from the Commonwealth Secretariat and the Governments of Israel, France, Fiji Islands, Solomon Islands, Tonga, Vanuatu, Australia and UNESCO.

SOPAC has attempted to ensure that the information in this product as accurate as possible. However, it does not guarantee that this information is totally accurate and complete. Therefore you should not rely solely on this information when making commercial decisions.

SITE-SPECIFIC EARTHQUAKE HAZARD DETERMINATIONS IN CAPITAL CITIES IN THE SOUTH PACIFIC

Report on

USAID Project

Earthquake Microzoning in Capital Cities in the South Pacific

Sub-Grant No. TA-MOU-95-C13-024

Principal Investigator

Avi Shapira

Geophysical Institute of Israel, Holon

Collaborating Investigators

Alfred Simpson, Graham Shorten

South Pacific Applied Geoscience Commission SOPAC, Suva

Marc Regnier

IRD (ORSTOM), Noumea

Implementing Organisations and Contributors

Geophysical Institute of Israel, Holon

Alona Malitzky, Veronic Avirav, Lea Feldman, David Kadosh, David Levi,

Uri Peled, Yossi Swartz, Illia Turetzky

South Pacific Applied Geoscience Commission SOPAC, Suva

Litea Biukoto, Monika Swamy, Geraldine Teakle, Suse Schmall, Les Allinson, Franck Martin

IRD (ORSTOM), Port Vila

Marc Regnier

Participating Member Country Organisations and Counterparts

Mineral Resources Department, Fiji Islands

Gajendra Prasad, Arvin Singh, Lasarus Vuetibau, Nilesch Kumar, Sakaria Vunisa, Eroni Tupua

Department of Geology, Mines and Water Resources, Vanuatu

Morris Stephen, Christopher Ioan

Department of Energy, Mines and Water Resources, Solomon Islands

Kenneth Bulehite, Alison Papabatu

Department of Lands, Survey & Natural Resources, Tonga

Kelepi Mafi

Contributing Organisations

Australian Geological Survey Organisation AGSO

Trevor Jones

TABLE OF CONTENTS

1	OBJECTIVE	6
2	INTRODUCTION	6
2.1	INVESTIGATIONS AND DEVELOPMENTS	6
2.2	REGIONAL SEISMO-TECTONIC SETTING.....	7
	Figure 1: Locality and Regional Seismo-Tectonic Map	7
3	SITE-SPECIFIC EARTHQUAKE HAZARD DETERMINATION PROCEDURE	9
3.1	THE NAKAMURA SITE-RESPONSE DETERMINATION METHOD	10
3.2	ZONATION USING GEOTECHNICAL AND NAKAMURA RESULTS	10
3.2.1	Geotechnical Input.....	10
	Box 1: Input Geotechnical Parameters	11
3.2.2	Grouping of Nakamura Results.....	11
	Figure 2: Areas Zoned for Earthquake Hazard in Suva, Port Vila, Honiara and Nuku'alofa	11
3.3	SITE-RESPONSE DETERMINATION (SRD) PROCEDURE	13
3.4	APPLICATION OF SITE-RESPONSE DETERMINATION THROUGH THE SVE METHOD	13
	Box 2: The SVE Approach.....	15
3.5	JUSTIFICATION OF METHODOLOGY	16
	Box 3: The NEHRP (Borcherdt) Method for Estimating Site-Dependent Response Spectra for Design.....	16
4	ASPECTS OF PROJECT DEVELOPMENT	18
4.1	DEVELOPMENT OF THE SEISMIC DATA ACQUISITION SYSTEM: PC-SDA.....	18
4.2	DEVELOPMENT OF SITE-RESPONSE SOFTWARE: GII-SRD PROGRAM.....	18
4.3	DEVELOPMENT OF THE MAPINFO GEOGRAPHIC INFORMATION SYSTEM (GIS).....	19
4.4	INSTALLATION, DEMONSTRATION AND TRAINING.....	19
4.4.1	First GII-USAID Seismic Microzoning Meeting and Workshop, Suva	20
	Box 4: Participants at 1 st Seismic Microzoning Meeting	20
4.4.2	Second GII-USAID Seismic Microzoning Meeting and Workshop, Suva	20
	Box 5: Participants at 2 nd Seismic Microzoning Meeting	20
4.4.3	Third GII-USAID Seismic Microzoning Meeting, Suva.....	21
	Box 6: Participants at 3 rd Seismic Microzoning Meeting.....	21
5	SEISMIC MICROZONATION OF SUVA, VITI LEVU, FIJI ISLANDS	22
5.1	INTRODUCTION, SUVA.....	22
5.2	TECTONIC SETTING, SUVA.....	22
5.3	REGIONAL AND LOCAL GEOLOGY, SUVA	23
	Figure 3: Lithology Map (including Borehole Positions), Suva	23
	Figure 4: Borehole Logs SB 323 to SB 321, Suva	25
	Figure 5: Borehole Logs SB 322 to SB 335, Suva	25
	Figure 6: Borehole Logs SB 133 to SB 148, Suva	25
	Figure 7: Borehole Logs SB 179 to SB 145, Suva	25
	Figure 8: Borehole Logs SB 199 to SB 030, Suva	25
5.4	HISTORY OF DAMAGING EARTHQUAKES, SUVA	31
	Figure 9: Large Shallow Earthquakes around Suva.....	31
	Table 1: Catalogue of Large Shallow Earthquakes, Suva	33
5.5	MICROTREMOR RECORDINGS - SITE-RESPONSE MEASUREMENTS, SUVA.....	36
	Table 2: Microtremor Site-Response Recordings, Suva.....	36
	Figure 10: Site-Response Spectra, Suva.....	39
5.6	ANALYSIS OF SITE-RESPONSE MEASUREMENTS AND ZONATION OF SUVA	44
	Table 3: Map Zones vs. Site-Response Models, Suva.....	44
	Table 4: Definition of Site-Response Models, Suva	44
	Figure 11: Diagrammatic Summary Cross-Section, Suva	46
5.7	SVE RESULTS AND INTERPRETATION, SUVA	46
	Figure 12: Site-Response Models and Acceleration-Response Functions, Suva	47
	Figure 13: Seismic Microzonation Site-Response Map, Suva.....	47
6	SEISMIC MICROZONATION OF PORT VILA, EFATE, VANUATU	50
6.1	INTRODUCTION, PORT VILA	50
6.2	TECTONIC SETTING, PORT VILA	50
6.3	REGIONAL AND LOCAL GEOLOGY, PORT VILA.....	51
	Figure 14: Lithology Map (including Borehole Positions), Port Vila.....	51
	Figure 15: Borehole Logs VB 040 to VB 043, Port Vila.....	53

	Figure 16: Borehole Logs VB 069 to VB 081, Port Vila.....	53
	Figure 17: Borehole Logs VB 081 to VB 075, Port Vila.....	53
	Figure 18: Borehole Logs VB 095 to VB 104, Port Vila.....	53
	Figure 19: Borehole Logs VB 121 to VB 117, Port Vila.....	53
6.4	HISTORY OF DAMAGING EARTHQUAKES, PORT VILA	59
	Figure 20: Large Shallow Earthquakes around Port Vila	59
	Table 5: Catalogue of Large Shallow Earthquakes, Port Vila.....	61
6.5	MICROTREMOR RECORDINGS - SITE-RESPONSE MEASUREMENTS, PORT VILA	69
	Table 6: Microtremor Site-Response Recordings, Port Vila	69
	Figure 21: Site-Response Spectra, Port Vila	74
6.6	ANALYSIS OF SITE-RESPONSE MEASUREMENTS AND ZONATION OF PORT VILA.....	81
	Table 7: Sediment thickness calculated from the observed resonance period in Bauerfield Airport area, Zone A, Port Vila	81
	Table 8: Sediment thickness calculated from observed resonance period in Zone B, Port Vila.....	82
	Table 9: Sediment thickness calculated from observed resonance period in the Tassiriki area, Zone C, Port Vila.....	82
	Table 10: Summary of general site-response observations and estimates of thickness, Port Vila.....	83
	Table 11: Map Zones vs. Site-Response Models, Port Vila	84
	Table 12: Definition of Site-Response Models, Port Vila.....	84
	Figure 22: Diagrammatic Summary Cross-Section, Port Vila.....	85
6.7	SVE RESULTS AND INTERPRETATION, PORT VILA	85
	Figure 23: Site-Response Models and Acceleration-Response Functions, Port Vila.....	86
	Figure 24: Seismic Microzonation Site-Response Map, Port Vila	86
7	SEISMIC MICROZONATION OF HONIARA, GUADALCANAL, SOLOMON ISLANDS.....	89
7.1	INTRODUCTION, HONIARA	89
7.2	TECTONIC SETTING, HONIARA	89
7.3	REGIONAL AND LOCAL GEOLOGY, HONIARA	89
	Figure 25: Lithology Map (including Borehole Positions), Honiara	90
	Figure 26: Borehole Logs HB 032 to HB 047, Honiara	92
	Figure 27: Borehole Logs HB 044 to HB 017, Honiara	92
	Figure 28: Borehole Logs HB 023 to HB 026, Honiara	92
7.4	HISTORY OF DAMAGING EARTHQUAKES, HONIARA	96
	Figure 29: Large Shallow Earthquakes around Honiara.....	96
	Table 13: Catalogue of Large Shallow Earthquakes, Honiara.....	98
7.5	MICROTREMOR RECORDINGS - SITE-RESPONSE MEASUREMENTS, HONIARA	104
	Table 14: Microtremor Site-Response Recordings, Honiara.....	104
	Figure 30: Site-Response Spectra, Honiara	106
7.6	ANALYSIS OF SITE-RESPONSE MEASUREMENTS AND ZONATION OF HONIARA	109
	Table 15: Sediment thickness calculated from observed resonance period in Zone B, Honiara	110
	Table 16: Map Zones vs. Site-Response Models, Honiara.....	110
	Table 17: Definition of Site-Response Models, Honiara.....	110
	Figure 31: Diagrammatic Summary Cross-Section, Honiara.....	111
7.7	SVE RESULTS AND INTERPRETATION, HONIARA	111
	Figure 32: Site-Response Models and Acceleration-Response Functions, Honiara	112
	Figure 33: Seismic Microzonation Site-Response Map, Honiara	112
8	SEISMIC MICROZONATION OF NUKU'ALOFA, TONGATAPU, TONGA	115
8.1	INTRODUCTION, NUKU'ALOFA	115
8.2	TECTONIC SETTING, NUKU'ALOFA	115
8.3	REGIONAL AND LOCAL GEOLOGY, NUKU'ALOFA.....	115
	Figure 34: Lithology Map (including Borehole Positions), Nuku'alofa	116
	Figure 35: Borehole Logs NB 008 to NB 011, Nuku'alofa.....	118
	Figure 36: Borehole Logs NB 010 to NB 003, Nuku'alofa.....	118
8.4	HISTORY OF DAMAGING EARTHQUAKES, NUKU'ALOFA.....	121
	Figure 37: Large Shallow Earthquakes around Nuku'alofa.....	121
	Table 18: Catalogue of Large Shallow Earthquakes, Nuku'alofa	123
8.5	MICROTREMOR RECORDINGS - SITE-RESPONSE MEASUREMENTS, NUKU'ALOFA	132
	Table 19: Microtremor Site-Response Recordings, Nuku'alofa.....	132
	Figure 38: Site-Response Spectra, Nuku'alofa.....	134
8.6	ANALYSIS OF SITE-RESPONSE MEASUREMENTS AND ZONATION OF NUKU'ALOFA	137
	Table 20: Map Zones vs. Site-Response Models, Nuku'alofa.....	137
	Table 21: Definition of Site-Response Models, Nuku'alofa	137
	Figure 39: Diagrammatic Summary Cross-Section, Nuku'alofa	138
8.7	SVE RESULTS AND INTERPRETATION, NUKU'ALOFA.....	138
	Figure 40: Site-Response Models and Acceleration-Response Functions, Nuku'alofa.....	139
	Figure 41: Seismic Microzonation Site-Response Map, Nuku'alofa	139

9	SUMMARY OF MICROZONATION RESULTS ACROSS ALL CITIES	142
9.1	GENERALISED GEOTECHNICAL RESULTS	142
	Table 22: NEHRP Site Classifications	143
9.2	GENERALISED NAKAMURA RESULTS AND INTERPRETATION	143
	Figure 42: Seismic shear-wave velocities for the surface layer (upper) and basement half-space (lower) in the four Pacific Cities	144
	Figure 43: Relationship between observed period of resonance (T), known thickness (H) and adopted shear-wave velocity (V_s) of the surface layer in the Pacific cities	145
	Figure 44: Nomogram for estimating the relationship between the depth of the surface layer and the possibility of resonance effects in buildings of a given height in Pacific cities	146
	Box 7: Nomogram method for estimating the relationship between ground resonance and building response	147
9.3	SUMMARY OF SVE RESULTS	147
	Figure 45: Acceleration-response curve for Suva with theoretical envelope of amplification; lower bound marks smoothed rock basement and upper bound joins peaks of resonance from layers of different thickness	148
	Table 23: Maximum amplification, period of resonance and probable heights of buildings susceptible to resonance for all Pacific city-zones	148
	Figure 46: Seismic-response zones: Predicted amplifications due to resonance, and probable heights of buildings affected, shown together with the likelihood of ground failure at the resonant frequency	149
10	CONCLUSIONS AND RECOMMENDATIONS	150
11	ACKNOWLEDGMENTS	152
12	REFERENCES	152
13	APPENDICES	156

1 Objective

The principal objective of the current project was the development of a functional, quantitative seismic hazard microzonation in each of four capital cities of the South Pacific.

The microzonation technique was based on site-specific earthquake hazard determinations developed from the SvE method and the other established techniques incorporated therein.

The purpose was to engender a heightened sense of awareness of the prevailing seismic hazard, not only in the four countries concerned, but also extending into the region and, concurrently, to develop skills, tools and attitudes in the region to deal with that hazard and reduce the attendant risks to the local populace.

Achieving the objective has involved the development of several lines of technology. These include a special seismic data-acquisition system; specialised software for estimating seismic response from actual measurements; a novel approach to estimate the site-specific hazard; and a geographic information system to analyse and present the results of the determinations for each city and support ongoing all-hazard and risk studies.

2 Introduction

Successful completion of the project *Earthquake Microzoning in Capital Cities in the South Pacific*, involved the collaboration of the Geophysical Institute of Israel (GII), the Institut de Recherche pour le Développement (IRD) New Caledonia, and the South Pacific Applied Geoscience Organisation (SOPAC), as well as the four countries engaged in the project. The project was carried out under USAID Project Grant No: TA-MOU-95-C13-024 (Shapira 1999), and covered the following cities (island and country shown in brackets):

- Suva (Viti Levu, FIJI ISLANDS)
- Port Vila (Efate, VANUATU)
- Honiara (Guadalcanal, SOLOMON ISLANDS)
- Nuku'alofa (Tongatapu, TONGA)

The project resulted in a site-specific earthquake hazard determination for each of these cities which is presented in the form of text, plots and maps in this report. Also presented are detailed summaries of the investigation and development activities associated with the tasks listed below, and other results arising from the project. Some of the information is in the process of being prepared as scientific publications. A conference paper summarising the results was prepared by Shorten et al. (1999).

The locations of the cities involved, set within the context of the regional seismicity and tectonics, are shown in Figure 1.

It must be stressed that this study is of a regional nature and there is generally in each country a paucity of data from which conclusions are drawn. Field observations are only at a reconnaissance level and zone boundaries may change with further work. For site-specific assessments, any observations and broad conclusions in this report should be checked by geotechnical specialists.

2.1 Investigations and Developments

The investigations and developments associated with site-response assessments were:

1. Development and installation of a seismic data acquisition system: the PC-SDA.
2. Characterising the seismo-tectonic setting of the four cities under study.
3. Development of the software for estimating the site response from seismic measurements: the GII-SRD program.
4. Implementation of a MapInfo-based geographical information system (GIS) for each of the cities in the project.
5. Collecting physical, geological and geotechnical data, borehole information and demographic data, modifying and installing them in the GIS.
6. Performing site-response measurements in Suva, Port Vila, Honiara and Nuku'alofa.

7. Analysis of the site-response measurements in association with geological and geotechnical information.
8. Preparing microzoning maps describing the resonant frequencies and expected amplification effects across the investigated cities.
9. Collaboration with countries engaged in the project, including involvement and training of local counterparts from each country in all of the above aspects of the project.

One of the main tasks of the project was to assess the seismic response of sites across the investigated cities. This one task absorbed much of the research time and finances in the three-year operation of the project.

2.2 Regional Seismo-Tectonic Setting

The broad distribution of earthquakes (post-1972 records) throughout the North and South Fiji and Lau Basins and island areas can be seen in Figure 1. The proximity to the cities in this study of concentrations of shallow earthquake activity (less than 70 km deep), of medium-high magnitude represents a major concern.

High levels of activity are marked by clustering of earthquake epicentres in the Fiji Fracture Zone; the Hunter Fracture Zone; the Hazel Holme Ridge; the New Hebrides Arc and San Cristobal Trench; the Tonga Trench (Aggarwal et al. 1972); and the proposed spreading centre immediately west of Fiji (Hamburger & Isacks 1993). The northern and western parts of the North Fiji Basin and the western Lau Basin are typically aseismic while the area north of Fiji is dominated by strike-slip deformation. The boundary between the Pacific and Indo-Australian Plates is convergent. In the North Fiji Basin, complex processes of active crustal deformation of back-arc extension are taking place (Hamburger & Isacks 1993; Cooper & Kroenke 1993). The North Fiji Basin is sandwiched between the Tonga and New Hebrides Trenches where there are two active subduction zones of notably opposite polarity. The Vityaz Trench marks a now-inactive subduction zone lying to the north of Fiji and the Solomon Islands.

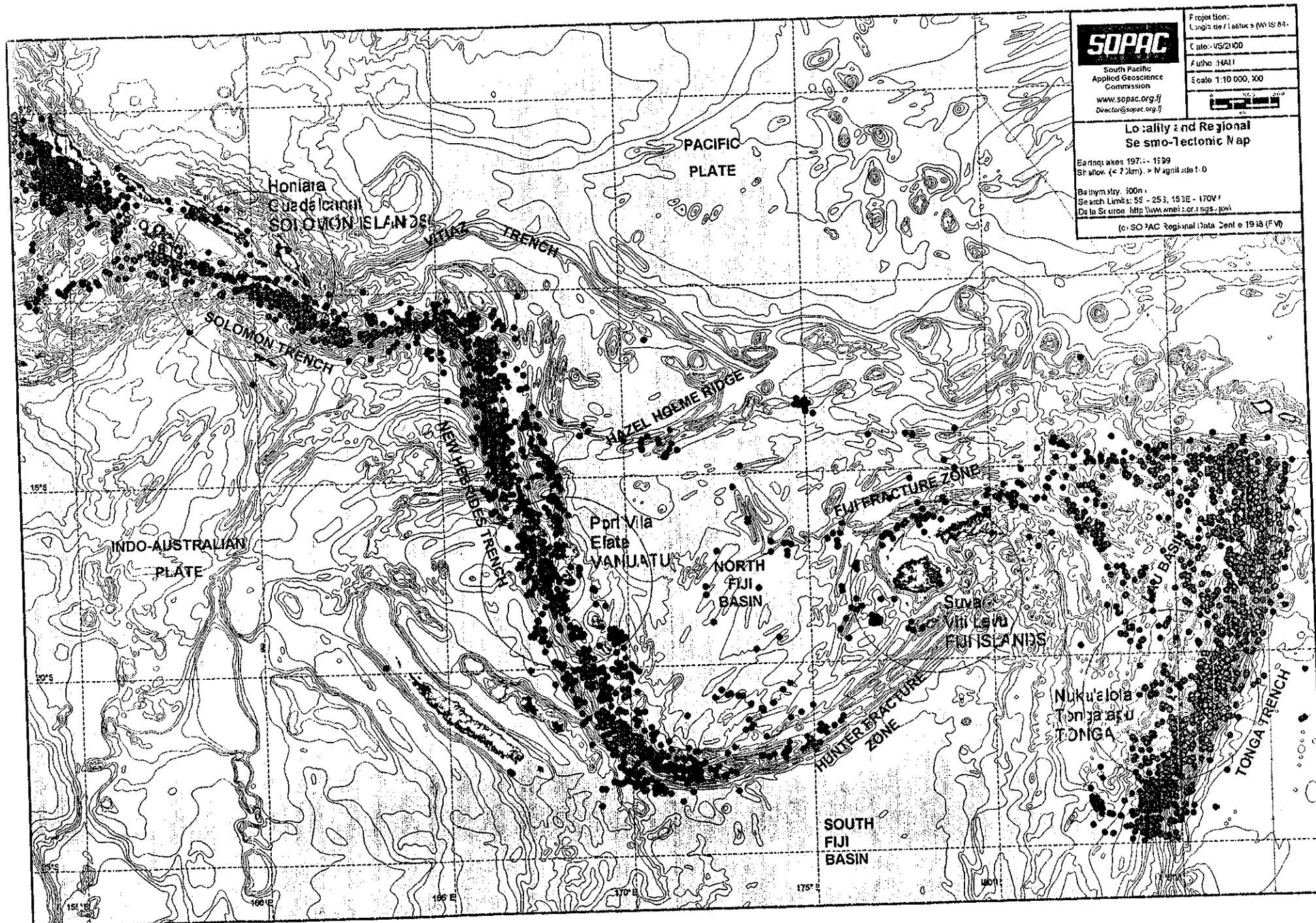
Effects of deep seismicity may also pose some risk to the cities in the study area. Hypocentres have generally been located in the upper mantle to depths of 545-655 km (Cooper & Kroenke 1993). The slab-like distribution of hypocentres in this region is consistent with other areas of active subduction. The authors point out that lithosphere at this depth possesses enough strength to support earthquake-generating stresses and to cause severe deformation of Pacific lithosphere subducted at the Tonga Trench.

Hofstetter et al. (2000) studied the relationship between frequency of occurrence and earthquake magnitudes in the seismogenic areas relevant to the four cities studied. They adopted a characteristic b -value for the entire study area of 1.27 which appears to be independent of depth or seismogenic region.

Because of lack of data in Tonga, Mafi & Shapira (2000) developed a local magnitude scale in terms of the estimated seismic moment. This device enables magnitude determinations of many seismic events which would otherwise not be possible.

(over page: p.8)

Figure 1: Locality and Regional Seismo-Tectonic Map



3 Site-Specific Earthquake Hazard Determination Procedure

All four cities, due to their proximity to active seismic zones, are vulnerable to strong earthquakes. However, damage during an earthquake is not controlled only by the earthquake source characteristics and focal distance. Shallow geological structures and surface soil conditions are also key parameters that can account for observed damage and site-response effects. A fast and reasonably accurate technique for assessing site response is to carry out a microtremor survey of the target area and apply the Nakamura method to analyse the data.

Microtremors are the continuous microscopic vibrations of the ground. They result from ever-present surface waves generated by such sources as human activities, wind and surf, as well as natural ground motions such as earthquakes.

The use of microtremors to characterise soft soils was developed by Nakamura (1989) to determine the resonant frequency of ground shaking and the degree of amplification arising from the shaking of soft soils overlying hard bedrock. This process of characterisation is referred to as site-specific earthquake hazard determination, more commonly known as seismic microzonation. Microseismic zones delineate areas which differ in seismic hazard due to variable amplification at specific sites. The seismic hazard is more acute for those buildings or structures having a natural period of resonance matching that of the ground on which it is built. The Nakamura method is described in more detail in Section 3.1.

To meaningfully prescribe risk parameters to building structures for the use by hazard managers and planners or otherwise, the seismic microzonation of a city should include:

1. Rigorously controlled microtremor recordings (in this case by the Nakamura/SRD method), processing and analysis undertaken in a repeatable step-by-step fashion so as to minimise operator bias and maximise reproducibility;
2. Calculation of the analytical response functions of the microtremor spectral ratios by applying the appropriate constraints (such as known geotechnical parameters, see Section 3.2 and Section 3.3 below);
3. Characterisation of the areas to be zoned by obtaining shear-wave velocity profiles (for example, through the Seismic Cone Penetrometer Method);
4. Use of earthquake ratios recorded at representative sites in each city zone to provide a control on the frequency information and provide better estimates of site amplification;
5. Determination of the natural building responses of characteristic building styles in each city zone, either through SDA and SRD or another method; and
6. Compilation of a reliable history of earthquakes for the regions surrounding the cities so as to achieve the degree of input required to determine the acceleration response of soft soils (using the SvE method, see Section 3.4 below) and produce a scientifically sound uniform hazard spectrum for each city zone.

To fulfil the goals of the project within the resources made available for the current study, seismic microzonation of the four Pacific cities was achieved by undertaking activities outlined in Steps 1, 2, and 6 above. Parameters required for activities in Steps 3, 4 and 5 above were estimated and an ad-hoc assessment of vulnerable buildings (see Chapter 9) was performed which was not within the original scope of this study. Nevertheless, it is recommended that an assessment of vulnerable buildings be repeated when resources can be made available to undertake the activities outlined in Steps 3, 4 and 5 above. A list of recommendations is given in Chapter 10.

A microzonation scheme for each city was achieved by firstly considering known geotechnical information and delineating zones where soft soils would be expected in the subsurface. Based on this geotechnical knowledge, microtremor sites were chosen across the cities and the spectral site responses determined using the Nakamura technique. By comparing the responses from the sites, the seismic microzones of each city were then mapped.

Since the Nakamura method gives a relatively accurate estimate for the natural resonant frequency of a site, but only a rough estimate of the amplification factor (Lermo & Chávez-García 1994), a more robust method was employed to estimate the latter.

The first step in such an approach was to calculate an analytical response function. The analytical response function was correlated with appropriately grouped spectral site responses and constrained by known geotechnical parameters. There should be one analytical response function for each zone in each

city. The function was calculated using the method of Joyner (1977), based on the work of Joyner & Chen (1975), and was incorporated in the SRD analysis described in Section 3.3.

The next step was to calculate acceleration-response functions, utilising regional earthquake hazard and the parameters determined from the analytical response function. This was achieved using the SvE method (Shapira & van Eck 1990, 1993) described in Section 3.4. The SvE calculations were based on a probability of 10% exceedance in an exposure time of 50 years.

The combined Nakamura, geotechnical, Joyner and, ultimately, SvE results enabled a complete microzonation of each city to be developed and mapped utilising GIS software (see Section 4.3). These maps (shown at the end of the chapter on each city) provide an interpretation of all the incorporated empirical and theoretical results. For engineering purposes, the microzonation of each city should be interpreted in conjunction with the respective acceleration-response curves.

3.1 The Nakamura Site-Response Determination Method

Nakamura's (1989) method considers microtremors to be constituted mainly of seismic surface waves that are generated by the constructive and destructive interference of the upward propagating body waves. Based on theoretical considerations as well as on some empirical evidence, Nakamura applied the assumption that the spectral ratio between the vertical motions on the surface and those of the horizontal motions on the interface between the rock and the soft layer is close to unity. Consequently, the ratio between the horizontal motions and the vertical motions on the free surface closely represents the transfer function of the soft layer to seismic shear waves (s-waves). The generation process of the surface waves (i.e. microtremors) basically implies that seismic energy is trapped between the free surface and the surface of the basement rock, focusing seismic energy in discrete frequencies. The fundamental frequency is known as the resonant frequency of the soft layer.

Nakamura's method attracted many researchers around the world looking for a simple, inexpensive technique to estimate the response of a site to seismic waves. World-wide experience has shown that the site effect is one of the major factors that control the intensity of damage caused during earthquakes and, consequently, is an important parameter in the process of estimating earthquake hazard and risk.

At the time this project was initiated in 1995, there were not many studies that incorporated this site effect in hazard assessment. There is now, however, a rapidly increasing wealth of literature that describes site-response studies and site investigations associated with the Nakamura method.

It is generally agreed that the Nakamura technique itself provides a realistic and reliable estimation of the fundamental frequency of the resonance of a soil layer, yet there still remains some debate as to its reliability in estimating the level of amplification. Nevertheless, some researchers are confident that the Nakamura method is capable of locating highly resonant areas where a widespread uniform soft layer has an abrupt interface with firmer material (Stephenson & Baguley 1996; Singh et al. 1998). The same authors also recommend that when resonance has been detected, other methods should be employed to characterise the area thoroughly.

3.2 Zonation using Geotechnical and Nakamura Results

3.2.1 Geotechnical Input

Geographic areas in each city were differentiated initially into like geotechnical zones based on known surface and sub-surface geology and geotechnical information on rock and soil material types. The areas zoned in each city, shown to the same scale, are delineated in Figure 2. The major limitation in this exercise was the restricted amount of subsurface and geotechnical information available in the four cities studied.

Static geotechnical parameters used as input into the Joyner method were either obtained from in-situ or laboratory procedures where available, or estimated (as were all dynamic geotechnical parameters) from similar situations in the published literature. The Joyner method, incorporated in the GII-SRD software, was used to calculate the non-linear seismic response of a system of horizontal soil layers underlain by a semi-infinite elastic medium representing bedrock.

No consideration was given in this report to factors such as the earthquake source mechanism and direction of fault propagation, which have been shown elsewhere to have a profound effect on motion generated at the source (W. R. Stephenson, pers. comm.).

Box 1: Input Geotechnical Parameters

<i>For surface soil layer:</i>
thickness (or depth)
natural density (bulk wet density)
pre-consolidation vertical effective stress
depth to water table
degree of saturation of phreatic zone
dynamic shear strength
shear modulus (low-strain)
shear velocity (low-strain)
<i>For the elastic substratum:</i>
density
shear velocity

The dynamic behaviour of the soil under effective stress conditions was specified in terms of the input parameters, or parameters developed from them in *cgs* units, shown in Box 1. Values for selected critical parameters are presented in a table in each of the four city-chapters following. Shear-wave velocity parameters were not measured directly, but were inferred, estimated or adopted from other studies as detailed in Section 9.

3.2.2 Grouping of Nakamura Results

The individual site responses were determined using the Nakamura technique. This required the computation of the spectral ratio of the average of each of two orthogonal horizontal components, arbitrarily the north-south (x) and east-west (y) components, relative to the vertical component (z) of the ground motion, ie. x/z and y/z . The directional set-up of the seismometer components was fixed so that, if required at a later date, directionality of wave propagation can be incorporated into the analyses.

The calculations were performed within the SRD software (described in Section 3.3). The spectral response curve determined for each site was plotted as spectral ratio versus frequency. Plots of the site-specific spectral responses can be found in each city-chapter of this report.

Grouping (or stacking) of the Nakamura site responses was based on the degree of correlation of the resonant frequency response curves and amplification characteristics of all recordings obtained across the area to be zoned.

The earlier-defined geotechnical zones were then compared to the distribution of the grouped site responses and used to define the boundaries of seismic microzones.

Where the frequency response of one seismic microzone matched, or only differed slightly from, that in another, and where the geotechnical parameters and subsurface geology did not differ markedly across that geographic area, then the boundary was removed to form a single zone. Conversely, if two sites lying within an area containing like geotechnical and subsurface parameters showed widely different spectral responses, a new boundary defined by the Nakamura site responses was delineated.

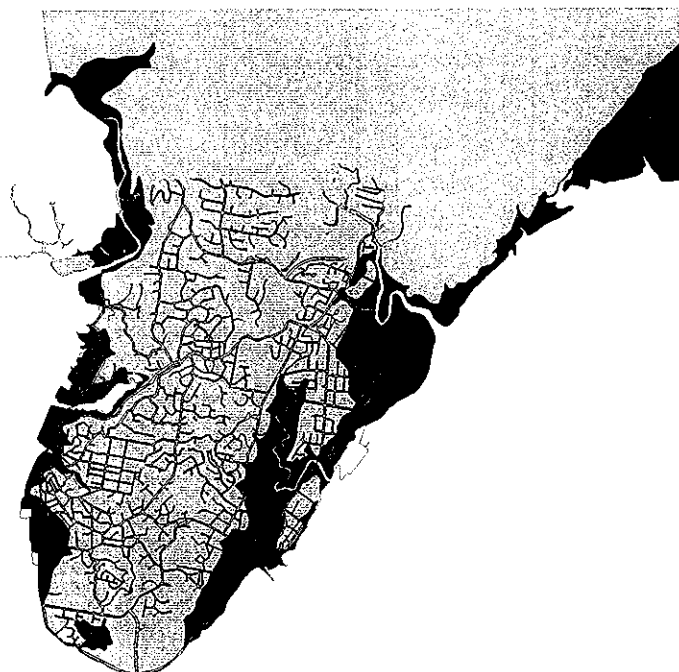
In this way, the initial geotechnical zones and their extents were adjusted by considering the groupings of Nakamura spectral site responses before finally being validated as seismic microzones.

As mentioned above, the Nakamura technique results in a good estimate of the resonant frequency of the soil layer, but does not necessarily give a reliable estimate of amplification. The next step was to fit a unique analytical function to each Nakamura stack, using the known and assumed geotechnical parameters and layer thickness for that zone (Section 3.3). This function was later incorporated within the SVE analysis (Section 3.4).

(over page: p.12)

Figure 2: Areas Zoned for Earthquake Hazard in Suva, Port Vila, Honiara and Nuku'alofa

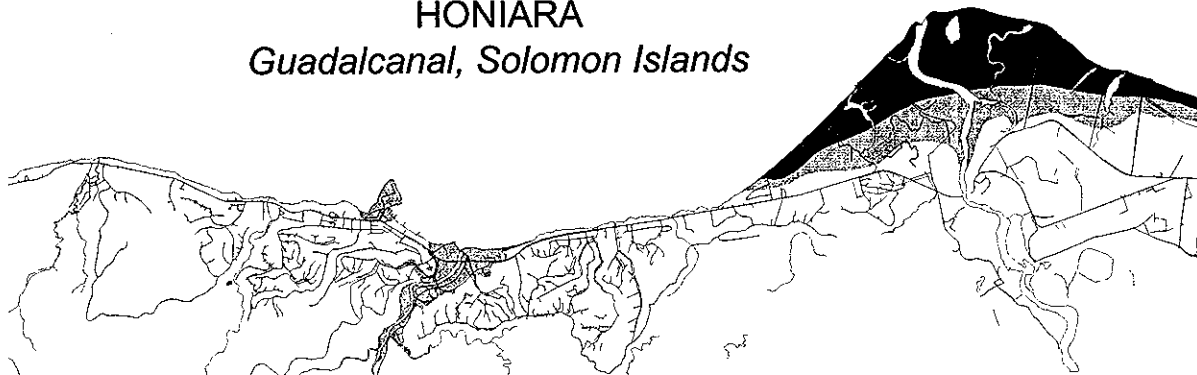
SUVA
Viti Levu, Fiji Islands



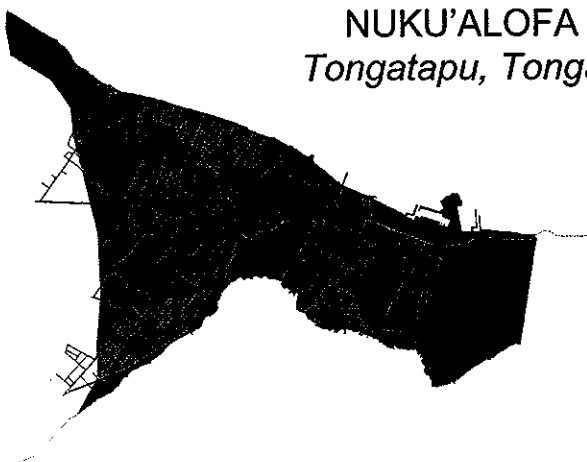
PORT VILA
Efate, Vanuatu



HONIARA
Guadalcanal, Solomon Islands



NUKU'ALOFA
Tongatapu, Tonga



SOPAC

South Pacific
Applied Geoscience
Commission

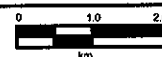
www.sopac.org.fj
Director@sopac.org.fj

Projection:
Non Earth

Date: 20/2/2001

Author: HAU

Scale: 1:100,000



**Areas Zoned for Earthquake
Hazard in Suva, Port Vila,
Honiara and Nuku'alofa**

(c) SOPAC Regional Data Centre 1998 (FM)

3.3 Site-Response Determination (SRD) Procedure

The SRD software was used to:

1. Calculate the spectral-ratio functions for individual sites within each city (see Section 3.2.2); and
2. Fit a subsurface model that will yield a theoretical response function which is similar to the observed pattern and which provides a more realistic estimate of the amplification level.

To minimise the uncertainty in estimating the amplification level by using the Nakamura method, we adhered to the concept that the empirical site-response function (i.e. the horizontal-to-vertical spectral ratio) should be matched to an analytical function based on a credible geotechnical model as explained earlier. The computation of the latter required the input of subsurface information using the computer code of Joyner.

Application of the Nakamura results is facilitated in the SRD program. In the first module, the SRD program allows the user to:

1. set the appropriate number and length of the seismic data acquisition period;
2. assign the window length;
3. choose the number of windows across the components;
4. assign the window shape; and
5. define the ratio-averaging method.

To satisfy the procedures outlined in Section 3 above, the consistency of processing and analysis of microtremor data collected in the four cities was maintained in all cases where possible. At each site, one recording of 3 or 4 minutes was acquired every 10 minutes for a duration of 30 or 40 minutes. The window chosen by the operator was box-shaped. The window length was set to 20 seconds in most cases except where the recording contained too much noise, and then it was reduced to 10 seconds. There were generally four windows chosen to be averaged, and in all cases the ratio of the averages (as opposed to the average of the ratios) was calculated to obtain the value of the Nakamura spectral ratio.

In the second module the SRD program also allows the computation of the analytical response function for a user-defined subsurface model, by integrating the non-linear site-response determination program of Joyner. In quantifying the seismic amplification at a site with soft soil, the most significant items of information required are the shear-wave velocities and the thickness of the soil layers. Shear-wave velocities measured down to several tens of metres depth are generally best for this purpose. In the absence of direct measurements, velocity profiles were estimated from geotechnical data, existing drillhole logs and p-wave velocity profiles.

Numerous scientific advances have recently been made in assessing site-related amplification of earthquake-induced ground motion. However, some sites covered with a significant depth of soft soil have not shown the high amplifications expected. Elsewhere, this effect has been shown to have been caused by a gradual change from soft surface soils to stiff basement rocks, or by the scattering of the arriving earthquake waves in the inhomogeneous strata underlying the soft surface materials (Stephenson & Baguley 1996).

3.4 Application of Site-Response Determination through the SvE Method

One of the main purposes of this project is quantification of the earthquake hazard in terms of site-specific, uniform-hazard, acceleration-response functions. These functions are calculated by application of the SvE method. The SvE method is described in full in Shapira & van Eck (1993). There is a semi-empirical approach that incorporates theoretical models of the earthquake source (Brune 1970; Boore 1983), empirical scaling laws of seismic parameters, empirical assessments of the long-term distribution of the seismicity in and around the region of interest, and empirically determined site-response functions.

The method was first tested in Israel in the early 1990s merely as a concept suggested for approaching the problem of assessing earthquake hazard in applied engineering terms (Shapira 1999). Through a combination of empirical and theoretical applications, the process of determining dynamic earthquake source parameters such as seismic moment, stress drop and rupture area in Israel (Shapira & Hofstetter 1993), was successfully demonstrated. The approach was then developed so as to address the problem of earthquake hazard assessment in less-developed areas or regions where true strong ground motions

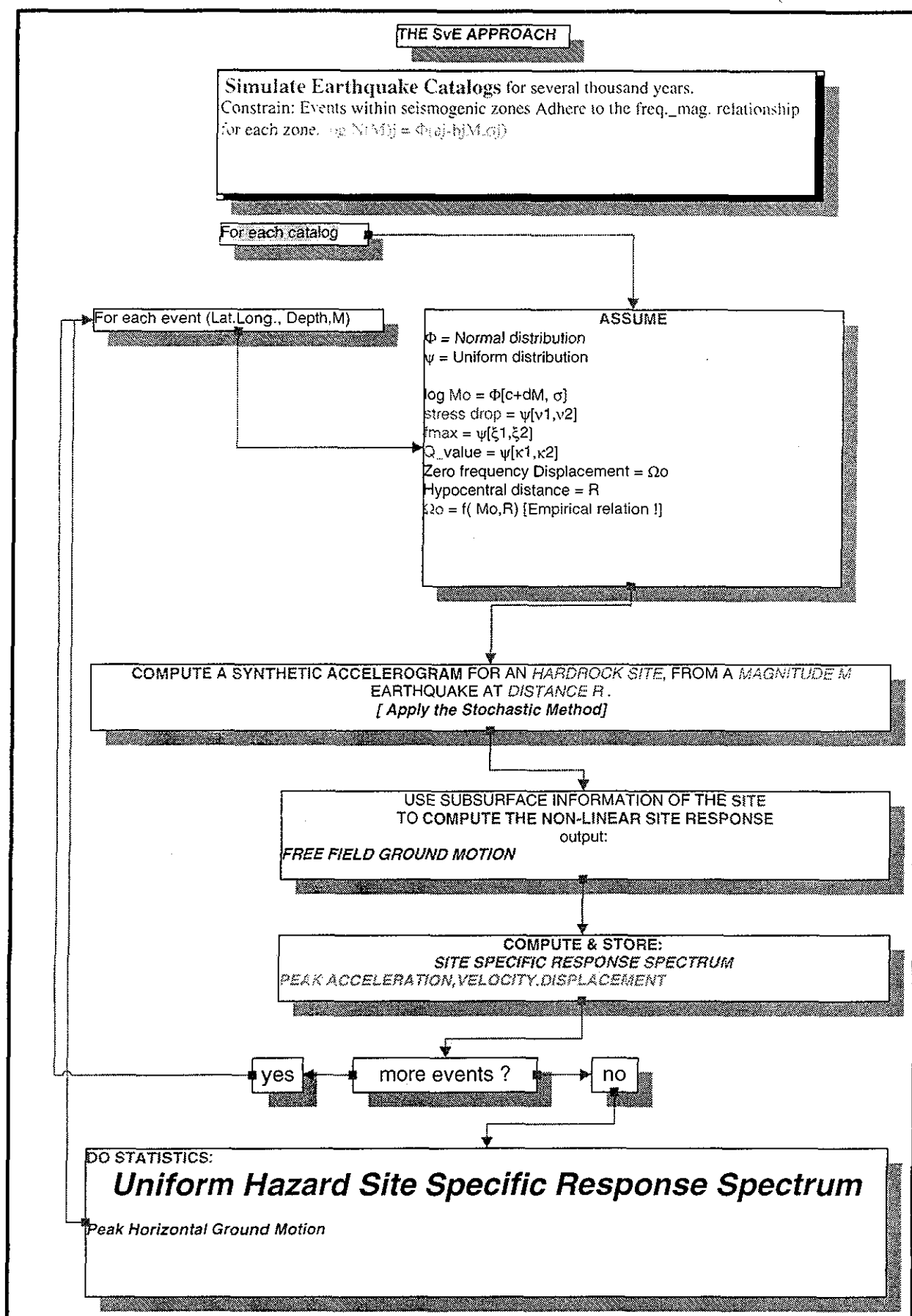
are not available. The SvE methodology of Shapira & Van Eck was formally defined at about the time that this project commenced.

As described by Shapira (1999) in a project report submitted to USAID (Grant No: TA-MOU-95-C13-024), and summarised in the schematic diagram in Box 2 below, the SvE method used in this project involved:

1. Definition of the seismogenic zones around the investigated site(s) and the corresponding seismicity parameters. These data define the parameters needed for simulating the seismicity which will affect the investigated sites in the future. The distribution of seismicity in the seismogenic zones relevant to the project areas was defined, and the frequency-magnitude relationships for each zone were estimated.
2. Determination of dynamic source parameters of earthquakes in the region(s) and their inter-relationships, e.g. the relationship between seismic moment and magnitude, attenuation of seismic energy with distance, and expected stress drop. Based on the stochastic approach, these data are used to synthesise expected ground motions (accelerograms) at the bottom of the surface layer(s) of the investigated site. Earthquake data from Tonga, Vanuatu and the Solomon Islands were used together with parametric data provided by the USGS/NEIC and ORSTOM (Vanuatu office) to determine an empirical attenuation function of the zero-frequency displacement level. The seismic moments of earthquakes in the region were then determined and a unified magnitude scale for the South Pacific region defined. Following this, the relationship to the commonly used m_b magnitude scale was developed.
3. Use of the synthetic accelerograms which correspond to hard-rock site conditions to compute the expected vibratory motions on the free surface of the investigated site by using the Joyner (1977) program), and taking into consideration possible site effects (due to soils and soft rocks overlying the hard rock layer). By application of the Nakamura (1989) empirical site-response determination method, discussed above, the site-response function of each zone in each city was determined.
4. Computation of the response spectrum from each of the synthetic site-specific accelerograms (Shapira & Avirav 1991) followed by the application of simple statistics in order to obtain the expected acceleration spectra for a prescribed probability, exposure time and damping ratio (in this project being 10% probability in 50 years with 5% damping).

A summary of the SvE results can be found at the end of each city-chapter of this report. The acceleration-response spectrum for each zone in each city is also plotted.

Box 2: The SVE Approach



3.5 Justification of Methodology

There are many microtremor techniques used to evaluate the site response of soft soils. Commonly used methods are the interpretation of Fourier amplitude spectra and the computation of spectral ratios relative to a firm reference station (Lermo & Chávez-García 1994).

A four-step microzonation method developed by Borchardt (1994) has recently gained popularity and has been adapted for use in revising the NEHRP seismic provisions (Crouse & McGuire 1996) in the United States. The Borchardt technique is described briefly in the box below.

Box 3: The NEHRP (Borchardt) Method for Estimating Site-Dependent Response Spectra for Design.

STEP 1:

Determine input ground-motion spectral levels for short-period (acceleration) or mid-period (velocity) bands from:

- (a) published maps showing effective peak ground acceleration (PGA), or
- (b) maps showing spectral ordinates.

Option (a) is preferred.

STEP 2:

Characterise local site conditions in terms of mean shear-wave velocity to a depth of 30 m by assigning:

- (a) site classification from a tabulation of physical descriptions of near-surface materials,
- (b) inferred mean shear-wave velocity with information on thickness and physical properties for each of the underlying layers, or
- (c) measured mean shear-wave velocity to a depth of 30 m (where shear-wave velocity is the shear-wave travel-time to 30 m).

Options (b) and (c) should yield more-accurate estimates of shear-wave velocity.

STEP 3:

Infer site-dependent, short-period and mid-period amplification factors that are:

- (a) average values specified with respect to reference ground condition used for determination of input ground-motion spectral levels (STEP 1a), or
- (b) determined from spectral ordinates (STEP 1b) from either:
 - (i) site classification (STEP 2a) and corresponding amplification factor for appropriate tabulated reference ground condition, or
 - (ii) mean shear-wave velocity (STEP 2b or 2c) and corresponding amplification factor for appropriate plotted reference ground condition.

STEP 4:

Calculate free-field, site-dependent response spectra, using input ground-motion spectral levels (from STEP 1), mean shear-wave velocity estimates (from STEP 2) and amplification factors (short- and long-period) (from STEP 3).

The present report forms just one element of a wider SOPAC *Pacific Cities* concept which is linked to the Australian Geological Survey Organisation (AGSO) *Australian Cities* project, both operationally and in terms of aims and desired outcomes. The description of urban earthquake hazard in Cairns by T. Jones (pers. comm.) and also in Granger et al. (1999) as part of the *Australian Cities* study is largely based on the NEHRP methodology and differs somewhat from the methodology adopted in this study. To facilitate an appreciation of the particular approach to seismic microzonation in the cities involved in the two projects, we have compared the methodologies adopted by each project below:

In our approach there are essentially four stages, as described in Section 3.1, 3.2, 3.3, and 3.4. These stages are broadly comparable with the stages of Granger et al.:

1. Granger et al., in their Stage 1, estimated regional earthquake hazard for Cairns based on the adoption and scaling of the appropriate spectral values proposed in the revision of the published Australian Standards AS1170.4-1973 earthquake hazard map for Australia by Somerville et al. (1998).

In our report, the regional earthquake hazard for each city forms a component of the input to the SvE procedure, and is developed through the creation of a synthetic earthquake catalogue based on the recorded history of seismicity within each city-region (see Section 3.4).

2. Granger et al., in their Stage 2, subdivided the city of Cairns into classes in the same manner as the NEHRP method described in the box above. However, these authors have reclassified some of the NEHRP classes slightly to suit the local conditions. The NEHRP classes, based as they are on conditions in California, are not always appropriate to other areas outside the original region for which they were specifically designed.

By contrast, our project develops, independently of the NEHRP classifications, classes or layer classifications that are specific to each city and to each zone within that city. A broad comparison of the resultant site classes in each city against the relative NEHRP classes is discussed in detail in Chapter 9.

As described in Section 3.1, and 3.2, the Pacific cities are zoned primarily on the basis of geotechnical material characteristics. The zones are ultimately constrained through groupings of similar Nakamura site spectra which provide a characteristic frequency of ground resonance, and some indication of the degree of amplification. In locations where the values were known, layer thickness and density are adopted together with a trial-and-error iterative process of varying shear-wave velocity within reasonable bounds to give a best-fit to the stacked Nakamura results in order to calculate the analytical response functions.

3. Site-amplification factors used by Granger et al. in their Stage 3 were determined from empirical values derived for Californian earthquakes and ground conditions. They used amplifications from Crouse & McGuire (1996) for two specific periods ($T = 0.3$ s and $T = 1.0$ s) which were adopted as anchor points to define the full range of amplifications across the appropriate frequency range.

In our project, specific amplification factors for each city-zone are derived from a comparison of the response function of a given zone output from the SvE procedure with that of the basement (or no-response) function over an appropriate range of frequencies. The amplification is measured in terms of acceleration, and is taken as the direct ratio, at a specific frequency, of the over-response function of the affected zone to the response function of the basement.

4. Granger et al., in their Stage 4, modified the results of Somerville et al. (1998) in the revision of the Australian Standard to produce response spectra for their site classes. Somerville et al. in turn used amplification factors of Crouse & McGuire to produce spectra recommended for Australia. Granger et al. used the response spectrum for rock (NEHRP Site Class A) unchanged but have slightly modified spectra from the other classes, preferring to use empirical factors of Crouse & McGuire in some cases, and amplification factors for $T = 1.0$ s unchanged from Crouse & McGuire for an input PGA of 0.1 g. Granger et al. produced response spectra for the four NEHRP Site Classes appropriate to Cairns across a range of periods $T \approx 0.03$ s to 3.0 s.

Our project produces spectral response functions that describe the earthquake hazard specifically for each zone in each city. These functions are derived through the SvE procedure by adopting Joyner function specific to each zone, and incorporating the synthetically derived, regional earthquake hazard for that region. Responses are calculated across a range of periods of $T = 0.1$ s to 10.0 s.

The advantage of the site-specific hazard determination and SvE procedures adopted for the Pacific cities is that site-response functions and acceleration-response spectra are developed specifically for the city and zone under study. In the Cairns study of Granger et al., by contrast, empirical responses developed for California were adapted to the local Cairns site conditions. Notwithstanding, the California study still provides probably the single best-researched example of the development of an earthquake microzonation scheme available.

4 Aspects of Project Development

4.1 Development of the Seismic Data Acquisition System: PC-SDA

Task leader: Veronic Avirav (GII)

Collaborators: Avi Shapira (GII), Les Allinson (SOPAC), Franck Martin (SOPAC), Lea Feldman (GII), David Levi (GII), David Kadosh (GII), Uri Peled (GII), Yossi Swartz (GII) and Marc Regnier (IRD /ORSTOM).

The PC-SDA was developed during the initial stages of the project. The first version was prepared in 1995. The PC-SDA manual (see Shapira & Avirav 1996) provides a detailed description of the system. Following is a brief description of the main characteristics of the PC-SDA.

The PC-SDA units that were used in the project are based on PC 486 computers operating under MS-DOS, which was the most advanced PC available at the time of the initiation of the project.

The PC-SDA enables simultaneous digital registration of up to 16 seismic channels. The analogue seismic input is digitised in a 12-bit word digitizer with a sampling rate of up to 100 samples per second per channel.

The recording can be made in both trigger mode (i.e., recording only when the input signal fulfils certain pre-defined conditions) and scheduled mode (i.e. start and end recording according to a pre-defined schedule).

The triggering is based on the STA/LTA algorithm (for a single channel) and coincidence criterion (a number of channels triggering within a prescribed time window).

The scheduled recording can be defined in terms of starting time and length of recording or in a periodic manner, i.e. t seconds are recorded every T minutes.

A GPS system is connected to the computer and provides accurate timing to the recorded signals.

The PC-SDA produces an output signal that is used to trigger a digital strong-motion accelerograph (optional).

A removable disk, installed on the computer in addition to the hard disk, enables automatic backup of any waveform data file that is created by the system (optional).

During the site-response recording measurements the PC-SDA system used three L4C seismometers (Mark Products, USA) with a 1 Hz natural frequency, one oriented vertically and two horizontally (oriented north-south and east-west). The output of the seismometers was amplified and filtered with a band-pass filter of 0.2 to 12.5 Hz. (Geotech, USA). Recording was made with a sampling rate of 50 or 100 samples/second/channel using the Periodic recording algorithm.

The PC-SDA system was the main tool for obtaining data to be used in the analysis associated with the project. It should be noted, however, that the rapid progress in the computer sciences and technology has imposed continuous maintenance problems for the system. Nowadays, it would be almost impossible to find and replace items such as motherboard for the PC 486, hard disks compatible with the old PC 486 and a similar A/D card for digitisation. Nevertheless, the organisations of SOPAC and GII have managed to keep these systems operational throughout the project.

4.2 Development of Site-Response Software: GII-SRD Program

Task leader: Alona Malitzky (GII)

Collaborators: Avi Shapira (GII), Illia Turetzky (GII).

The GII-SRD was written for the interactive analysis of site-response measurements. The current GII-SRD software is a second generation to the program developed at the initial stage of the project. The GII-SRD is based on another software product, especially developed for this project, under the name of GII-SDP (Seismic Data Processing) by Malitzky & Shapira (1996). While the GII-SDP supports the need for phase picking, location and magnitude determinations, the GII-SRD enables the analysis of the recorded waveform in the spectral domain. Both use a common library of the calibration data of each seismic channel. Those data are produced by a special application embedded in the GII-SDP.

4.3 Development of the MapInfo Geographic Information System (GIS)

Task leader: Graham Shorten (SOPAC)

Collaborators: Monika Swamy (SOPAC), Litea Blukoto (SOPAC), Geraldine Teakle (SOPAC), and Lasarusua Vuetibau (MRD)

The GII-USAID project on seismic microzoning of four Pacific capital cities dovetails neatly into the wider responsibilities of SOPAC in hazard and risk assessment in its Pacific Island member countries, concurrently being undertaken in the *Pacific Cities* project.

SOPAC has developed a geographic information system (GIS) database in MapInfo software for the four cities covered in the current project. As well as recording the location and results of the measurements of microseisms, the database captures all existing physical, geotechnical, cadastral, assets, population and utilities information for each city including an image backdrop for the information. Hazard zonations, specifically earthquake site-response zonations, have been developed for each city using this information base. Subsequently the zonations will be combined and queried with other relevant databases to assess risk to life and property in the cities studied for a given scenario.

The *Pacific Cities* approach promotes the development of this GIS database as an all-embracing tool for providing a framework or infrastructure for the spatial data management. Information from fields as diverse as geology, meteorology, physiography, engineering, town planning and demography is stored in a single database in multiple layers. Interactions between layers are possible, and the results of numerical modelling are incorporated through the generation of various disaster scenarios.

One of the cornerstones of the project has been the building-assets survey for each city, which seeks to individually assess each building for a series of characteristics related to its potential performance under earthquake, cyclone, flooding or unfavourable foundation conditions. Attempts are now being made to link this information through to the various city council and census demographic databases.

Ultimately, the risk to population and property can be measured through the GIS by considering the way in which hazards, in this particular case earthquake hazards, interact with, and affect, these community assets.

The geographic information system should ideally be able to answer any question posed it by a user of the system such as a town planner or disaster manager. The reality, of course, is that the basic data must first be input into the system.

GIS databases will be made available to national disaster-management authorities in the respective member countries, and kept updated by SOPAC and the country concerned. The databases have the potential to be used to assist town planning, post-disaster rehabilitation, the insurance industry, aid donors and reconstruction authorities, amongst other users.

4.4 Installation, Demonstration and Training

A preliminary trip to the collaborating countries and their capital cities, Suva, Port Vila, Honiara and Nuku'alofa, was undertaken from 12th to 28th February, 1996. The project leader Avi Shapira was accompanied throughout the region by a delegation from Suva which included Alf Simpson, Director of SOPAC, Trevor Jones, a seismologist previously seconded to MRD from the Australian Geological Survey (AGSO), and Graham Shorten, a geological engineer of SOPAC. The aim of the visits was for the project leaders to become acquainted with researchers and technicians in the region, assess seismic-monitoring conditions and technical and logistical requirements, set up communication protocols and explain the scope the project.

Various staff of the Geophysical Institute of Israel between them collectively visited all countries over the course of the project in order to install the equipment in each country and train the counterparts in its use.

A number of trips were made by various members of the SOPAC team to work with the counterparts in-country, and counterparts were invited on an individual basis to work in SOPAC in Suva at various times to receive training in techniques related to the project. In addition, counterparts took part in two special training workshops held in Suva.

4.4.1 First GII-USAID Seismic Microzoning Meeting and Workshop, Suva

3rd - 15th October, 1997

The first meeting, workshop and series of lectures in October 1997, brought together under the one roof for the first time all of the participants in the project. The workshop was held at SOPAC headquarters in Suva directly following the 1997 SOPAC Annual Session. This ensured the maximum attendance of relevant parties. Participants from all the four participating countries attended, as well the leader of the project Dr Avi Shapira and several of his technical staff and representatives from SOPAC and observer nations.

Box 4: Participants at 1st Seismic Microzoning Meeting

Counterparts:		Visiting Resource Persons:	
Gajendra Prasad	Fiji Islands	Avi Shapira	Geophysical Institute of Israel
Arvin Singh	Fiji Islands	Alona Malitzky	Geophysical Institute of Israel
Eroni Tupua	Fiji Islands	Marc Regnier	IRD (ORSTOM), Port Vila
Nilesh Kumar	Fiji Islands	Trevor Jones	AGSO, Canberra
Sakaraia Vunisa	Fiji Islands	Yves Lafoy	IRD (ORSTOM), Noumea
Chris Ioan	Vanuatu		
Stephen Morris	Vanuatu	Local Presenters:	
Alison Papabatu	Solomon Islands	Gajendra Prasad	Mineral Resources Department of Fiji
Kelepi Mafi	Tonga	Arvin Singh	Mineral Resources Department of Fiji
Rennie Vaiomo'unga	Tonga	Lasarusua Vuetibau	Mineral Resources Department of Fiji
Lameko Talia	Samoa	Graham Shorten	SOPAC
Observer:		Facilitator:	
Cathy Baldassary	IRD (ORSTOM), Noumea	Litia Waradi	SOPAC

4.4.2 Second GII-USAID Seismic Microzoning Meeting and Workshop, Suva

15th - 22nd April 1998

The second training workshop, in April 1998, followed up on the first meeting/workshop, that was held in October 1997. The objective of this training was to ensure that at the end of the programme the trainees fully understood the mechanics and manner of using appropriate microzonation techniques, and ultimately were able to use the system effectively in their home countries.

The main business of the workshop was to summarise the ongoing seismic microtremor measurements in Suva, Nuku'alofa, Honiara and Port Vila, analyse the results, and produce seismic site-response maps for each city as a preliminary step in the production of seismic hazard maps.

The following counterparts spent a one-week attachment at SOPAC in April 1998 attending and contributing to the penultimate workshop sponsored by the Geophysical Institute of Israel GII-USAID, the Second Seismic Microzoning Workshop:

Box 5: Participants at 2nd Seismic Microzoning Meeting

Counterparts:		Visiting Resource Persons:	
Gajendra Prasad	Fiji Islands	Avi Shapira	Geophysical Institute of Israel
Arvin Singh	Fiji Islands	Marc Regnier	IRD (ORSTOM), Port Vila
Lasarusua Vuetibau	Fiji Islands		
Eroni Tupua	Fiji Islands		
Nilesh Kumar	Fiji Islands		
Sakaraia Vunisa	Fiji Islands	SOPAC Resource Persons:	
Stephen Morris	Vanuatu	Graham Shorten	SOPAC
Alison Papabatu	Solomon Islands	Litea Biukoto	SOPAC
Kelepi Mafi	Tonga	Monika Swamy	SOPAC

4.4.3 Third GII-USAID Seismic Microzoning Meeting, Suva

8th - 18th March 1999

The final meeting for the GII-USAID project was held in Suva in March 1999, where the principals met to finalise the details of the output of the project, and present the outcomes to the wider Suva community in a public address. As well, the principals travelled to Nuku'alofa to present the outcomes of the project there in a similar public address, and to take the opportunity to upgrade the project hardware and software. They also took advantage of being in the region to make a presentation in Apia in order to set the scene for a parallel project to be undertaken in Apia, as a result of a request to SOPAC by the Government of Samoa, flowing on from the GII-USAID project.

Box 6: Participants at 3rd Seismic Microzoning Meeting

Counterparts:		SOPAC Resource Persons:	
Lasarus Vuetibau	Fiji Islands	Graham Shorten	SOPAC
Kelepi Mafi	Tonga	Geraldine Teakle	SOPAC
Lameko Talia	Samoa	Litea Biukoto	SOPAC
Visiting Resource Persons:		Monika Swamy	SOPAC
Avi Shapira	Geophysical Institute of Israel	Facilitator:	
Alona Malitzky	Geophysical Institute of Israel		
Marc Regnier	IRD (ORSTOM), Port Vila		
		Sisilia Gravelle	SOPAC

5 Seismic Microzonation of Suva, Viti Levu, Fiji Islands

5.1 Introduction, Suva

Task leader: Gajendra Prasad (Mineral Resources Department of Fiji)

Collaborators: Arvin Singh (Mineral Resources Department of Fiji), Lasarusa Vuetibau (Mineral Resources Department of Fiji)

Suva, with its population of over 100,000, is a major regional centre. It houses a large range of industries and the headquarters of many regional organisations. It has an important harbour, foreign embassies, and the main campus of the University of the South Pacific. The city is prone to earthquake damage as demonstrated by the effects of the magnitude 6.8 Suva earthquake of 1953, which caused levels of damage indicating intensities of around MM 8 in Suva. There are extensive areas of landfill underlain by a considerable thickness of soft muds, particularly in the city and port, that are expected to amplify shaking associated with earthquakes, and where liquefaction phenomena may occur.

The first site-response measurements in Suva were made in 1996 (Singh & Prasad 1997) using an EARSS/L3C4D recording system brought from New Zealand and operated by the staff of the New Zealand Institute of Geological and Nuclear Sciences (GNS). GNS, under a separate project, were contracted by UNDHA-SPPO to work with MRD to prepare a site-amplification map for Suva on behalf of the Suva Earthquake Risk Management Plan. Initial measurements were made at the locations of the Mineral Resources Department (MRD) and SOPAC offices, Raiwaqa Reservoir, Royal Suva Yacht Club, Suva Fire Station and at locations in the Suva city centre.

Under the UNDHA-SPPO contract the MRD used a combination of GII and GNS systems during 1997 to perform measurements at further locations across Suva. Some of the sites had to be re-measured in 1998, partly to ensure similarity between the two different recording systems used in Suva for site-response determinations. Both GNS and MRD were co-operative in making these data available to the project. In addition, it should be noted that GNS subsequently converted data collected into a format readable by GII-SRD software. The conversion and method of data analysis may have produced the occasional differences noticed between the levels of amplification of the Nakamura site-response spectra plotted in the report by Singh et al. (1998) and those plotted in this report.

MRD and GNS compiled a first draft of a microzonation map for Suva in 1997-8. Following the Second Seismic Microzoning Meeting later in 1998, a revised, and more accurate, microzonation map was produced by the current project, which also detailed the effects of amplification of earthquake accelerations in Suva.

Details in digital format of geographical information for Suva including geological boundaries, borehole locations and logs, seismic microzone boundaries and investigation sites, road and cadastral plans, digital terrain model and orthophotograph can be found in Biukoto et al. (2001c).

5.2 Tectonic Setting, Suva

Viti Levu lies on the Fiji Platform, surrounded by zones of seismicity, the most active being that forming the northern edge of the platform. The platform itself is postulated to have experienced clockwise rotation since the Eocene and uplift and formation of extensional basins, and there is evidence for a late-stage palaeo-collision in the northwestern corner.

Focal-mechanism studies by Everingham (1983) suggest that the Viti Levu plate region currently lies in a zone of east-west tension. Although Viti Levu is generally located away from well-defined zones of seismicity, nevertheless Suva has been affected on several occasions by earthquakes occurring in a poorly defined zone of seismicity to the south of the island. The damaging earthquake of 1953 (Houtz 1962a; Everingham 1984) is the prime example. Shorten (1990) has related the focal location and mechanism of the earthquake to a northwest-trending fault system some 15 km west of Suva. An apparently related fault system affects the southern end of Suva Harbour and there are unconfirmed indications of activity on this fault system within the last several thousand years.

Research by Jones (1998) suggested that there is a ten-percent probability of exceedance of a spectral ground acceleration of 0.68 g in Suva in any 50-year period. Jones further indicated that peak horizontal ground accelerations (PGA) are about 40% of the spectral acceleration values, or around 0.28 g.

5.3 Regional and Local Geology, Suva

The morphology of the Suva peninsula is largely controlled by block faulting and tilting. The peninsula is essentially a tilted block of sedimentary rocks controlled by north- and northeast-trending fault zones on the harbour side and to the east in Laucala Bay. Suva Harbour itself is a graben flanked by two zones of northeast-trending faulting. These systems are further modified by northwest-trending fault zones, some of which may be recently active, which progressively down-drop the land surface to seaward (Shorten 1990).

The distribution of lithologies in Suva, together with the locations of boreholes, is shown in Figure 3. Suva peninsula is composed of several Mio-Pliocene formations of weak, fine-grained and largely calcareous rocks making up the Medrausucu Group (P. Rodda, pers. comm.). The most widely exposed rock-type in Suva is fine-grained marl containing thin, intercalated volcanic ash beds; the Suva Marl. A thin (maximum thickness around 25 m) limestone formation, the Lami Limestone, and a sandstone formation, the Veisari Sandstone, successively underlie the Suva Marl, but are exposed only in the core of a breached monocline in the Walu Bay area as well as at Lami, west of Suva. In regard to earthquake response, there is expected to be little variation among the various rock types of the Medrausucu Group. This group of formations is underlain by volcanic basement which is exposed a short distance north of the city in the form of the Vago Volcanics.

The formations have been faulted and uplifted to their current position, and dissected by episodes of fluvial erosion over the last several hundred thousand years. During the maximum of the last glacial stage about 18,000 years ago, streams arising from the Suva Peninsula and hinterland occupied deep valleys which graded to a sea level then about 120 m below present level. Sea-level rise since about 10,000 years ago resulted in rapid changes to base level for rivers and streams draining the Suva Peninsula and surrounds.

Keep-up coral reef growth was initiated on bedrock high points along the glacial-stage shoreline, and reef growth has persisted up until the present time. In the areas marginal to the current shoreline, however, the nearshore reefs were eventually swamped by prograding alluvial fans and decreasing circulation and deposition of fine sediment as sea level approached its present elevation.

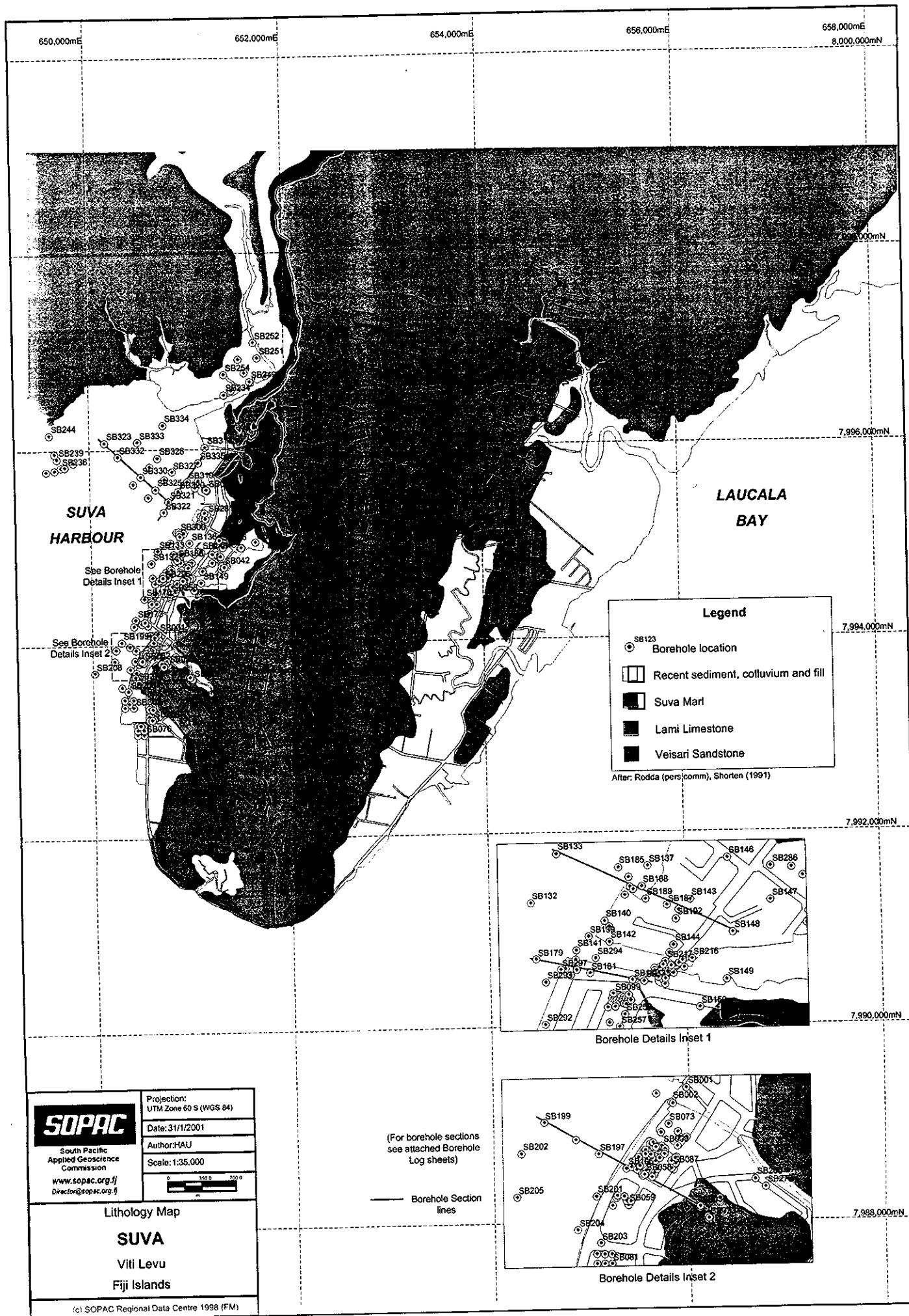
A rising base level gave rise to deposition of thick sequences of fine-grained sediments in the drowned river valleys, particularly as sea level approached its present elevation. At about 4,500 y BP, sea level stabilised at approximately its present position. Deposition has continued within the older stream channels resulting in accumulations of silt and organic deposits up to 50 m thick close inshore and up to 90 m thick in the harbour. These infilled channels occur within all the drowned river systems on both sides of the Suva Peninsula and beneath the low-lying coastal areas.

During this century, various reclamations were carried out in coastal areas, particularly in the present port area, Walu Bay industrial, and central business district areas. Artificial fills are of variable thickness and generally consist of irregularly compacted rubble of andesite, basalt, marl and sandstone.

Selected borehole sections shown in Figures 4-8 serve to illustrate the subsurface distribution of engineering soil and rock types classified according to the Unified Soil Classification System (USBR 1973). The borehole logs are accompanied by logs of soil strength, where these are available, based mainly on Standard Penetration Test N-values. Details of the legend for the soil-type logs and instructions on the interpretation of the strength logs are given in Appendices 1-3.

(over page: p.24)

Figure 3: Lithology Map (including Borehole Positions), Suva



(over page: p.26)

Figure 4: Borehole Logs SB 323 to SB 321, Suva

(over page: p.27)

Figure 5: Borehole Logs SB 322 to SB 335, Suva

(over page: p.28)

Figure 6: Borehole Logs SB 133 to SB 148, Suva

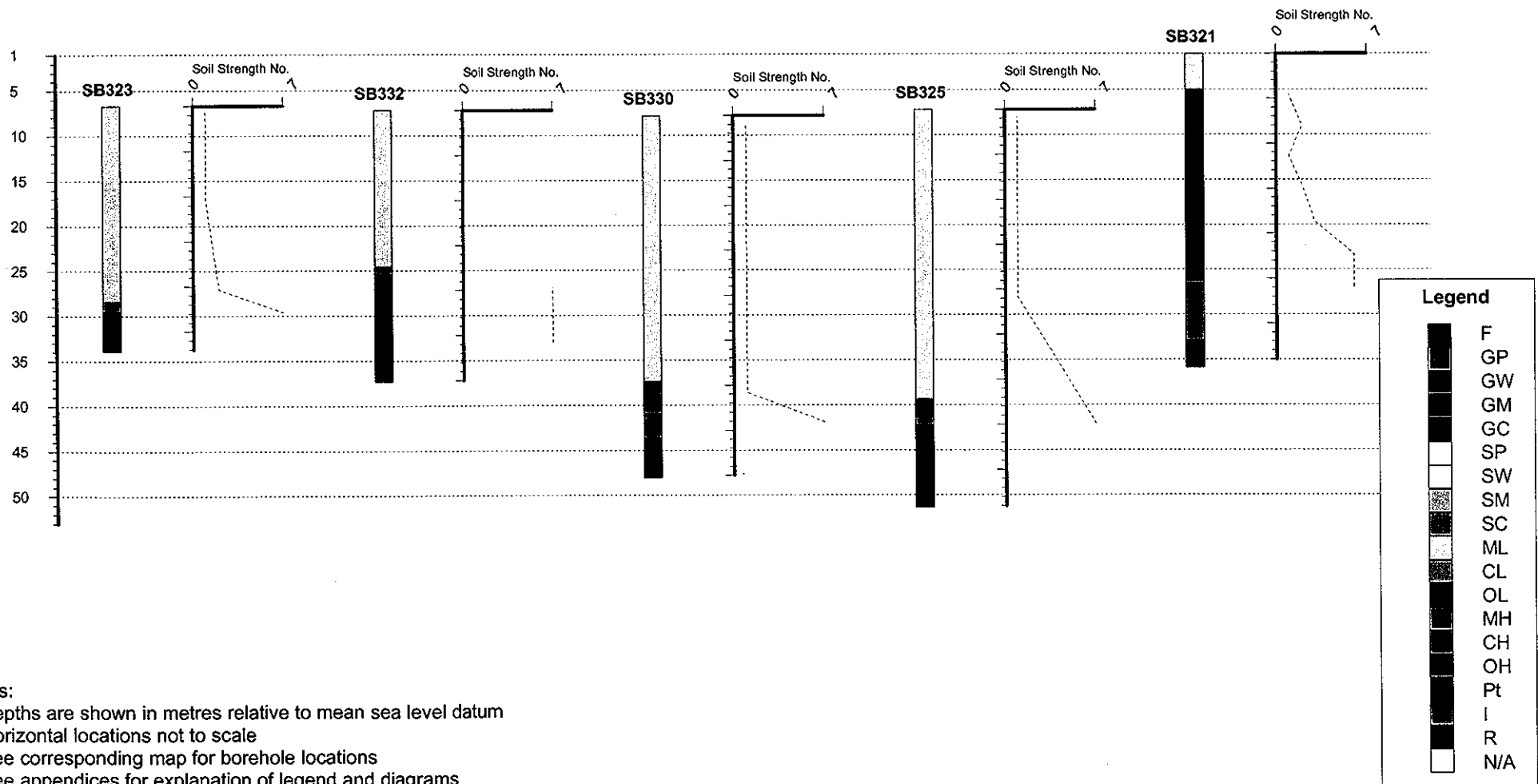
(over page: p.29)

Figure 7: Borehole Logs SB 179 to SB 145, Suva

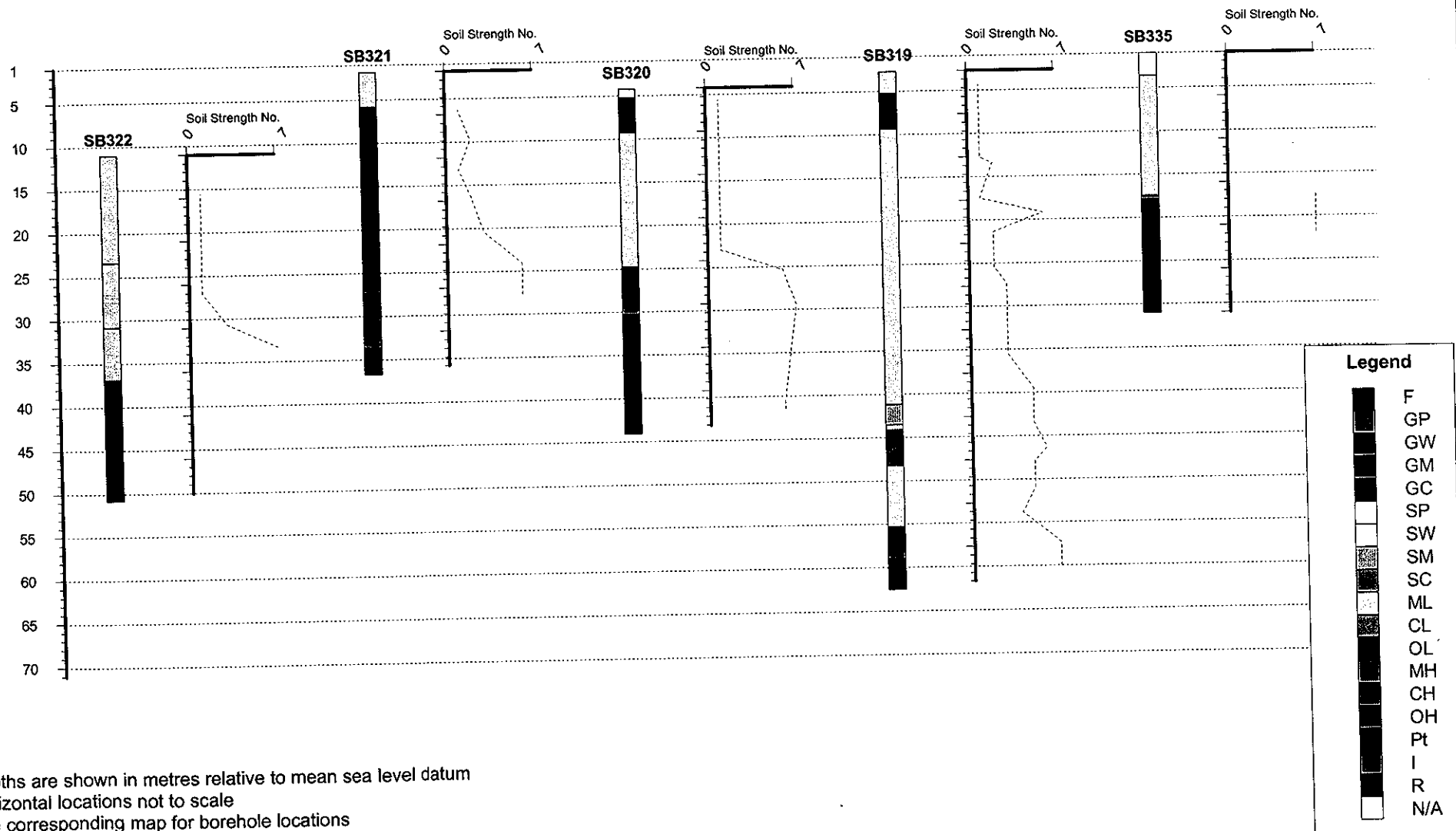
(over page: p.30)

Figure 8: Borehole Logs SB 199 to SB 030, Suva

Borehole Logs Suva Viti Levu, Fiji Islands



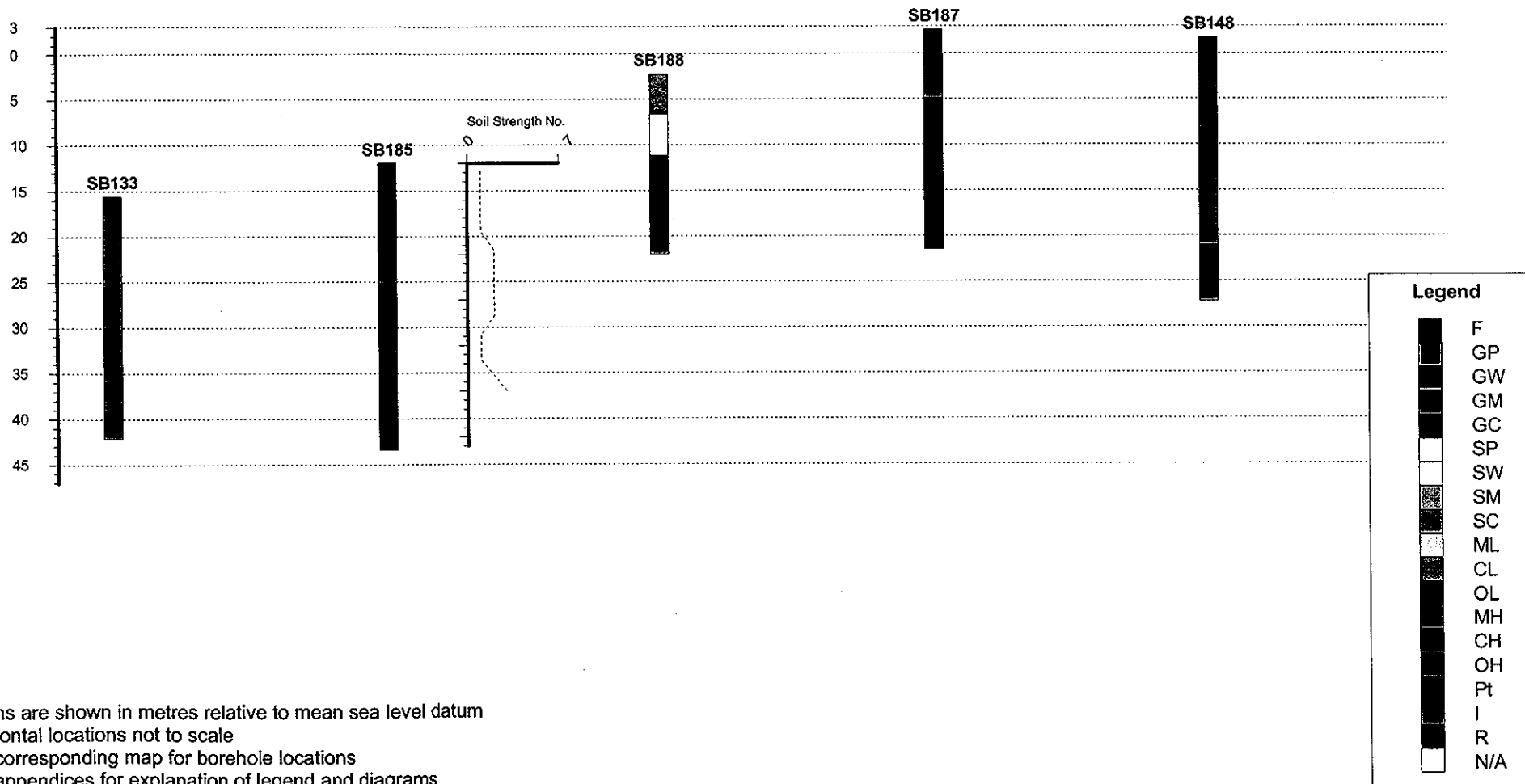
Borehole Logs Suva Viti Levu, Fiji Islands



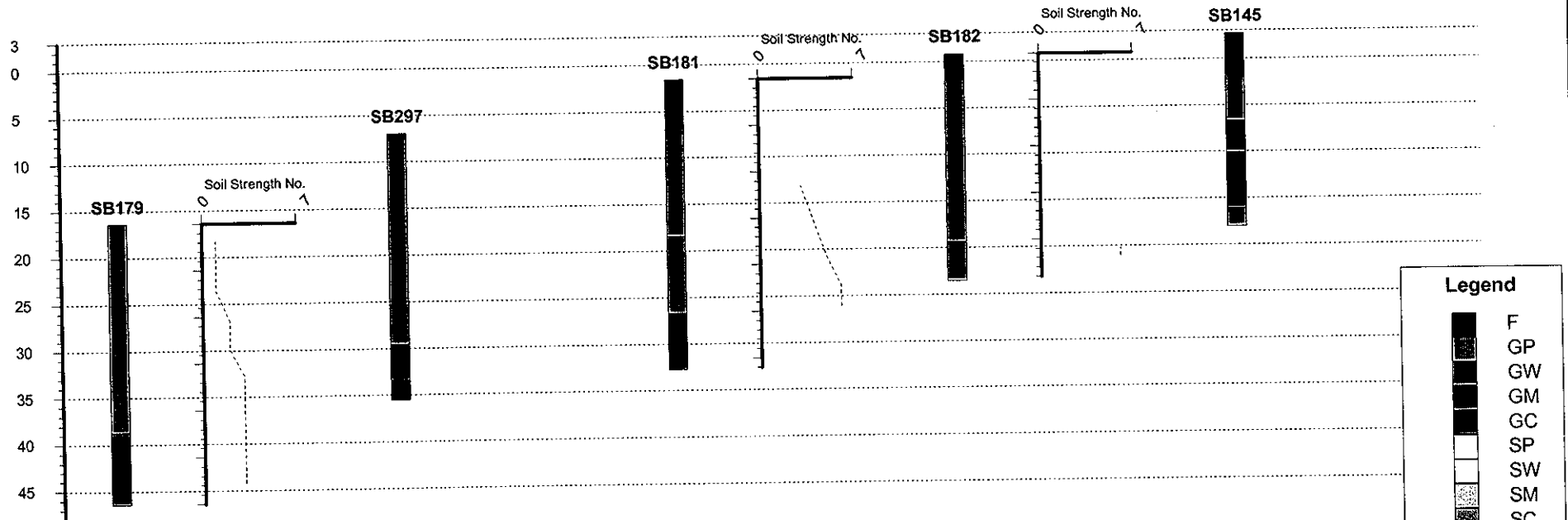
Notes:

1. Depths are shown in metres relative to mean sea level datum
2. Horizontal locations not to scale
3. See corresponding map for borehole locations
4. See appendices for explanation of legend and diagrams

Borehole Logs Suva Viti Levu, Fiji Islands



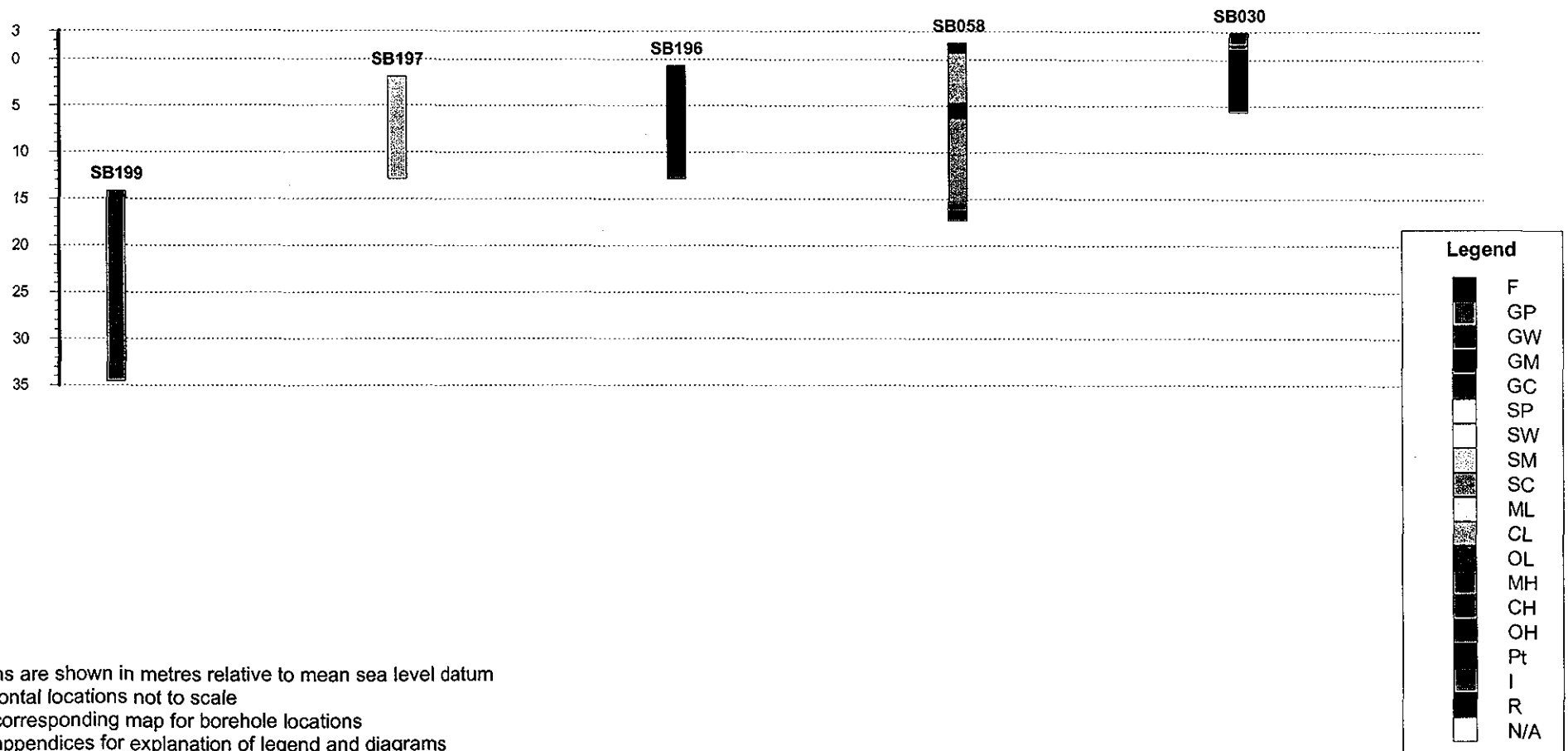
Borehole Logs Suva Viti Levu, Fiji Islands



Notes:

1. Depths are shown in metres relative to mean sea level datum
2. Horizontal locations not to scale
3. See corresponding map for borehole locations
4. See appendices for explanation of legend and diagrams

Borehole Logs Suva Viti Levu, Fiji Islands



5.4 History of Damaging Earthquakes, Suva

The epicentres of large shallow earthquakes (magnitude > 5 , focal depth < 70 km) for the period 1973-1998, as well as earlier historical events, within an arbitrary 250 km radius of Suva are shown in Figure 9 and catalogued in Table 1.

Suva is located in the Southeast Viti Levu Zone of earthquake activity defined by Jones (1998). Jones' work summarised reports by others of a number of strong earthquakes which have occurred in this zone since the October 1869, Mw 6.1 event. Not all major events in the zone have been felt in Suva.

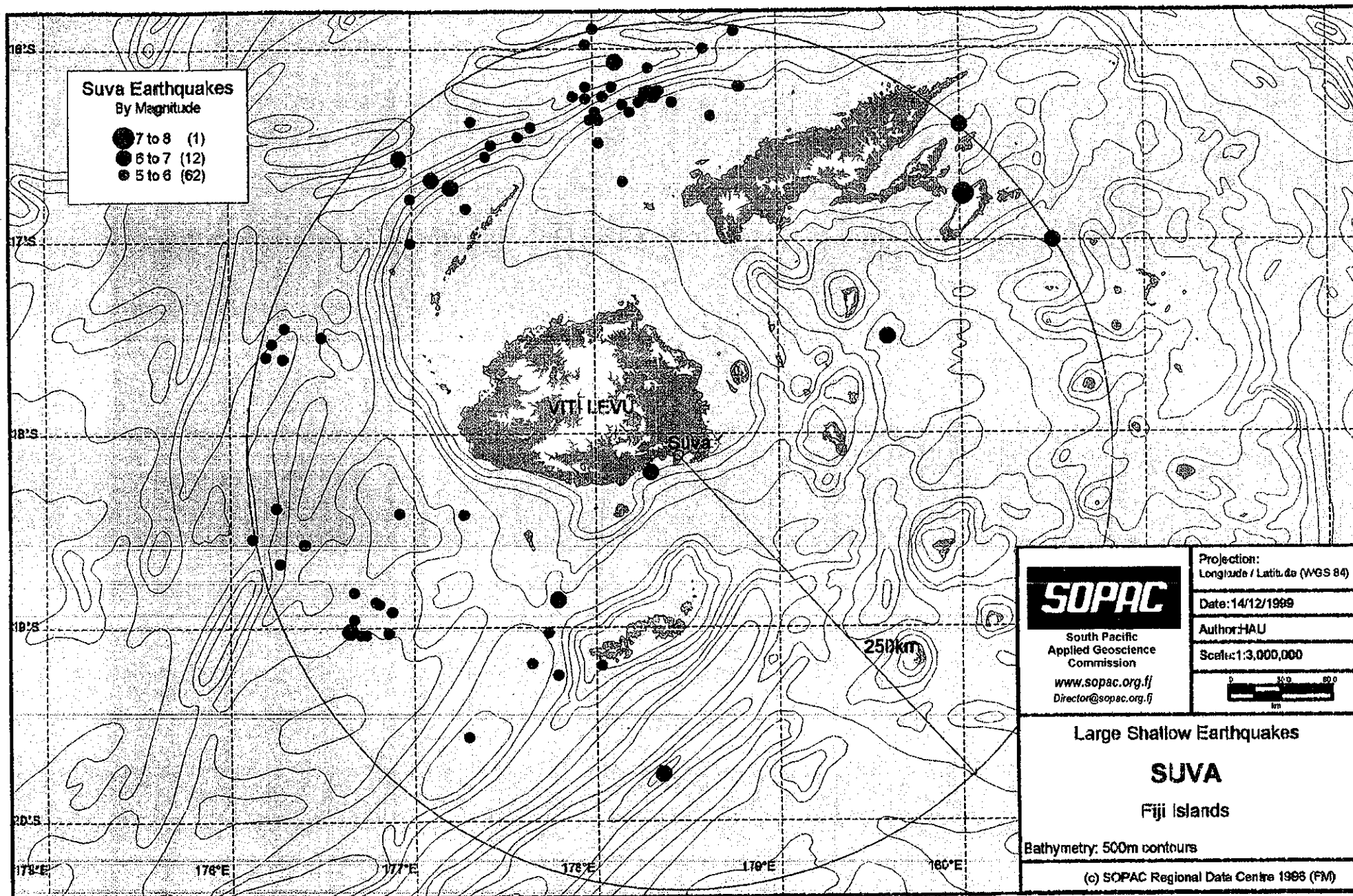
1932: In 1932, the Mw 6.6 Koro earthquake caused felt intensities in Suva of MM 4-5.

1953: Apart from several minor events, the most significant earthquake to affect Suva was the 1953 Suva earthquake of Mw 6.8, followed by a Mw 5.8 aftershock. Houtz (1962a) provided the definitive description of this event and its effects on Suva and Everingham (1987) also reported on the event. The main shock caused felt intensities of MM 7 in Suva and MM 8 in surrounding areas and caused a submarine landslide that initiated a tsunami. Two people were killed as a result of the earthquake and five more as a result of the tsunami. A large number of government buildings were damaged and many of the bridges in the region were destroyed or damaged. The main Suva wharf and the reclaimed area inshore were damaged to the extent that the wharf had to be replaced. There has been a much greater degree of development in the city area since 1953, so that an event of even similar intensity would cause far greater damage today.

1961: Other, smaller, events include the 1961, Mw 4.5 earthquake in the same zone which was described by Houtz (1962b) and Everingham (1987).

(over page: p.32)

Figure 9: Large Shallow Earthquakes around Suva



(over page: p.34-35)

Table 1: Catalogue of Large Shallow Earthquakes, Suva

Circle Search: Earthquakes for Suva	
Circle Centre Point:	Latitude: 18.1130 S Longitude: 178.4580 E
Radius:	250 km
Magnitude Range:	5.0-9.0
Depth Range:	0-70 km

Date	Origin Time (UTC)	Latitude	Longitude	Depth (km)	Magnitude	Solution	Recorder	Epicentral Distance from Suva (km)
3-Oct-19		-16.40	180.00	10	6.8	mb		
21-Jun-28		-17.00	-179.50	10	6.9	mb		
11-Nov-31		-16.20	178.80	10	5.8	mb		
8-Mar-32		-17.50	179.60	10	6.5	mb		
13-Feb-50	101300.00	-18.86	177.79		6.5	mb		
15-Sep-53	122700.00	-18.20	178.30		6.7	mb		
11-Sep-56	143200.00	-16.24	178.33		6.3	mb		
19-Jun-57		-16.57	176.93	10	6.5	mb		
17-Apr-63		-19.76	178.36	10	6.4	mb		
5-Jun-64	191316.00	-16.38	177.33	25	5.2	mb		
21-Jun-64	222121.00	-16.33	178.01	18	5.0	mb		
5-Mar-66	154505.00	-17.60	176.20	31	5.4	mb		
12-Jul-67	211453.00	-16.10	178.30	33	5.3	mb		
20-Jan-68	164127.00	-16.20	178.10	21	5.6	mb		
3-Feb-68	051619.00	-17.50	176.50	33	5.1	mb		
7-Mar-68	025454.00	-16.00	178.60	33	5.1	mb		
26-Aug-68	092559.00	-16.26	177.96	25	5.7	mb		
1-Jan-69	092500.00	-16.22	178.36	33	5.3	mb		
13-Oct-70	140226.00	-18.54	176.12	33	5.1	mb		
27-Dec-70	020645.00	-16.20	178.79	29	5.1	mb		
20-Jul-71	173420.00	-19.57	177.30	33	5.5	mb		
5-Sep-72	184126.00	-16.20	177.96	33	5.3	mb		
6-Sep-72	055528.00	-15.98	177.96	33	5.2	mb		
25-Feb-75	192751.40	-16.25	178.05	33	5.0	mb	GS	209
2-Mar-77	050523.60	-16.37	177.98	33	5.5	mb	GS	198
19-Sep-77	124946.20	-16.37	178.03	22	5.5	mb	GS	197
20-Feb-78	090155.60	-16.46	177.59	32	5.0	mb	GS	205
4-Mar-79	235337.50	-16.56	177.41	33	5.9	Ms	GS	204
29-Mar-79	144956.20	-17.53	176.23	11	5.0	mb	GS	244
10-Sep-79	085437.90	-16.35	178.64	33	5.3	mb	GS	195
24-Sep-79	061315.50	-17.61	176.29	33	5.0	mb	GS	235
16-Nov-79	152125.70	-16.76	-179.98	33	7.0	UK	BRK	222
10-Sep-80	120309.60	-18.67	176.27	33	5.3	mb	GS	239
23-Dec-80	095342.60	-16.29	178.16	33	5.9	mb	GS	203
20-Feb-82	091703.90	-16.71	177.23	14	5.5	mb	GS	202
7-Aug-82	012029.52	-16.23	178.28	33	5.1	mb	GS	208
16-Jul-83	155009.98	-19.03	177.74	33	5.1	mb	GS	125
19-Jul-83	060928.40	-19.19	177.65	33	5.1	mb	GS	146
2-Aug-83	131510.06	-16.41	177.66	33	5.0	mb	GS	206
13-Aug-83	153002.65	-19.20	178.03	33	5.1	mb	GS	128
20-Dec-83	160607.90	-16.49	178.03	24	5.5	mb	GS	185
29-Feb-84	012700.05	-18.57	176.40	33	5.7	Ms	GS	222
21-Mar-84	182037.70	-16.28	178.43	8	5.0	mb	GS	202
28-Jun-84	023331.86	-18.42	177.28	10	5.4	Ms	GS	129
12-Oct-84	182147.30	-16.68	177.11	13	6.5	Ms	BRK	213
12-Oct-84	190001.15	-16.72	177.22	11	6.1	Ms	BRK	202
18-Oct-85	100820.46	-17.45	176.30	33	5.0	mb	GS	239
18-May-87	182725.15	-16.28	178.25	20	5.0	mb	GS	203
18-May-87	183319.65	-16.22	178.30	33	5.4	mb	GS	210
15-Feb-88	200535.49	-16.25	178.28	10	5.0	mb	GS	206
24-Jul-89	100345.85	-18.87	176.79	31	5.7	Ms	BRK	195
24-Jul-89	101124.23	-18.82	176.67	33	5.6	Ms	BRK	203
24-Jul-89	105310.56	-18.88	176.81	19	5.6	Ms	BRK	193
10-Aug-89	192520.69	-19.04	176.71	33	5.2	mb	GS	210
11-Aug-89	032700.60	-19.04	176.74	20	5.1	mb	GS	207
11-Aug-89	065554.38	-18.92	176.88	33	5.2	mb	GS	188
14-Aug-89	175108.76	-19.02	176.65	33	6.0	Ms	BRK	214
14-Aug-89	181240.74	-19.01	176.66	33	5.4	mb	GS	213
14-Aug-89	181553.80	-18.96	176.67	33	5.5	mb	GS	209
14-Aug-89	190233.44	-19.03	176.86	33	5.3	mb	GS	196
2-Feb-90	144909.48	-18.41	176.92	10	5.7	Ms	GS	165

Date	Origin Time (UTC)	Latitude	Longitude	Depth (km)	Magnitude	Solution	Recorder	Epicentral Distance from Suva (km)
28-Sep-90	123334.93	-16.69	178.16	33	5.3	mb	GS	160
5-Nov-90	124736.96	-17.01	176.99	33	5.0	mb	GS	197
18-Feb-91	101032.04	-18.57	176.41	27	5.1	mb	GS	221
18-Feb-91	134743.51	-18.38	176.25	33	5.2	mb	GS	234
24-Mar-91	063922.00	-16.83	177.30	11	5.2	mb	GS	187
15-Jan-95	045431.94	-16.50	177.44	33	5.3	Mw	HRV	208
30-Apr-95	025540.21	-16.78	176.99	42	5.9	Mw	GS	214
5-Aug-95	194249.29	-16.25	177.89	33	5.7	Mw	HRV	213
18-Jun-96	135534.21	-16.07	178.12	33	6.0	Mw	HRV	228
27-Dec-96	024947.23	-16.07	178.14	33	5.5	mb	GS	228
6-Oct-97	065714.42	-16.33	178.20	22	5.0	mb	GS	199
23-Feb-98	031448.13	-15.90	178.00	33	5.2	Mw	HRV	249
2-Nov-98	035032.46	-19.25	177.79	33	5.7	Mw	HRV	143
24-Dec-98	235605.54	-15.91	178.77	33	5.2	Mw	HRV	245

5.5 Microtremor Recordings - Site-Response Measurements, Suva

Microtremor recordings were originally made at eight sites in Suva by this project in conjunction with the Mineral Resources Department of Fiji (MRD). The same sites were used again in the later, more comprehensive study, by GNS and MRD which also made recordings at an additional 48 other locations in Suva.

Stacked groups of site-response spectra are shown together with the appropriate spectral models in Figure 10, and the site characteristics are summarised in Table 2. The locations of recording sites are shown at the end of the Suva chapter (see Figure 13).

Data collection and analysis by GNS/MRD was undertaken from 15th March to 16th April 1997. Spectral ratios from all sites were later re-computed at SOPAC and MRD using the SRD software.

Staff of the Seismology Section of MRD selected the best sites for microtremor measurements. Some sites close to trees, power poles or mechanical jacks were moved at least 50 m away to minimise noise due to swinging movement or pounding. Sites 21, 22 and 23 were moved from their planned locations because they were beside trees, power poles or mechanical jacks, or inaccessible. Measurement at site 40 was repeated because the initial recording had been interrupted by noise.

The instruments that were used for all recordings were the single-component 1-Hz Mark Products L4C transducers supplied by the current GII-USAID project. These have a nominal damping of 67% of critical. Earthquake recorders used in the GNS/MRD study were Kelunji recorders manufactured by the Seismology Research Centre of Melbourne. Recorder settings in the form of software (Seismology Research Centre 1990) were provided by the Centre for the Nakamura method. GNS used a Macintosh Powerbook as the interface between the earthquake recorder and transducer.

For all microtremor measurements, care was taken to use north-south and east-west transducers for their respective directions. These transducers could have been used interchangeably in the surveys because both were horizontal components, but preservation of the correct alignments allows for the possible future investigation of directional effects.

The total duration for completing the 56 microtremor sites was eight days. Some delays were encountered due to bad weather. Some recordings were done late at night or early in the morning to minimise local noise from traffic. The recordings were done for two periods at a single site and each period lasted 10 minutes. The sampling rate for the microtremor signal was set to 40 per second and the anti-aliasing frequency was 15 Hz. Before recording at any site a calibration signal was generated to show that all transducer components were in working order. The set-up time for each site lasted at least 35 minutes.

(over page: p.37-38)

Table 2: Microtremor Site-Response Recordings, Suva

Site Response Table, Suva

SUVA Site No.	Amplification Factor	Amplified Frequency Hz	Site Response Class	UTC Date	UTC Time	WGS84 UTM Easting	WGS84 UTM Northing	Locality
1	3.3	0.4	D	120397	0423	1966140	3871462	Lands and Survey Bld.
2	1.8	0.9	A	130397	0301	1966207	3876623	Tamavua Bridge, Lami end, west side of road
3	2.4	2.6	C	170397	1653	1966291	3875556	East side of Foster Road, south side of jail
4	4	0.6	A	180397	0041	1965833	3875136	Seaward end of Rona St., south side
5	2.7	0.7	A	180397	0637	1965928	3875053	South side of Rona St., opposite road junction
6	2.6	1.3	C	180397	0557	1966034	3874962	South side of Rona St., junction with Foster Rd.
7	2.7	0.62	A	180397	0337	1966113	3874913	South side of Syria St., half-way between Foster and Leonidas Sts.
8	4.7	0.65	A	150397	0313	1966219	3874836	East side Leonidas St, opposite end of Syria St.
9	1.6	0.85	C	180397	0254	1966417	3875116	Near SW end of Steel Factory
10	2.1	0.8	A	170397	0233	1965705	3874862	Fiji Naval Squadron Bld., opposite end of Eliza St.
11	4.2	0.56	A	180397	0453	1965601	3874727	NW corner of May St. at Jellicoe Rd., Kings Wharf
12	6.2	0.35	A	180397	0520	1965434	3874333	SW corner of Usher St and Jellicoe Rd., Kings Wharf
13	1.8	1.2	B	160397	0451	1965472	3874095	Near Telephone Exchange Bld., Edward St.
14	2	0.4	B	160397	0402	1965399	3873979	NE side of Central St., near SE corner of Parking Bld.
15	2.1	0.9	B	160397	0320	1965444	3873962	NE side of Central St., beside alleyway.
16	3.8	0.65	D	160397	0532	1965528	3873899	South side of Renwick Rd. at junction with Pratt St.
17	1.5	1	B	160397	0213	1965397	3873887	Near eastern end of YWCA Bld. at end of alleyway from Central St.
18	1.5	0.62	A	160397	0133	1965293	3873741	Near NW corner of Civic Centre
19	1.7	0.85	C	160397	0052	1965364	3873660	Between Suva City Council and Olympic Pool Blds.
20	1.5	0.65	B	160397	0005	1965355	3873436	Near North end of FDB Bld (in Joe's Carpark)
21	1.8	0.55	B	170397	2329	1965396	3873232	Near NE corner of Suva Travelodge
22	3.1	0.68	A	170397	2240	1965360	3873140	Near SW corner of Suva Travelodge
23	1.2	0.62	C	150397	2303	1965485	3873223	On northern driveway to Govt. Blds.
24	1.6	1.1	C	160397	2320	1965929	3871594	North side of road, at western end of bridge over Leveti Creek
25	1.3	1.1	C	150397	0207	1966252	3871498	End of driveway to Hotel and Catering School
26	1.5	0.7	C	170397	0045	1967781	3872554	South side of Sunderland Rd., near Uluetuni Ck.
27	1	1.2	C	170397	0010	1967843	3872724	West side of Sunderland Rd., beside driveway to USP
28	1.1	1	B	150397	2220	1968095	3872845	SW corner of National Gymnasium carpark off Laucala Bay Rd.
29	3.2	0.68	B	150397	2131	1968232	3872871	South side of Laucala Bay Rd. at entrance to National Gymnasium

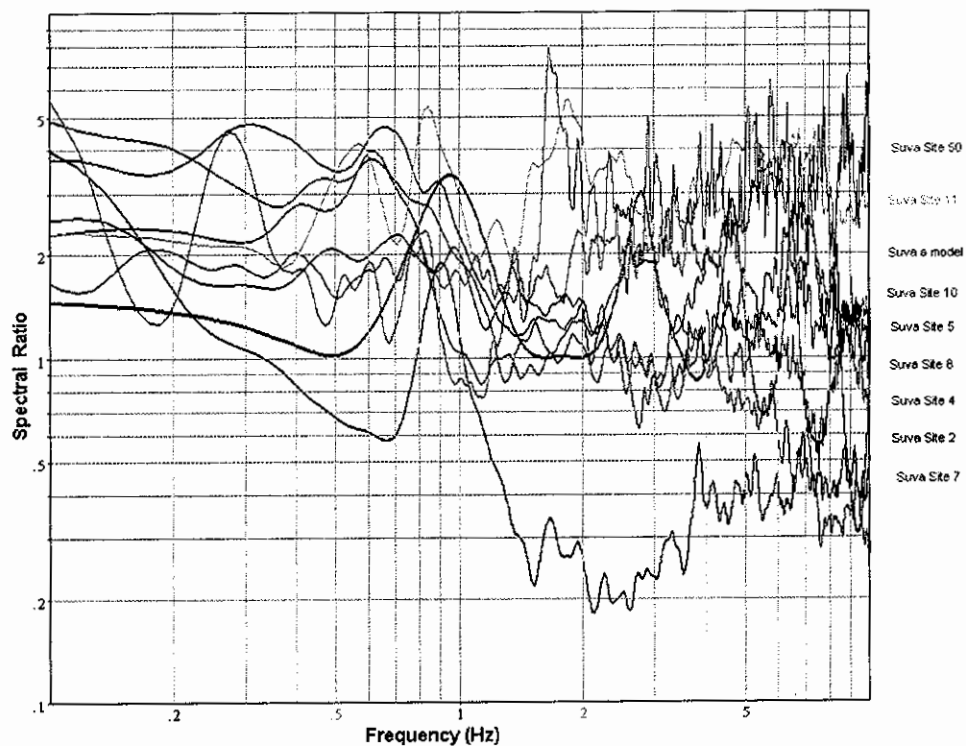
Site Response Table, Suva

SUVA Site No.	Amplification Factor	Amplified Frequency Hz	Site Response Class	UTC Date	UTC Time	WGS84 UTM Easting	WGS84 UTM Northing	Locality
30	2.5	0.38	B	170397	1741	1969146	3874030	North side of bridge over Vatuwaqa River, east side of road
31	2	0.7	B	150397	0118	1969195	3874194	South side of Viria Rd., opposite Govt. Printer Bld.
32	2.2	0.8	B	140397	2330	1968639	3874663	West side of Vatuwaqa River bridge, north side of road
33	2.8	0.55	A	170397	2145	1968574	3874865	Near northern corner of Raiwaqa Sewage Treatment Plant
34	3.3	0.9	A	140397	2212	1969985	3874923	South of bend in Rifle Range Rd., near Fiji Telecom station.
35	6.4	1.3	A	150497	1312	1970149	3875033	On Rifle Range Road opposite Fiji Telecom receiving station
36	1.9	1.2	A	150397	1935	1969864	3876091	At junction of Golf Link and Nokonoko Rds., west side of bridge
37	1.3	0.7	B	150397	1831	1969966	3876187	On Nokonoko Rd. east side of Samabula River, north side of road
38	1.4	1	A	150597	1806	1970073	3876249	On Nokonoko Rd., opposite bend in Samabula River
39	1.4	0.8	C	150397	1712	1970163	3876308	On Nokonoko Rd., north side of road
40	2.1	0.85	D	140397	2012	1970322	3876351	Junction of Nokonoko and Sekoula Rds., SE corner
41	0.85	1.4	D	130397	2315	1969765	3877058	East side of Cunningham Rd., opposite Dairy Factory
42	1.8	0.75	D	130397	2355	1969865	3877073	North side of Kings Rd. east side of Wainitarawau Creek
43	1	0.6	D	140397	1941	1971346	3876781	Opposite FEA Power House, south side
44	2.6	0.75	D	070497	2331	1971167	3878095	Nadera, Ministry of Education property
45	3	0.8	D	080497	0030	1968138	3879313	Tamavua Hospital complex
46	2.6	0.6	D	080497	0337	1967231	3878564	Tamavua Heights, near Wailoku Reservoir
47	2.2	0.9	D	080497	2238	1967425	3876762	Tamavua, Mead Rd., Pillay Park
48	1.6	0.8	D	080497	0835	1967596	3875547	Samabula South, near Old Peoples Home, Totoya St.
49	3.5	0.65	D	080497	2323	1966274	3875978	Korovou, Suva Gaol, near St. Elizabeth's Home
50	2.3	0.85	A	080497	1000	1965819	3873859	Suva Central, Carpark of Provident Building (Downtown Boulevard)
51	2.7	0.48	D	090497	0009	1967224	3873400	Toorak, Flagstaff Park - south side
52	2.2	0.55	D	090497	0356	1966346	3872477	Domain, Fell Place
53	2.5	0.4	D	130497	2348	1967136	3871756	Muanikau, St. Mary's Convent
54	1.4	0.65	D	150497	0328	1947565	3884358	Vunikawai Seismic Station
55	2	0.85	D	200497	2115	1966171	3874560	Edinburgh Drive cave
56	2.5	0.55	D	160497	1308	1966728	3876125	Reservoir Rd. valley on Veisari Sandstone

(over page: p.40-43)

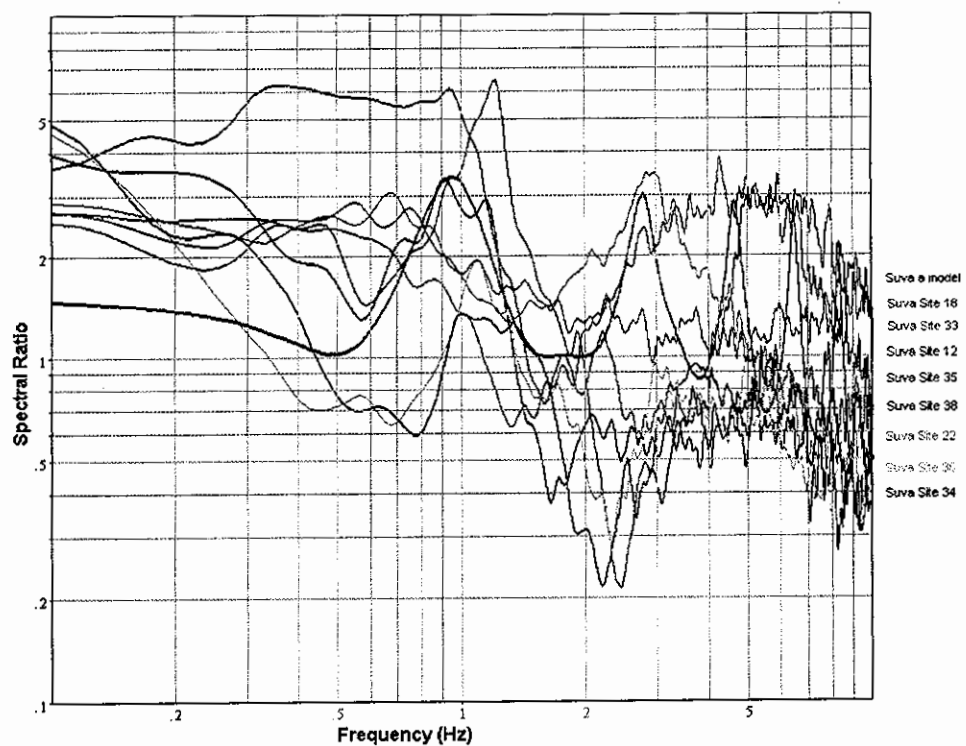
Figure 10: Site-Response Spectra, Suva

SUVA SITE RESPONSE SPECTRA ZONE A - STACK 1



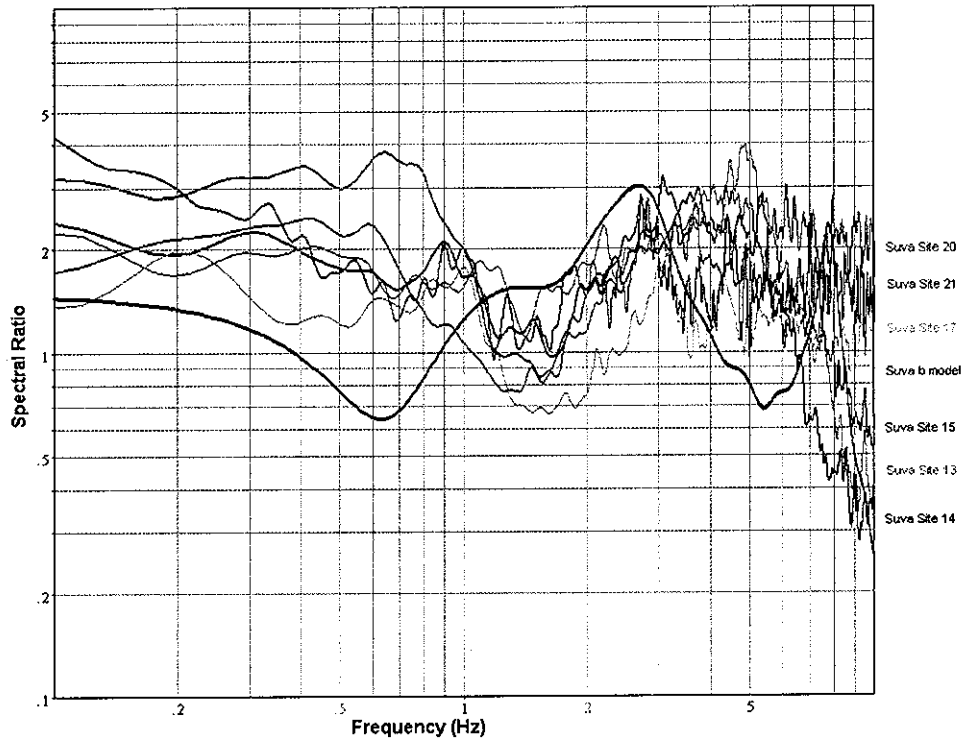
a

SUVA SITE RESPONSE SPECTRA ZONE A - STACK 2



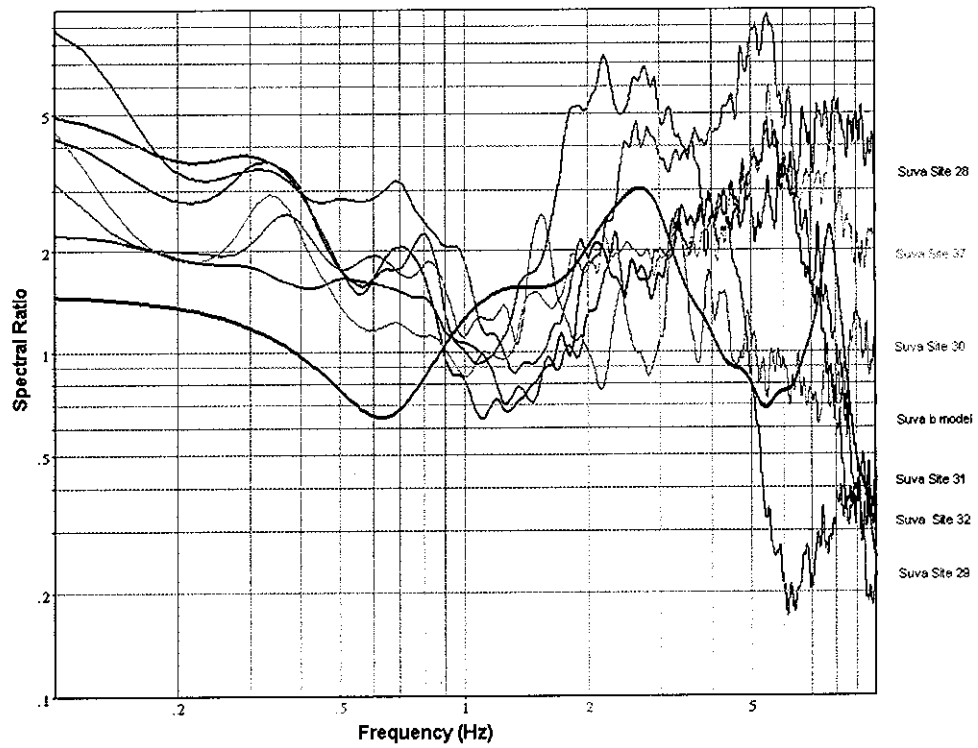
b

SUVA SITE RESPONSE SPECTRA ZONE B - STACK 1



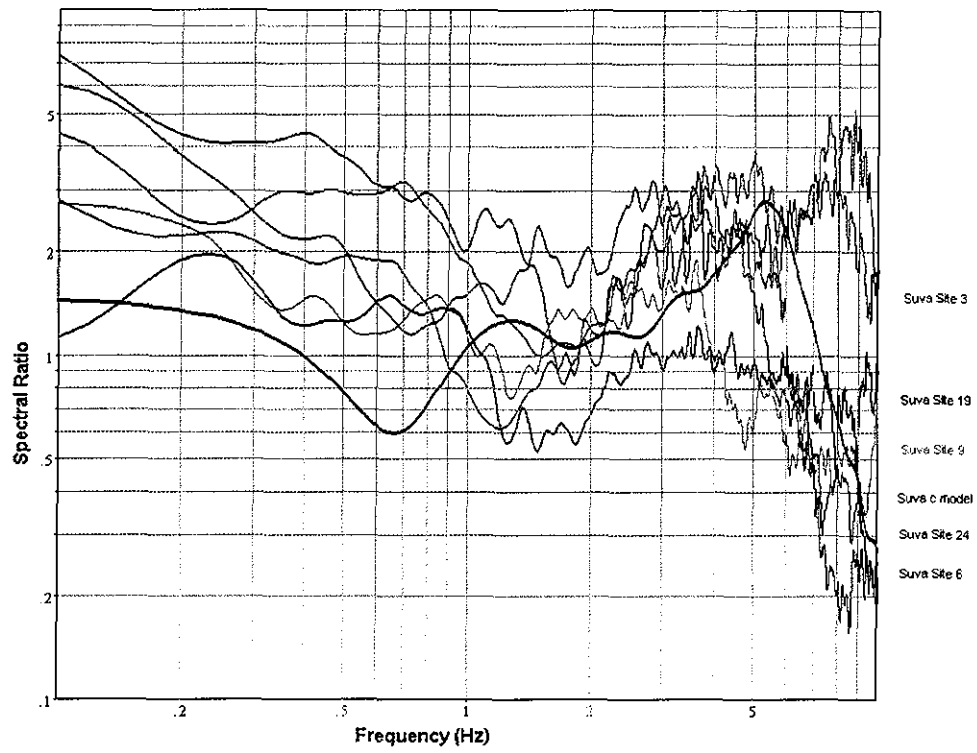
c

SUVA SITE RESPONSE SPECTRA ZONE B - STACK 2



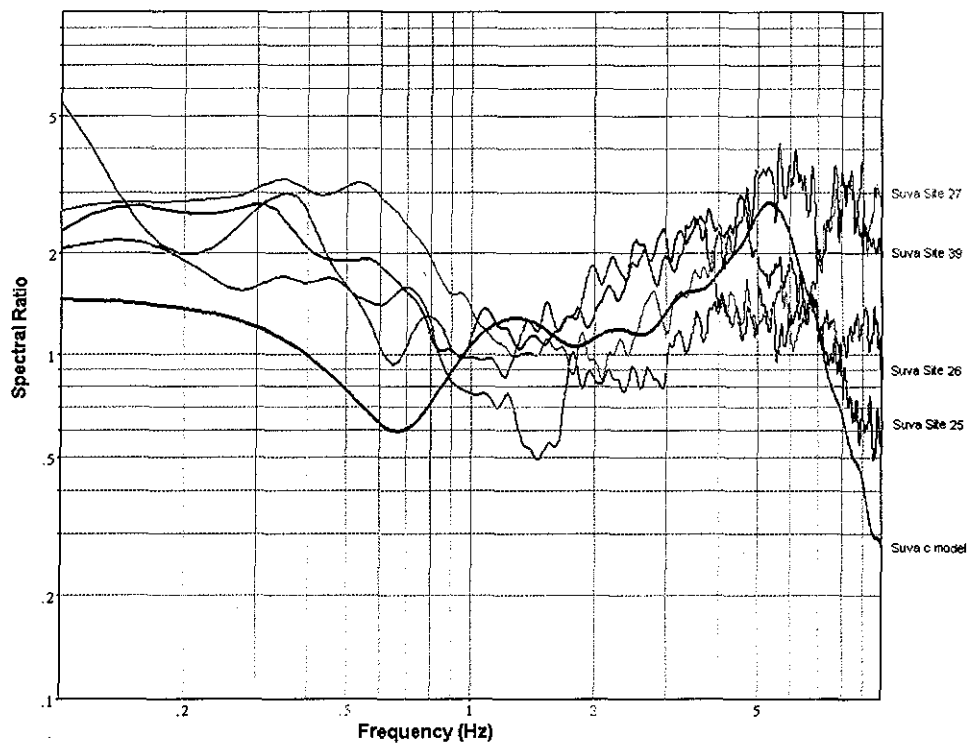
d

SUVA SITE RESPONSE SPECTRA ZONE C - STACK 1



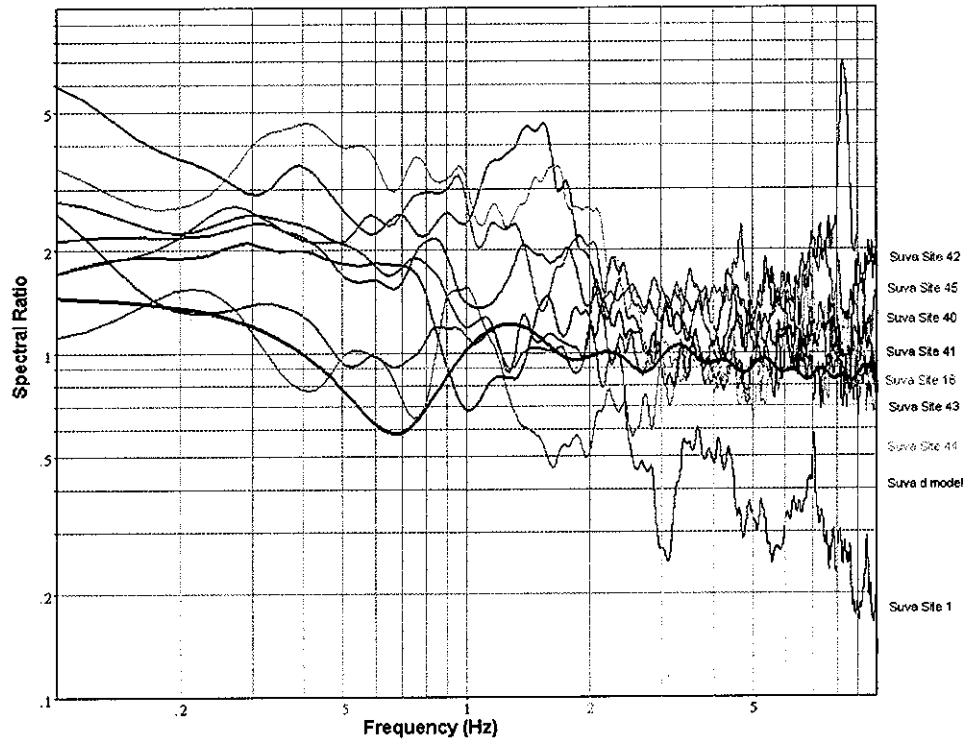
e

SUVA SITE RESPONSE SPECTRA ZONE C - STACK 2

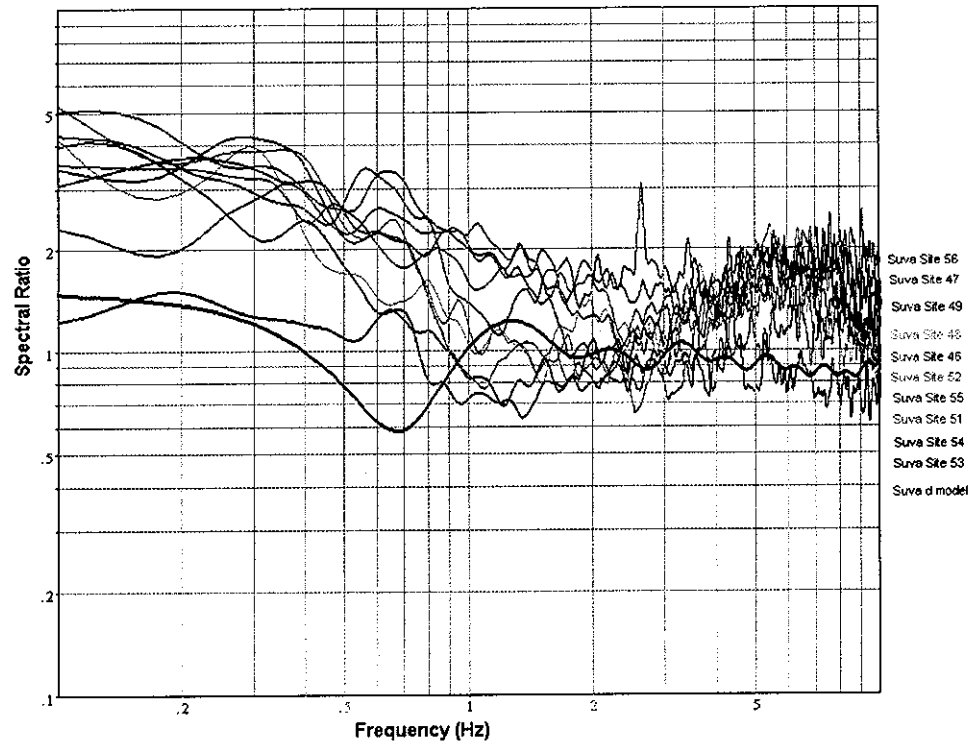


f

SUVA SITE RESPONSE SPECTRA ZONE D - STACK 1



SUVA SITE RESPONSE SPECTRA ZONE D - STACK 2



5.6 Analysis of Site-Response Measurements and Zonation of Suva

The GNS/MRD study subdivided the Suva area into four principal classes of possible earthquake response. These classes were developed based on Nakamura site-response evaluations, topography, geomorphology, depth to bedrock from borehole data and other available geological data. Details of the earthquake shaking-susceptibility mapping process undertaken by the GNS/MRD study team were presented in detail by Hull et al. (1997). The earthquake shaking-susceptibility classes developed in their report are:

- Class A Fine-grained sediments and fill more than 20 m thick, overlying Suva Marl
- Class B Fine-grained sediments and fill 10-20 m thick, overlying Suva Marl
- Class C Shallow coastal deposits and fill less than 10 m thick, overlying Suva Marl
- Class D Suva Marl and equivalent rocks with thin (< 5 m) regolith, fill or sediment cover

Resonant sites are characterised by a narrow resonant peak between frequencies of 0.5 and 3 Hz. Several Suva sites, chosen because they were expected on the basis of geological mapping to show resonant amplification, are clearly resonant according to the criteria outlined above. In each case the spectrum has a characteristic resonant peak, and the amplitude falls off at low frequencies above the peak.

In other, possibly resonant sites, testing has produced spectra which have some features consistent with resonance. However reservations must be held in each of these cases as the spectrum does not fall to low values at high frequencies.

Other sites have spectra that indicate a non-resonant or low response. Some other sites are also non-resonant, though the spectra are not of a uniformly low value. It is difficult to comment on these sites without further investigation, other than to remark that the method strictly applies only to sites where Rayleigh waves or mixtures of s-waves and p-waves propagate in a soft layer lying on a stiff layer. At some sites, the peaks are broad, and their frequencies imply quite shallow resonant layers that are likely to be of little importance in determining damage to structures. No significance should be attached to the sizes of the spectral ratios obtained from the sites classified as non-resonant.

The data from the GNS/MRD study were re-analysed using the SRD software, and four soil models were adopted which fitted the observed site responses and known geological conditions. The four corresponding zones developed by the current study are broadly comparable with the GNS/MRD zones in surface-layer thickness and distribution.

The characteristic resonant frequencies of the spectral models and corresponding zone names are shown in Table 3, and the critical parameters defining the spectral models are shown in Table 4.

Table 3: Map Zones vs. Site-Response Models, Suva

Map Zones - Suva	Characteristic Resonant Frequency (Hz)	Applicable Models
A	1.0	Suva a
B	2.7	Suva b
C	5.2	Suva c
D	No Resonance	Suva d

Table 4: Definition of Site-Response Models, Suva

Model	Layer	Thickness (m)	Shear Velocity (m/s)	Density (g/cm ³)	Geotechnical Description
Suva a	1	40	140	1.45	weak organic silt
	2	Half-space	350	1.80	Suva Marl basement
Suva b	1	15	140	1.45	weak organic silt
	2	Half-space	350	1.80	Suva Marl basement
Suva c	1	8	140	1.45	weak organic silt
	2	Half-space	350	1.80	Suva Marl basement
Suva d	1	3	140	1.45	colluvium /fill
	2	Half-space	350	1.80	Suva Marl basement

A diagrammatic, generalised cross-section of subsurface conditions and their relationship to the adopted subsurface models is shown in Figure 11.

The spectral models are compared in Figure 12a, and the acceleration-response functions for each zone are shown in Figure 12b.

The GNS report (Hull et al. 1997) identified four major limitations in their study of Suva. The first was the universal one of sampling. The spectral ratio is only known at discrete locations, and it is possible that unsampled areas might have high amplifications.

The second limitation identified by Hull et al. was the small-strain nature of the microtremors measured. The stress-strain character of soils is non-linear, so that during strong shaking both the amplification and the resonant frequency will fall. The strength of shaking at which non-linear effects become important depends upon the soil material, and is generally higher for more plastic materials. In the case of the Suva city area, soil plasticity is well documented, but the level at which non-linear effects become important here remains an area for further research.

Researchers from GNS suggested that the thickness of fine-grained sediment might not be a significant control on whether a site in the Suva area will show resonance (as determined by microtremor analysis) in earthquake shaking. They attributed possible causes for their results, including the following:

1. Borehole logs identify the presence of fine-grained material, but do not characterise its state of consolidation (and hence do not indicate its stiffness)
2. There is not a sharp shear-wave velocity contrast between the bedrock marl and the overlying unconsolidated thick sediments
3. There may be significant relief on the bedrock/sediment contacts that prevents trapping of seismic waves within low-velocity layers to cause resonance
4. Shear-wave velocity slowly increases with depth of Holocene-age sediment overlying Suva Marl
5. Resonant sites occur only where some particular layer, such as organic-rich sediment or other geological character, is present, and this character only occurs where total sediment thickness is in excess of 10 m

Earlier research has been undertaken on the geotechnical properties of the organic silts of Suva (Shorten 1993a, b; 1995). These works indicate that the above assumptions 1 and 2 (and to a large extent 4) of Hull et al. are incorrect, and that more emphasis must be given to the other assumptions, 3 and 5. Contrary to the assertions of the GNS report, the divisions in borehole logs were made specifically on engineering properties and not on grain size alone, and there is quite a definite (though not large) velocity contrast between the organic silt and the weak rocks of the Suva Marl. There may be, however, a velocity gradation at the very base of the Holocene organic silt through into underlying late Pleistocene channel-fill sands and peats.

The GNS/MRD study found that the amount of information available on the thickness of sediments in the study area was limited outside the downtown Suva area. Here, site classification was based only on surficial geological and topographic information, and sediment thickness was based on similar, though better-controlled, data transposed from the Suva city area. Notwithstanding, even where they acknowledged that good subsurface depth-control was available, the GNS/MRD study concluded that there was still not a good correlation between sediment more than 10 m thick and site resonance determined from microtremor measurements. Hull et al. suggested, correctly, that down-hole information on shear-wave velocity for resonant and non-resonant sites is required to understand better the likely cases of resonance from microtremor analysis.

This study of 56 sites by the GNS/MRD team within the greater Suva district showed only a moderate correlation between estimates of likely earthquake shaking response based on surficial and limited subsurface geology and those based upon the Nakamura method of microtremor response.

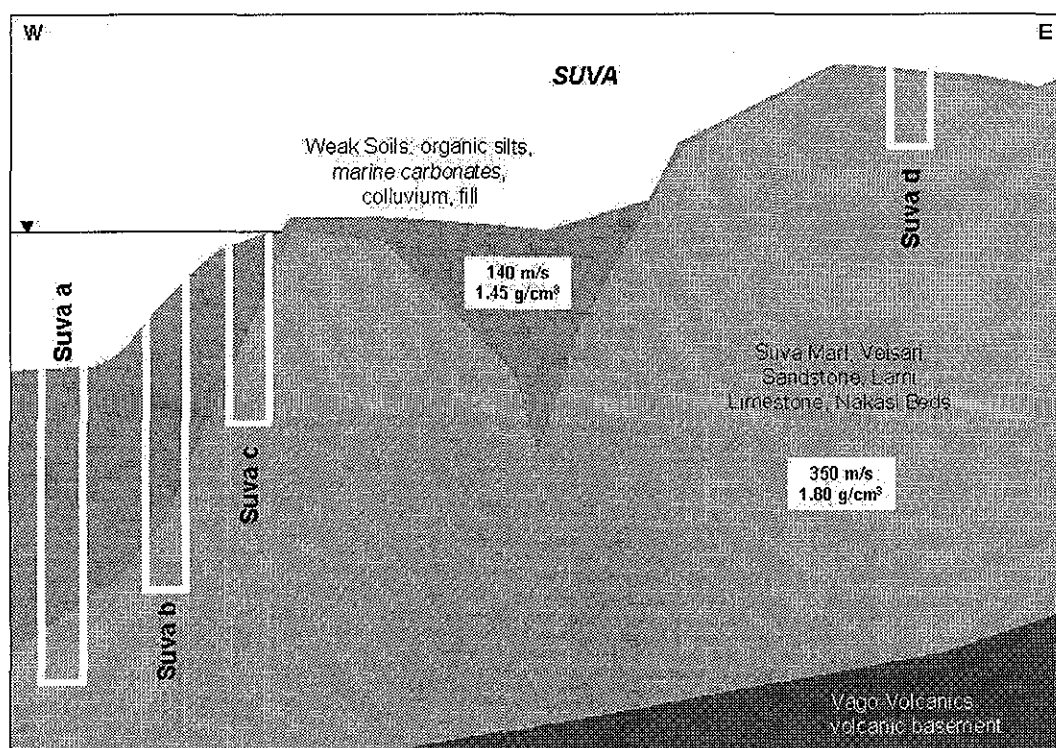
The GNS/MRD team concluded that site resonance does not occur on Suva Marl rock type or other bedrock types in the greater Suva district. Nor does it occur where the sediment thickness is known or estimated to be less than 10 m. Their interpretation of the results further suggested that depth of sediment, even where it exceeds 10 m, does not seem to be a significant control on site resonance as measured by microtremor analysis. They observed site resonance at only about 30% of the sites measured in areas where Holocene sediments exceed about 10 m (Class A and Class B). In their opinion, microtremor analysis did not reveal a higher proportion of resonant sites where unconsolidated sediment exceeds a depth of 20 m.

The GNS/MRD report went on to state that, as assessed by Nakamura's microtremor spectral-ratio technique, soft-soil amplification of earthquake motion in Suva is important in a few easily identified locations, where shaking is expected to be amplified during both low-intensity and moderate-intensity earthquakes. In the less likely event of strong shaking, the non-linear effects of liquefaction and of ground failure will limit such amplifications.

However, some of these findings of the GNS/MRD study are at odds with the conclusions of the current study. We suggest that there is resonance in all Classes A, B and C, albeit accompanied by a continuous shift in the frequency of resonance with increasing thickness, and that there is a definite increase in amplification with thickness of the surface layer. The discrepancy in the findings might be partly due to the fact that the GNS/MRD team did not have access to accurate borehole information with which to compare the microtremor results. The other confusing factor, as they suggest, could be the significant relief known to occur on the sediment-rock interface.

The factors that control site resonance in the greater Suva district are not well understood. Better control of the subsurface geotechnical parameters, and particularly shear-wave velocity, is required to understand better the earthquake shaking response in Suva. The GNS/MRD report recommended that future seismic-hazard assessment work in the Suva region should be carried out at sites where preliminary mapping shows possible site-related amplification, and where there is a large investment in structures which would be damaged in the event of amplified shaking. The greatest deficiency in the Suva region data from a seismic microzoning point of view is the lack of either shear-modulus data, or shear-wave velocity data, as functions of depth. The way in which shear-wave velocity changes with depth controls the amplification of earthquake shaking, and it would be valuable to know the shear-wave velocity at some major control points. Such a characterisation of shear-wave velocities could be achieved by applying a Seismic Cone Penetration Test (SCPT) at sites where significant amplification is expected.

Figure 11: Diagrammatic Summary Cross-Section, Suva



5.7 S_vE Results and Interpretation, Suva

Compared with the other three cities in the study, Suva is relatively distant from most of the large earthquake-generating zones. Consequently, as compared to the other investigated cities in the South

Pacific, the expected free-surface accelerations and the acceleration-response values are low. Assuming that the peak ground acceleration (PGA) corresponds to the spectral acceleration level at high frequencies (low periods), we obtain $PGA = 0.35 \text{ g}$ for a 10% probability of exceedance in 50 years, which is comparable to the findings from an independent study by Jones (1998).

The city is divided into four zones, each of them characterised by the acceleration-response function shown in Figure 12b and Figure 13. The mapped distribution of seismic microzones in Suva is shown in Figure 13.

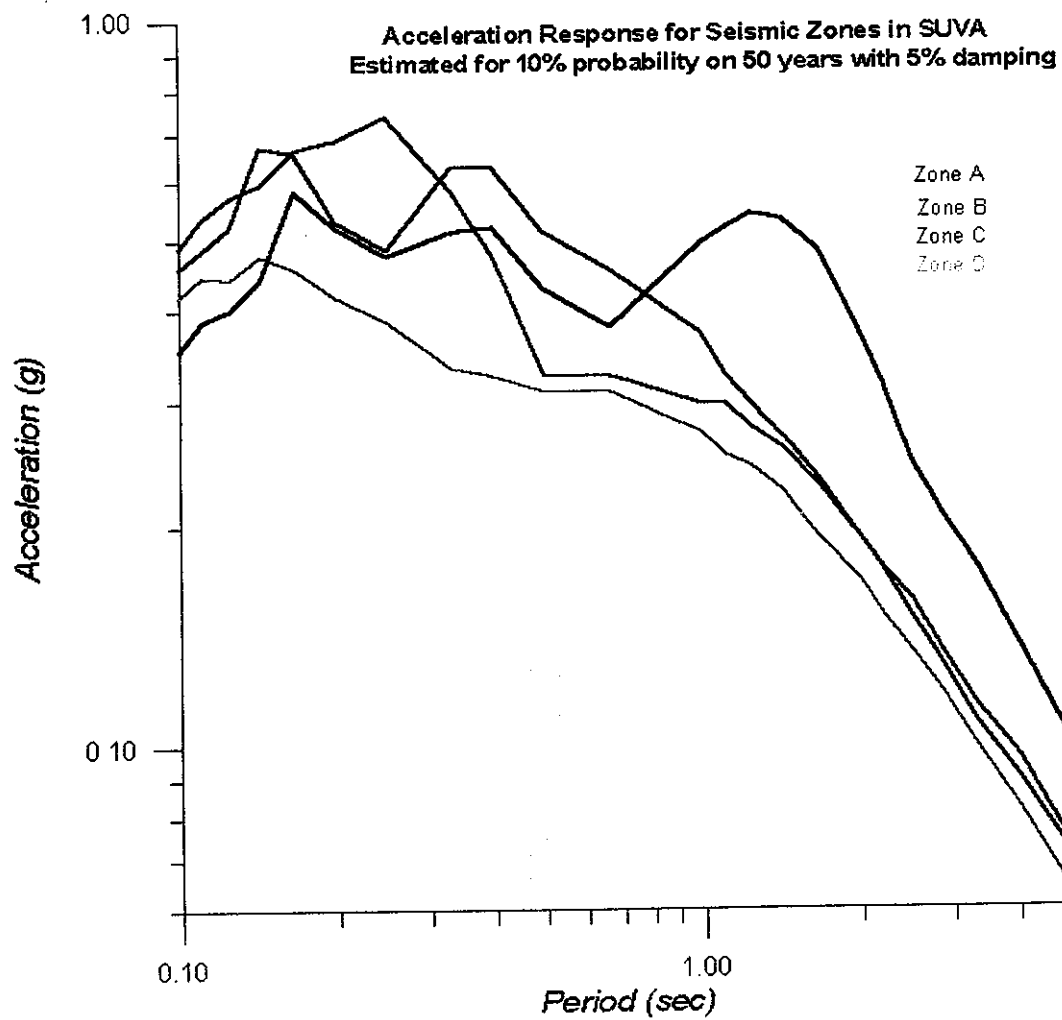
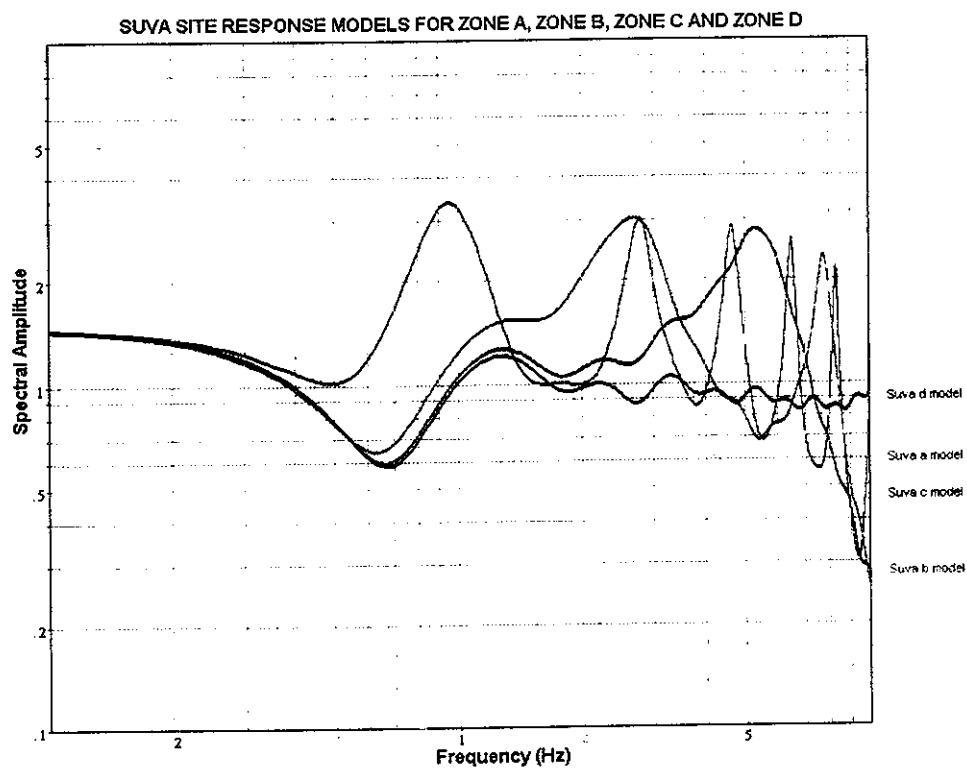
Using these functions, we suggest that Zone D represents an area with no site effects. The accelerations in the period range 0.2-0.5 seconds for Zones B and C may reach 0.7 g. This finding suggests that small buildings (1-4 floors) in these areas, as compared to other parts of the city, are vulnerable to earthquake ground shaking. Likewise, tall buildings (more than 8 floors) may be at highest risk if located in Zone A where the period of ground resonance was measured at around 1.0 seconds.

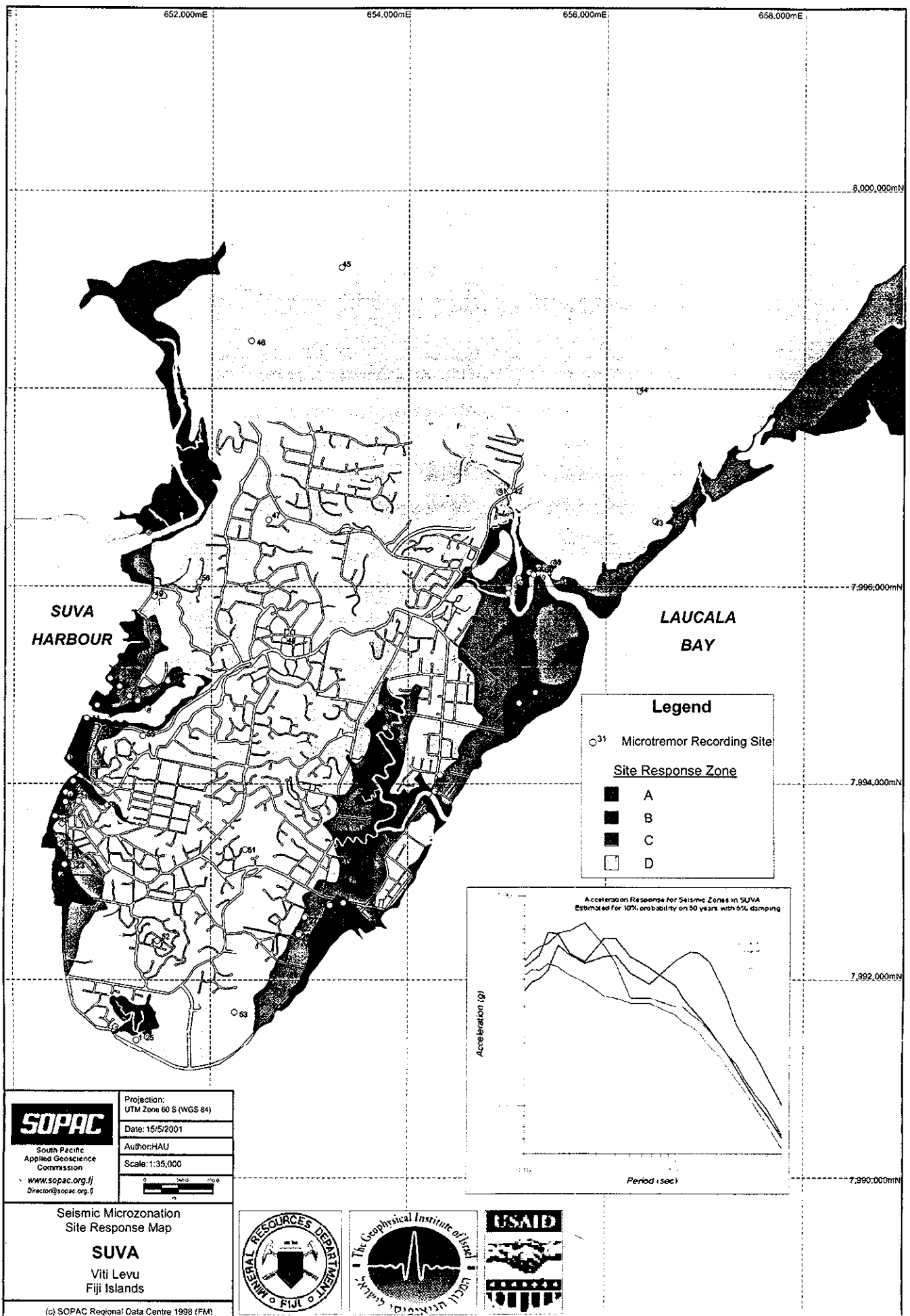
(over page: p.48)

Figure 12: Site-Response Models and Acceleration-Response Functions, Suva

(over page: p.49)

Figure 13: Seismic Microzonation Site-Response Map, Suva





6 Seismic Microzonation of Port Vila, Efate, Vanuatu

6.1 Introduction, Port Vila

Task leader: Marc Regnier (IRD (ORSTOM), Port Vila)

Collaborators: Morris Stephen (Geology, Mines and Water Resources, Vanuatu), Christopher Ioan (Geology, Mines and Water Resources, Vanuatu)

Port Vila, with a population of 50,000, is the capital and a major centre of tourism and commerce for the whole Vanuatu group. It houses a number of foreign embassies and regional organisations.

The city is often affected by discernible tremors and has suffered recorded damage from earthquakes in 1880 and 1974.

Although there is much less land reclamation over soft harbour muds than in Suva Harbour, the presence of suspected modern fault activity in the northern lobe of the harbour gives cause for concern. Palaeo-sinkholes in the limestone basement rock, which onshore are filled with fine-grained colluvial soils and, in places, anthropogenic fill, appear to significantly amplify earthquake effects. The area of most concern, however, is the alluvial plain lying to the north of the city proper and fringing Mele Bay, which incorporates the airport and expanding industrial and urban areas. Amplification of low-frequency earthquake shocks has been observed here in practice and is very likely to occur in future. In one case, it was reported that racks of glass plate stacked in the yard of a glass manufacturer on the Mele Road were broken, although affected differentially depending on the orientation of the racks. The felt intensity of the same event in the main city area was negligible.

Site-response measurements in Port Vila were carried out jointly by the Department of Geology, Mines and Water Resources and an IRD (ORSTOM) seismology group which has been attached to the Department for a significant period of time but has, only recently, relocated to IRD (ORSTOM) headquarters in Noumea. The IRD (ORSTOM) representative and task leader for this project, Dr Marc Regnier, also provided assistance to the Nuku'alofa program of microseismic zonation.

Details in digital format of geographical information for Port Vila including geological boundaries, borehole locations and logs, seismic microzone boundaries and investigation sites, road and cadastral plans, digital terrain model and orthophotograph can be found in Biukoto et al. (2001b).

6.2 Tectonic Setting, Port Vila

Seismology in Port Vila is dominated by shallow events related to subduction at the New Hebrides Trench, immediately west of the island Efate. Even though Port Vila does not lie in an identified major seismic zone, strong earthquakes have to be expected due to the city's geographical location close to this major plate boundary. Data from the permanent IRD (ORSTOM) network show that the zone including the western side of Efate island, where Port Vila is located, has a complex pattern of seismicity, and numerous faults and active clusters can be recognised.

Diagrams of cumulative co-seismic slip versus time give a maximum-magnitude earthquake of 8.6 for the New Hebrides subduction zone. A mean return period of 480 years for this maximum magnitude has been estimated from a Gutenberg-Richter frequency-magnitude diagram (R. Pillet, pers. comm.). Along the New Hebrides island arc, the average recurrence interval for a magnitude 8 earthquake is about 10 years.

The coastline of Efate to the north of Port Vila is marked by a series of uplifted terraces. A summary of the work investigating the ages of the terraces, assumed to be a result of co-seismic uplift, is provided in Howorth (1985). These terraces are not apparent on the shores of Port Vila harbour. However, it appears from recent investigations of submarine morphology by SOPAC that the harbour is formed in a down-dropped structural block and there is good evidence of drowned terraces.

Based on the record of Holocene uplift in southwest Efate, Howorth produced a provisional frequency-magnitude plot for seismicity in the Port Vila area which indicates that a magnitude 7 earthquake is likely every 10 years, magnitude 7.5 every 30 years and magnitude 7.8 every 100 years. Howorth assumed co-seismic uplift (accompanying magnitude > 7 earthquakes) for a series of at least seven distinct terraces rising up to 13 m and dating back to 6,000 years BP. He deduced average uplift rates of around 1.5 mm per year.

Howorth (1983) described the formation of Port Vila Harbour, Mele Bay and the Erakor Lagoons as being the result of gross subsidence and uneven displacement on a mega-landslide (translational block-sliding

as part of tectonic erosion on the island margin facing the trench) affecting the entire southwest corner of Efate. He postulated a shallow slip surface at the base of the limestone carapace, but the failure surface probably extends into the volcanic superstructure itself.

Inspection of the fault systems forming the harbour, and the results of a seismic survey carried out by a SOPAC team in 1996, provided evidence that the major fault surfaces are discontinuous and scalloped. This supports Howorth's proposal that the harbours, lagoons, islands and plateaux around Port Vila are part of a series of tilted and differentially submerged, jostled blocks of an island-scale mega-landslide.

An east-west fault forming the southern edge of the northern lobe of Port Vila harbour, immediately north of Iririki island, appears to have experienced very recent vertical movement. Here, the modern sediment surface of the northern harbour lobe has been tilted southward at around 5° in strong contrast to the near-horizontal sediment surfaces in the other two lobes of the harbour.

6.3 Regional and Local Geology, Port Vila

The geology of Efate island and, in particular, of the city Port Vila is fairly uncomplicated. Efate is a large Plio-Quaternary volcano-sedimentary island. It is made of prevailingly volcanic eruptive rocks and ash deposits, the Efate Pumice Formation (1.6 Ma) with the younger Basalt Volcanoes Formation (0.7 Ma) cropping out on the north side. Its formation has also been controlled by episodes of significant tectonic uplift and, as a result, it is fringed by large Quaternary limestone and sedimentary terraces uplifted to around 600 m above sea level.

The distribution of lithologies in Port Vila, together with the locations of boreholes, is shown in Figure 14. The city itself is located largely on a formation of raised limestone terraces up to a height of 120 m, referred to in this report as the Port Vila limestone. The volcanic substratum, the Rentabau tuffs (a sub-unit of the Efate Pumice Formation), generally does not crop out in the Port Vila area but lies at some depth beneath the limestone cover. Howorth (1983) recorded a pumice formation of the Rentabau tuffs exposed in the cliff of an uplifted block above the road to the main wharf. Yet another exposure of tuff occurs in a cliff face midway between the central business district and Erakor Lagoon.

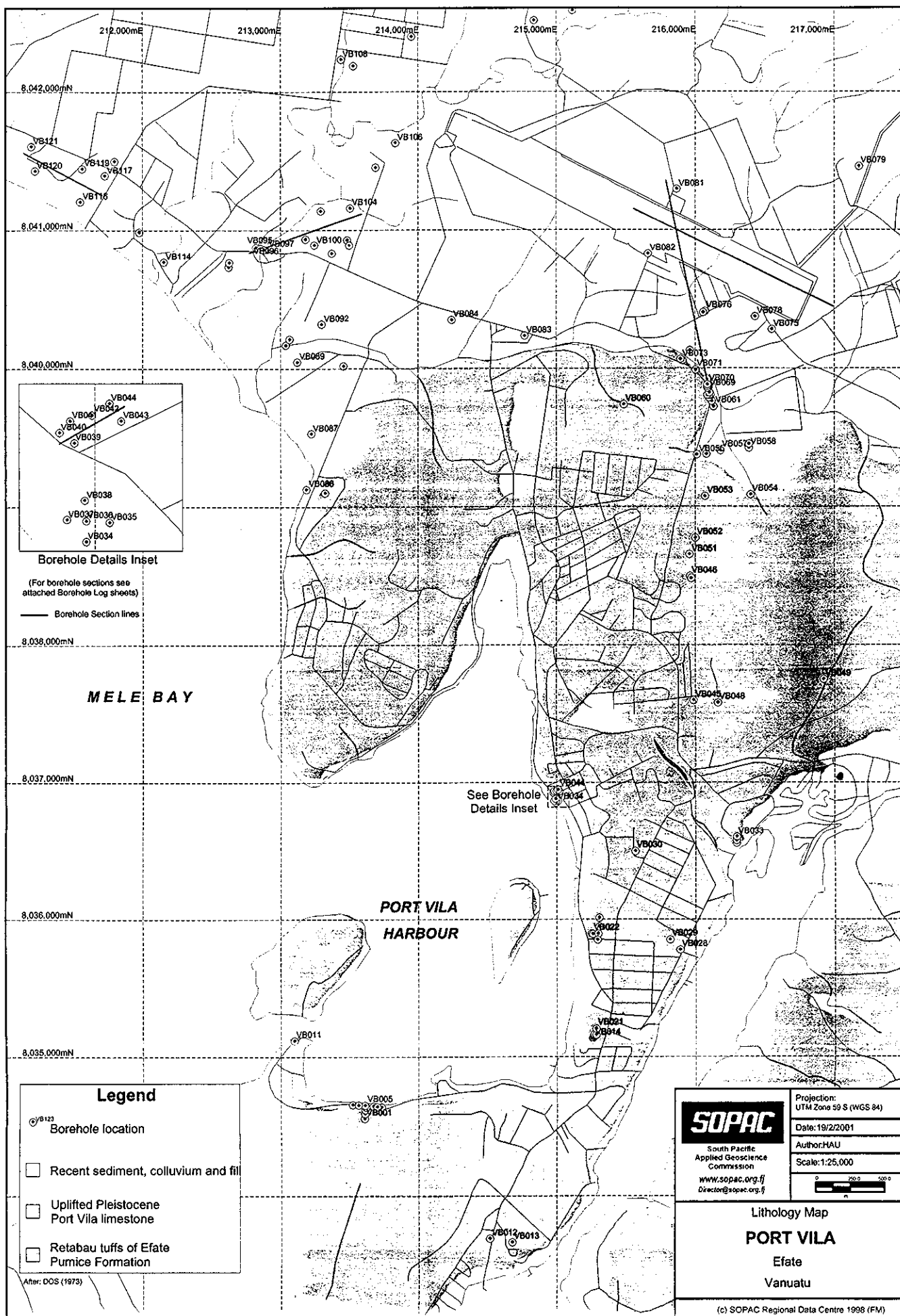
Faulting in two roughly conjugate directions has divided the physiography of the city area into a checker-board scheme of horsts and grabens. The numerous faults have facilitated differential uplift and subsidence of blocks. Due to this uneven topography soil thickness is very variable within the Port Vila area but, on average, is only several metres thick. Only at a very few places can significant thicknesses of soil be observed. Some of these are man-made fills. Borehole data commonly show a layer, 20 to 30 m thick, of variably weathered limestone mixed with sand and gravel deposits below the thin soil layer.

Lying to the north of Port Vila, and bordered to the west by Mele Bay, is a large graben filled with a significant thickness (at least several tens of meters) of light volcanic sediments. At Tagabe, on the southern edge of the graben, the log of a borehole drilled in 1979 describes clayey and sandy sediments down to at least 30 m depth, and identified the groundwater table at 6 m depth. The graben, which is located very close to the city, has the potential for future development, especially around the Bauerfield Airport, where it forms a distinct geological and pedological unit (Quantin 1980).

Selected borehole sections shown in Figures 15-19 serve to illustrate the subsurface distribution of engineering soil and rock types classified according to the Unified Soil Classification System (USBR 1973). The borehole logs are accompanied by logs of soil strength, where these are available, based mainly on Standard Penetration Test N-values. Details of the legend for the soil-type logs and instructions on the interpretation of the strength logs are given in Appendices 1-3.

(over page: p.52)

Figure 14: Lithology Map (including Borehole Positions), Port Vila



(over page: p.54)

Figure 15: Borehole Logs VB 040 to VB 043, Port Vila

(over page: p.55)

Figure 16: Borehole Logs VB 069 to VB 081, Port Vila

(over page: p.56)

Figure 17: Borehole Logs VB 081 to VB 075, Port Vila

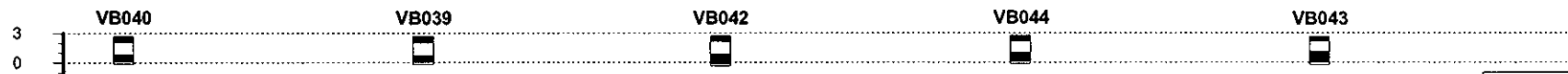
(over page: p.57)

Figure 18: Borehole Logs VB 095 to VB 104, Port Vila

(over page: p.58)

Figure 19: Borehole Logs VB 121 to VB 117, Port Vila

Borehole Logs Port Vila Efate, Vanuatu

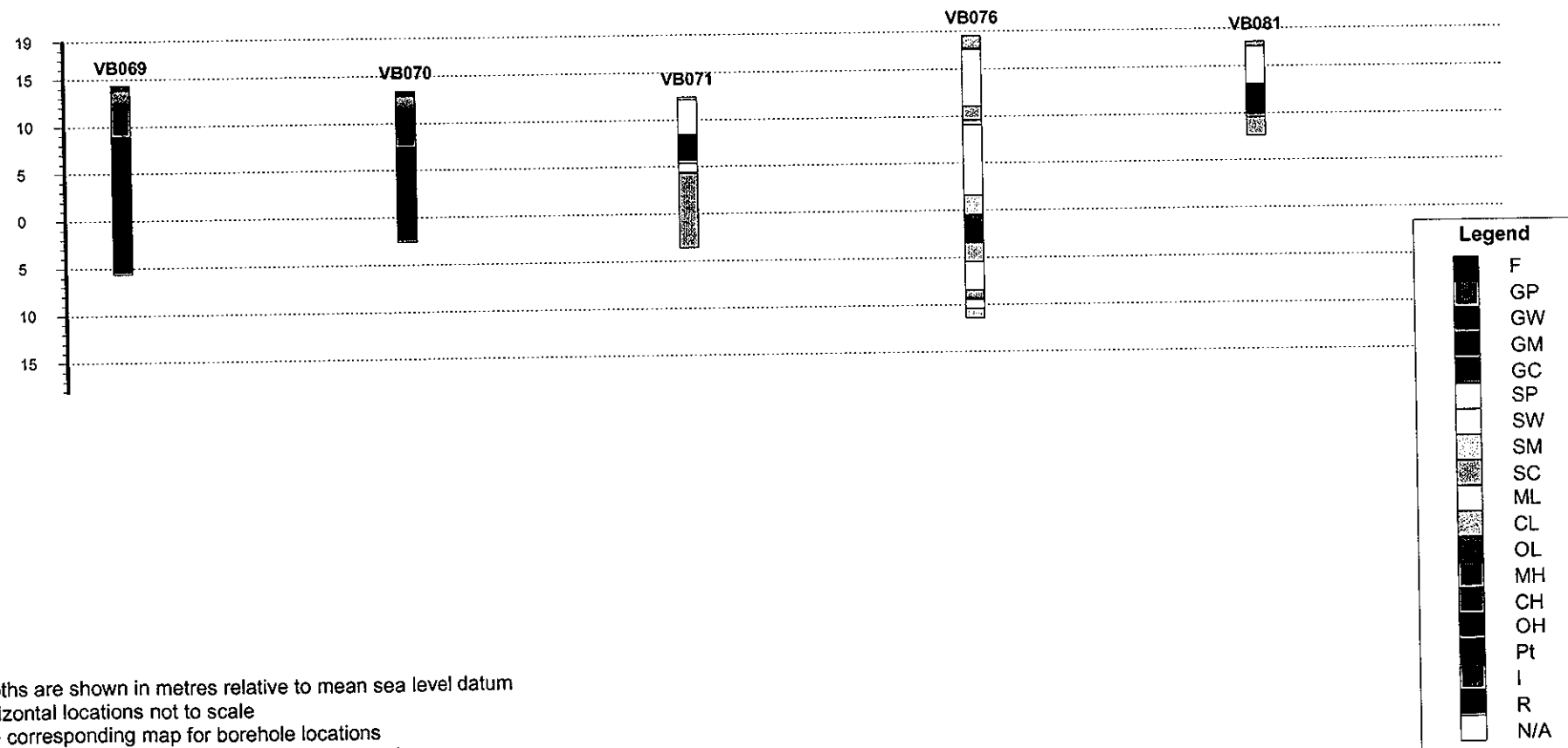


Legend	
	F
	GP
	GW
	GM
	GC
	SP
	SW
	SM
	SC
	ML
	CL
	OL
	MH
	CH
	OH
	Pt
	I
	R
	N/A

Notes:

1. Depths are shown in metres relative to mean sea level datum
2. Horizontal locations not to scale
3. See corresponding map for borehole locations
4. See appendices for explanation of legend and diagrams

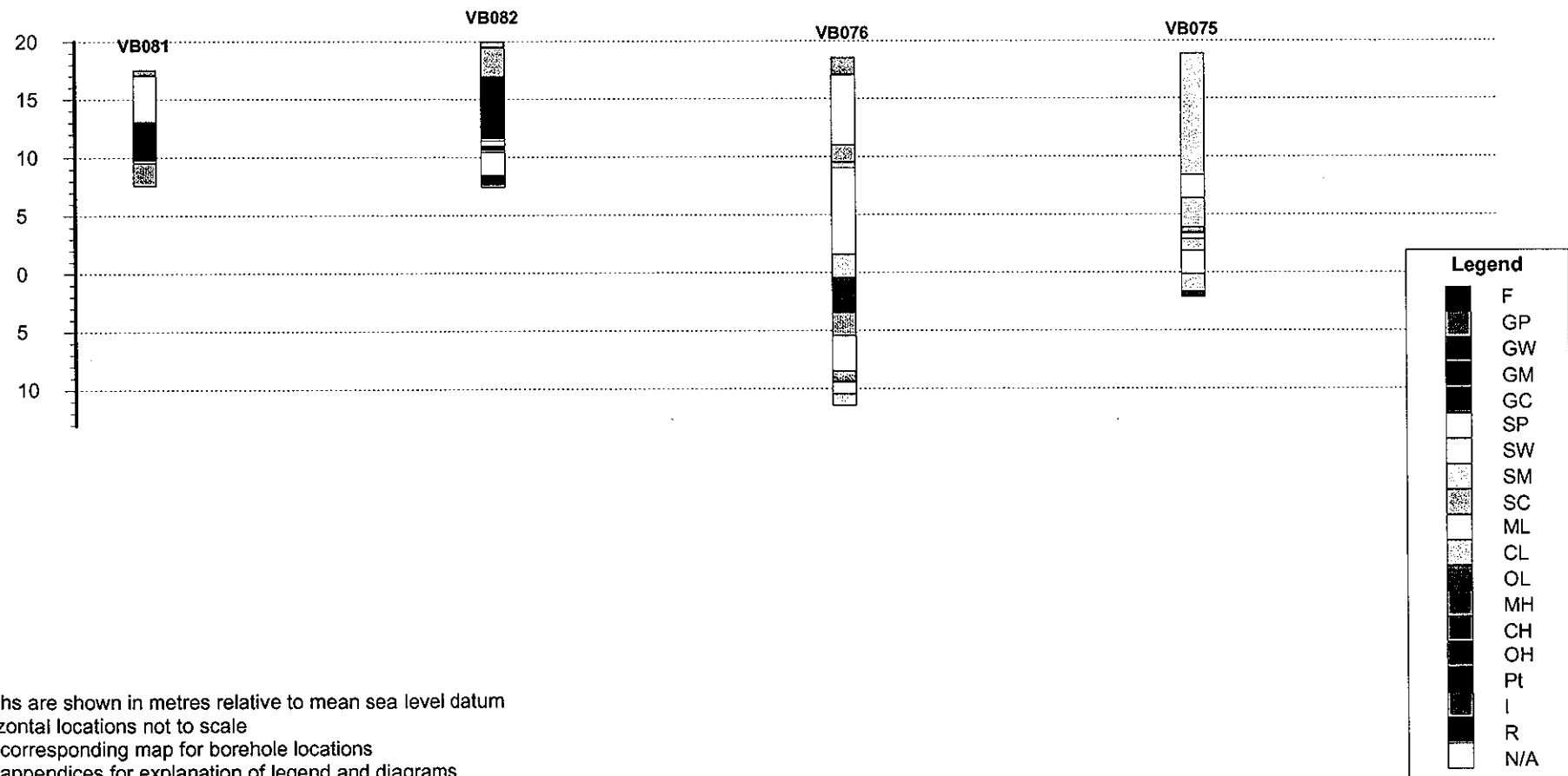
Borehole Logs Port Vila Efate, Vanuatu



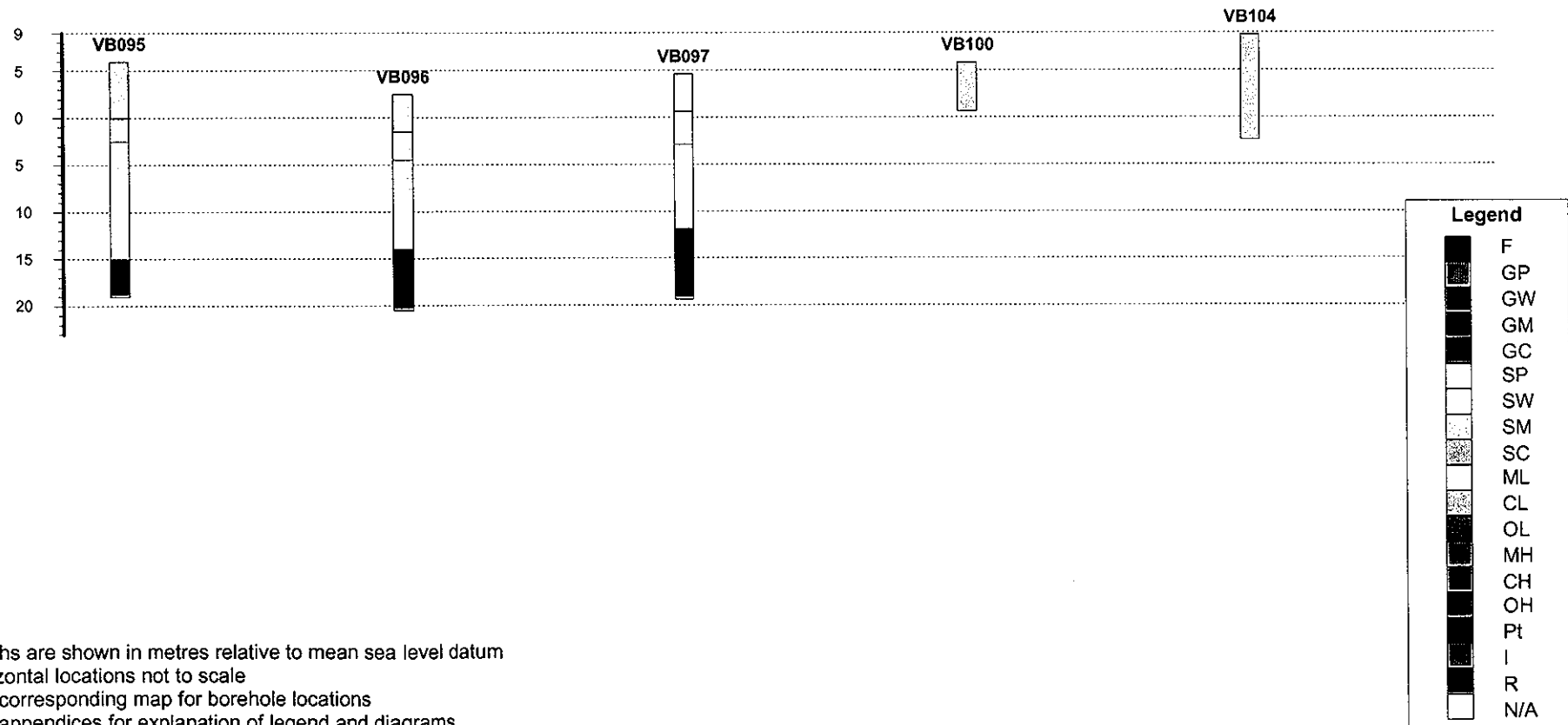
Notes:

1. Depths are shown in metres relative to mean sea level datum
2. Horizontal locations not to scale
3. See corresponding map for borehole locations
4. See appendices for explanation of legend and diagrams

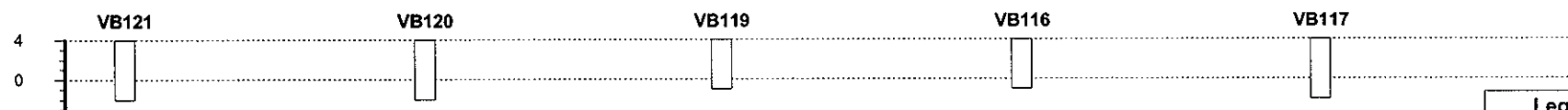
Borehole Logs Port Vila Efate, Vanuatu



Borehole Logs Port Vila Efate, Vanuatu



Borehole Logs Port Vila Efate, Vanuatu



Legend	
	F
	GP
	GW
	GM
	GC
	SP
	SW
	SM
	SC
	ML
	CL
	OL
	MH
	CH
	OH
	Pt
	I
	R
	N/A

Notes:

1. Depths are shown in metres relative to mean sea level datum
2. Horizontal locations not to scale
3. See corresponding map for borehole locations
4. See appendices for explanation of legend and diagrams

6.4 History of Damaging Earthquakes, Port Vila

The epicentres of large shallow earthquakes (magnitude > 5, focal depth < 70 km) for the period 1973-1998, as well as earlier historical events, within an arbitrary 250 km radius of Port Vila are shown in Figure 20 and catalogued in Table 5.

Port Vila has been affected by a number of major earthquakes (Wong & Greene 1988). The great majority of earthquakes ever recorded in Vanuatu have been of relatively small magnitude and only a few have caused any damage. The historical account, at least, shows that there has never been a catastrophic event, although in some cases material damage has been major. Louat & Baldassari (1989) reported few cases of damage to buildings over a 100-year period.

1880: The event of 1880 generated a seiche in the harbour that inundated extensive areas of the harbour islands and stranded large numbers of fish in the vegetated areas well above sea level.

1927: Eyewitness accounts from Port Vila suggest that the largest tsunami experienced there was as a result of the 24th January 1927 event of Ms 7.1 centred on south Malekula. The tsunami entered the harbour and apparently caused seiching and flooding of the shoreline up to several metres above the normal tide levels. This event is not registered in Table 5 or shown on Figure 20, as its origin and magnitude are uncertain.

1950: An event with a magnitude near 7 occurred about 100 km southwest of Efate in 1950.

Between 1961 and 1978, a series of large earthquakes (Ms > 5.5) recorded in the vicinity of Efate ranged up to around magnitude 6.0 with an isolated example of Ms 6.5.

1961: A small tsunami was recorded in Port Vila harbour after the 23rd July 1961 (Ms 6.0) event 100 km south of Port Vila.

1965: On 12th August 1965, an Ms 6.3 earthquake in the north of the group was felt with intensity MM 7 in Efate.

1974: The 30th June 1974 (Ms 5.7) event about 25 km south of Port Vila resulted in cracks in newly constructed multi-storey buildings and rock-falls from cliffs in the city.

The ORSTOM-Cornell network began operating in 1978, and Prevot & Chatelain (1984) reported that *only four earthquakes of large magnitude had been recorded in the archipelago since the inception of the network. The largest was the Mere Lava event near Santo.*

1979: The remaining three occurred to the west of Efate. The first on 17th August 1979 (Ms 6.1) occurred 35 km off Efate. It was followed nine days later by a second shock (Ms 6.0), some 20 km to the north of the first.

1980: The largest, 12th May 1980 (Ms 6.1), was the Mere Lava event near Santo that caused relatively major damage but no casualties.

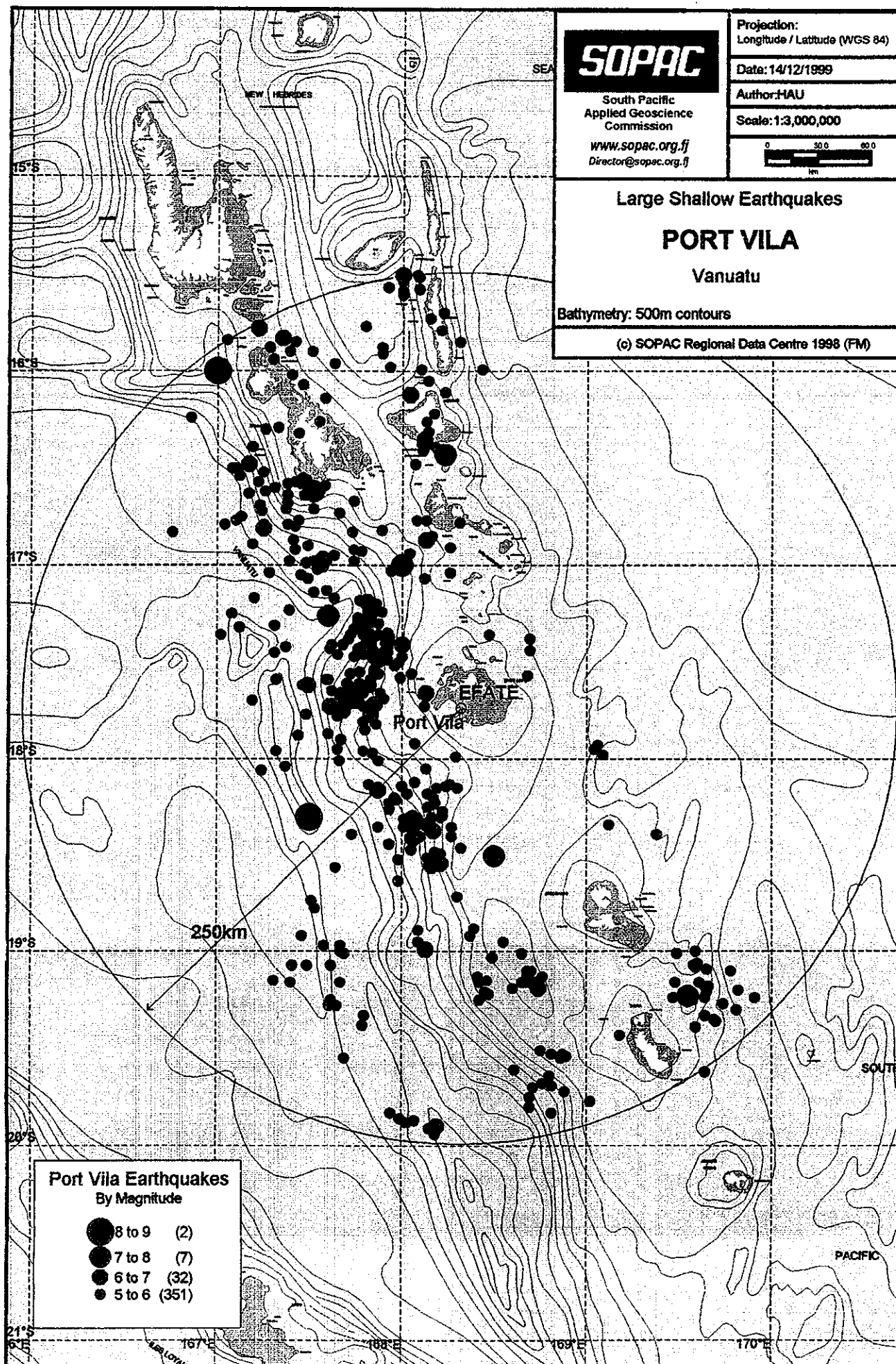
1981: The earthquake of 15th July 1981 (Ms 7.0) occurred approximately 85 km northwest of Efate and was reported to have caused damage in Port Vila. This earthquake was notable for having occurred in an area that had not experienced any large earthquakes in the preceding 75 years.

According to Prevot & Chatelain (1984), each of the earthquakes was preceded by swarms around the zone where the aftershocks occurred, in areas of characteristically low seismicity, and even to the rear of the arc, east of Efate. The swarms occurred up to eight hours before each main shock, and the aftershock zone expanded quickly over the following days to cover areas 5 to 10 times greater than normal for earthquakes of such magnitudes. Even though an earthquake of 7th July 1981 was centred some distance offshore of Efate, the region of aftershocks spread onto the island itself.

Prevot & Chatelain estimated that the greatest possible magnitude for the archipelago is 7.6 on the basis of calculated energy release in earthquakes since the beginning of the century. Based on this, they estimated that the maximum likely predicted intensity for Efate (and the Port Vila region in particular) would be MM 8, and up to MM 9, allowing for deleterious ground conditions such as occur in the Mele area. They did not, however, discount the possibility of intensities as high as MM 12 in the archipelago. Notwithstanding, Port Vila appears on the basis of their estimates to have a significantly lower return period for high-intensity events than the more active region around Santo.

(over page: p.60)

Figure 20: Large Shallow Earthquakes around Port Vila



(over page: p.62-68)

Table 5: Catalogue of Large Shallow Earthquakes, Port Vila

Circle Search: Earthquakes for Port Vila	
Circle Centre Point:	Latitude: 17.7432 S Longitude: 168.3142 E
Radius:	250 km
Magnitude Range:	5.0-9.0
Depth Range:	0-70 km

Site-Specific Earthquake Hazard Determinations in Capital Cities in the South Pacific

Date	Origin Time (UTC)	Latitude	Longitude	Depth (km)	Magnitude	Solution	Recorder	Epicentral Distance from Port Vila (km)
9-Aug-01		-16.00	167.00		8.4	Ms		239
13-May-03	063400.00	-17.00	168.00	60	7.9	Ms		88
22-Mar-25	084100.00	-18.50	168.50	50	7.6	Ms		85
2-Dec-50	195100.00	-18.30	167.50	60	8.1	Ms		105
24-Feb-73	073827.00	-19.19	168.74	59	6.0	mb	GS	166
8-Apr-73	124102.00	-15.78	167.22	35	6.4	Ms	GS	246
21-Apr-73	203035.70	-15.88	167.28	33	5.3	mb	GS	233
5-Jun-73	020712.50	-17.30	167.80	12	5.2	mb	GS	73
5-Jun-73	031225.80	-17.19	167.81	24	6.5	UK	PAS	80
5-Jun-73	090432.90	-17.34	167.79	21	5.0	mb	GS	71
8-Jun-73	010111.40	-17.47	167.74	21	5.9	UK	BRK	68
9-Jun-73	042702.80	-17.46	167.65	27	5.0	mb	GS	76
13-Jun-73	094825.20	-19.18	169.66	24	5.7	mb	GS	213
19-Jul-73	162531.20	-15.79	168.21	28	5.5	mb	GS	215
27-Jul-73	160832.60	-17.22	167.85	15	5.1	mb	GS	75
9-Aug-73	193329.80	-19.01	168.65	45	5.0	mb	GS	144
27-Aug-73	134831.60	-15.99	168.10	11	5.7	mb	GS	195
2-Sep-73	160633.50	-19.25	167.62	33	5.2	mb	GS	182
27-Oct-73	075338.20	-17.98	169.09	29	5.3	mb	GS	86
10-Nov-73	092116.50	-19.07	167.41	12	5.4	mb	GS	174
4-Dec-73	153039.00	-16.50	167.10	9	5.3	mb	GS	188
15-Dec-73	225702.90	-16.77	168.13	7	5.6	mb	GS	109
16-Jan-74	104510.90	-17.45	167.89	30	5.3	mb	GS	54
28-Feb-74	125929.70	-19.20	169.82	14	5.5	mb	GS	226
14-Mar-74	213523.00	-19.16	167.67	33	5.2	mb	GS	170
5-May-74	081750.30	-17.45	167.91	33	5.6	Ms	GS	53
26-May-74	013211.20	-17.70	167.75	13	6.1	UK	PAS	59
26-May-74	021526.40	-17.77	167.48	31	5.2	mb	GS	88
26-May-74	055240.20	-17.32	167.12	53	5.5	mb	GS	134
26-May-74	081450.00	-17.72	167.68	8	5.1	mb	GS	67
26-May-74	100242.10	-17.73	167.79	27	5.0	mb	GS	55
26-May-74	152424.00	-17.62	167.49	7	6.2	mb	GS	88
28-Jun-74	180635.20	-17.97	167.84	26	5.1	mb	GS	56
30-Jun-74	083346.50	-17.99	168.29	61	5.7	mb	GS	27
30-Jun-74	125001.60	-19.16	168.67	32	5.7	mb	GS	161
5-Aug-74	141301.30	-16.59	167.58	42	5.1	mb	GS	149
19-Nov-74	065029.00	-16.07	167.46	42	5.2	mb	GS	205
4-Jan-75	020039.40	-17.07	168.12	62	5.0	mb	GS	76
5-Mar-75	102709.80	-19.53	168.87	55	5.6	mb	GS	205
25-Mar-75	210528.90	-16.55	167.46	14	5.1	mb	GS	160
10-Jun-75	071911.50	-17.36	167.02	33	5.1	mb	GS	143
1-Jan-76	184338.20	-16.79	167.25	25	5.5	Ms	GS	154
25-May-76	003908.40	-19.77	169.02	70	5.1	mb	GS	235
25-May-76	180117.90	-17.36	167.79	20	5.5	mb	GS	70
6-Jun-76	205345.50	-16.29	167.33	18	5.1	mb	GS	191
8-Jun-76	092217.60	-16.30	167.26	13	5.6	Ms	GS	194
5-Jul-76	024252.90	-16.39	167.19	22	5.4	mb	GS	191
4-Sep-76	161554.70	-19.21	169.65	38	5.0	mb	GS	214
9-Nov-76	012536.70	-18.13	168.26	32	5.0	mb	GS	42
30-Nov-76	075617.20	-19.19	168.60	53	5.0	mb	GS	162
20-Dec-76	100419.90	-17.41	167.83	33	5.1	mb	GS	62
24-Jan-77	144117.60	-17.35	167.92	38	5.0	mb	GS	59
27-Jan-77	045053.30	-17.36	167.87	25	5.0	mb	GS	63
28-Jan-77	180051.80	-17.44	168.69	14	5.6	Ms	GS	52
28-Jan-77	235451.20	-17.38	168.69	16	5.0	mb	GS	56
9-Apr-77	211614.60	-19.08	169.59	25	5.5	UK	BRK	199
9-Apr-77	215108.10	-19.09	169.65	15	5.0	mb	GS	205
10-Apr-77	005416.50	-19.00	169.59	18	5.0	Ms	GS	193
11-Apr-77	052820.90	-19.25	169.56	39	5.0	mb	GS	212
16-May-77	111430.70	-17.42	167.92	30	5.3	Ms	GS	54
23-May-77	120909.20	-17.65	167.62	11	5.0	mb	GS	74

Date	Origin Time (UTC)	Latitude	Longitude	Depth (km)	Magnitude	Solution	Recorder	Epicentral Distance from Port Vila (km)
25-May-77	191853.80	-17.73	167.61	13	5.2	mb	GS	74
10-Jul-77	023714.60	-19.13	168.41	12	5.5	mb	GS	153
10-Jul-77	031108.10	-19.22	168.47	21	5.1	mb	GS	163
11-Jul-77	191051.20	-19.15	168.46	20	5.3	mb	GS	155
25-Jul-77	224104.50	-19.16	168.42	30	5.1	mb	GS	156
16-Aug-77	061516.70	-19.28	167.65	12	5.5	mb	GS	183
16-Aug-77	070301.30	-18.97	167.58	33	5.1	mb	GS	155
22-Sep-77	234144.40	-15.94	167.30	25	5.1	mb	GS	226
9-Nov-77	084439.70	-16.24	166.86	27	5.2	mb	GS	227
3-Dec-77	163526.40	-17.59	167.32	10	5.4	mb	GS	106
14-Feb-78	231648.00	-15.58	168.09	33	5.4	mb	GS	240
21-Mar-78	175307.90	-17.50	167.88	27	5.2	mb	GS	52
21-Mar-78	191405.90	-17.61	167.77	23	5.4	mb	GS	59
8-May-78	163538.00	-17.02	167.54	33	5.4	mb	GS	115
8-May-78	190539.40	-16.98	167.59	33	5.1	mb	GS	114
13-May-78	040726.20	-16.99	167.48	15	5.3	mb	GS	120
23-May-78	050347.70	-16.14	167.58	47	5.2	mb	GS	193
3-Jul-78	030533.10	-18.25	168.14	33	5.3	mb	GS	58
1-Sep-78	041642.10	-17.41	168.00	32	6.2	UK	BRK	49
8-Sep-78	060248.60	-15.96	167.63	39	5.3	mb	GS	209
9-Sep-78	122333.70	-17.49	167.92	27	5.0	mb	GS	50
28-Sep-78	132232.20	-17.46	167.91	33	5.0	mb	GS	52
22-Nov-78	050257.80	-19.61	168.61	33	5.1	mb	GS	208
29-Nov-78	111050.80	-15.51	168.08	33	5.5	mb	GS	248
6-Dec-78	095234.70	-19.33	167.80	22	5.3	mb	GS	183
23-Jan-79	214320.20	-17.50	167.86	33	5.3	mb	GS	55
27-Jan-79	001815.00	-18.54	168.21	25	6.3	Ms	GS	89
8-Apr-79	053839.30	-18.48	168.18	32	5.3	mb	GS	82
10-May-79	145725.80	-19.91	168.15	33	5.1	mb	GS	239
29-May-79	054600.10	-16.93	167.78	39	5.3	mb	GS	105
14-Jun-79	215716.30	-17.66	167.79	27	5.2	mb	GS	56
21-Jun-79	145741.80	-15.61	168.00	33	5.1	mb	GS	238
10-Jul-79	162508.00	-18.95	168.55	56	5.3	mb	GS	136
15-Jul-79	183947.00	-19.10	168.70	55	5.4	mb	GS	155
9-Aug-79	144418.20	-19.94	168.18	42	5.1	mb	GS	243
14-Aug-79	105703.80	-18.53	168.20	39	5.3	mb	GS	88
17-Aug-79	125907.40	-17.72	167.85	17	6.2	UK	BRK	49
17-Aug-79	141834.70	-17.72	167.71	23	5.4	mb	GS	63
17-Aug-79	151826.50	-17.65	167.75	39	5.7	Ms	GS	60
17-Aug-79	181716.30	-17.90	167.67	15	5.0	Ms	GS	70
26-Aug-79	114724.50	-17.67	167.68	10	6.2	UK	PAS	67
26-Aug-79	165612.20	-17.29	167.76	33	5.1	mb	GS	77
2-Sep-79	183747.20	-17.59	167.59	33	5.3	mb	GS	78
19-Sep-79	184420.00	-17.36	168.47	33	5.0	mb	GS	45
5-Dec-79	085354.80	-18.15	168.30	48	5.1	mb	GS	44
8-Dec-79	083133.70	-15.85	168.31	34	5.6	mb	GS	209
11-Dec-79	052819.50	-19.10	168.68	51	5.1	mb	GS	155
16-Dec-79	063347.70	-17.46	167.79	19	5.2	mb	GS	63
24-Dec-79	120549.30	-18.23	167.93	26	5.0	mb	GS	67
12-Jun-80	175553.50	-17.31	167.81	32	5.1	mb	GS	71
6-Jul-80	051843.20	-18.35	168.27	43	5.1	mb	GS	66
9-Oct-80	061137.00	-19.24	169.64	33	5.2	Ms	GS	217
9-Oct-80	104413.20	-19.18	169.64	33	5.2	Ms	GS	211
9-Oct-80	113256.40	-19.27	169.74	33	5.9	UK	BRK	226
3-Dec-80	203643.00	-17.95	169.04	33	5.2	mb	GS	79
5-Dec-80	173933.90	-16.50	167.08	35	5.0	mb	GS	189
15-Jul-81	075908.47	-17.26	167.60	30	7.1	Ms	BRK	92
15-Jul-81	090043.61	-17.07	167.49	35	5.2	mb	GS	115
15-Jul-81	100120.17	-16.92	167.42	33	5.0	mb	GS	131
15-Jul-81	165126.12	-17.62	167.46	38	5.0	mb	GS	91
15-Jul-81	221052.79	-17.56	167.72	32	5.2	mb	GS	66

Date	Origin Time (UTC)	Latitude	Longitude	Depth (km)	Magnitude	Solution	Recorder	Epicentral Distance from Port Vila (km)
15-Jul-81	232041.77	-17.59	167.60	31	5.5	Ms	GS	77
17-Jul-81	005734.69	-17.17	167.63	33	5.1	mb	GS	95
17-Jul-81	101915.44	-17.42	167.37	33	5.0	mb	GS	106
19-Jul-81	044259.36	-17.14	167.52	46	5.5	Ms	GS	106
19-Jul-81	153046.79	-17.25	167.08	27	5.1	mb	GS	141
29-Jul-81	050913.10	-16.75	167.13	33	5.0	mb	GS	166
31-Jul-81	000103.76	-16.87	167.41	33	5.0	mb	GS	136
9-Aug-81	202442.21	-17.04	167.28	33	5.0	mb	GS	134
18-Jan-82	042337.75	-17.29	167.81	44	6.0	Ms	BRK	73
27-Jan-82	010401.75	-17.47	168.00	33	5.1	mb	GS	44
26-Feb-82	211801.88	-18.01	167.87	44	5.0	mb	GS	55
27-Feb-82	052838.95	-16.11	168.23	25	5.0	mb	GS	180
1-May-82	174649.59	-15.85	167.42	33	5.3	Ms	GS	229
19-Aug-82	044048.22	-19.07	169.58	38	5.6	mb	GS	197
5-Oct-82	091432.51	-15.59	168.00	17	5.8	mb	GS	240
12-Mar-83	084946.35	-18.12	168.07	35	5.8	Ms	GS	48
26-Apr-83	111537.43	-15.99	168.43	33	5.5	mb	GS	193
26-Jun-83	155419.03	-17.87	167.60	13	5.1	mb	GS	77
27-Jun-83	082510.42	-18.13	167.82	32	5.0	mb	GS	67
15-Jul-83	031804.73	-18.95	168.09	33	5.0	mb	GS	135
3-Aug-83	181742.23	-17.40	167.91	33	5.6	Ms	GS	57
5-Aug-83	052543.44	-17.30	167.87	33	5.7	Ms	GS	67
5-Aug-83	070238.81	-17.24	167.84	15	5.3	mb	GS	75
11-Dec-83	130252.88	-18.36	168.05	54	5.5	mb	GS	73
5-Mar-84	044804.37	-17.04	168.26	33	5.2	mb	GS	78
5-Mar-84	114233.25	-16.94	168.04	33	5.1	mb	GS	93
21-Mar-84	170447.04	-17.17	167.20	32	5.3	mb	GS	134
1-Apr-84	212809.63	-17.64	167.80	33	5.0	mb	GS	55
29-Apr-84	223400.44	-18.06	167.24	33	5.2	mb	GS	118
18-May-84	095505.19	-17.73	168.12	43	5.2	mb	GS	20
28-May-84	174726.84	-15.84	167.05	33	5.2	Ms	GS	249
16-Jul-84	181630.58	-18.49	168.21	24	5.2	mb	GS	83
25-Jul-84	130928.48	-16.67	167.74	40	5.0	mb	GS	133
18-Aug-84	132458.30	-17.62	167.83	23	5.1	mb	GS	53
2-Oct-84	013708.12	-18.63	167.98	6	5.9	Ms	GS	104
2-Oct-84	132240.97	-18.52	167.98	14	5.5	mb	GS	93
2-Oct-84	194149.19	-18.51	168.14	24	5.5	mb	GS	86
3-Oct-84	143043.18	-18.44	167.93	37	5.0	mb	GS	87
3-Dec-84	131313.43	-19.16	168.65	38	5.3	Ms	GS	160
5-Dec-84	120229.72	-15.70	168.22	33	5.3	Ms	GS	226
17-Feb-85	194048.00	-19.25	168.42	33	5.0	mb	GS	166
28-Feb-85	111016.83	-19.16	168.74	48	5.5	mb	GS	163
1-Apr-85	010453.00	-16.69	167.23	42	5.0	mb	GS	163
12-May-85	152342.18	-17.01	167.57	32	5.1	mb	GS	112
25-Jun-85	141757.81	-19.51	168.75	61	5.0	mb	GS	200
3-Jul-85	155548.77	-17.24	167.83	28	6.7	Ms	BRK	75
1-Aug-85	080129.35	-18.88	168.39	38	5.1	mb	GS	125
7-Aug-85	132146.56	-18.92	168.37	33	5.2	mb	GS	130
8-Sep-85	180740.05	-17.62	167.71	10	5.3	mb	GS	65
4-Jan-86	095253.34	-17.55	167.77	23	5.1	mb	GS	61
4-Jan-86	133633.73	-17.56	167.85	26	5.3	Ms	GS	53
5-Jan-86	212804.95	-19.83	168.81	47	5.3	mb	GS	236
7-Jan-86	080846.56	-17.43	167.61	25	5.3	Ms	GS	82
31-Mar-86	070850.00	-17.23	167.39	33	5.0	mb	GS	113
12-Apr-86	121246.19	-17.54	167.85	22	5.2	mb	GS	54
14-Jun-86	232923.38	-19.10	169.78	15	5.9	Ms	BRK	214
14-Jun-86	233741.80	-19.06	169.60	16	5.3	mb	GS	199
7-Jul-86	163306.10	-17.33	167.74	27	5.1	mb	GS	75
2-Aug-86	111852.07	-18.20	167.96	33	5.0	mb	GS	62
23-Sep-86	133015.37	-16.62	167.26	19	5.7	Ms	GS	166
7-Oct-86	140344.57	-16.60	167.31	10	5.7	mb	GS	165

Date	Origin Time (UTC)	Latitude	Longitude	Depth (km)	Magnitude	Solution	Recorder	Epicentral Distance from Port Vila (km)
25-Oct-86	204701.80	-17.66	168.13	30	6.2	Ms	BRK	20
19-Nov-86	115237.18	-19.55	167.69	33	5.3	mb	GS	210
19-Nov-86	171155.36	-18.89	168.09	47	5.3	mb	GS	128
20-Nov-86	131424.95	-16.26	167.55	60	5.7	mb	GS	182
13-Dec-86	183152.46	-17.95	167.65	17	5.6	Ms	GS	73
14-Dec-86	112252.76	-17.96	167.79	10	5.0	mb	GS	60
16-Dec-86	081827.75	-18.01	167.66	10	5.2	mb	GS	75
28-Dec-86	114733.85	-19.21	168.45	50	5.2	mb	GS	162
11-Feb-87	075612.91	-15.83	167.35	23	6.6	Ms	BRK	234
17-Feb-87	041957.65	-19.68	168.76	33	5.6	mb	GS	218
17-Feb-87	051743.39	-19.69	168.81	33	5.3	mb	GS	221
26-Feb-87	043035.82	-19.70	168.71	43	5.2	mb	GS	220
26-Feb-87	043608.41	-19.80	168.69	49	5.4	mb	GS	230
7-Mar-87	061117.02	-16.02	167.40	35	5.6	mb	GS	213
29-Mar-87	091734.93	-17.24	167.89	21	5.4	Ms	GS	71
16-Jul-87	002305.62	-17.66	167.88	37	5.0	mb	GS	46
28-Sep-87	071538.24	-18.40	168.27	31	5.9	Ms	GS	73
28-Sep-87	114708.61	-18.41	168.06	30	6.8	Ms	GS	78
28-Sep-87	121651.98	-18.40	168.10	31	5.3	mb	GS	75
28-Sep-87	134613.95	-18.55	168.16	25	6.5	Ms	GS	90
28-Sep-87	150102.22	-18.14	168.00	54	5.0	mb	GS	54
28-Sep-87	230937.10	-18.34	168.12	31	5.2	mb	GS	69
30-Sep-87	013928.09	-18.16	167.87	51	6.3	Ms	GS	66
8-Nov-87	060604.72	-18.35	167.87	23	5.3	mb	GS	81
18-Nov-87	122758.97	-19.24	169.91	49	5.0	mb	GS	236
26-Nov-87	172854.73	-16.35	168.12	18	6.3	Ms	GS	155
27-Nov-87	130552.62	-16.26	168.13	32	5.5	mb	GS	164
27-Nov-87	131122.61	-16.31	168.14	28	5.3	Ms	GS	159
27-Nov-87	133318.05	-16.37	168.12	28	6.4	Ms	GS	152
27-Nov-87	173536.04	-16.22	168.17	30	5.0	mb	GS	168
21-Jan-88	082222.93	-18.18	168.14	44	5.9	Ms	GS	51
22-Jan-88	231329.13	-19.55	168.86	42	5.0	mb	GS	207
7-Feb-88	033316.48	-17.66	167.74	10	5.4	mb	GS	61
7-Feb-88	040531.33	-17.56	167.87	22	5.3	mb	GS	50
16-Feb-88	214230.16	-18.46	168.32	38	5.1	mb	GS	78
5-Mar-88	120649.63	-18.14	168.24	47	5.4	Ms	GS	44
26-Mar-88	094239.39	-18.26	167.93	17	5.1	mb	GS	70
30-Apr-88	065010.64	-17.05	167.45	47	5.2	mb	GS	118
5-May-88	075750.03	-18.20	168.17	35	5.3	Ms	GS	53
17-Jul-88	131211.58	-17.82	167.86	33	5.1	mb	GS	49
13-Aug-88	123621.62	-16.52	167.25	33	5.3	mb	GS	176
20-Aug-88	081937.64	-16.48	167.17	21	6.1	Ms	PAS	184
20-Aug-88	083101.34	-16.54	167.12	12	5.1	mb	GS	183
22-Aug-88	023538.32	-16.63	167.17	10	5.1	mb	GS	172
16-Sep-88	062729.76	-17.93	169.06	33	5.5	Ms	BRK	81
14-Feb-89	145306.21	-17.45	167.31	33	5.1	Ms	GS	111
8-Mar-89	035721.57	-19.13	168.68	65	5.2	mb	GS	157
24-Apr-89	203255.84	-17.48	167.84	27	5.1	mb	GS	58
24-Apr-89	204111.54	-17.40	167.83	34	5.7	Ms	BRK	64
25-Apr-89	031117.46	-17.42	167.78	15	5.0	mb	GS	67
18-Jul-89	235239.48	-17.57	168.68	41	5.2	mb	GS	43
20-Jul-89	172221.24	-17.41	167.83	33	5.1	mb	GS	63
11-Aug-89	011219.96	-18.71	168.30	42	5.0	mb	GS	106
17-Aug-89	110310.64	-17.70	167.19	10	5.2	mb	GS	119
17-Nov-89	153557.89	-17.39	167.93	27	5.7	Ms	BRK	56
29-Nov-89	155955.39	-18.32	168.15	23	5.1	mb	GS	66
1-Jan-90	172138.88	-19.15	167.31	10	5.2	mb	GS	188
9-Jan-90	184354.45	-19.88	168.03	33	5.0	Ms	GS	237
28-Jan-90	111530.32	-16.73	167.66	26	5.1	mb	GS	131
5-Mar-90	163812.57	-18.32	168.06	20	7.0	Ms	GS	68
5-Mar-90	171039.57	-18.35	168.01	33	5.4	mb	GS	74

Date	Origin Time (UTC)	Latitude	Longitude	Depth (km)	Magnitude	Solution	Recorder	Epicentral Distance from Port Vila (km)
8-Mar-90	101514.57	-18.47	168.05	17	5.2	mb	GS	84
7-Apr-90	182556.39	-18.05	168.13	36	5.2	mb	GS	39
7-Jul-90	203557.24	-15.52	168.09	33	5.2	mb	GS	247
22-Jul-90	012609.44	-19.13	168.76	45	5.0	mb	GS	160
17-Sep-90	000524.58	-18.34	169.12	41	5.1	mb	GS	107
17-Sep-90	020914.07	-18.39	169.38	33	5.4	mb	GS	133
23-Sep-90	175402.96	-17.73	167.61	10	6.2	Ms	GS	74
24-Sep-90	014420.25	-17.61	167.70	20	5.1	mb	GS	67
24-Sep-90	015801.92	-17.59	167.83	25	5.5	Ms	GS	53
2-Oct-90	074827.97	-17.63	167.83	26	5.3	mb	GS	52
2-Oct-90	080826.37	-17.62	167.80	19	5.5	Ms	GS	56
5-Nov-90	132254.53	-17.50	167.98	33	5.3	mb	GS	44
14-Dec-90	150002.78	-15.90	167.39	55	5.0	Ms	GS	226
27-Dec-90	180141.73	-19.53	168.81	59	5.2	mb	GS	204
18-Feb-91	161506.59	-19.03	168.49	39	5.7	mb	GS	143
14-Mar-91	135049.05	-19.38	167.79	33	5.0	mb	GS	189
28-Mar-91	072236.86	-18.31	168.01	29	5.2	mb	GS	69
28-Mar-91	075831.94	-18.21	167.97	26	5.3	Ms	GS	62
5-Jun-91	144713.11	-19.01	169.49	27	5.0	mb	GS	186
6-Jul-91	190012.56	-16.71	167.52	26	5.2	Ms	GS	141
11-Jul-91	020228.21	-16.77	167.44	28	5.1	mb	GS	142
3-Oct-91	202010.21	-17.03	167.94	10	5.7	Ms	GS	88
3-Oct-91	202417.38	-16.82	167.89	10	5.9	Ms	BRK	111
3-Oct-91	204331.16	-16.85	168.16	15	5.6	Ms	GS	99
6-Oct-91	075133.67	-16.77	168.08	22	5.2	Ms	GS	109
12-Dec-91	061301.23	-18.18	168.03	33	5.0	mb	GS	56
4-Mar-92	125525.01	-17.38	167.71	43	5.0	mb	GS	76
17-Mar-92	003809.38	-18.39	167.73	33	5.3	mb	GS	94
20-Mar-92	081646.66	-18.29	168.22	42	5.0	mb	GS	61
22-Mar-92	204520.64	-17.45	167.92	33	5.3	mb	GS	53
7-Apr-92	224729.45	-16.87	168.13	16	6.0	Ms	BRK	98
8-Apr-92	030127.59	-16.91	168.26	18	5.6	Ms	GS	92
8-Apr-92	133656.43	-16.78	168.31	14	5.8	Ms	GS	105
10-Apr-92	030142.52	-17.58	167.99	34	5.3	mb	GS	39
13-Aug-92	005750.67	-16.64	167.48	33	5.2	mb	GS	150
10-Sep-92	201057.09	-17.22	167.82	20	5.5	mb	GS	78
11-Sep-92	065353.15	-17.36	167.72	23	5.4	Ms	GS	75
19-Sep-92	232809.33	-15.73	168.15	20	5.1	mb	GS	222
15-Oct-92	144023.31	-19.16	169.61	20	5.3	mb	GS	207
17-Oct-92	020601.99	-19.35	169.69	57	5.3	mb	GS	229
17-Oct-92	025150.92	-19.23	169.55	11	7.0	Ms	BRK	209
17-Oct-92	054758.11	-19.24	169.47	33	5.2	mb	GS	205
17-Oct-92	114103.30	-19.16	169.48	33	5.3	mb	GS	199
17-Oct-92	141233.13	-19.36	169.70	39	5.1	mb	GS	230
17-Oct-92	181023.88	-19.33	169.64	36	5.3	mb	GS	224
19-Oct-92	120330.13	-19.39	169.59	20	5.8	Ms	GS	226
18-Nov-92	163645.19	-16.77	167.10	22	5.3	Ms	GS	167
11-Dec-92	022251.84	-17.52	167.96	33	5.4	mb	GS	44
17-Jan-93	053606.35	-19.72	168.88	30	5.2	Mw	HRV	226
10-Feb-93	001632.33	-19.43	169.18	10	5.2	mb	GS	207
22-Apr-93	180340.79	-16.32	167.44	33	5.0	mb	GS	182
3-May-93	232756.51	-19.64	168.80	33	5.1	mb	GS	215
9-Jul-93	130309.51	-17.37	167.93	16	5.9	Mw	GS	58
9-Jul-93	130849.33	-17.44	167.84	23	5.0	mb	GS	60
9-Jul-93	163706.33	-17.45	167.78	10	5.0	mb	GS	65
9-Jul-93	231747.95	-17.55	167.77	28	5.1	mb	GS	61
25-Jul-93	053746.39	-16.83	167.73	33	5.3	Mw	HRV	118
29-Sep-93	093920.67	-18.97	167.67	34	5.5	mb	GS	151
29-Sep-93	094848.27	-18.92	167.46	34	5.4	mb	GS	157
29-Sep-93	100920.04	-18.77	167.53	34	5.1	mb	GS	140
29-Sep-93	120708.08	-19.07	167.49	35	5.4	mb	GS	170

Date	Origin Time (UTC)	Latitude	Longitude	Depth (km)	Magnitude	Solution	Recorder	Epicentral Distance from Port Vila (km)
29-Sep-93	125029.90	-18.73	167.51	33	5.0	mb	GS	138
29-Sep-93	140748.80	-19.07	167.62	42	5.4	mb	GS	163
29-Sep-93	144427.73	-19.01	167.69	34	5.2	mb	GS	154
30-Sep-93	223620.88	-19.28	167.61	44	5.0	mb	GS	185
2-Oct-93	042340.61	-19.00	167.67	10	5.0	mb	GS	154
15-Nov-93	224519.35	-18.56	167.64	48	5.2	mb	GS	115
22-Jan-94	053701.12	-17.69	167.90	33	5.0	mb	GS	43
16-Feb-94	064858.04	-18.99	168.13	13	6.5	Ms	BRK	139
26-Feb-94	174550.37	-17.65	167.78	28	5.4	Mw	HRV	57
6-Apr-94	121344.97	-17.37	167.82	17	6.2	Mw	HRV	66
6-Apr-94	121958.39	-17.43	167.76	10	5.2	mb	GS	68
10-Apr-94	051826.90	-17.41	167.68	29	5.4	Mw	HRV	77
17-Apr-94	061439.17	-15.90	167.51	39	5.7	Mw	HRV	220
7-Jul-94	001925.41	-19.30	169.81	33	5.2	mb	GS	233
13-Jul-94	002514.43	-16.64	167.47	33	5.4	mb	GS	150
13-Jul-94	023556.02	-16.62	167.52	33	7.3	Ms	GS	150
13-Jul-94	024347.10	-16.64	167.38	33	5.6	mb	GS	156
13-Jul-94	031319.31	-16.81	167.25	33	6.7	Mw	HRV	152
13-Jul-94	080951.75	-16.57	167.22	29	5.3	mb	GS	173
13-Jul-94	090156.67	-16.90	167.49	23	5.2	mb	GS	127
13-Jul-94	134807.93	-16.57	167.42	25	5.3	mb	GS	160
14-Jul-94	000924.70	-16.58	167.45	19	5.9	Ms	GS	157
14-Jul-94	075306.32	-17.13	167.59	36	5.2	Ms	GS	102
14-Jul-94	082538.77	-16.71	167.37	30	5.7	Mw	HRV	152
14-Jul-94	112633.47	-16.80	167.42	21	5.3	Mw	HRV	140
15-Jul-94	131149.60	-16.58	167.38	28	5.0	mb	GS	161
15-Jul-94	160430.49	-16.56	167.48	33	5.2	mb	GS	158
15-Jul-94	192043.38	-16.72	167.24	33	5.0	mb	GS	160
17-Jul-94	220458.06	-16.68	167.38	33	5.6	Mw	HRV	153
23-Jul-94	133956.46	-16.79	167.04	33	5.2	Ms	GS	171
23-Jul-94	195306.81	-16.79	167.38	33	5.0	mb	GS	144
24-Jul-94	175540.38	-16.97	167.57	20	6.6	Ms	BRK	116
24-Jul-94	203752.43	-16.98	167.39	33	5.3	Mw	HRV	129
25-Jul-94	215208.72	-16.98	167.52	33	5.1	mb	GS	118
29-Jul-94	075328.47	-16.98	167.74	13	5.9	Mw	GS	103
29-Jul-94	124224.06	-16.95	167.63	33	5.3	mb	GS	113
29-Jul-94	131251.23	-16.92	167.74	36	5.4	Mw	HRV	109
3-Aug-94	182401.16	-17.31	167.31	40	5.2	Mw	HRV	116
10-Aug-94	140657.03	-16.89	167.19	33	5.5	Mw	HRV	152
15-Aug-94	105853.87	-17.62	167.79	33	5.4	mb	GS	56
1-Oct-94	150331.31	-17.85	167.80	25	5.7	Mw	HRV	55
1-Oct-94	163520.79	-17.75	167.68	16	6.5	Ms	GS	66
1-Oct-94	174637.58	-17.77	167.83	33	6.3	Ms	GS	51
1-Oct-94	175416.71	-17.96	167.32	33	5.1	mb	GS	107
1-Oct-94	181622.20	-18.04	167.37	33	5.4	Ms	GS	105
1-Oct-94	210128.36	-17.81	167.79	24	5.3	mb	GS	55
1-Oct-94	232856.24	-17.64	167.79	18	5.4	Mw	HRV	57
1-Oct-94	235359.40	-17.88	167.44	33	5.4	Mw	HRV	94
2-Oct-94	101432.38	-17.56	168.05	10	5.4	Mw	HRV	34
2-Oct-94	103545.48	-17.78	167.65	33	5.2	mb	GS	70
18-Jan-95	121437.12	-19.16	167.40	36	5.5	mb	GS	183
22-Jun-95	075710.92	-16.41	168.11	33	5.8	Mw	GS	148
7-Nov-95	160810.18	-17.92	168.07	33	5.2	Mw	HRV	32
13-Jan-96	000723.94	-19.54	168.89	33	5.3	Mw	HRV	207
11-Feb-96	205025.48	-16.39	168.18	18	5.4	mb	GS	149
18-Sep-96	041144.40	-19.75	168.69	31	5.7	Mw	HRV	225
26-Jan-97	144116.64	-17.18	167.77	37	5.4	Mw	HRV	84
23-Mar-97	154939.68	-19.17	168.74	33	5.5	Mw	HRV	163
3-Apr-97	004441.52	-16.05	168.14	50	5.0	mb	GS	188
27-Apr-97	003132.54	-19.17	168.73	41	6.1	Mw	GS	163
9-Jun-97	012131.77	-19.62	169.64	33	5.2	Mw	HRV	249

Site-Specific Earthquake Hazard Determinations in Capital Cities in the South Pacific

Date	Origin Time (UTC)	Latitude	Longitude	Depth (km)	Magnitude	Solution	Recorder	Epicentral Distance from Port Vila (km)
21-Jul-97	123029.98	-17.41	167.62	33	5.3	Mw	HRV	82
28-Aug-97	214207.61	-17.40	167.91	33	5.5	Mw	HRV	57
18-Oct-98	031538.42	-16.86	166.79	33	5.0	mb	GS	188
19-Oct-98	012501.20	-17.30	167.72	33	6.0	Mw	HRV	79
19-Oct-98	022334.68	-17.24	167.84	33	5.1	Ms	GS	75
14-Feb-99	211224.58	-15.51	168.00	10	6.0	Mw	GS	249
15-Feb-99	051907.37	-15.54	168.00	33	5.4	Ms	GS	245
2-Apr-99	170547.11	-19.90	168.19	10	6.2	Mw	GS	238
2-Apr-99	183816.97	-19.86	167.99	10	5.2	mb	GS	236
2-Apr-99	195610.81	-19.83	167.94	10	5.0	mb	GS	233
6-Apr-99	003313.36	-19.87	168.07	10	5.0	mb	GS	236
15-Jul-99	142625.76	-18.23	168.18	33	5.2	mb	GS	55
15-Jul-99	154459.24	-18.15	168.19	43	5.0	mb	GS	47
22-Aug-99	124045.96	-16.12	168.04	33	6.5	Mw	GS	182
26-Nov-99	132115.42	-16.43	168.23	33	7.5	Mw	HRV	144
26-Nov-99	133834.26	-15.98	167.93	33	5.7	mb	GS	199
26-Nov-99	134643.54	-15.88	167.89	33	5.3	mb	GS	210
26-Nov-99	144120.86	-15.77	167.80	33	5.5	mb	GS	225
26-Nov-99	152529.86	-15.91	167.89	33	5.0	mb	GS	208
26-Nov-99	193609.40	-16.48	168.07	33	5.5	mb	GS	141
26-Nov-99	220320.01	-15.57	167.92	33	5.9	Mw	GS	243

6.5 Microtremor Recordings - Site-Response Measurements, Port Vila

Microtremor recordings were made at 100 sites within the Port Vila and Bauerfield Airport areas during May 1997 and from September to November 1997.

Stacked groups of site-response spectra are shown together with the appropriate spectral models in Figure 21, and the site characteristics are summarised in Table 6. The locations of recording sites are shown at the end of the Port Vila chapter (see Figure 24).

At each site, the ambient noise was recorded for 3 minutes every 10 minutes during one hour. The recorded microtremors were analysed using the Nakamura technique to recover the polarisation characteristics of the wave field.

Approximately sixty percent of the sites surveyed exhibit site responses that actually show no amplification at frequencies up to 10 Hz. At around 10 Hz in the spectrum, some scattering occurs due to small variations in soil-layer thickness and/or weak topographic irregularities.

The Nakamura technique is known to be essentially efficient in the presence of a strong velocity contrast between the uppermost soft layers and the underlying basement. In that situation it can provide robust estimate of the s-wave resonance frequency and it has been shown (Lachet & Bard 1994) that similar results are then obtained by using incident s waves from earthquakes to compute the response spectrum.

(over page: p.70-73)

Table 6: Microtremor Site-Response Recordings, Port Vila

Site Response Table, Port Vila

PORT VILA Site No.	Amplification Factor	Amplified Frequency Hz	Site Response Class	UTC Date	UTC Time	WGS84 UTM Easting	WGS84 UTM Northing	Locality
0	1.8	4.8		130597	0920			Mines Department
1	1.8	9.0	D	140597	0900	215,668.08	8,037,035.58	Eluk à coté de chez Gaston
2	1.0	7.3	D	140597	1040	214,162.42	8,033,583.36	Hotel le Lagon (haut du golf)
3	1.2	9.0	D	140597	1010	214,947.64	8,034,127.81	Hotel le Lagon (Entree)
4	0.8	2.0	D	150597	1130	214,744.97	8,033,608.44	Ecole de Pango (cote Pilioko)
5	1.0	5.0	D	150597	1020	213,930.12	8,032,889.56	Number three chez Dominique
6	2.0	7.0	C	160597	1430	214,652.91	8,034,603.82	Haut de Number three
7	1.2	9.0	C	160597	1528	214,336.82	8,034,585.55	Ardimani wharf
8	2.5	3.5	B	160597	1010	214,301.04	8,034,726.48	Star wharf
9	2.4	4.4	B	190597	0910	213,456.38	8,034,602.37	Rondpoint Travaux Public
10	1.0	9.5	D	200897	1010	215,347.44	8,034,756.20	Au Bon Marche Nbr 2
11	1.1	1.4	D	200897	1010	215,293.32	8,035,252.72	Museum
12	2.0	10.0	D	200897	0850	215,438.82	8,035,839.14	Sea side Paama (show ground)
13	1.2	8.0	D	210897	1000	215,845.53	8,035,800.32	Vila Central Hospital
14	2.7	8.1	D	210897	0910	216,078.75	8,036,191.72	Terrain du Parlement
15	1.8	8.0	D	220897	1010	215,217.25	8,036,142.33	Independence Park
16	1.4	7.0	D	220897	1101	215,446.19	8,036,535.57	Ancienne Maison President
17	3.2	10.0	C	220897	1440	215,488.41	8,036,789.92	Tour Telecom
18	1.5	1.8	D	220897	1536	215,791.50	8,037,022.72	Maison des scouts
19	4.0	10.0	C	220897	0848	215,423.59	8,037,129.35	Natai fish market
20	2.1	2.6	B	250897	1000	215,117.46	8,036,411.14	Club Vanuatu
21	1.1	5.0	D	250897	1050	215,244.65	8,036,771.92	Hotel Rossi
22	1.5	3.3	B	250897	1430	214,909.52	8,036,888.63	Foyer Catholique
23	1.4	8.5	D	250897	1520	215,198.21	8,037,028.76	Radio Vanuatu
24	0.9	1.2	D	250897	0840	214,923.19	8,037,097.26	Ministry of Public Works
25	1.4	8.0	D	260897	0942	214,946.08	8,037,329.63	Terrain vague INTV
26	1.1	7.5	D	260897	1100	215,161.57	8,037,832.21	Roger Brand
27	2.4	7.0	B	260897	1350	214,754.14	8,037,844.44	Stade a cote du Prison
28	2.8	7.0	C	260897	1540	215,335.24	8,037,414.93	Le Meridien
29	3.2	6.2	C	260897	0800	216,306.06	8,036,692.81	Erakor Bridge
30	2.2	4.8	C	270897	0857	217,289.56	8,036,553.50	Korman Stadium

Site Response Table, Port Vila

PORT VILA Site No.	Amplification Factor	Amplified Frequency Hz	Site Response Class	UTC Date	UTC Time	WGS84 UTM Easting	WGS84 UTM Northing	Locality
31	2.2	6.7	C	270897	1000	217,459.59	8,037,144.23	Terrain vague Tassiriki
32	1.5	4.2	C	270897	1042	217,079.58	8,037,080.03	Bellevue Estate
33	2.0	9.0	D	270897	1340	217,052.17	8,037,448.34	Ex National Housing Cooperation
34	1.1	7.0	D	270897	1440	215,580.55	8,038,052.50	Station GPS
35	1.8	7.5	D	270897	1550	215,718.14	8,037,805.15	U.S.P.
36	1.5	9.0	D	270897	1403	216,222.72	8,037,320.37	Simbolo
37	1.4	6.5	D	280897	1500	215,430.41	8,038,733.94	Propriete Siske (Anaburu)
38	1.2	8.0	D	280897	0750	215,255.25	8,038,868.77	Anaburu chez Job Esau
39	2.0	8.0	C	290897	0840	215,096.13	8,038,698.94	Devans magasin Peter Chan
40	1.6	9.0	C	290897	0940	215,050.44	8,038,865.74	A cote Seven Stars
41	1.2	7.5	C	290897	1140	215,072.47	8,039,203.08	Grandes citernes Ohlen
42	1.1	7.0	D	290897	1240	215,769.33	8,039,300.63	Stade Antoine Rossi
43	2.1	8.5	C	290897	0920	214,935.40	8,038,203.89	LCM Store
44	1.1	5.1	D	010997	1020	214,816.59	8,038,561.04	Ohlen
45	2.8	8.0	D	010997	1340	215,282.77	8,039,328.03	Eglise Assemble de Dieu
46	1.1	4.4	C	010997	1440	214,612.64	8,038,876.76	Man Pless
47	1.8	6.0	C	010997	1540	214,629.30	8,039,203.06	Tebakor chez Jimmy Moli
48	1.2	6.2	D	010997	1010	214,872.57	8,039,086.05	Au Bon Marche Tebakor
49	0.9	1.7	D	020997	1110	214,713.39	8,039,358.21	Ancien depotoir (Teumutotoe)
50	6.2	2.6	SINK HOLE	02 09 97	1350	214,707.63	8,039,590.40	Ohlen Fresh Wind (Taavara)
51	2.8	8.8	C	02 09 97	0810	215,168.47	8,039,542.82	Derrier Fresh Water School
52	2.2	7.6	C	03 09 97	1000	216,011.19	8,038,841.01	Terrain Agriculture Tagabe
53	1.4	2.3	A	03 09 97	1100	215,425.10	8,040,215.22	Derriere bureeau Air Club
54	3.0	1.0	A	03 09 97	1400	215,303.49	8,040,920.98	Route Aviation Civil Bauerfield
55	2.4	0.8	A	03 09 97	1450	214,648.04	8,041,443.04	Bureau Aviation Civil Bauerfield
56	3.6	8.2	A	03 09 97	1540	215,019.13	8,041,550.34	Ancien bout de piste Bauerfield
57	4.0	1.2	A	03 09 97	0830	216,105.25	8,040,982.00	Plantation Furay amont Tagabe
58	1.2	1.5	B	04 09 97	1030	216,795.64	8,039,998.24	Plantation Furay en face de Switi
59	3.1	0.9	A	04 09 97	1400	216,005.07	8,040,338.21	Plantation Declaire vers Saparua
60	2.1	0.8	A	04 09 97	1500	214,158.59	8,041,713.26	Tagabe vers la route Black Sand

Site Response Table, Port Vila

PORT VILA Site No.	Amplification Factor	Amplified Frequency Hz	Site Response Class	UTC Date	UTC Time	WGS84 UTM Easting	WGS84 UTM Northing	Locality
61	-	-	A	04 09 97	1540	213,863.13	8,040,395.02	Rondpoint Tagabe
62	-	-	A	04 09 97	1030	214,547.81	8,040,359.19	Route pres de l' abattoir
63	2.2	8.3	A	08 09 97	1406	212,962.10	8,041,811.84	Black Sand cote Tagabe
64	1.0	8.0	A	08 09 97	1518	212,855.54	8,039,690.55	Black Sand cote La Colle
65	2.9	0.5	A	08 09 97	0820	212,528.00	8,040,218.35	Kawenu field
66	1.8	4.2	B	09 09 97	0920	214,323.66	8,038,019.70	Sauma Malapoa Estate
67	1.2	4.2	D	09 09 97	1020	214,072.81	8,037,845.20	Tengaru Plateau pointe Malapoa
68	1.8	8.2	D	09 09 97	1400	213,439.73	8,037,744.96	Sumalapa Transmateur TVL
69	2.2	8.2	C	09 09 97	1456	213,651.13	8,038,138.42	Plateau Matnaalu avant Malapoa
70	1.1	8.2	D	09 09 97	0750	214,162.10	8,038,747.04	Matantapoa en face Malapoa Coll.
71	0.9	2.5	D	10 09 97	0920	214,113.91	8,038,413.64	Matnaniu haut de Manples
72	1.0	6.4	D	10 09 97	1230	214,318.34	8,039,029.27	Pusupe village Manples
73	3.0	9.7	D	10 09 97	1450	214,169.73	8,039,332.95	Ecole d' Embassade
74	3.5	9.0	C	10 09 97	0804	215,827.09	8,036,647.43	Anglican Church
75	1.1	8.0	D	11 09 97	0910	214,662.77	8,039,995.11	Ohlen Fresh Wind cote Nord
76	1.4	5.0	C	11 09 97	1010	215,243.12	8,040,024.89	Ohlen Fresh Wind cote Est
77	1.5	3.5	B	11 09 97	1350	215,814.66	8,039,649.71	Ohlen Fresh Wind BH1
78	3.8	7.1	C	11 09 97	1450	215,512.90	8,039,701.34	Green Hill (Valea) en face SMET
79	0.8	4.5	D	11 09 97	0820	214,299.50	8,039,884.70	Malapoa derriere Sumalapa
80	1.0	7.8	D	12 09 97	1030	213,409.89	8,039,008.60	Ancienne station radio malapoa
81	1.2	5.2	D	05 11 95	1430	213,173.88	8,037,092.87	Derriere Malapoa
82	3.1	7.8	C	05 11 97	1000	213,083.75	8,038,163.60	Anaburu chez Festa
83	2.1	5.8	D	05 11 97	1130	215,398.51	8,038,455.16	Motis Nabatu (vers Kaiviti)
84	1.0	5.0	D	06 11 97	1430	215,179.68	8,035,577.82	Nabatu cote seaaide
85	3.0	4.0	C	06 11 97	1530	215,665.40	8,035,320.05	Dock PWD apres Fisheries
86	0.9	2.0	D	06 11 97	0840	215,066.66	8,034,960.95	Nabatri derriere Inomakas store
87	1.5	6.0	C	07 11 97	1020	214,935.02	8,034,534.98	Magasin rondpoint hotel le lagon
88	1.0	8.2	D	07 11 97	1410	214,558.55	8,033,939.60	Route wharf Erakor
89	1.2	4.0	D	07 11 97	0900	214,433.32	8,033,459.43	Imperial
90	2.1	8.5	C	11 11 97	1000	215,762.19	8,037,335.18	Fresh water football field

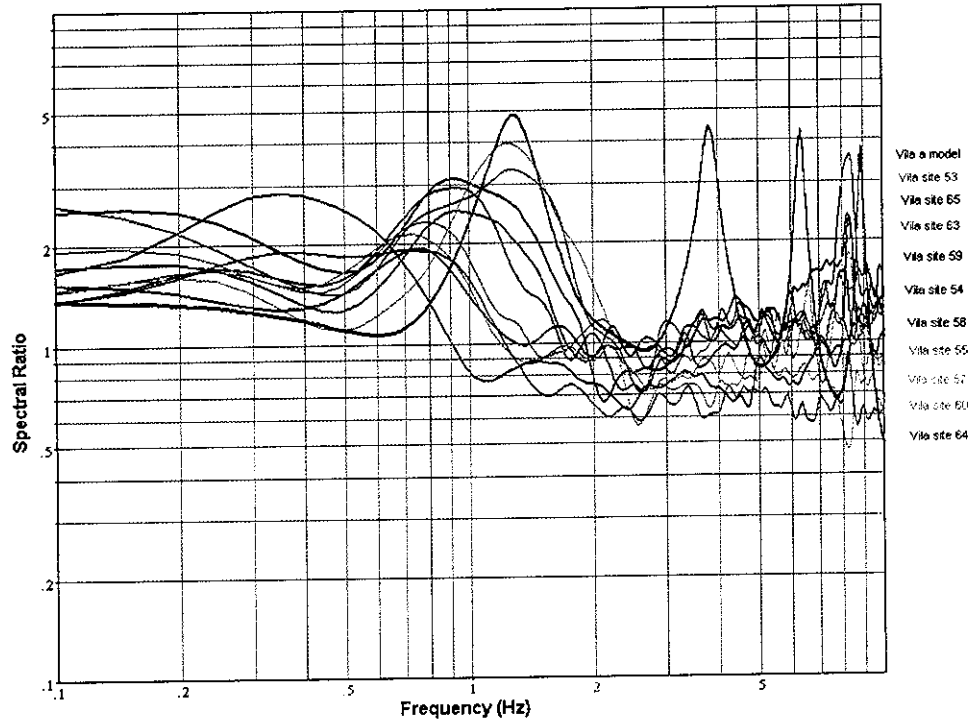
Site Response Table, Port Vila

PORT VILA Site No.	Amplification Factor	Amplified Frequency Hz	Site Response Class	UTC Date	UTC Time	WGS84 UTM Easting	WGS84 UTM Northing	Locality
91	1.2	9.0	D	11 11 97	1420	215,863.11	8,038,506.86	Lycee L A B
92	1.1	5.3	D	11 11 97	1550	215,253.68	8,038,101.23	Hollen white wood
93	1.4	7.0	D	11 11 97	1400	215,462.79	8,039,053.81	Vila east school
94	1.8	8.2	D	12 11 97	1510	215,745.05	8,036,390.60	Hotel Talimoru
95	1.2	8.5	D	12 11 97	0840	215,673.13	8,036,176.08	Tassiriki apres rondpoint
96	2.0	9.0	D	13 11 97	1000	216,037.82	8,036,896.65	Tassiriki entre habitats
97	1.9	8.2	D	13 11 97	1400	216,494.39	8,036,988.43	Derriere eglise pare nabatu
98	2.0	7.0	D	13 11 97	0840	215,498.55	8,035,068.37	Tagabe 400m amont st. pompage
99	1.6	5.0	B	14 11 97	1050	216,170.50	8,039,670.72	Terrain vague apres Hotl le Lagon
100	1.1	7.2	D	14 11 97	1400	215,039.78	8,033,866.75	

(over page: p.75-80)

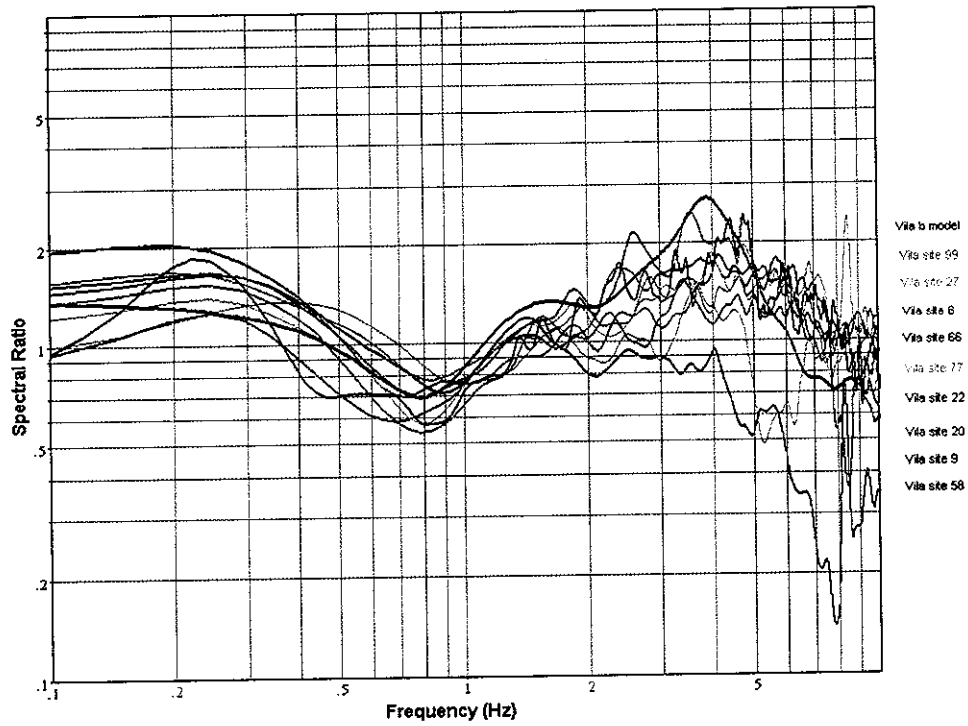
Figure 21: Site-Response Spectra, Port Vila

PORT VILA SITE RESPONSE SPECTRA ZONE A



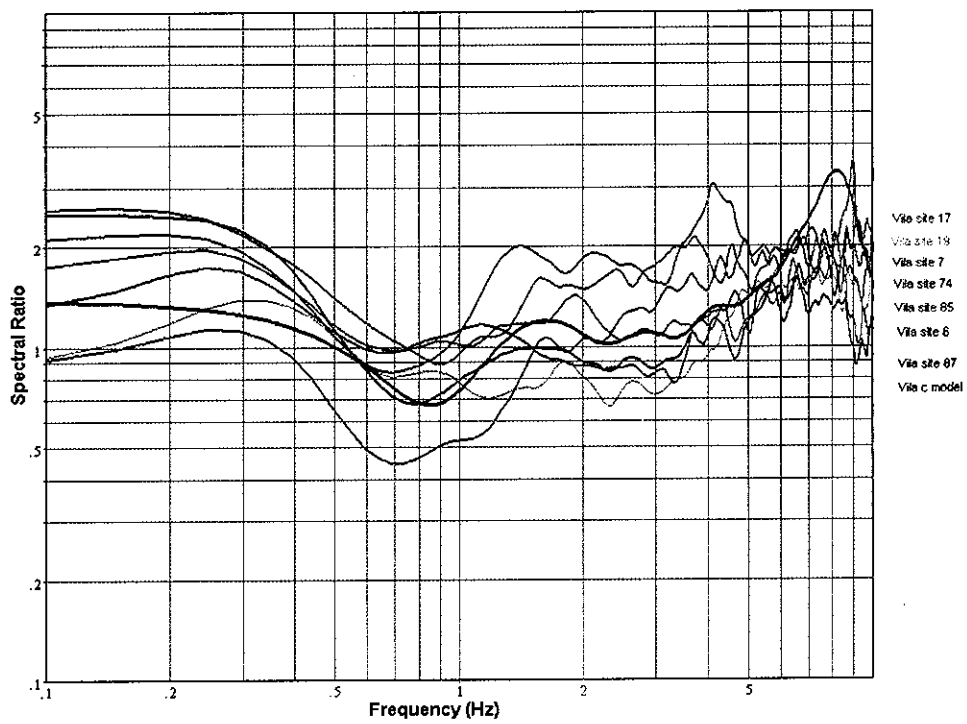
a

PORT VILA SITE RESPONSE SPECTRA ZONE B



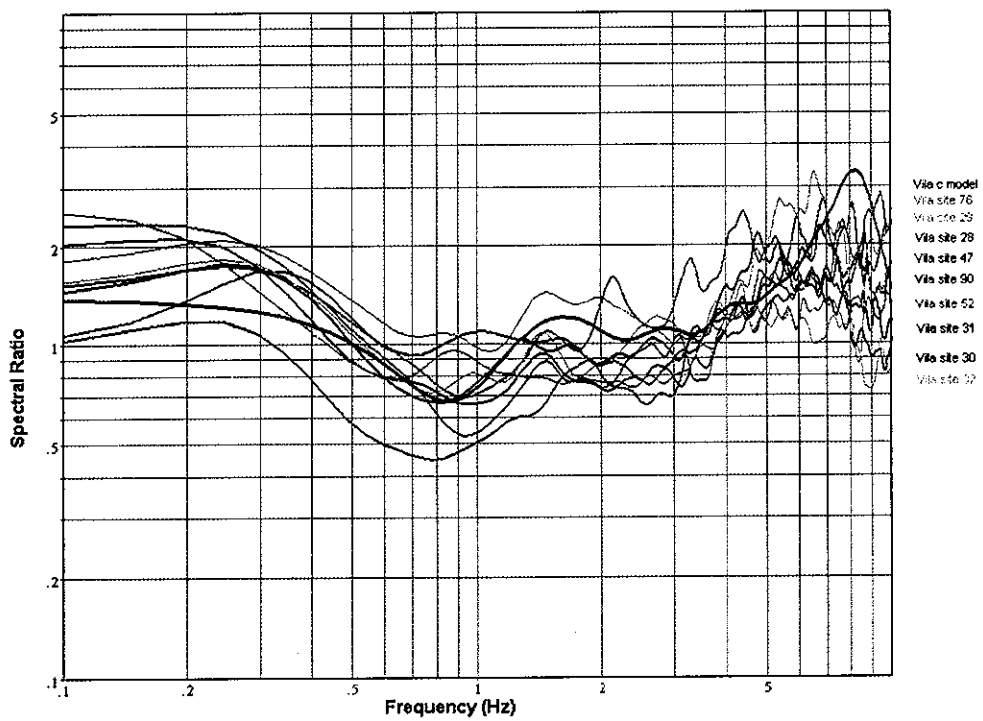
b

PORT VILA SITE RESPONSE SPECTRA ZONE C - STACK 1



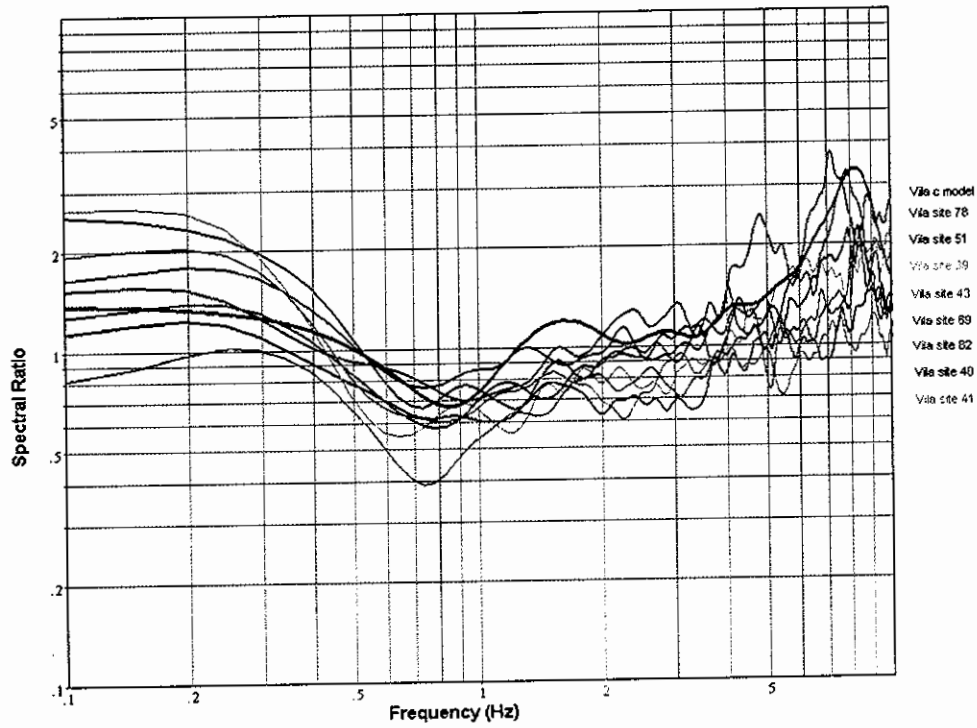
c

PORT VILA SITE RESPONSE SPECTRA ZONE C - STACK 2



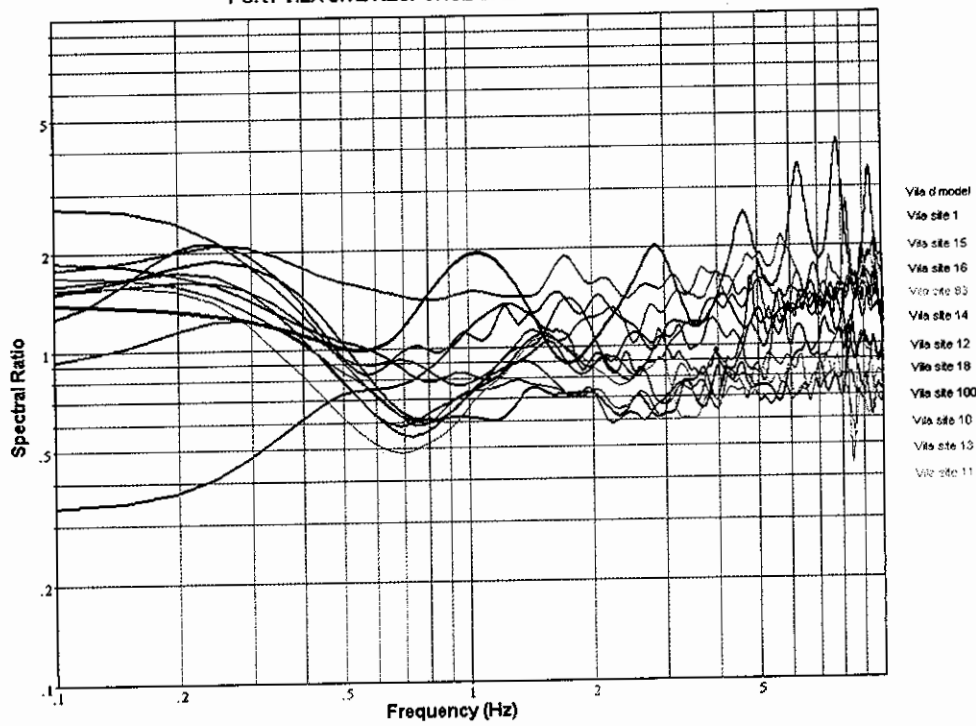
d

PORT VILA SITE RESPONSE SPECTRA ZONE C - STACK 3



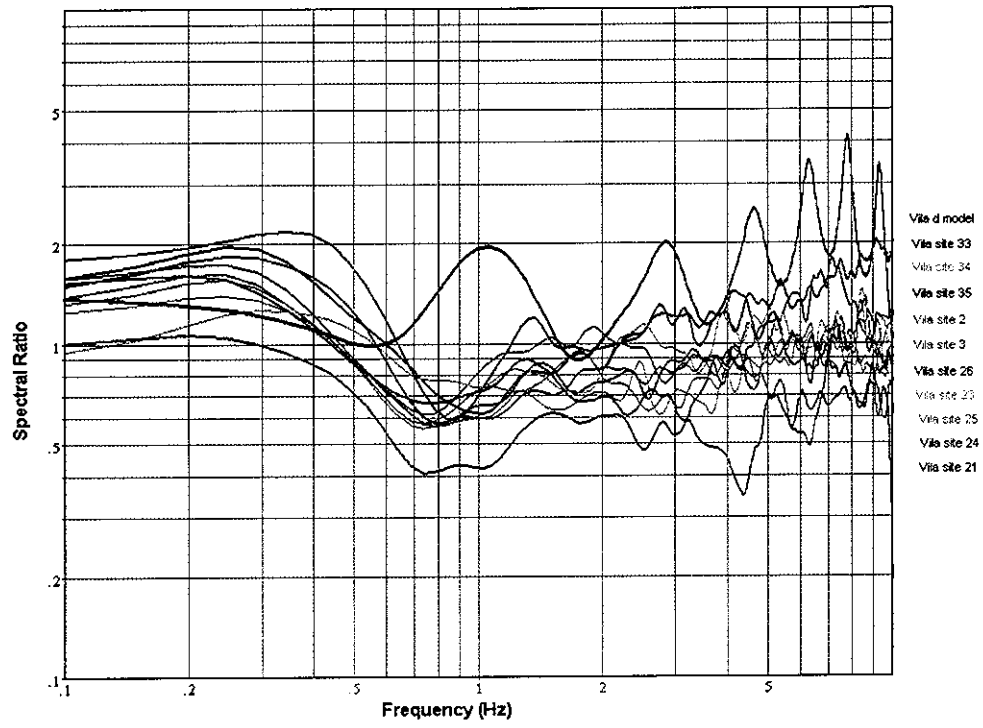
e

PORT VILA SITE RESPONSE SPECTRA ZONE D - STACK 1



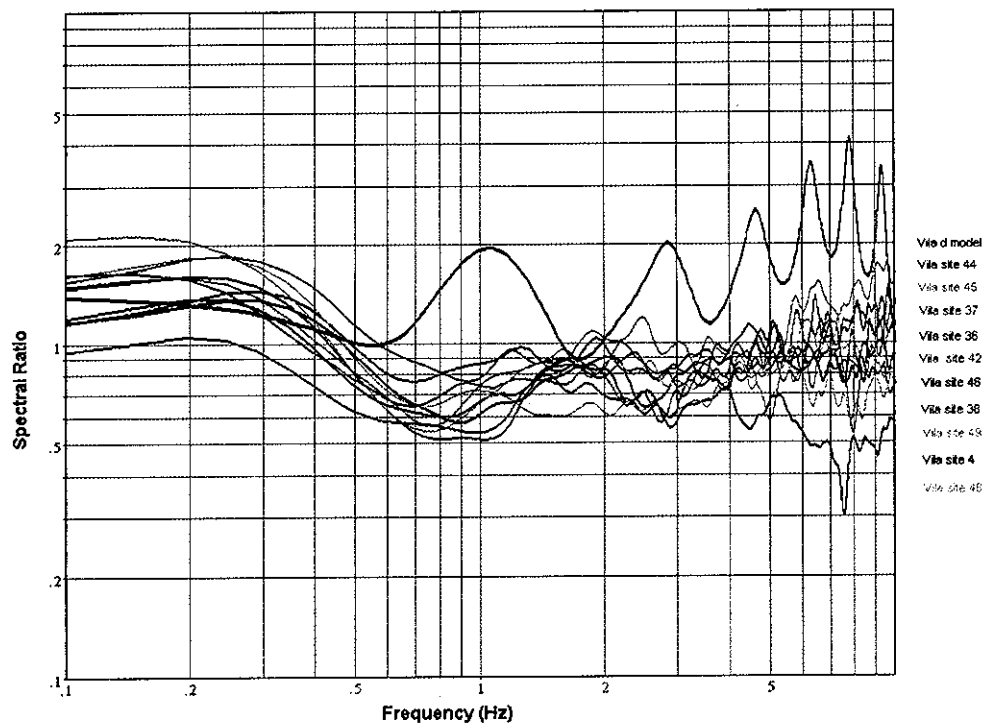
f

PORT VILA SITE RESPONSE SPECTRA ZONE D - STACK 2



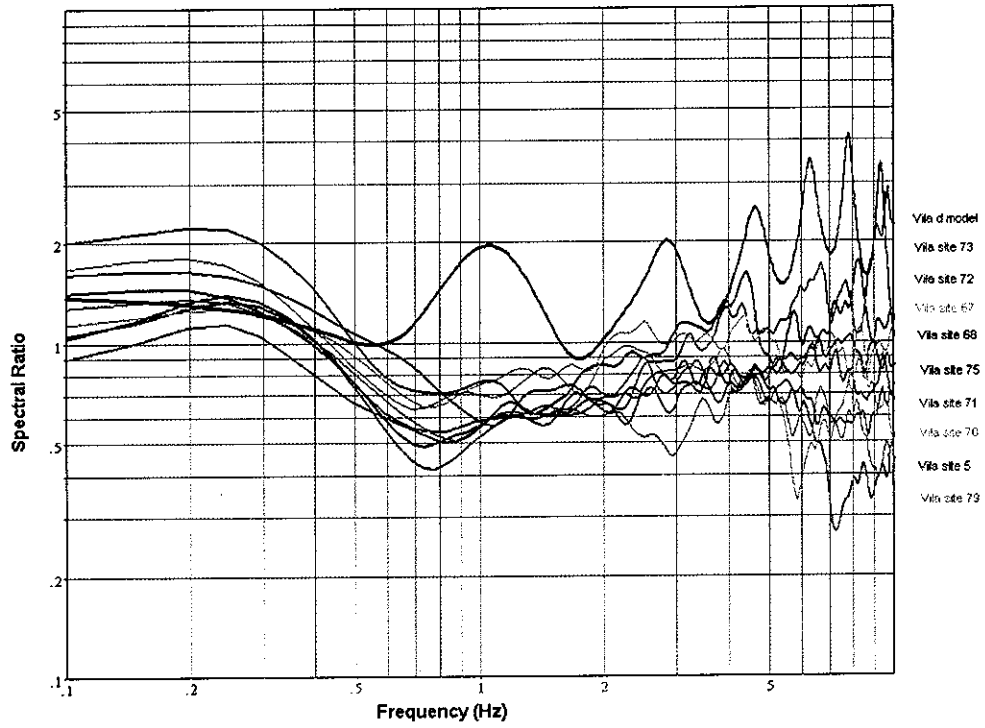
g

PORT VILA SITE RESPONSE SPECTRA ZONE D - STACK 3



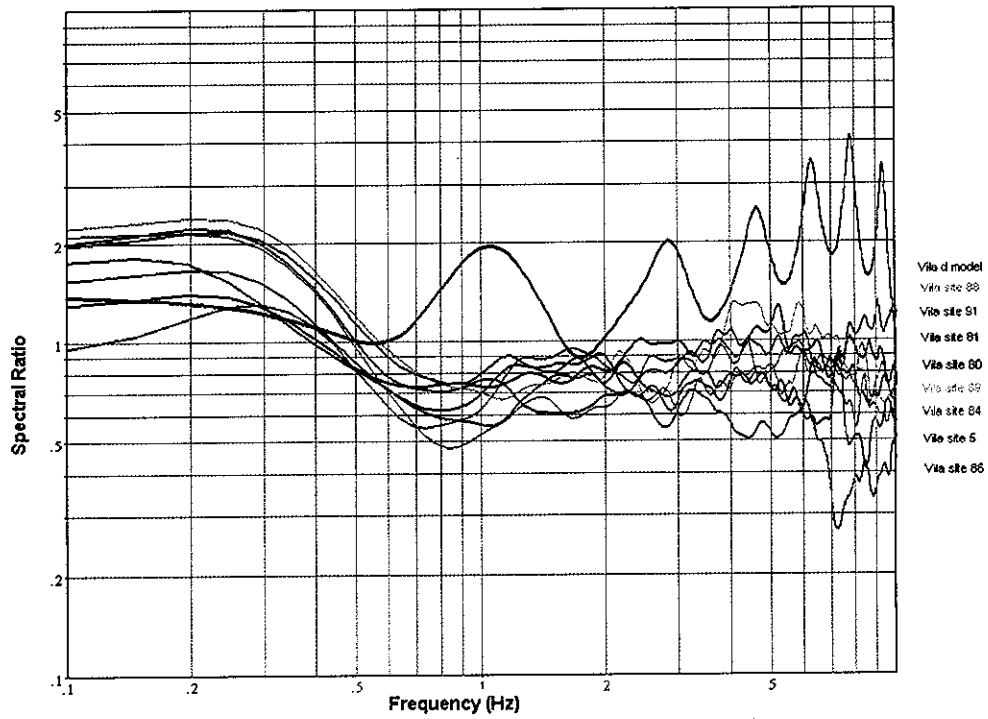
h

PORT VILA SITE RESPONSE SPECTRA ZONE D - STACK 4



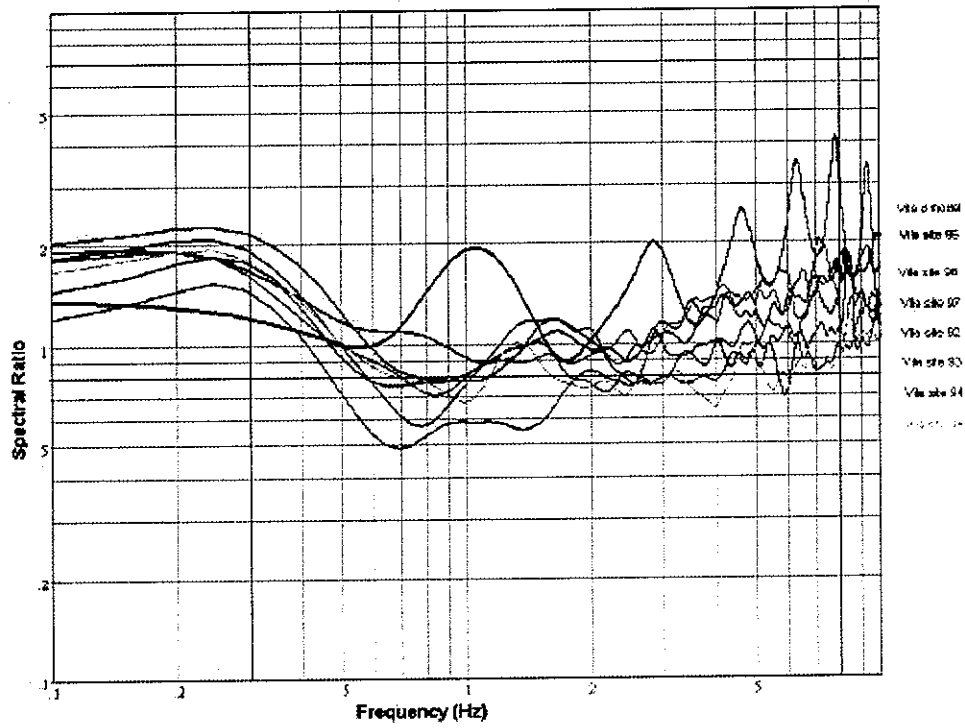
i

PORT VILA SITE RESPONSE SPECTRA ZONE D - STACK 5



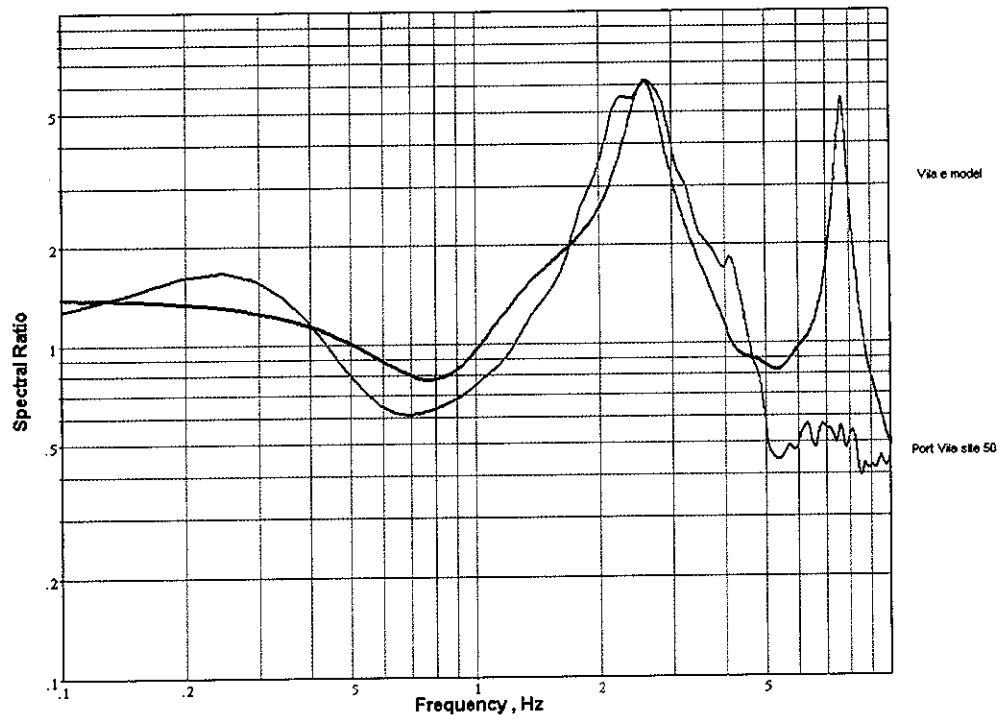
j

PORT VILA SITE RESPONSE SPECTRA ZONE D - STACK 6



k

SITE RESPONSE SPECTRA FOR PORT VILA SITE 50



l

6.6 Analysis of Site-Response Measurements and Zonation of Port Vila

A number of models were developed to fit the various results from the microseismic measurements across Port Vila. Seven models were chosen for the range of available results, having various combinations of layer thickness, s-wave velocity and density.

The thickness of the surface layer was estimated from the measured resonance period according to the relationship: $T = 4H/V_s$ where T = period in seconds, H is the thickness of the layer in metres, and V_s is the shear-wave velocity in m/s. The estimated sediment thickness for selected sites is summarised in Tables 7-10 below.

The characteristic resonant frequencies of the spectral models and corresponding zone names are shown in Table 11, and the critical parameters defining the spectral models are shown in Table 12.

A diagrammatic, generalised cross-section of subsurface conditions and their relationship to the adopted subsurface models is shown in Figure 22.

The spectral models are compared in Figure 23a, and the acceleration-response functions for each zone are shown in Figure 23b.

Similarities among some of the models allowed a grouping into five distinct classes for mapping for zonation purposes. In the case of Port Vila, the class distinction is made by grouping the geological units together with the range of frequencies that correspond to high spectral amplitudes.

Readers should note that amplification factors discussed in this section are based on Nakamura site responses only.

Zone A is represented by only one style of model behaviour. The zone outlines an extensive area of weak silts and sands - at least 20 metres thick - in alluvial or coastal deposits overlying either Port Vila limestone basement or volcanic basement rocks. The model suggests that the thickness of the sedimentary layers increases to over 60 m towards the west.

Figure 21a shows the site responses for the area around Bauerfield Airport (sites 53 to 63), north of Port Vila and part of the larger Mele terrace. They are characterised by two peaks, one at low frequencies around 1 Hz, and another at higher frequencies between 8 and 9 Hz. The peak at low frequencies is observed systematically at each site from that area, but with a variation in position and amplitude. Assuming a constant shear-wave velocity over the considered area, the resonance peak move-out implies a thickness variation of the soft-material layer responsible for the resonance. Table 7 shows estimates of the sediment thickness at these sites for a range of s-wave velocity appropriate for soft volcano-sedimentary material.

Table 7: Sediment thickness calculated from the observed resonance period in Bauerfield Airport area, Zone A, Port Vila

Site	V_s , Adopted Shear Velocity (m/s)	T , Measured Resonant Period (seconds)	H , Calculated Sediment Thickness (m)
Tagabe (53)	120	0.80	24
Air Club (54)	120	1.11	33
Civil Aviation (55)	120	1.25	37
Civil Aviation (56)	120	1.05	31
Airstrip (57)	120	0.80	24
Plant Furay (59)	120	1.11	33
Plant Declaire (60)	120	1.33	40
Abattoir (63)	120	1.43	43
Black Sands (64)	120	1.43	43
La Colle (65)	120	2.22	67

The second peak centred at 8.2 Hz is not observed on all sites from the Bauerfield Airport area. It could be related to a sand layer which is observed in many places in this area, up to the base of Mt Bernier, that limits the Mele volcano-sedimentary terrace to the north. At Tagabe, on the southern edge of the Mele terrace, the log of a borehole drilled in 1979 describes clayey and sandy sediments down to at least 30 m depth. The location of the borehole lies between site 53 (inferred 24 m thickness) and site 64 (inferred 43 m thickness), indicating that the values of thickness inferred through site-response measurements are in the correct order of magnitude.

Zone B incorporates two models, showing similar responses. The first model represents reclaimed bay areas of fill placed over weak, nearshore carbonate sediments around 10-15 m thick (R. Smith, pers. comm.). These sediments in turn overlie the Port Vila limestone basement. The second model represents a zone of colluvium and dump-site fill, at least 10 m thick, in a sinkhole in karstic limestone basement.

The evaluated response functions from Zone B show slight amplification, with a maximum amplification factor of 3, over a broad range of frequencies. Figure 21b is a compilation of the responses in reclaimed lands located in the harbour area including sites 8 and 9, the city area, and three sites along the city waterfront (sites 20, 22 and 27), including the best-fit analytical site-response function representing the Vila b model. There is no single, distinct pick of resonance, but rather a broad zone of resonance amplification centred at 4 Hz. In both areas, the surface of the reclaimed land is fairly small and the thickness of the fill is assumed from nearby seismic-reflection records to be of the order of 5 m at the waterfront area and up to about 10 m at the wharf platforms. Assuming a shear-wave velocity of 200 m/s (Fah et al. 1997) for the fill material over the bedrock and modern reef flat, the estimated thickness is comparable with the values in Table 8. The broad range of frequencies seen in the response functions are possibly due the effect of a near-shore sediment layer lying between the fill and the limestone basement.

The sediment thickness estimated from the measured resonance period according to the relationship: $T = 4H/V_s$ for each site is summarised in Table 8 below.

Table 8: Sediment thickness calculated from observed resonance period in Zone B, Port Vila

Site	V_s , Adopted Shear Velocity (m/s)	T, Measured Resonant Period (seconds)	H, Calculated Sediment Thickness (m)
reclaimed areas	200	0.20-0.33	10-16

Zone C incorporates two models in which a range of conditions give similar responses. These conditions include high relief, 2-5 m of weathered in-situ soils or colluvium and in places, faulted or deeply weathered and weakened limestone rock overlying Port Vila limestone basement.

Sites 29, 30 and 31 are located in Tassiriki around the bend between the two inland lagoons (see location map Figure 24). The spectral responses from these sites are included in Figure 21d with other Zone C site responses, and the best-fit analytical function representing Vila c model, in Figure 21c, e. This is a flat and sediment-filled area, at the junction of major faults forming the troughs in which the lagoons are located. The maximum amplitude of the spectral ratio is variable (between 2 and 3), over a frequency range of 5 to 7 Hz. Table 9 gives the possible ranges of sediment thickness as a function of the shear-wave velocity.

Table 9: Sediment thickness calculated from observed resonance period in the Tassiriki area, Zone C, Port Vila

Site	V_s , Adopted Shear Velocity (m/s)	T, Measured Resonant Period (seconds)	H, Calculated Sediment Thickness (m)
Tassiriki area	110	0.14-0.20	4-6

Zone D incorporates all areas encompassing sites where there was no amplification of the site response at all. Figure 21f-k is a compilation of the site responses from Zone D, including the best-fit analytical site-response function representing Vila d model.

Site 50 is a unique site. Figure 21l shows the site response at site 50, which is located on man-made fill along the main road to the airport near the northern limit of the city. This location had been used for many years as a dump site. Its resonant frequency is centred on 2.5 Hz with an amplification factor between 6 and 7. The best-fit analytical response is given by the Vila e model which assumes a shear-wave velocity in the upper layer of 100 m/s, suggesting a corresponding thickness of 10 m. The observed amplification factor at that site is not representative of site responses measured elsewhere in Port Vila.

The deep, trough-like valley in which the dump was located is a sinkhole feature that was probably already partly filled with colluvium before dumping was initiated. This situation may be representative of other troughs that have been surveyed in Port Vila during this project. In general, though, the responses of sites located at the bottom of such troughs show only a slightly higher site-amplification factor, about 2 to 3, at frequencies between 5 and 10 Hz compared to most other sites across Port Vila.

Table 10 summarises the variation in representative site-response parameters and computer-model parameters across Port Vila. Based on these observations, on the soil map (Quantin 1980), the topographic map and drillhole information provided by the Geology, Mines and Water Resources Department, we have prepared a zoning map of the Port Vila and Bauerfield Airport areas. We have also modelled the subsurface at some sites where the amplification site factor was above 2. The modelling process is based on matching the observed response functions with an analytical function that is calculated by assuming shear-wave velocities, densities and thicknesses of the layers underlying the surface. The computations associated with each model are made by using the program of Joyner (1977). In the modelling process, a very good fit to the observed resonance frequencies is achieved while the amplification factor is matched within 10% accuracy.

Table 10: Summary of general site-response observations and estimates of thickness, Port Vila

Site No.	Site name	Observed		Estimated by Modelling			
		Measured Resonant Frequency (Hz)	T Measured Resonant Period (seconds)	Preliminary Amplification from Site-Response Results	Adopted Model	V Adopted Shear Velocity (m/s)	H Calculated Sediment Thickness (m)
57	Bauerfield	1.2	0.83	4	Vila a	120	25
50	Depotoire	2.5	0.40	6	Vila e	100	10
8	Wharf	4	0.25	3	Vila b	200	13
29	Tassiriki	5-7	0.20-0.14	3	Vila c	110	4-6
78	Olhen	7	0.14	4	Vila c	110	4
82	Malopoa	8	0.12	3.2	Vila c	110	3.5
74	Ec. Francaise	9	0.10	3.5	Vila c	110	3

Based on the analysis of the observed site responses, the Port Vila and Bauerfield areas have been divided into a system of four zones, three of which are characterised by a predominant resonant frequency and a range of expected site-amplification factors. A site with no amplification factor would not be included in any of the first three zones, no matter what the shape of the spectral ratio function but, instead, would be placed in a special no-response zone. The sinkhole dump site, site 50, remains as a unique case.

To a first approximation, the relationship between the height of a building and its fundamental period of vibration can be expressed by the crude formula: $T = (\text{number of storeys})/10$. Two groups of building are considered in Port Vila: low-rise (1 to 5 storeys; $T = 0.1-0.5$) and high-rise (more than 5 storeys; $T > 0.5$) buildings. If the natural period of the ground matches the period of the building, then resonance may occur and increase the probability of damage to the building.

The four zones on the map (and the site responses typifying those zones) are as follows:

Zone A: Low resonant frequency < 1 Hz, thick surface sedimentary layer, found only in the Bauerfield area. Possible resonance effects for very high-rise building (more than 8-10 storeys). Note that for map Zone A, the Vila a model is the most applicable model with amplified frequencies of around 1.2 Hz. The Vila a model does not fit site 65, which has amplified frequencies of around 0.4 Hz. As mentioned earlier, this is perhaps a result of sediment thickness increasing across the zone from east to west towards Mele Bay.

Zone B: Resonant frequency between 3 and 5 Hz. Found in the reclaimed areas and in a transition zone between Bauerfield area and Port Vila. Possible resonance for medium- to high-rise building (5 to 10 storeys).

Zone C: Resonant frequency between 5 and 10 Hz. Found in some areas with shallow sediments (up to a few metres) over limestone basement or areas with complex topography (cliff lines, narrow grabens). Possible resonance for low-rise building (1 to 3 storeys, the most common structure in the Port Vila area).

Zone D: No site resonance. Limestone terraces and plateaux with little or no topographic variation.

Site 50: Resonant frequency at 2.5 Hz with high amplifications affecting medium-height buildings. Thick colluvium and anthropogenic fill in deep sinkholes.

This extensive study was aimed mainly at identifying locations within Port Vila that may exhibit unusual site effects during strong earthquakes. We have applied the Nakamura method over 100 sites across Port Vila and obtained rough estimations of the resonance frequencies and amplifications of the superficial layers. The Nakamura (1989) approach, based on seismic noise measurements, has gained great

popularity and is used by many across the globe. However, it is by now well known that this approach may fail at locations where amplification effects are only marginal. Even when a strong amplification is observed, the amplification factor is often not accurately determined and should be substantiated with additional geological and/or geophysical information.

Except for specific areas within Port Vila which exhibit amplification effects of engineering significance, most of the city area seems to be immune to site effects resulting from either soft sediments overlying hard rocks or from abrupt variations in topography. Despite the limitations inherent in the measurements and their interpretations, we may fairly assume that significant amplifications (say, with factor greater than 2), if they exist, would have been detected. For example, there is no resonance pattern associated with areas close to the harbour coastline where soft materials might be expected to accumulate. However, this is not true for the lagoons to the east of Port Vila where strong ground shaking has been reported during earthquakes. As a rule, we observed significant effects due to the topography in the site responses up to 10 Hz. The only sites where such large effects have been observed are located on the highest points in the city. Above 10 Hz, the complexity of the spectral ratio at some sites located on rocks could also indicate topographic effects, but buildings are unlikely to be affected much by resonance in this high-frequency band.

Earthquakes are felt frequently in the Port Vila and Bauerfield regions. Surprisingly, there are very few cases of reported damage to buildings over an approximately 100-year period (Louat & Baldassari 1989). There is also no reported dramatic site effect across Port Vila, but there are a few places where earthquakes are more strongly felt than elsewhere. These locations are coincident on the map with zones characterised by a resonant frequency. One location is along the Mele Bay road in the Bauerfield area (resonance around or below 1 Hz), where anomalous glass breakage during earthquakes has been reported. Other places that have experienced stronger shaking are spread along the shore of the inland lagoon system, starting from the Tassiriki area (the narrow neck that connects the two inland lagoons) which is characterised by a resonant frequency between 5 and 10 Hz affecting mostly low-rise buildings. It is clear that the strong shaking experienced at these locations is linked to ground-motion amplification due to significant soil thickness.

Table 11: Map Zones vs. Site-Response Models, Port Vila

Map Zones - Port Vila	Characteristic Resonant Frequency (Hz)	Applicable Models
A	1.2	Vila a
B	3.8	Vila b
C	7.5	Vila c
D	No Resonance	Vila d
Sinkhole/Dump Site 50	2.5	Vila e

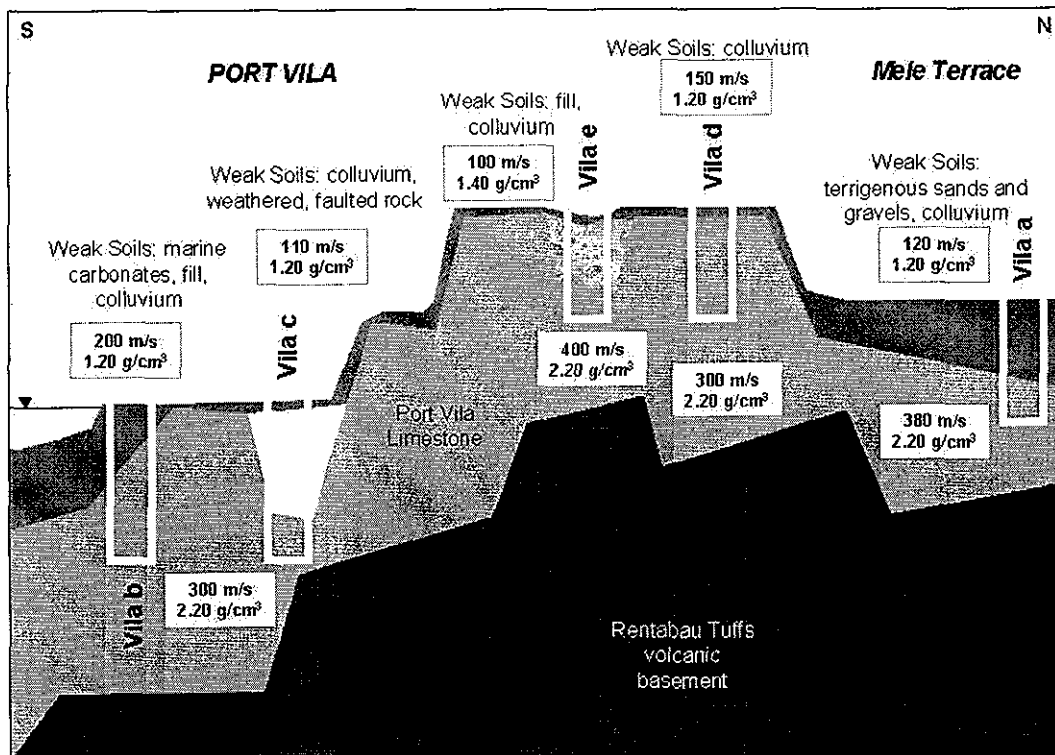
Table 12: Definition of Site-Response Models, Port Vila

Model	Layer	Thickness (m)	Shear Velocity (m/s)	Density (g/cm ³)	Geotechnical Description
Vila a	1	25	120	1.20	weak sediments
	2	Half-space	380	2.20	Port Vila limestone/tuff basement
Vila b	1	15	200	1.20	reclaimed areas/weak sediments
	2	Half-space	300	2.20	Port Vila limestone basement
Vila c	1	3.8	110	1.20	in-situ soils, weathered limestone
	2	Half-space	300	2.20	Port Vila limestone basement
Vila d	1	2.5	150	1.20	in-situ soils
	2	Half-space	300	2.20	Port Vila limestone basement
Vila e	1	10	100	1.40	dump site /in-situ soils
	2	Half-space	400	2.20	Port Vila limestone basement

In conclusion, the majority of sites in the Port Vila city area showed no significant site effects. In most places in the city, a significant thickness of uplifted, terraced limestone occurs over a basement of volcanic rocks and ash deposits, yielding no site effects. Site-amplification factors can be increased locally by both abrupt topographic effects and very localised, thick accumulations of sediments and soil controlled by block faulting and karst development. Both the surface geology and the results from seismic

zonation indicate a thicker sedimentary fill (up to several tens of metres) around the Bauerfield Airport and in the Mele terrace area. Low resonant frequencies (around and below 1 Hz) and amplification factors of the order of 2 were observed over this large area flanking Port Vila city. Any building development in this area should take these results into account.

Figure 22: Diagrammatic Summary Cross-Section, Port Vila



6.7 S_vE Results and Interpretation, Port Vila

Among the four investigated cities, Port Vila is at highest seismic hazard and risk. Estimated peak ground acceleration (PGA) values exceed 1.0 g. This is an extremely high level of acceleration that probably could not be accommodated by earthquake engineering. Given that the hazard assessments in this study are made for a prescribed probability of 10% in an exposure time of 50 years, the requirements are possibly too high a safety requirement for Port Vila. The risk level that is ultimately accepted is a matter of a governmental policy that will need to consider the socio-economic implication of that decision. These issues are not addressed in the current report.

We divided the city into four zones. Regnier et al. (2000) discussed the microzonation of expected site effects across Port Vila. The acceleration-response functions that characterise each zone are shown in Figure 23b and Figure 24. The mapped distribution of seismic microzones in Port Vila is shown in Figure 24.

Evidently, the highest risk to tall buildings is in Zone A, and to low- and medium-rise buildings it is in Zone B, Zone C and at the unique site 50. However, the results also feature a very dramatic effect of the non-linear behaviour of the soft soil layers. The evaluated spectral acceleration levels in Zone A ($T < 0.3$ sec), Zone B ($T < 0.2$ sec) and site 50 ($T < 2.0$ sec) are lower than those expected for buildings on hard rock. The physical interpretation of this observation is that the soft surface material is unable to transmit elastic energy and develops plastic deformation that absorbs the seismic energy. If this deformation occurs on or close to the surface, buildings will probably collapse due to foundation failure.

With respect to seismic hazards, Port Vila is definitely in a serious situation. From the engineering point of view, the adoption of the results obtained does not seem to be practical. A long-term multidisciplinary strategy to deal with earthquake hazards in Port Vila must be developed as soon as possible.

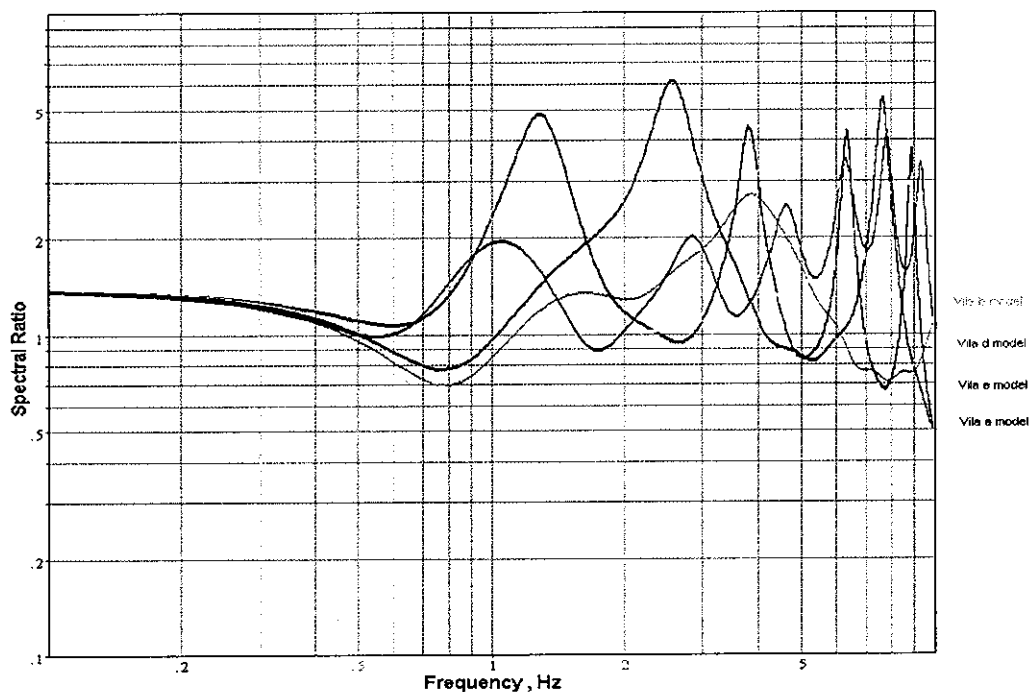
(over page: p.87)

Figure 23: Site-Response Models and Acceleration-Response Functions, Port Vila

(over page: p.88)

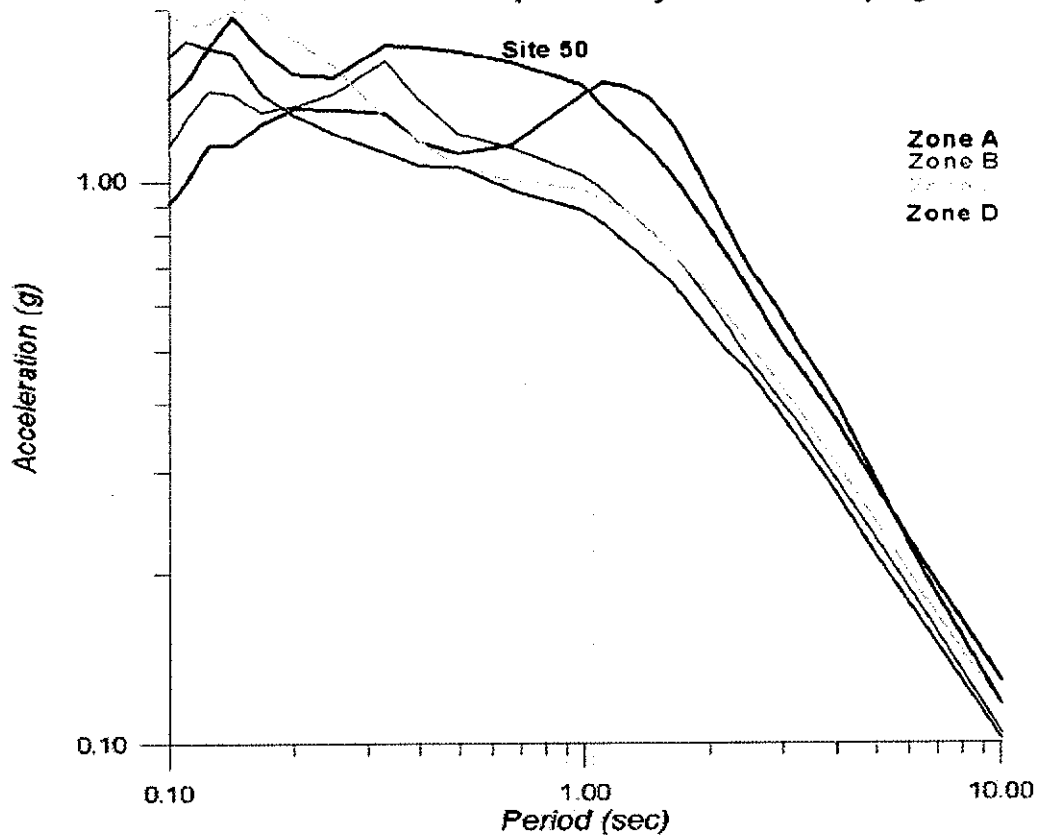
Figure 24: Seismic Microzonation Site-Response Map, Port Vila

PORT VILA SITE RESPONSE MODELS FOR ZONE A, ZONE B, ZONE C, ZONE D, ZONE E

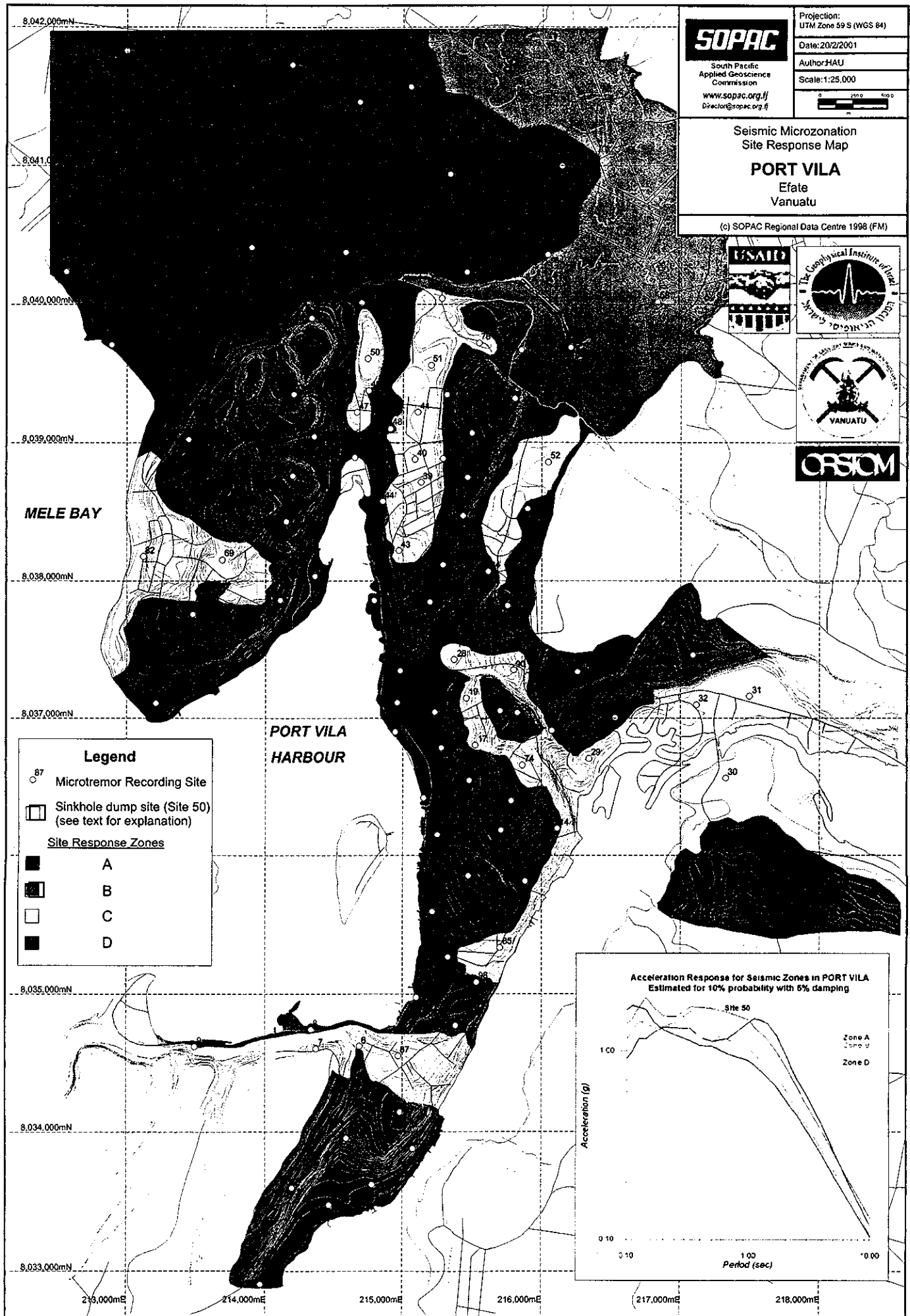


a

Acceleration Response for Seismic Zones in PORT VILA
Estimated for 10% probability with 5% damping



b



7 Seismic Microzonation of Honiara, Guadalcanal, Solomon Islands

7.1 Introduction, Honiara

Task Leader: Kenneth Bulehite (Energy, Water and Mineral Resources, Solomon Islands)

Collaborators: Alison Papabatu (Energy, Water and Mineral Resources, Solomon Islands), Uri Peled (GII)

Honiara is the capital and the major commercial and administrative centre in the Solomon Islands. It forms the base for a number of regional organisations and commercial ventures.

In the past, Honiara appears to have been shielded from the worst effects of large earthquakes occurring in the subduction zone related to the San Cristobal Trench close to the southwestern side of Guadalcanal. However, even though Honiara does not lie on an identified seismic zone, strong earthquakes have to be expected due to the city's geographical location close to the plate boundary.

Honiara is another city that, as a result of its geography, has little area available for urban expansion except for an alluvial plain on the eastern outskirts of the city. Similarly to the situation in Port Vila, the alluvial plain of the delta of the Lungga River has become a site for industrial growth, and it is in this setting that thick layers of weak sediment give rise to the potential for amplification of low-frequency earthquake shaking. The Honiara Hospital is a critical facility that is founded on another thick deposit of weak sediments at the mouth of the Mataniko River, closer to the inner city area.

The Department of Energy, Mines and Water Resources in conjunction with staff from the Geophysical Institute of Israel carried out site-response measurements in Honiara.

Details in digital format of geographical information for Honiara including geological boundaries, borehole locations and logs, seismic microzone boundaries and investigation sites, road and cadastral plans, digital terrain model and orthophotograph can be found in Swamy et al. (2001).

7.2 Tectonic Setting, Honiara

Oceanic crust was upraised in Late Miocene time to form the basement of Guadalcanal (Kroenke 1984). During this time, subduction began south of Guadalcanal and Bougainville at the New Britain and San Cristobal Trenches. Overthrusting of the old North Solomon Arc and folding of the Malaita and Santa Isabel oceanic sequences to form the Malaita Anticlinorium began as subduction commenced along the New Britain-South Solomon Trench.

Creation of the new northeast-dipping subduction zone on the south side of Guadalcanal and formation of the South Solomon Arc, entrapping North Solomon back-arc basin crust, transformed the New Georgia Basin from a back-arc basin to an inter-arc basin. Arc volcanism and plutonism on Guadalcanal, Bougainville and the Tabar-Feni Islands was accompanied by continued overthrusting of the old North Solomon Arc and folding of the Malaita Anticlinorium.

Due to its location at the northern edge of the new trench, Guadalcanal is experiencing uplift, more rapidly on the southern side than on the northern where Honiara is located.

7.3 Regional and Local Geology, Honiara

The gross geology of the area around Honiara is essentially one of a series of weak sedimentary cover rocks, predominately volcano-conglomerates, lithic sandstones and limestones, over a seaward (northward)-tilted basement of volcanic rocks. These formations are blanketed near the coast by superficial deposits of fringing Holocene coral reefs and associated carbonates, as well as prograding deltaic deposits associated with major rivers. The distribution of lithologies in Honiara, together with the locations of boreholes, is shown in Figure 25.

According to Hackman (1979) the structure is controlled essentially by faulting; north-northwest trending faults are the most persistent along their strike, and many of these structures are high-angle reverse faults which have contributed to composite horsting of the pre-Pliocene basement. Northeast-trending faults are prominent in association with the Mbelapoke Hill crater; their initiation was probably contemporaneous with Plio-Pleistocene volcanicity.

The Mbonehe Limestone, about 100 m thick, is predominately a poorly bedded, recrystallised, biomicrite or calcarenite of late Early Miocene to Middle Miocene age. The formation rests non-conformably on an eroded platform of Poha microdiorite, and dips generally at 10°-25° NE.

Hackman states that the Lungga Beds consists of three distinct facies: in the south the Plio-Pleistocene Mataniko Siltstone is composed of about 400 m of volcanic arenites and wackes with turbidite features. Around Honiara and Mount Austen, the Pleistocene Honiara Beds, about 400 m thick, forms a sequence of calcareous volcanic arenites and rudites: these phase westwards into the Saghalu Conglomerate, which form a mantle of volcanoclastic rudites derived from the northwest. The Kombito Marl is a lagoonal back-reef facies of the Honiara Beds.

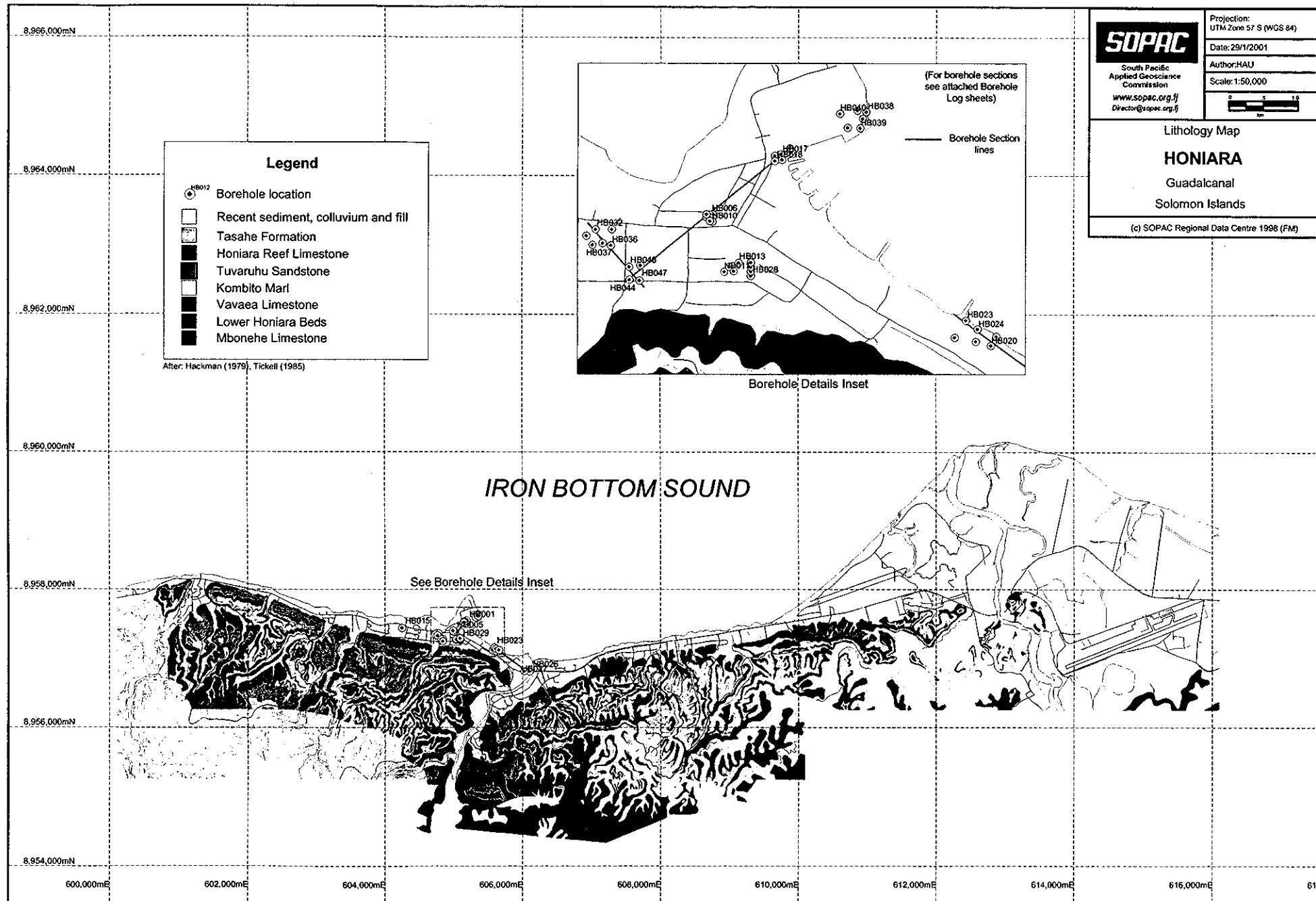
In the Honiara town area, the Honiara Beds are capped by about 60 m of corallgal biolithite and derived debris, forming the Honiara Reef Limestone. These are associated with a series of terraces, ranging in height from 700 m above sea level to 100 m below.

Most of the coast is fringed with Recent extinct, emergent coral reef, which is currently being swamped by alluvium derived from the major rivers. Extensive alluvium occurs in valleys along the courses of the Lungga, Poha and Umasani Rivers. In the coastal-fringe area of the city, excavations and boreholes indicate a predominance of Recent carbonate gravels, sands and silts to depths of between 10 and 30 m.

Selected borehole sections shown in Figures 26-28 serve to illustrate the subsurface distribution of engineering soil and rock types classified according to the Unified Soil Classification System (USBR 1973). The borehole logs are accompanied by a log of soil strength where these are available, based mainly on Standard Penetration Test N-values. Details of the legend for the soil-type logs and instructions on the interpretation of the strength logs are given in Appendices 1-3.

(over page: p.91)

Figure 25: Lithology Map (including Borehole Positions), Honiara



(over page: p.93)

Figure 26: Borehole Logs HB 032 to HB 047, Honiara

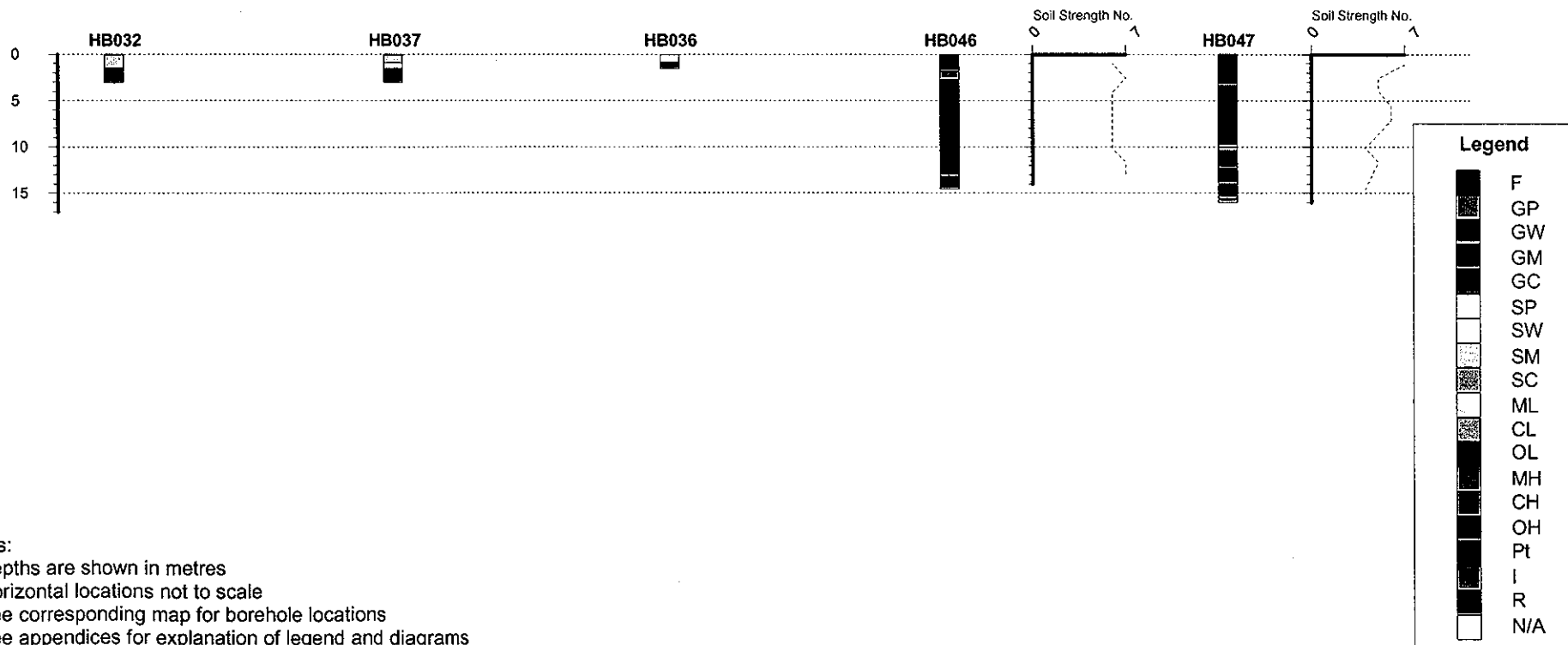
(over page: p.94)

Figure 27: Borehole Logs HB 044 to HB 017, Honiara

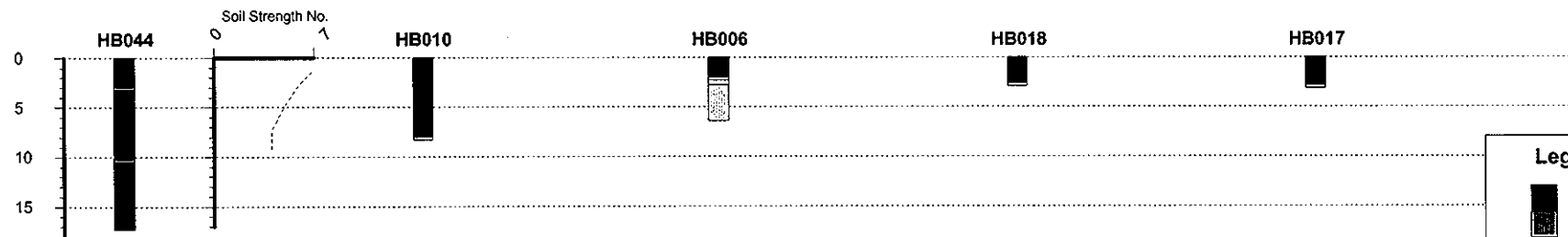
(over page: p.95)

Figure 28: Borehole Logs HB 023 to HB 026, Honiara

Borehole Logs Honiara Guadalcanal, Solomon Islands



Borehole Logs Honiara Guadalcanal, Solomon Islands

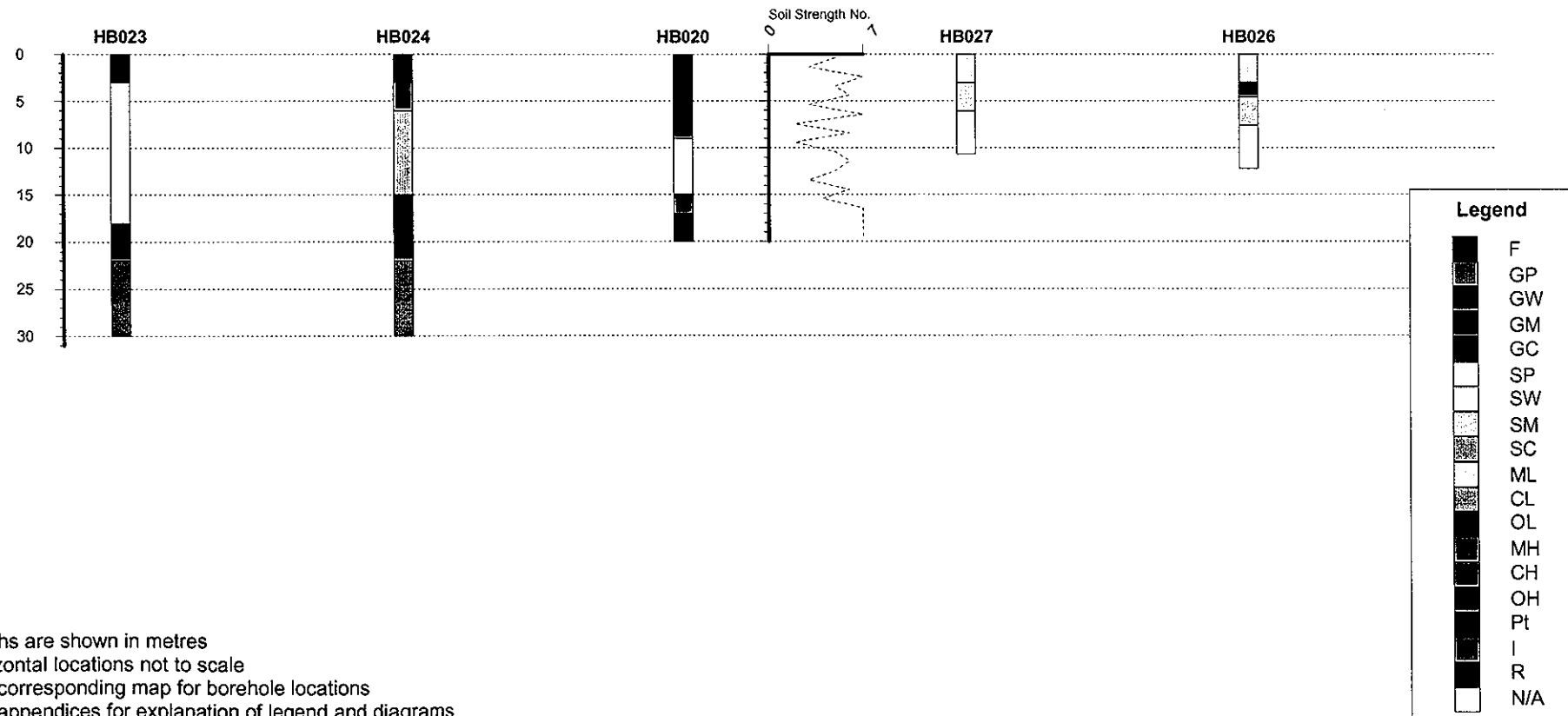


Legend	
	F
	GP
	GW
	GM
	GC
	SP
	SW
	SM
	SC
	ML
	CL
	OL
	MH
	CH
	OH
	Pt
	I
	R
	N/A

Notes:

1. Depths are shown in metres
2. Horizontal locations not to scale
3. See corresponding map for borehole locations
4. See appendices for explanation of legend and diagrams

Borehole Logs Honiara Guadalcanal, Solomon Islands



Notes:

1. Depths are shown in metres
2. Horizontal locations not to scale
3. See corresponding map for borehole locations
4. See appendices for explanation of legend and diagrams

7.4 History of Damaging Earthquakes, Honiara

The epicentres of large shallow earthquakes (magnitude > 5, focal depth < 70 km) for the period 1973-1998, as well as earlier historical events, within an arbitrary 250 km radius of Honiara are shown in Figure 29 and catalogued in Table 13.

Earthquakes originating near the southern side of Guadalcanal, in the Marau Sound Sea have damaged the city of Honiara. Some of the reported cases had the potential to cause injury or loss of life in Honiara (Tuni 1981).

1977: The 1977 earthquake caused considerable damage in Honiara although there was no loss of life (Thompson & Tuni 1977). The seven main shocks felt within the first 8 hours of the event ranged in magnitude between 5.2 and 7. The maximum intensity felt in Honiara was MM 7. The Hong Kong and Shanghai Bank (NPF Building) in the centre of Honiara city was seriously damaged when non-structural concrete-block in-fill walls cracked and separated from the steel column frame. The water main from Tuvaruhu was ruptured, and piers on the main wharf settled. Most non-reinforced buildings in the Chinatown and Mataniko areas were cracked and some collapsed. According to Hackman (1979) and Tuni (1981), nearly all buildings constructed in flat coastal areas on poorly consolidated coralline beach deposits and river alluvium experienced damage.

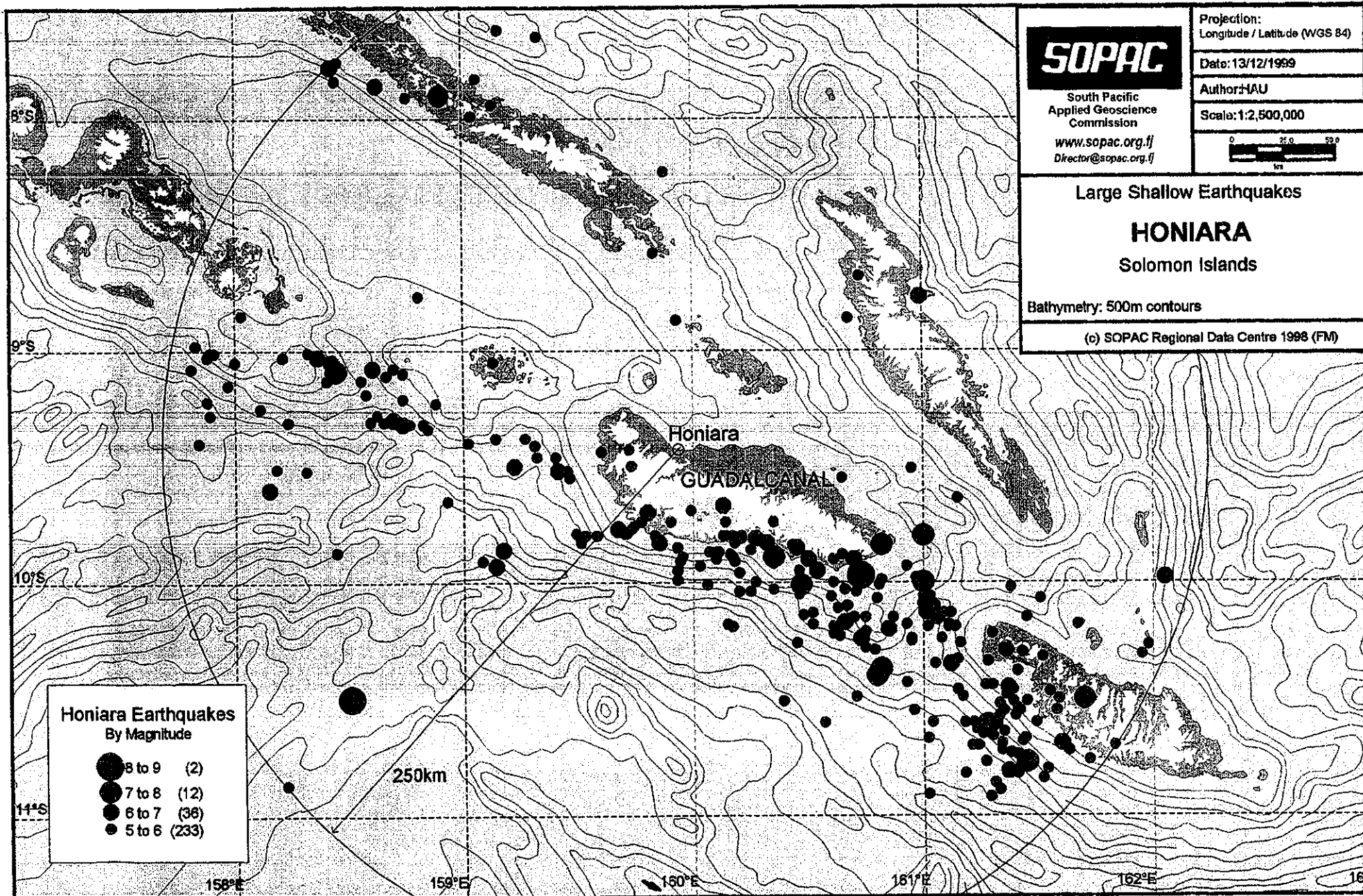
1984: In the 1984 Ms 7.5 earthquake (Tuni 1986), severe shaking occurred for about 15-20 seconds and major damage occurred to the NBSI Building housing the Australian High Commission at Point Cruz. The structure of the building was severely damaged and the building was declared unsafe for occupation at the time.

The Department of Works of the Ministry of Transport, Works and Utilities, in trying to counter potential earthquake damage in Honiara and Solomon Islands has, as a matter of policy, adopted standards from developed countries for building development (Standards Australia 1993, 1998). However, it has not yet developed a national legislative framework to govern the whole construction and building industry.

The location of damage that has occurred during previous earthquake events suggests that earthquake shaking is amplified by the Recent sediments overlying the Honiara Beds and Honiara Reef Limestone.

(over page: p.97)

Figure 29: Large Shallow Earthquakes around Honiara



(over page: p.99-103)

Table 13: Catalogue of Large Shallow Earthquakes, Honiara

Circle Search: Earthquakes for Honiara		
Circle Centre Point:	Latitude:	9.4256 S
	Longitude:	159.9591 E
Radius:	250 km	
Magnitude Range:	5.0-9.0	
Depth Range:	0-70 km	

Date	Origin Time (UTC)	Latitude	Longitude	Depth (km)	Magnitude	Solution	Recorder	Epicentral Distance from Honiara (km)
12-Apr-26	083200.00	-10.00	161.00	60	7.5	Ms		130
3-Oct-31	191300.00	-10.50	161.70	25	7.9	Ms		224
15-Dec-35	070700.00	-9.80	161.00	60	7.6	Ms		121
30-Apr-39	025500.00	-10.50	158.50	25	8.1	Ms		198
8-Jan-61	053900.00	-9.90	160.50	50	6.5	ML		77
13-Feb-63	181300.00	-9.90	160.70	30	6.5	ML		88
25-Jul-64	224700.00	-9.70	159.80	21	5.6	ML		44
17-Jul-65	072000.00	-9.70	159.80	41	6.0	ML		44
27-Nov-65	120100.00	-9.70	159.80	41	6.0	ML		44
15-Jun-66	005900.00	-10.40	160.80	31	7.8	Ms		141
5-Jan-69	132600.00	-7.90	158.90	47	7.5	Ms		204
29-Jun-72	162200.00	-9.90	160.10	40	5.5	ML		55
14-Feb-73	093258.80	-9.93	160.93	62	5.9	mb	GS	120
9-Jun-73	082127.30	-10.29	161.36	70	6.6	UK	PAS	181
25-Jul-73	060838.70	-8.68	160.73	69	5.5	mb	GS	117
31-Jul-73	204452.20	-8.77	160.99	30	6.3	UK	PAS	134
10-Sep-73	181101.80	-10.24	161.08	68	5.0	mb	GS	152
8-Jan-74	152408.40	-10.18	161.67	56	5.3	mb	GS	205
14-Jan-74	233210.60	-9.64	161.15	53	5.6	mb	GS	133
21-Jan-74	114928.70	-8.86	160.68	38	5.4	mb	GS	100
24-Jan-74	150630.40	-10.02	161.38	69	5.2	mb	GS	169
9-Apr-74	202536.00	-10.05	160.46	25	5.1	mb	GS	88
8-Jun-74	215605.20	-9.55	160.65	34	5.4	mb	GS	77
12-Jun-74	212721.20	-10.18	160.93	33	5.4	mb	GS	135
25-Jun-74	165827.10	-9.51	160.95	35	5.0	mb	GS	108
15-Aug-74	033558.00	-9.05	159.13	59	5.5	mb	GS	99
9-Mar-75	231310.00	-9.15	157.97	13	5.0	mb	GS	219
15-Mar-75	031436.60	-9.83	159.51	30	5.2	mb	GS	66
28-Apr-75	083649.90	-8.85	158.03	41	5.6	mb	GS	220
8-May-75	152757.00	-9.87	160.11	38	5.1	mb	GS	51
24-Aug-75	143531.60	-9.74	159.90	45	5.4	mb	GS	34
15-Sep-75	034335.20	-7.65	159.33	60	5.2	mb	GS	208
3-Oct-75	141617.10	-10.13	160.52	56	5.8	mb	GS	98
14-Nov-75	222746.00	-10.07	161.51	67	5.4	mb	GS	183
5-Jun-76	082007.20	-10.09	161.01	61	6.6	UK	PAS	136
6-Jun-76	033228.20	-10.10	161.05	54	5.5	mb	GS	140
11-Jun-76	152626.00	-10.13	161.09	52	5.4	mb	GS	145
16-Jun-76	221231.10	-10.14	161.01	68	5.4	mb	GS	139
19-Jun-76	062213.00	-10.46	161.15	47	5.1	mb	GS	172
28-Jun-76	121556.00	-9.11	158.66	53	5.0	Ms	GS	146
8-Nov-76	020917.30	-9.95	159.93	9	5.1	mb	GS	57
22-Dec-76	202646.60	-10.55	161.58	66	5.1	mb	GS	215
24-Dec-76	120032.50	-8.87	159.93	68	5.1	mb	GS	61
19-Jan-77	235942.40	-9.69	159.99	25	5.4	mb	GS	29
21-Jan-77	200858.10	-10.66	161.30	51	5.1	mb	GS	200
20-Apr-77	231310.40	-9.83	160.32	33	6.8	UK	PAS	59
20-Apr-77	231840.80	-9.90	160.61	33	5.9	mb	GS	88
20-Apr-77	234250.50	-9.89	160.35	19	7.6	UK	PAS	66
20-Apr-77	234913.10	-9.84	160.82	33	7.5	Ms	GS	105
20-Apr-77	235617.60	-9.82	160.29	33	5.7	mb	GS	56
21-Apr-77	000249.00	-9.67	160.13	33	6.1	mb	GS	33
21-Apr-77	000527.70	-9.80	160.21	33	5.5	mb	GS	49
21-Apr-77	004433.50	-10.87	158.22	33	5.7	mb	GS	248
21-Apr-77	010709.60	-9.83	160.18	32	5.5	mb	GS	50
21-Apr-77	012032.80	-9.89	159.95	32	5.5	mb	GS	51
21-Apr-77	013404.80	-9.92	160.35	33	5.1	mb	GS	68
21-Apr-77	013752.70	-9.50	159.73	33	5.2	mb	GS	26
21-Apr-77	032658.80	-9.83	160.31	22	5.4	mb	GS	59
21-Apr-77	033426.60	-9.91	160.18	33	5.2	mb	GS	58
21-Apr-77	034430.00	-9.74	159.77	33	5.0	mb	GS	41

Date	Origin Time (UTC)	Latitude	Longitude	Depth (km)	Magnitude	Solution	Recorder	Epicentral Distance from Honiara (km)
21-Apr-77	040744.50	-9.85	159.93	27	5.1	mb	GS	47
21-Apr-77	042409.60	-9.97	160.73	33	8.1	UK	PAS	103
21-Apr-77	050628.50	-10.15	160.70	33	5.8	mb	GS	113
21-Apr-77	055418.00	-9.98	160.74	33	5.3	mb	GS	104
21-Apr-77	063103.90	-9.88	160.16	31	5.3	mb	GS	54
21-Apr-77	065322.00	-9.99	160.82	21	5.0	mb	GS	113
21-Apr-77	071851.10	-10.24	160.73	33	6.0	Ms	GS	123
21-Apr-77	080454.80	-10.04	160.25	20	5.1	mb	GS	75
21-Apr-77	093658.00	-10.15	160.75	51	5.0	mb	GS	117
21-Apr-77	094538.20	-10.28	160.75	33	5.6	mb	GS	127
21-Apr-77	102603.10	-9.95	160.46	33	5.0	mb	GS	80
21-Apr-77	161235.50	-10.18	160.15	20	5.4	mb	GS	86
21-Apr-77	165311.50	-10.19	160.63	12	5.4	Ms	GS	111
22-Apr-77	024324.00	-9.87	160.10	22	5.1	mb	GS	51
22-Apr-77	031100.20	-10.17	160.66	51	6.2	UK	PAS	112
22-Apr-77	071845.20	-10.12	161.05	48	5.2	mb	GS	141
22-Apr-77	121103.70	-9.89	160.17	33	5.3	mb	GS	56
22-Apr-77	132036.30	-9.91	159.94	33	5.3	mb	GS	53
22-Apr-77	182511.00	-10.03	160.66	25	5.3	mb	GS	101
22-Apr-77	191340.30	-9.74	160.14	20	5.1	mb	GS	39
23-Apr-77	053337.30	-10.06	160.60	1	5.0	mb	GS	98
23-Apr-77	060421.50	-10.81	161.40	33	5.1	mb	GS	219
23-Apr-77	162950.20	-9.96	160.20	26	5.2	mb	GS	64
23-Apr-77	183851.90	-9.86	160.25	33	5.0	mb	GS	57
24-Apr-77	010421.50	-10.00	160.74	33	5.0	mb	GS	106
24-Apr-77	062852.30	-9.87	160.07	29	5.4	mb	GS	50
27-Apr-77	131423.20	-10.21	160.63	56	5.1	mb	GS	113
29-Apr-77	055911.70	-9.99	159.93	8	5.1	mb	GS	62
29-Apr-77	155859.20	-10.29	160.79	13	5.1	mb	GS	132
1-May-77	083529.50	-9.88	160.65	19	5.5	mb	GS	91
2-May-77	204418.20	-9.93	160.03	33	5.1	mb	GS	55
7-May-77	093918.80	-9.74	160.35	16	5.1	mb	GS	55
11-May-77	223400.20	-10.24	160.95	51	5.2	mb	GS	140
16-May-77	181046.60	-10.19	161.11	43	5.0	mb	GS	151
20-May-77	235627.60	-10.22	160.61	33	5.7	Ms	GS	113
27-May-77	225813.30	-9.40	159.02	33	5.3	mb	GS	102
28-May-77	130424.50	-10.03	160.35	10	5.0	mb	GS	78
18-Jun-77	221049.60	-9.77	159.67	11	6.1	UK	PAS	48
2-Jul-77	005509.00	-9.95	160.54	16	6.0	UK	PAS	85
30-Jul-77	140025.80	-10.60	161.49	34	5.0	mb	GS	211
8-Aug-77	125845.00	-10.57	161.33	32	5.8	mb	GS	196
6-Sep-77	043327.90	-10.35	161.05	61	5.5	mb	GS	157
30-Sep-77	035817.90	-10.32	161.52	33	5.2	mb	GS	196
22-Oct-77	021608.90	-10.06	161.03	48	5.1	mb	GS	137
5-Nov-77	060257.60	-10.11	161.00	70	5.6	mb	GS	136
22-Dec-77	175826.50	-9.95	160.70	33	5.1	mb	GS	99
2-Apr-78	022403.40	-9.80	160.14	47	5.0	mb	GS	45
20-Apr-78	071839.50	-8.98	157.83	27	5.2	mb	GS	238
29-Apr-78	042110.40	-9.85	160.45	46	6.2	mb	GS	71
16-Jun-78	071151.10	-9.08	157.81	44	5.2	mb	GS	238
25-Jun-78	231520.00	-10.74	161.41	46	5.0	mb	GS	215
25-Jul-78	072906.20	-9.65	158.93	33	5.0	mb	GS	115
9-Sep-78	095453.40	-9.98	160.97	33	5.2	mb	GS	126
2-Oct-78	154647.20	-10.76	161.72	66	5.0	mb	GS	242
8-Nov-78	182636.80	-10.89	161.33	33	5.1	mb	GS	220
9-Nov-78	001703.10	-10.84	161.52	33	5.1	mb	GS	231
9-Nov-78	005128.30	-10.81	161.37	29	6.1	UK	PAS	217
9-Nov-78	034518.70	-10.82	161.37	33	5.0	mb	GS	217
10-Nov-78	122334.60	-10.73	161.38	33	5.3	mb	GS	211
10-Nov-78	171354.40	-10.72	161.63	33	5.3	mb	GS	232

Date	Origin Time (UTC)	Latitude	Longitude	Depth (km)	Magnitude	Solution	Recorder	Epicentral Distance from Honiara (km)
12-Nov-78	081114.30	-10.54	161.41	61	5.2	mb	GS	201
13-Nov-78	162407.30	-10.92	161.29	21	5.2	Ms	GS	220
14-Nov-78	011959.10	-10.50	161.59	68	5.0	mb	GS	214
29-Dec-78	161022.90	-10.47	161.55	69	5.1	mb	GS	208
31-Dec-78	230051.80	-10.34	161.28	66	5.3	mb	GS	176
23-Apr-79	225842.80	-9.28	157.89	33	5.0	mb	GS	227
21-May-79	145530.10	-10.13	161.12	56	5.3	mb	GS	149
29-May-79	062452.80	-7.91	158.75	47	5.1	mb	GS	213
19-Jul-79	102633.40	-9.89	160.36	33	5.0	mb	GS	67
23-Oct-79	081901.40	-10.60	161.31	33	6.2	UK	BRK	196
23-Oct-79	093609.70	-10.60	161.18	33	5.0	mb	GS	185
23-Oct-79	095106.70	-10.61	161.28	22	7.2	UK	BRK	195
23-Oct-79	100342.10	-10.60	161.04	33	5.6	mb	GS	175
23-Oct-79	100724.70	-10.63	161.23	33	5.7	mb	GS	192
23-Oct-79	103805.00	-10.82	161.18	33	5.3	mb	GS	203
23-Oct-79	104026.10	-10.70	161.21	33	5.5	mb	GS	196
23-Oct-79	111959.20	-10.49	161.17	33	5.2	mb	GS	177
23-Oct-79	114156.70	-10.70	161.24	33	5.0	mb	GS	198
23-Oct-79	135510.30	-10.60	161.22	33	5.4	mb	GS	189
23-Oct-79	150732.90	-10.15	161.45	33	5.5	mb	GS	181
27-Oct-79	070856.80	-10.72	161.34	33	5.3	mb	GS	208
6-Nov-79	113831.50	-9.50	159.22	30	6.5	UK	PAS	81
22-Feb-80	211542.10	-10.69	161.60	68	6.1	UK	PAS	227
18-Jun-80	045403.60	-8.23	159.88	68	5.0	mb	GS	131
26-Jun-80	072008.20	-9.13	158.55	33	5.3	mb	GS	157
26-Jun-80	072612.60	-9.10	158.73	33	5.2	mb	GS	139
26-Jun-80	083945.20	-9.19	158.57	65	5.2	mb	GS	154
21-Dec-80	182541.10	-9.05	158.42	28	6.5	UK	PAS	173
3-Jan-81	190950.80	-9.84	160.43	32	5.6	mb	GS	69
31-Mar-81	220631.50	-9.31	158.59	7	5.3	mb	GS	150
4-Sep-81	234449.70	-9.79	159.49	38	5.4	mb	GS	65
4-Oct-81	101817.32	-10.55	161.42	57	5.1	mb	GS	202
4-Oct-81	102742.04	-9.41	159.31	23	5.7	mb	GS	71
7-Oct-81	020513.90	-9.25	158.11	33	5.1	mb	GS	204
9-Oct-81	121940.23	-9.98	162.05	50	6.5	Ms	PAS	236
6-Jan-82	090138.22	-10.52	161.33	70	5.5	mb	GS	192
5-Mar-82	002758.52	-10.86	161.31	49	5.2	mb	GS	216
12-May-82	064231.04	-10.23	160.64	35	5.3	mb	GS	116
17-Jul-82	093534.41	-9.05	158.00	33	5.0	mb	GS	218
14-Aug-82	052940.56	-10.10	160.67	33	5.1	mb	GS	107
2-Nov-82	103346.58	-10.38	161.41	63	5.2	mb	GS	190
2-Jan-83	125406.75	-9.80	159.83	33	5.3	mb	GS	43
15-Feb-83	011431.21	-10.30	161.43	42	5.1	mb	GS	187
2-May-83	034626.65	-9.31	158.23	33	5.0	mb	GS	189
6-Sep-83	010558.76	-9.31	158.65	37	5.5	mb	GS	143
1-Oct-83	030544.59	-10.11	160.63	33	5.4	mb	GS	105
7-Feb-84	213321.49	-10.01	160.47	18	7.7	Ms	PAL	85
7-Feb-84	224700.15	-10.21	160.75	33	5.3	mb	GS	121
8-Feb-84	003951.09	-9.81	160.27	27	6.4	Ms	GS	54
8-Feb-84	075748.25	-10.19	160.17	15	5.1	mb	GS	87
8-Feb-84	082949.33	-10.00	160.61	23	5.0	mb	GS	95
27-Feb-84	014212.91	-10.26	160.45	33	5.2	mb	GS	106
27-Apr-84	040245.93	-10.55	161.35	62	5.2	mb	GS	196
12-Jul-84	030232.19	-10.46	161.39	37	5.5	mb	GS	193
21-Dec-84	012621.41	-9.22	157.88	39	5.2	mb	GS	229
27-Sep-85	033908.52	-9.83	159.85	31	6.9	Ms	GS	45
19-Nov-85	082015.32	-9.01	157.91	9	5.2	mb	GS	229
20-Apr-86	091718.25	-10.91	161.02	33	5.1	mb	GS	201
29-Nov-86	035238.76	-10.19	160.61	51	5.0	mb	GS	110
11-Dec-86	195612.58	-10.49	160.71	61	5.5	mb	GS	143

Date	Origin Time (UTC)	Latitude	Longitude	Depth (km)	Magnitude	Solution	Recorder	Epicentral Distance from Honiara (km)
17-Jan-87	112201.61	-10.77	161.27	51	5.7	Ms	BRK	206
2-Jul-87	192123.66	-9.38	159.14	18	5.0	mb	GS	90
8-Sep-87	050811.90	-10.68	161.43	60	5.0	mb	GS	211
10-Aug-88	043826.17	-10.37	160.82	34	7.4	Ms	GS	140
10-Aug-88	045640.23	-10.04	160.71	33	5.9	mb	GS	107
10-Aug-88	050929.14	-10.43	160.93	33	5.0	mb	GS	153
10-Aug-88	051541.49	-9.87	158.44	33	5.3	mb	GS	173
10-Aug-88	052018.35	-10.01	160.81	33	5.1	mb	GS	113
10-Aug-88	063842.89	-10.20	160.85	39	6.6	Ms	GS	130
10-Aug-88	071830.72	-9.80	160.17	33	5.2	mb	GS	47
10-Aug-88	103432.69	-10.14	160.48	35	5.6	mb	GS	97
10-Aug-88	153433.06	-10.55	160.96	33	5.4	Ms	GS	165
10-Aug-88	192404.33	-10.51	160.39	33	5.0	Ms	GS	128
10-Aug-88	211913.13	-10.18	160.52	41	5.3	Ms	GS	102
10-Aug-88	224125.99	-10.67	161.02	33	5.0	Ms	GS	180
13-Aug-88	162026.01	-10.01	160.06	33	5.2	mb	GS	65
14-Feb-89	062021.33	-10.45	161.37	31	6.4	Ms	GS	191
15-May-89	233433.65	-9.80	159.53	23	5.9	mb	GS	62
28-May-89	040323.51	-9.23	158.88	10	5.1	mb	GS	120
18-Oct-89	114050.22	-10.15	161.06	45	6.1	mb	GS	145
18-Oct-89	123516.96	-10.18	161.11	69	5.4	mb	GS	151
14-Dec-89	191353.85	-10.44	161.27	37	5.8	Ms	GS	182
1-Jan-90	144900.69	-10.51	161.39	36	5.2	mb	GS	196
15-May-90	200732.17	-10.15	161.05	57	5.5	mb	GS	143
10-Jul-90	031759.29	-10.35	161.12	66	6.2	mb	BRK	163
26-Jul-90	192739.47	-9.34	158.84	33	5.2	mb	GS	122
21-Sep-90	034825.49	-10.26	161.16	54	5.4	mb	GS	160
6-Nov-90	172754.71	-7.62	159.16	39	5.5	mb	GS	217
9-Feb-91	161858.37	-9.93	159.14	10	6.9	Ms	GS	105
9-Feb-91	163032.53	-9.86	159.17	10	6.4	Ms	GS	98
13-Feb-91	164452.09	-9.91	159.08	21	5.5	mb	GS	110
23-Jun-91	050315.43	-7.83	159.06	60	5.3	mb	GS	202
6-Aug-91	212302.77	-9.55	159.46	18	5.0	mb	GS	55
26-Sep-91	091450.45	-9.28	158.62	25	5.2	mb	GS	147
3-Oct-91	154614.34	-10.15	160.87	45	5.1	mb	GS	127
14-Oct-91	155812.79	-9.09	158.44	23	7.1	Ms	GS	170
14-Oct-91	161657.22	-9.08	158.60	31	6.4	Ms	GS	153
14-Oct-91	165553.01	-9.03	158.36	18	6.1	Ms	GS	181
14-Oct-91	193151.80	-9.21	158.73	26	5.0	Ms	GS	137
15-Oct-91	033022.15	-9.03	158.21	16	5.0	mb	GS	196
15-Oct-91	090717.41	-9.13	158.40	25	5.1	mb	GS	174
13-Nov-91	021453.90	-9.01	158.32	29	5.2	mb	GS	185
13-Nov-91	223017.64	-8.77	158.80	33	5.2	mb	GS	146
27-Dec-91	041946.69	-9.01	157.89	33	5.8	mb	GS	231
27-Dec-91	171427.24	-9.03	157.88	10	5.3	mb	GS	232
27-Apr-92	042140.50	-9.38	159.27	10	5.2	mb	GS	75
17-May-92	154649.04	-7.94	159.13	50	5.0	mb	GS	187
19-May-92	144250.70	-9.46	159.32	32	5.6	Ms	GS	70
29-Jun-92	000705.26	-10.67	161.44	58	5.5	mb	GS	212
6-Jul-92	005533.01	-10.60	160.57	10	5.1	mb	GS	145
25-Aug-92	020713.01	-10.04	160.20	26	5.5	Ms	GS	73
25-Aug-92	021055.13	-10.00	160.27	33	5.1	mb	GS	72
5-Dec-92	143722.38	-9.77	159.73	34	5.1	mb	GS	45
30-Dec-92	062526.67	-7.99	159.04	50	5.6	mb	GS	188
14-May-93	212945.04	-10.82	161.36	24	5.4	mb	GS	217
29-May-93	145125.19	-10.06	161.00	63	5.0	mb	GS	133
4-Aug-93	074510.06	-10.82	161.41	32	5.4	Mw	HRV	221
17-Aug-93	203512.72	-9.51	158.18	26	5.1	mb	GS	194
13-Sep-93	215201.45	-10.31	161.95	16	5.4	Mw	HRV	239
22-Oct-93	081927.08	-10.48	161.36	67	5.4	Mw	HRV	192

Date	Origin Time (UTC)	Latitude	Longitude	Depth (km)	Magnitude	Solution	Recorder	Epicentral Distance from Honiara (km)
29-Oct-93	014347.56	-10.25	160.95	52	5.1	mb	GS	141
26-Nov-93	232004.17	-9.60	158.15	17	6.2	Ms	GS	199
21-Feb-94	053132.12	-10.27	161.98	29	5.2	mb	GS	240
9-Mar-94	165837.63	-9.44	159.60	10	5.8	Mw	HRV	38
27-Mar-94	134512.26	-10.33	161.15	54	5.4	mb	GS	164
18-Apr-94	192158.80	-9.46	159.40	19	5.1	mb	GS	61
26-Jun-94	215515.38	-9.76	159.74	30	5.5	mb	GS	43
22-Jul-94	165748.42	-7.78	158.42	19	6.0	Mw	HRV	248
25-Jul-94	154645.86	-7.76	158.45	29	5.6	mb	GS	247
19-Oct-94	125408.40	-9.52	159.45	5	5.5	Mw	HRV	56
20-Nov-94	025715.62	-9.79	159.71	23	5.8	mb	GS	48
5-Dec-94	162009.36	-8.58	159.83	49	5.8	mb	GS	94
14-Dec-94	072853.25	-9.52	159.41	16	6.1	Mw	GS	60
16-Apr-95	132347.59	-9.80	159.58	20	5.6	mb	GS	58
1-May-95	182934.59	-10.57	161.40	32	5.7	Mw	GS	201
11-Jun-95	195333.90	-9.08	158.69	25	5.1	Ms	GS	144
22-Sep-95	200539.25	-10.07	160.80	42	5.6	Mw	HRV	116
23-Sep-95	014504.73	-10.44	161.30	36	5.3	mb	GS	184
2-Nov-95	160841.01	-9.79	159.70	12	5.8	Mw	HRV	49
7-Jan-96	080029.95	-10.65	161.26	33	5.4	Mw	HRV	196
31-Mar-96	013931.78	-10.19	161.02	64	5.4	Mw	HRV	143
8-Apr-96	204639.13	-10.70	161.83	61	5.5	Mw	HRV	248
11-Apr-96	112426.92	-10.80	161.54	42	5.9	mb	GS	230
2-Aug-96	125529.30	-10.77	161.45	33	7.1	Ms	GS	220
28-Aug-96	160145.25	-10.64	161.35	32	5.6	mb	GS	202
5-Sep-96	125203.18	-10.33	161.15	33	5.1	mb	GS	164
29-Dec-96	204923.57	-10.19	161.14	52	5.2	Mw	HRV	154
6-Oct-97	183530.31	-9.32	158.82	33	5.3	mb	GS	125
6-Oct-97	190805.16	-9.32	158.76	33	5.3	mb	GS	132
6-Oct-97	205244.61	-9.30	158.69	33	6.1	Mw	GS	139
10-Oct-97	184552.40	-9.32	158.73	33	6.0	Mw	HRV	135
14-Dec-97	170223.36	-10.13	161.00	65	5.0	mb	GS	137
18-Dec-97	210319.96	-9.80	160.13	33	5.1	mb	GS	45
28-Feb-98	221512.05	-7.84	158.44	44	5.7	Mw	GS	241
10-Apr-98	073331.74	-9.81	160.21	33	5.1	mb	GS	50
10-Oct-98	042658.38	-10.51	161.45	33	5.0	mb	GS	202
25-Nov-98	180525.81	-7.79	158.60	47	6.2	Mw	GS	234
17-Dec-98	135555.13	-10.14	161.02	33	5.2	Mw	HRV	140
29-Mar-99	014335.87	-10.69	161.34	33	5.4	Ms	GS	205
2-Jul-99	182940.08	-10.22	161.30	64	5.1	mb	GS	171
26-Sep-99	235032.52	-9.43	159.72	58	5.2	mb	GS	26
19-Oct-99	133648.84	-9.52	158.31	33	5.3	mb	GS	181

7.5 Microtremor Recordings - Site-Response Measurements, Honiara

The Seismology Section of the Department of Energy, Mines & Water Resources carried out microtremor recordings at 24 sites within the Honiara city boundaries.

Stacked groups of site-response spectra are shown together with the appropriate spectral models in Figure 30, and the site characteristics are summarised in Table 14.

The locations of recording sites is shown at the end of the Honiara chapter (see Figure 33).

The recording sites were selected by the staff of the seismology section to cover the full range of site conditions. The areas of main interest were the industrial areas, downtown Honiara and the densely populated areas such as Chinatown, New Chinatown, and the Lord Howe Settlement. The microtremor recording sites were carefully selected to avoid areas that were constantly subjected to cultural noise such as produced by factory machinery and traffic.

The gain settings for the recording amplifier differ from one site to another. Site 19 (PWD Workshop) near the Mataniko River, site 2 (Soap Factory) and site 3 (R & R Engineering) on the Lungga River delta at Ranadi, and site 15 (USP Centre Hall) at Lawson Tama were set at 58 dB. Microtremors at site 14 (Lord Howe Settlement) on the eastern side of the Mataniko River delta plain were recorded at 46 dB, and all remaining sites were recorded at 52 dB.

Microtremor data were recorded for at least 30 minutes at each site according to equipment and procedures described in Section 4.1. The SRD software was used to analyse the microtremor data collected according to the Nakamura method. Several samples of spectral ratios were obtained for each site, from which the average spectral ratio was calculated.

The sites which are relatively close to the wave-dominated shoreline at Ranadi on the Lungga River delta, such as R & R Engineering and the School of Marine Studies, seem to exhibit very large amplifications in the low-frequency range (0.2-0.9 Hz). This effect may have been caused by standing waves from the pounding of surf on the sandy strand of Ranadi Beach.

The data quality from some of the sites was very low; some seismograms continuously displayed transient cultural noise (clipped in amplitude) and hence data analysis for these sites was not possible.

(over page: p.105)

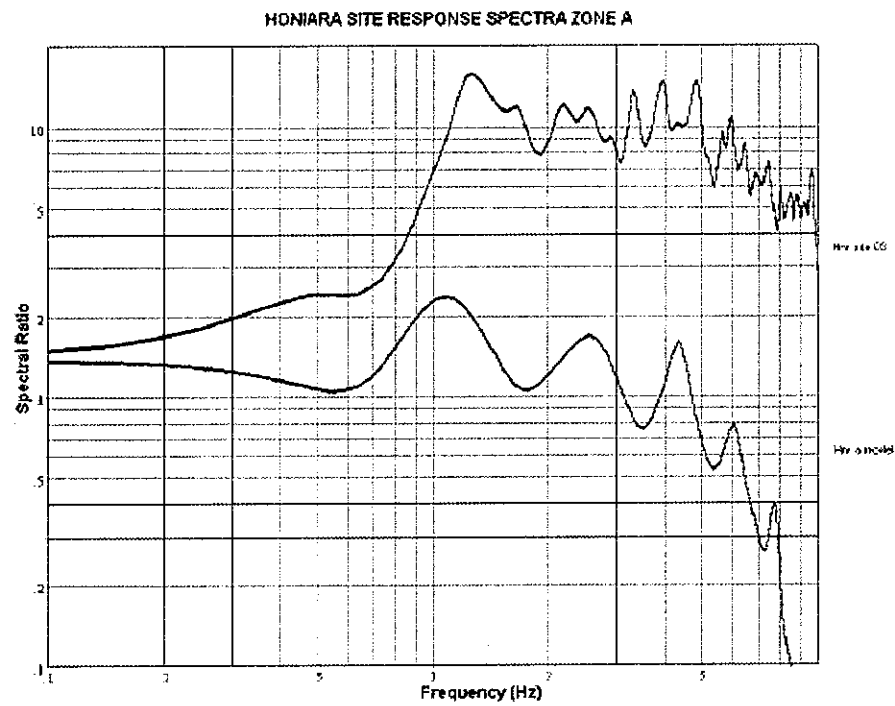
Table 14: Microtremor Site-Response Recordings, Honiara

Site Response Table, Honiara

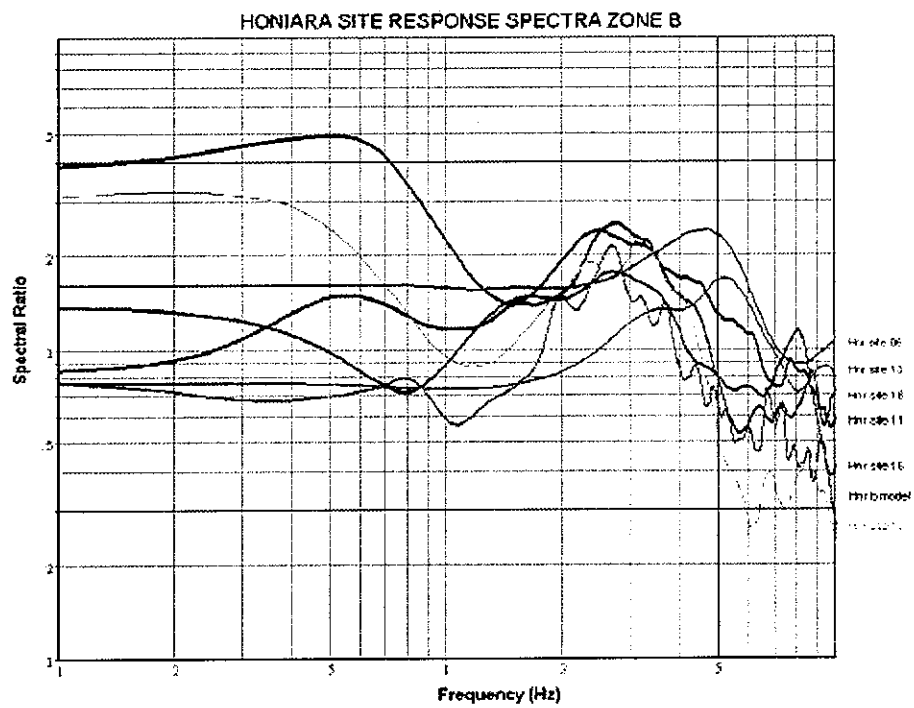
HONIARA Site No.	Amplification Factor	Amplified Frequency Hz	Site Response Class	UTC Date	UTC Time	WGS84 UTM Easting	WGS84 UTM Northing	Locality
1	1	No Res	C	031097	0025	609,764.76	8,957,544.69	School of Marine Studies, Ranadi
2	Data Corrupted	-	-	170398	1540	611,190.65	8,958,464.05	Soap Factory, Ranadi
3	5	1.3	A	310398	1505	610,416.60	8,957,943.26	R & R Engineering, Ranadi
4	1	No Res	C	220398	1043	612,062.82	8,958,235.61	ROC Rice Farm, Ranadi
5	1	No Res	C	311097	0445	604,921.92	8,956,980.32	(Old ATC) Admin Centre, Vavay
6	3	5	B	311097	0315	606,066.28	8,956,386.32	Honiara Secondary School
7	1	No Res	C	220398	1534	607,247.83	8,956,970.06	Bahai Centre
8	Data Corrupted	-	-	290398	1431	605,615.35	8,957,033.58	Victory Bldg, Main Market, Pt Cruz
9	1	No Res	C	230398	1140	605,674.92	8,957,075.82	Main Market, Pt Cruz
10	Data Corrupted	-	-	290398	1538	605,020.38	8,957,255.58	Hong Kong Palace, Pt Cruz
11	2.5	2.7	B	020498	1531	604,997.99	8,957,371.11	NBSI/ANZ, Pt Cruz
12	1	No Res	C	300398	1032	605,115.29	8,957,623.40	SIPA, Head Office, Pt Cruz
13	3	5	B	021097	0400	605,280.93	8,957,766.16	Wharf, Port Area, Pt Cruz
14	Data Corrupted	-	-	240398	1527	606,374.12	8,956,892.68	Lord Howe Settlement, Mataniko
15	2	3	B	230398	1018	606,472.59	8,956,603.85	USP Centre, Mutipurpose Hall, Lawson Tama
16	3	2	B	250398	0912	606,601.42	8,956,786.15	Main Road, Lawson Tama
17	1	No Res	C	250398	1016	606,739.14	8,956,880.63	Hospital, Hostel Wing
18	2.5	2.5	B	011097	2350	605,846.86	8,956,980.15	Sea King Restaurant, PWD
19	Data Corrupted	-	-	020498	1432	606,018.66	8,956,916.65	PWD Workshop
20	1	No Res	C	021097	0230	604,555.21	8,957,481.85	Art Gallery, Govt Bldg
21	1	No Res	C	260398	1052	605,005.88	8,957,448.98	Mobil Depot, Pt Cruz
22	Data Corrupted	-	-	260398	0929	604,751.33	8,957,285.98	National Museum, Pt Cruz
23	Data Corrupted	-	-	250398	1138	606,199.88	8,956,621.96	China Town
24	Data Corrupted	-	-	250398	1437	605,687.45	8,956,454.81	Number 3, New China Town

(over page: p.107-108)

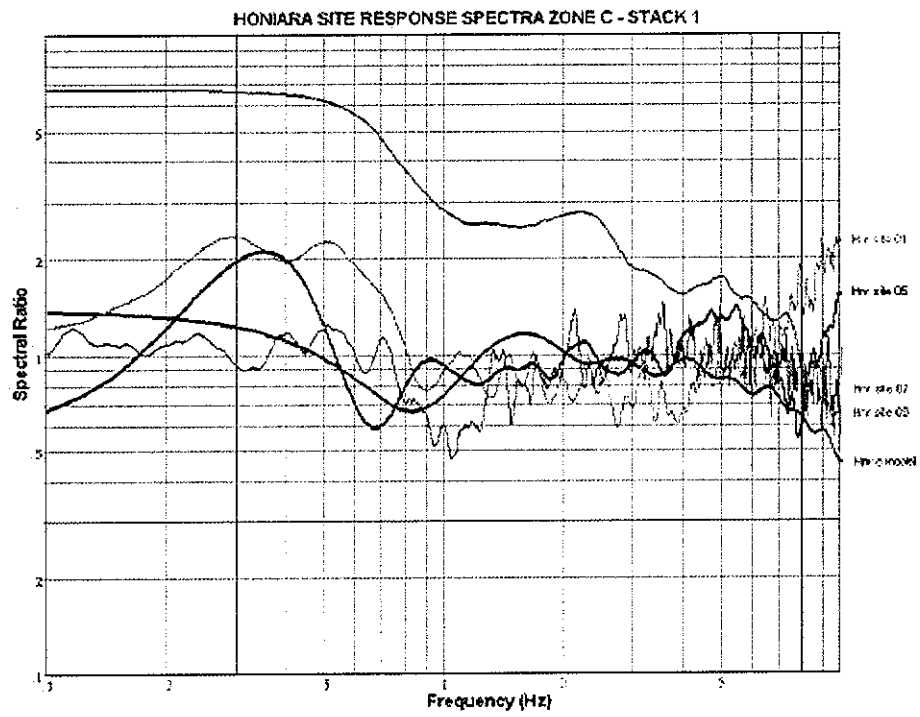
Figure 30: Site-Response Spectra. Honiara



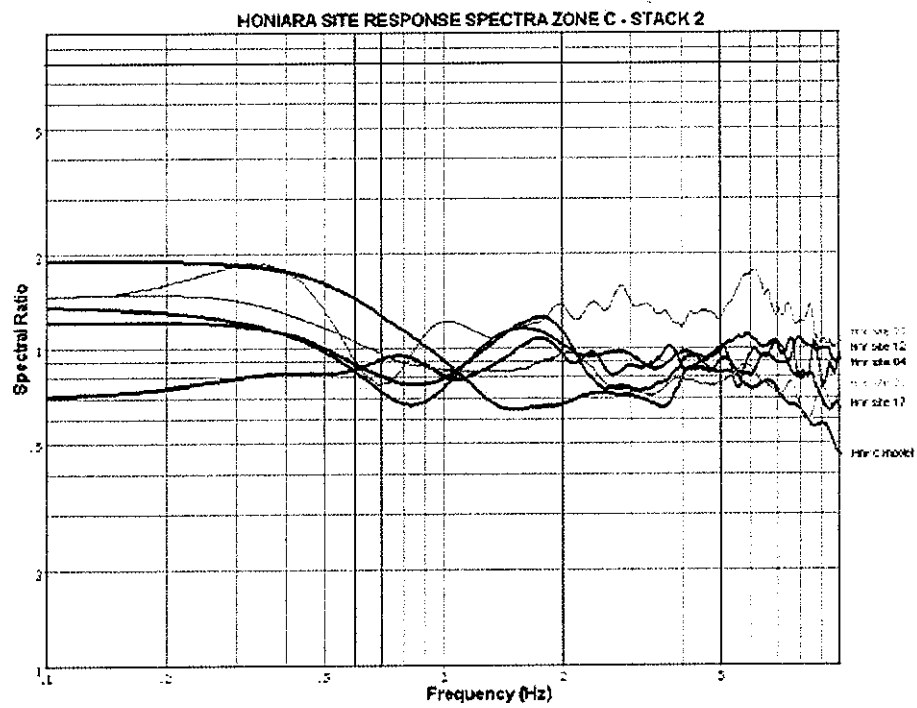
a



b



c



d

7.6 Analysis of Site-Response Measurements and Zonation of Honiara

A number of models were developed to fit the various results from the microtremor measurements across Honiara. Modelling of the subsurface was undertaken for sites where an amplification factor greater than 2 was observed. The modelling process is based on matching the observed response functions with an analytical function that is calculated by assuming shear-wave velocity, density and thickness of the layers underlying the surface. The estimated sediment thickness for each site is summarised in Table 15 below.

Three models were chosen for the range of available results, having various combinations of layer thickness, shear-wave velocity and density. The characteristic frequencies of the spectral models and corresponding zone names are shown in Table 16, and the critical parameters defining the spectral models are shown in Table 17.

A diagrammatic, generalised cross-section of subsurface conditions and their relationship to the adopted subsurface models is shown in Figure 31.

The spectral models are compared in Figure 32a, and the acceleration-response functions for each zone are shown in Figure 32b. The analytical response functions of the models are plotted in Figure 32a and Figure 33.

Each model refers to a distinct class or zonation for mapping purposes. It should be noted that the Honiara dataset is incomplete due to corruption of several data files and an inconsistency in gain settings during data collection. For this reason, the data collected at sites 2, 8, 10, 14, 19, 22, 23, and 24 were not incorporated into the interpretation. These sites have been marked on the Seismic Microzonation Site-response Map of Honiara (end of this chapter) for location reference so that the sites can be re-occupied at a later date. A preliminary interpretation is described below using the remaining 16 site responses.

Zone A is characterised by the Hnr a model, a two-layer plus half-space model. The top layer consists of 20 to 35 m of surficial, weak, coastal-deltaic sediments and the second layer, 30 m of weakly cemented Honiara Reef Limestone overlying terrigenous conglomerates of the Honiara Beds. Although the characterisation of the zone is inferred from one site-response recording only, the response was distinct, and characterised by high-amplitude magnification at a low frequency.

Zone B is characterised by the Hnr b model, a one-layer plus half-space model. The surface layer consists of 10 to 20 m of weak, nearshore alluvial and carbonate sediments overlying the Honiara Beds. The characteristics of this zone were again distinct, with mid-frequency (*circa* 3 Hz), high-amplitude magnification responses.

Zone C is characterised by the Hnr c model, a one-layer plus half-space model. The top layer consists of a very thin layer (0 to 5 m) of the Honiara Beds and/or coastal sediments, overlying basement. The site responses in this zone had very low or no amplification and for mapping purposes, define the no-response zone.

The evaluated site-response function from Zone A (Figure 30a) shows high amplification at a frequency of about 1.2 Hz. The response function was calculated from microtremor recordings at Honiara site 3, namely R & R Engineering in Ranadi, on the seaward edge of the Lungga River delta. The gain settings at site 3 were set incorrectly, and as can be seen from the graph, there has been an artificial increase in the amplification (to 30+), making true characterisation of resonant amplification difficult. However, it is the sharp change of phase (from 0.7 Hz to 1.2 Hz) in the prominent primary mode (peaking at 1.2 Hz) that characterises the response and hence a distinct class or zone. The thickness of the weak, top layer of Zone A was estimated to be around 30 m from limited subsurface information. Assuming a shear-wave velocity of 200 m/s, a modelled thickness of 20 to 35 m is to be expected. A water bore drilled north of Henderson Airport during WWII is reported by Baker (1950) to have found clay with intercalated sands and gravels to at least 150 m.

For resonant ground amplification at a frequency of 1.2 Hz, it can be estimated that 8-10 storey buildings constructed in that zone could be at higher risk of damage due to the ground amplification if the natural resonance of the building matches that of the ground. Although this is a crude estimate (since other factors such as building-to-ground coupling effects need to be considered), further data collection in Zone A should enable a more accurate analysis to be made of the types of building that might be affected.

The evaluated site-response functions from Zone B indicate considerable amplification, with factors ranging from 2 to 3. Figure 30b shows a compilation (stack) of site responses from site 13 (Wharf), site 11 (Point Cruz), site 18 (Sea King Restaurant), site 16 (Main Road), site 15 (USP Centre) and site 6 (Honiara Secondary School). Most of these sites are located on soft sediments around the estuarine flats of the Mataniko River.

It can be seen from the graph that amplification of the response at most sites occurs at approximately 3 Hz, although amplification at site 6 and site 13 occurs at a slightly higher frequency, 5 Hz. A shear-wave velocity of 200 m/s for the weak upper layer was assumed, and the thickness can be estimated theoretically from the measured resonance period according to the relationship: $T = 4H/V_s$. Note also, that site 21, although located in Zone B, actually has a typical Zone C response (no response, see Figure 30c). The result for site 21 is ambiguous and data acquisition should be repeated.

Table 15: Sediment thickness calculated from observed resonance period in Zone B, Honiara

Site	V_s , Adopted Shear Velocity (m/s)	T, Measured Resonant Period (seconds)	H, Calculated Sediment Thickness (m)
Point Cruz (11)	200	0.35	18
USP Centre (15)	200	0.32	16
Main Road (16)	200	0.35	18
Wharf (13)	200	0.20	10
Honiara School (6)	200	0.21	11

The thickness adopted for layer 1 in the Hnr b model is 19 m, to give a close correspondence with the site-response functions. This choice is supported by borehole logs from the commercial downtown area and from the vicinity of the lower Mataniko River, indicating a thickness of at least 14 m of medium-dense sands lying below sea level. Tickell (1985) records 9 m of gravel in a borehole in the Mataniko valley at Tuaruhu.

From the model above, buildings of 3 to 4 storeys in Zone B might be considered at higher risk of damage if the natural resonance of the building matches that of the ground in practice.

Site responses from microtremor recordings have been assigned to Zone C on the basis that they show very low (or no) amplification over all frequencies (Figure 30c, d). The compilation includes spectral ratios from site 21 (Mobil Depot), site 12 (SIPA), site 4 (ROC Rice Farm), site 20 (Art Gallery), site 1 (Marine School), site 5 (Admin Centre), site 7 (Bahai Centre) and site 9 (Main Market). As can be seen from the graph, the spectral ratio of site 9 appears to have a high amplification but, again, this is due to an incorrect gain setting resulting in an artificially high response. Site 9 is more comparable with a no-amplification response spectrum.

Table 16: Map Zones vs. Site-Response Models, Honiara

Map Zones - Honiara	Characteristic Resonant Frequency (Hz)	Applicable Models
A	1.3	Hnr a
B	3.0	Hnr b
C	No Resonance	Hnr c

Table 17: Definition of Site-Response Models, Honiara

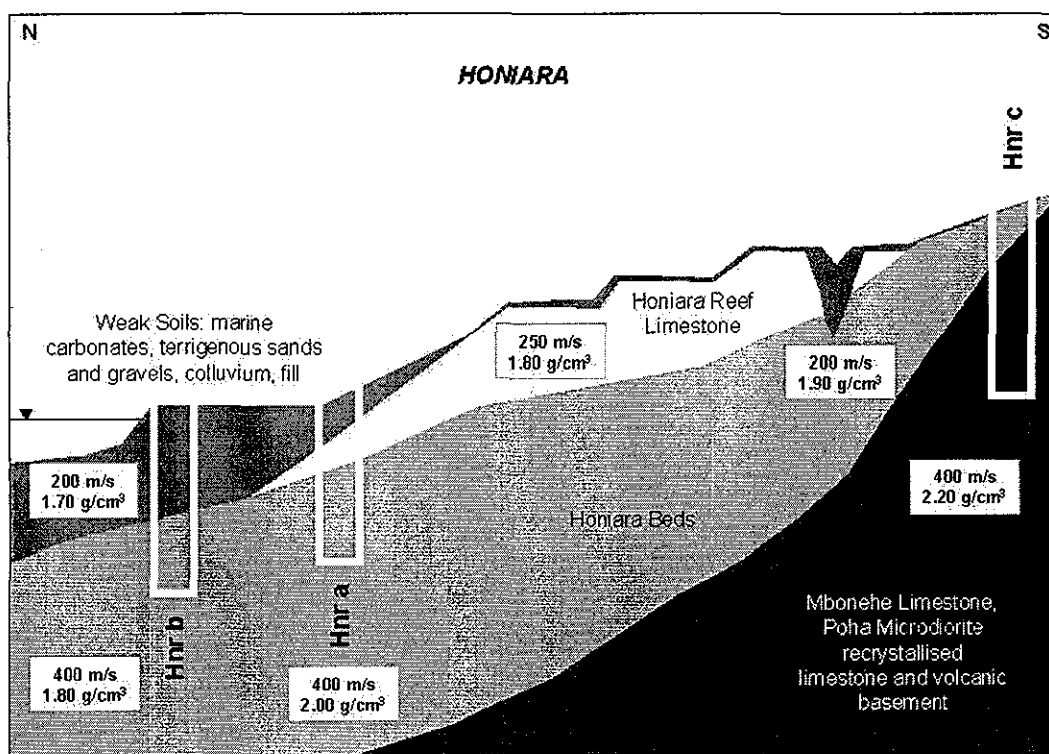
Model	Layer	Thickness (m)	Shear Velocity (m/s)	Density (g/cm ³)	Geotechnical Description
Hnr a	1	35	200	1.70	weak sediments
	2	30	250	1.80	Honiara Reef Limestone
	3	Half-space	400	2.00	Honiara Beds
Hnr b	1	19	200	1.70	weak sediments
	2	Half-space	400	1.80	Honiara Beds
Hnr c	1	5	200	1.90	Honiara Beds
	2	Half-space	400	2.20	basement

The majority of the Zone C spectral ratios have medium-high spectral amplitudes below approximately 0.7 Hz, but this should not be seen as representing an amplified primary mode. The seismometer does not effectively record true response below 0.7 to 0.5 Hz, so that this component of the response spectra

cannot be properly interpreted. The Hnr c model has been chosen as the best-fit model for all response spectra in Zone C.

A zonation map of Honiara (Figure 33) has been prepared using the site-response analysis, the surface geology map (Hackman 1979) and the topographic map (SOLMAP 1988). Zone A is characterised by thick (20 to 35 m), weak, estuarine surface sediments with a low resonant frequency, < 1.3 Hz. These characteristics might result in greater damage to 8-10 storey buildings where the natural resonance of the building matches the ground shaking. Zone B is characterised by thinner sediments (10 to 20 m) with a resonant frequency of 3 Hz, potentially causing amplification in buildings of 3 to 4 stories. Zone C is a non-resonant (no-amplification) zone with a very thin surface layer (0 to 5 m) of the Honiara Beds overlying basement.

Figure 31: Diagrammatic Summary Cross-Section, Honiara



7.7 SvE Results and Interpretation, Honiara

Peak ground acceleration (PGA) estimates for Honiara yield a value of 0.5 g. Based on site-response investigations we divided Honiara into three zones. The acceleration-response functions that characterise these zones are shown in Figures 32b and 33.

The distribution of seismic microzones in Honiara is shown in Figure 33.

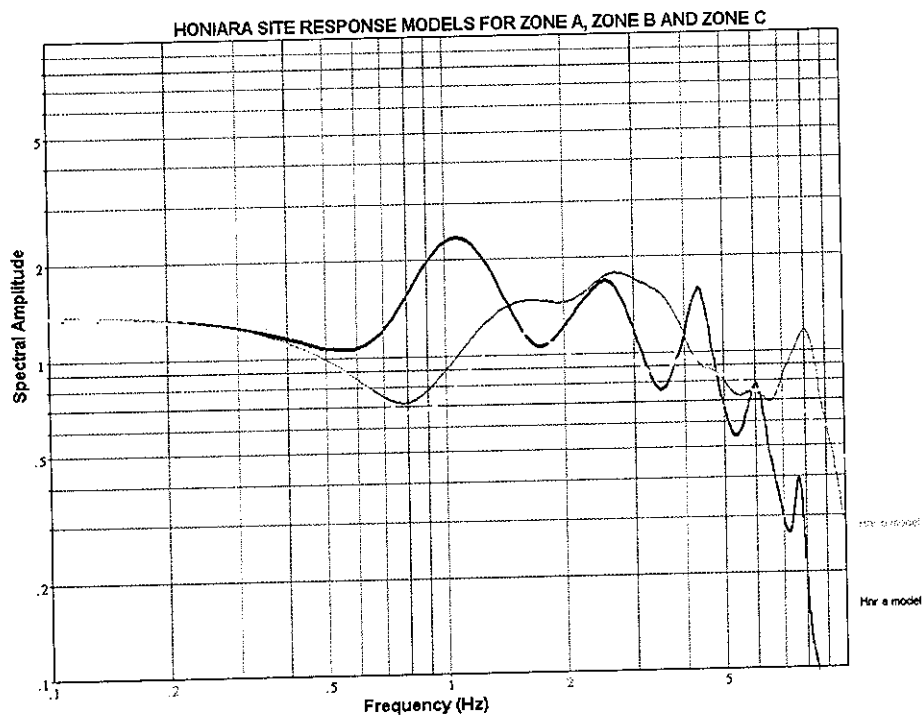
The area characterised as Zone C does not show significant site effects, and the estimated acceleration levels are similar to those expected on hard rock sites. Slightly higher accelerations are expected to develop in structures/buildings with natural periods of 0.1-0.4 s (1-5 floors) that are located in Zone B. The worst conditions are in Zone A. Our results show that for the prescribed probability of occurrence, we should expect significant non-linear effects of the soils that may be accompanied by surface deformation. Here again, the lower accelerations over a wide spectrum are the result of the absorption of seismic energy by the soft soil, possibly by transforming elastic motions into plastic deformation.

(over page: p.113)

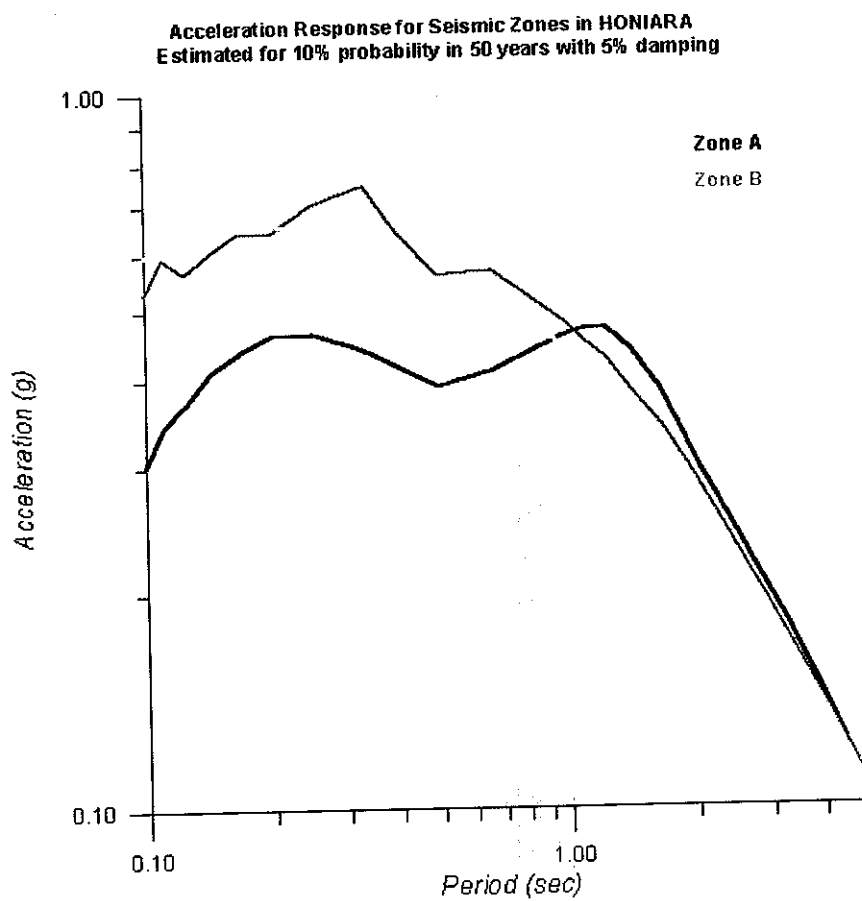
Figure 32: Site-Response Models and Acceleration-Response Functions, Honiara

(over page: p.114)

Figure 33: Seismic Microzonation Site-Response Map, Honiara

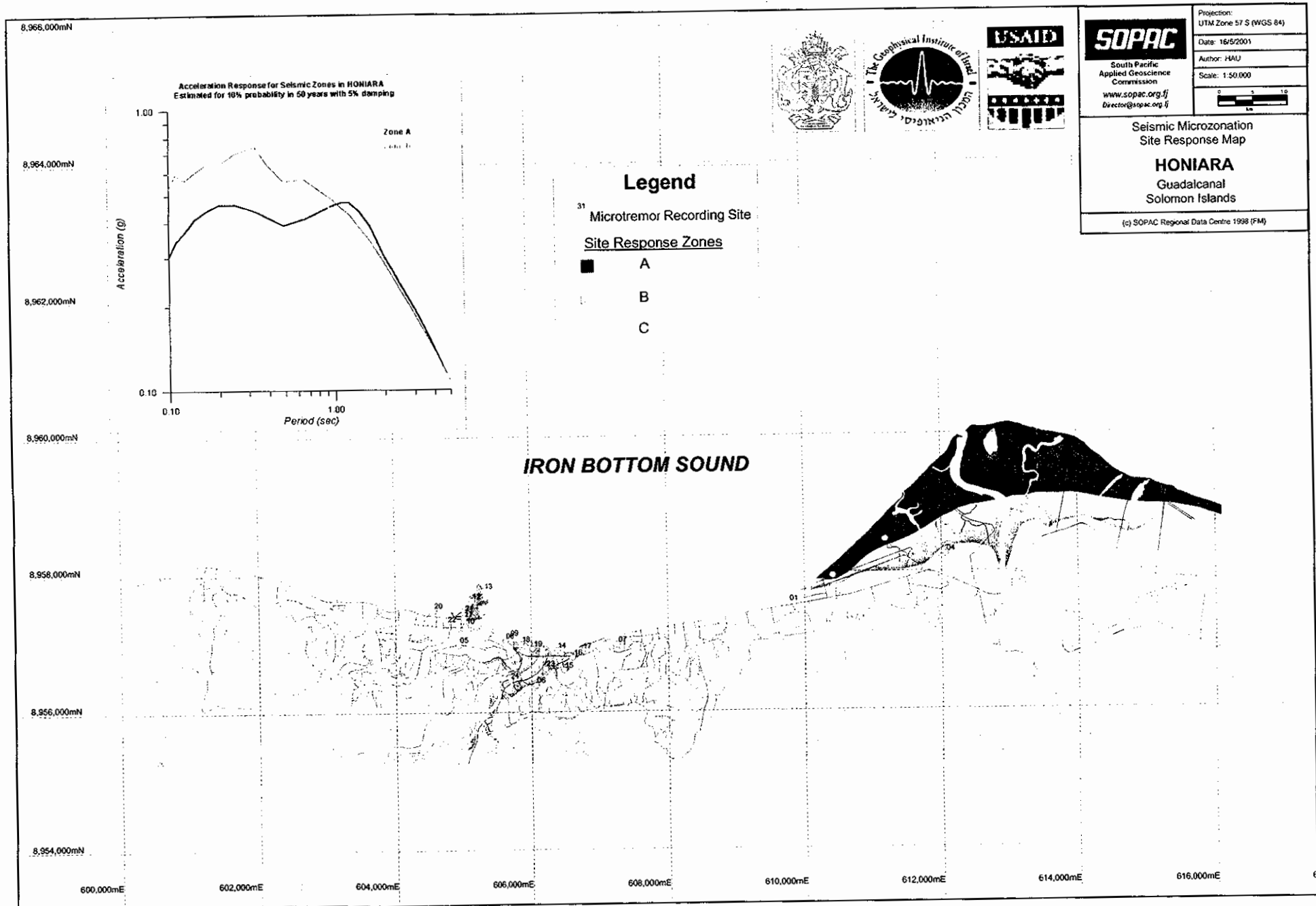


a



b

BEST AVAILABLE COPY



8 Seismic Microzonation of Nuku'alofa, Tongatapu, Tonga

8.1 Introduction, Nuku'alofa

Task leader: Kelepi Mafi (Lands, Survey & Natural Resource, Tonga)

Collaborators: Marc Regnier (IRD-ORSTOM, Noumea)

Nuku'alofa is the capital city of Tonga and has a population of some 25,000. Much of the development in the city is low-rise, and the majority of larger buildings are probably founded in weak limestone or surficial tuffaceous deposits. Several metres of weathered in-situ soils overlie these formations. Much of Nuku'alofa is founded on Recent carbonate sediments. Areas of weak organic sediment with a high groundwater table exist in the city area but are largely undeveloped at present.

The first few microtremor sites in Nuku'alofa were instrumented during 1997. However, due to technical difficulties in the initial program, most of the site information was measured during 1998 in a new program carried out with the assistance of Dr. M. Regnier of IRD (ORSTOM) who had gained experience with the GII system during site measurements in Port Vila.

Details in digital format of geographical information for Nuku'alofa including geological boundaries, borehole locations and logs, seismic microzone boundaries and investigation sites, road and cadastral plans, digital terrain model and orthophotograph can be found in Biukoto et al. (2001a).

8.2 Tectonic Setting, Nuku'alofa

The Tongan Islands are located on the crest of the Tonga Ridge, which is an active fore-arc bordering the Tonga Trench at the Pacific Plate boundary (Roy 1990). The ridge is divided into separate fault blocks (Cunningham & Anscombe 1985) whose surfaces are less than 200 m deep and have an irregular limestone cap, the emergent portions of which form islands. The southern (Tongatapu) block includes the islands Tongatapu and 'Eua. Tongatapu was formed by progressive uplift and tilting of pure carbonate deposits on the plate over-riding the Tonga subduction zone. The island has also received distal tuffaceous contributions as a result of volcanic action nearby in the Tonga group.

Emergent Pliocene-Pleistocene reef limestones on Tongatapu led early researchers (Lister 1891, Davis 1928) to propose that the island had been uplifted in the south and tilted down towards the north. Taylor (1978) envisaged that Tongatapu evolved on an inclined substrate that was slowly emerging so that the southern high point provided a nucleus for later leeward reef development. If uplift and tilting are still proceeding on Tongatapu, then Roy suggests that tectonism is now occurring at a much slower rate than eustatic changes.

Even though Nuku'alofa does not lie in an identified seismic zone, strong earthquakes have to be expected due to the city's geographical location close to the plate boundary at the Tonga Trench.

8.3 Regional and Local Geology, Nuku'alofa

Nuku'alofa is founded principally on a series of uplifted, recrystallised limestones blanketed by tuffs derived from nearby volcanic centres. Superficial Holocene fringing coral reefs and associated carbonate and organic-rich deposits occur in the coastal and lagoon areas. The distribution of lithologies in Nuku'alofa (after Cowie & Orbell 1991), together with the locations of boreholes, is shown in Figure 34.

Roy (1990) characterised the geology of Tongatapu as an uplifted carbonate platform made up of Pliocene and Pleistocene limestone, referred to in this report as the Nuku'alofa limestone. The formation is 130-250 m thick and overlies Pliocene and older volcanoclastics. The limestone is elevated above present sea level and reaches a maximum height of 65-70 m at the southern end of the island. Wilde & Hewitt (1983) and Orbell et al. (1985) noted that, as with all the Tongan islands, the soils of Tongatapu are rich in volcanic material, and attributed this to the fact that they are principally composed of now-extensively degraded volcanic ash (tephra). Harrison (1993) places the thickness of soils blanketing the limestones between 1 and 10 m with an average of 3 m.

Units of late Pleistocene and Holocene age veneer the Pliocene/ Pleistocene limestone core. Late Pleistocene volcanism has left a thick andesitic tephra over the northwestern coast and a thinner tephra of the same age covers the eastern and southern areas of the island. Along the southern and eastern coasts, erosion has exposed an older, underlying tephra.

Holocene (Recent) deposits have accumulated in beach, tidal-flat and lagoonal environments to form the northern coastal fringe, and the intertidal flats on the northwestern side of the island and the bottom

sediments of Fanga-uta Lagoon. Carbonate gravels and sands are generally concentrated towards the northern, seaward margin and at the eastern extremities of the Nuku'alofa peninsula (Cowie & Orbell 1991). Poorly drained organic sediments are concentrated towards the lagoon, surrounding the high ground of the raised carbonate platform at the Fakafanua Estate, and in back-barrier areas to the west of the city. Significant artificial fill has been placed along the ocean waterfront esplanade and in the various wharf areas including the Vuna and Queen Salote wharves.

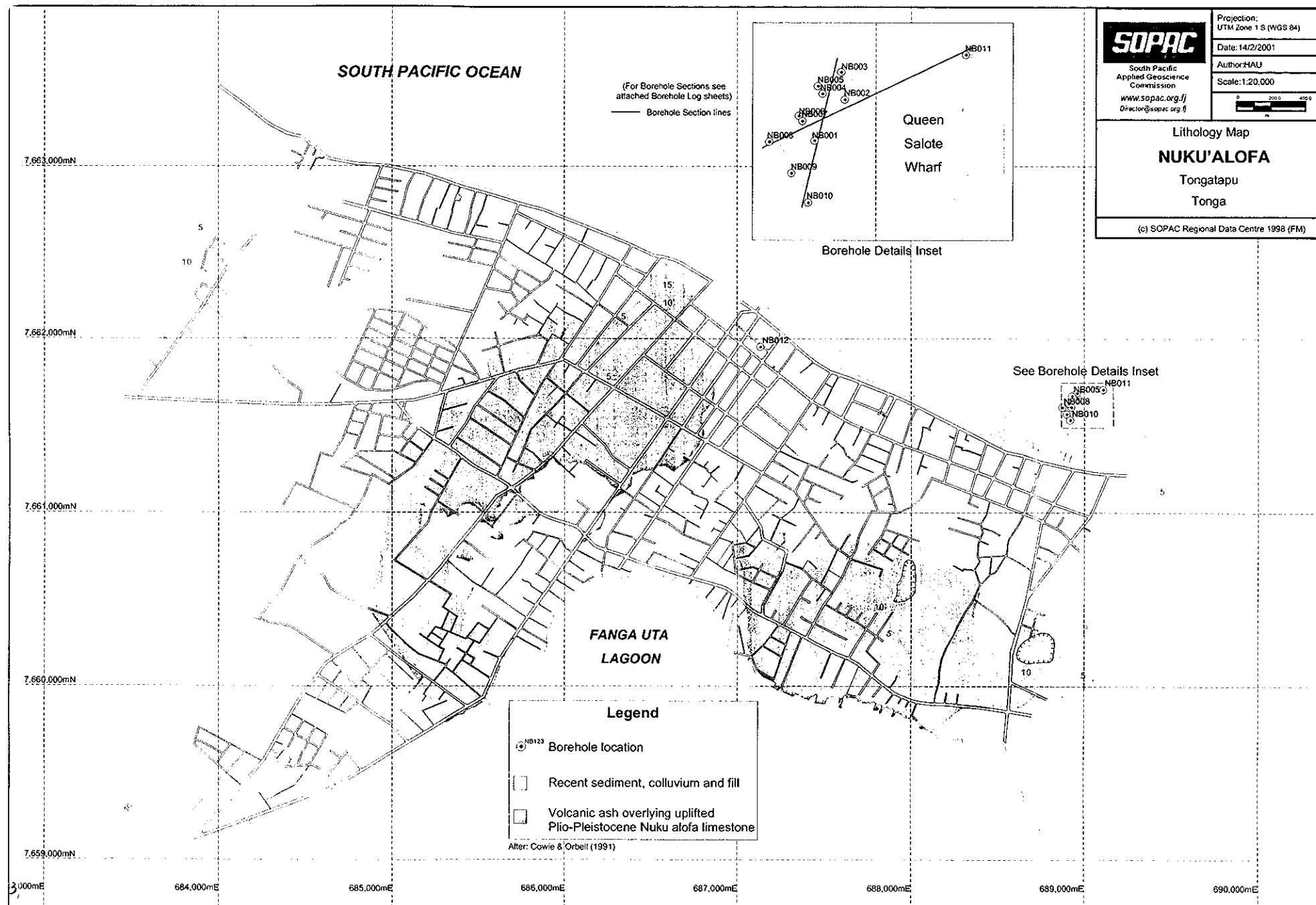
Boreholes at the Queen Salote wharf indicate carbonate gravels, sands and silts extending to the surface of the carbonate platform at around RL -20 m.

Selected borehole sections shown in Figures 35-36 serve to illustrate the subsurface distribution of engineering soil and rock types classified according to the Unified Soil Classification System (USBR 1973). The borehole logs are accompanied by logs of soil strength where these are available, based mainly on Standard Penetration Test N-values. Details of the legend for the soil type logs and instructions on the interpretation of the strength logs are given in Appendices 1-3.

(over page: p.117)

Figure 34: Lithology Map (including Borehole Positions), Nuku'alofa

BEST AVAILABLE COPY



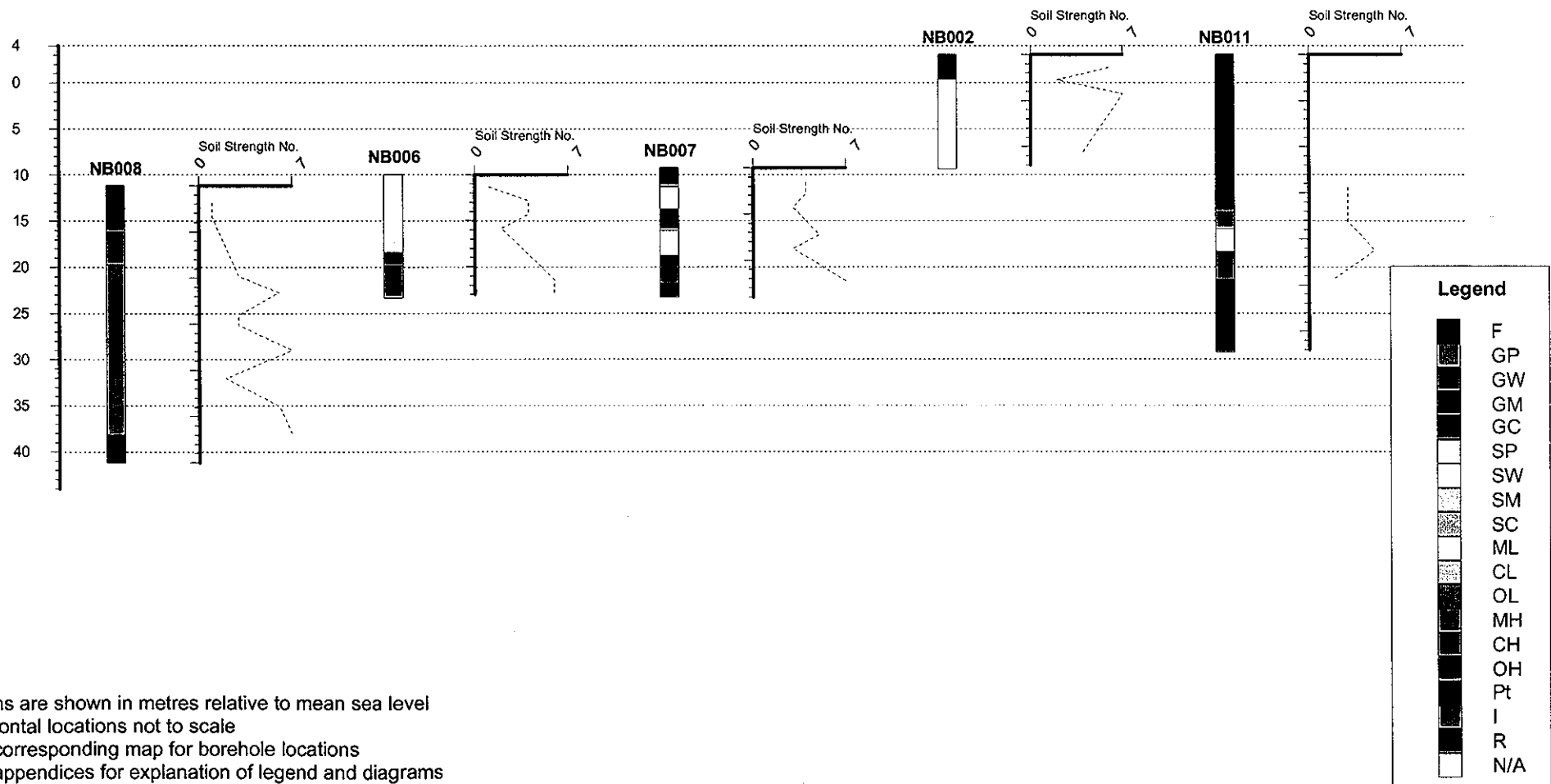
(over page: p.119)

Figure 35: Borehole Logs NB 008 to NB 011, Nuku'alofa

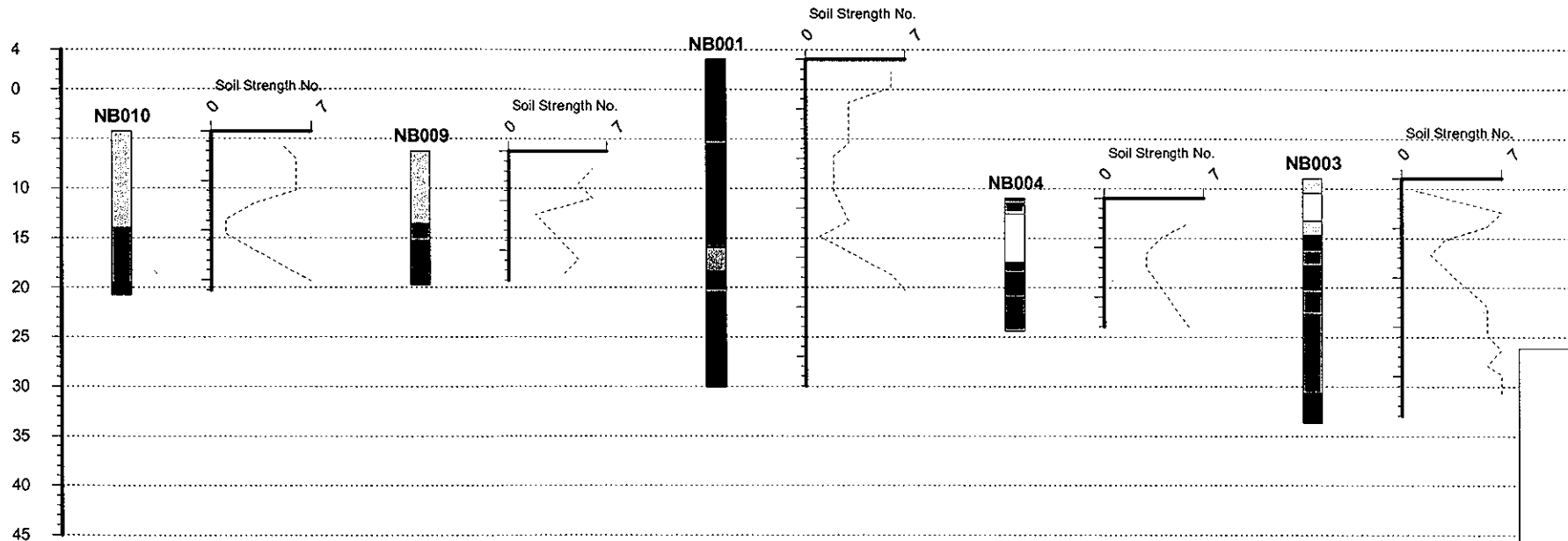
(over page: p.120)

Figure 36: Borehole Logs NB 010 to NB 003, Nuku'alofa

Borehole Logs Nuku'alofa Tongatapu, Tonga



Borehole Logs Nuku'alofa Tongatapu, Tonga



Legend

	F
	GP
	GW
	GM
	GC
	SP
	SW
	SM
	SC
	ML
	CL
	OL
	MH
	CH
	OH
	Pt
	I
	R
	N/A

Notes:

1. Depths are shown in metres relative to mean sea level
2. Horizontal locations not to scale
3. See corresponding map for borehole locations
4. See appendices for explanation of legend and diagrams

8.4 History of Damaging Earthquakes, Nuku'alofa

The epicentres of large shallow earthquakes (magnitude > 5, focal depth < 70 km) for the period 1973-1998, as well as earlier historical events, within an arbitrary 250 km radius of Nuku'alofa are shown in Figure 37 and catalogued in Table 18.

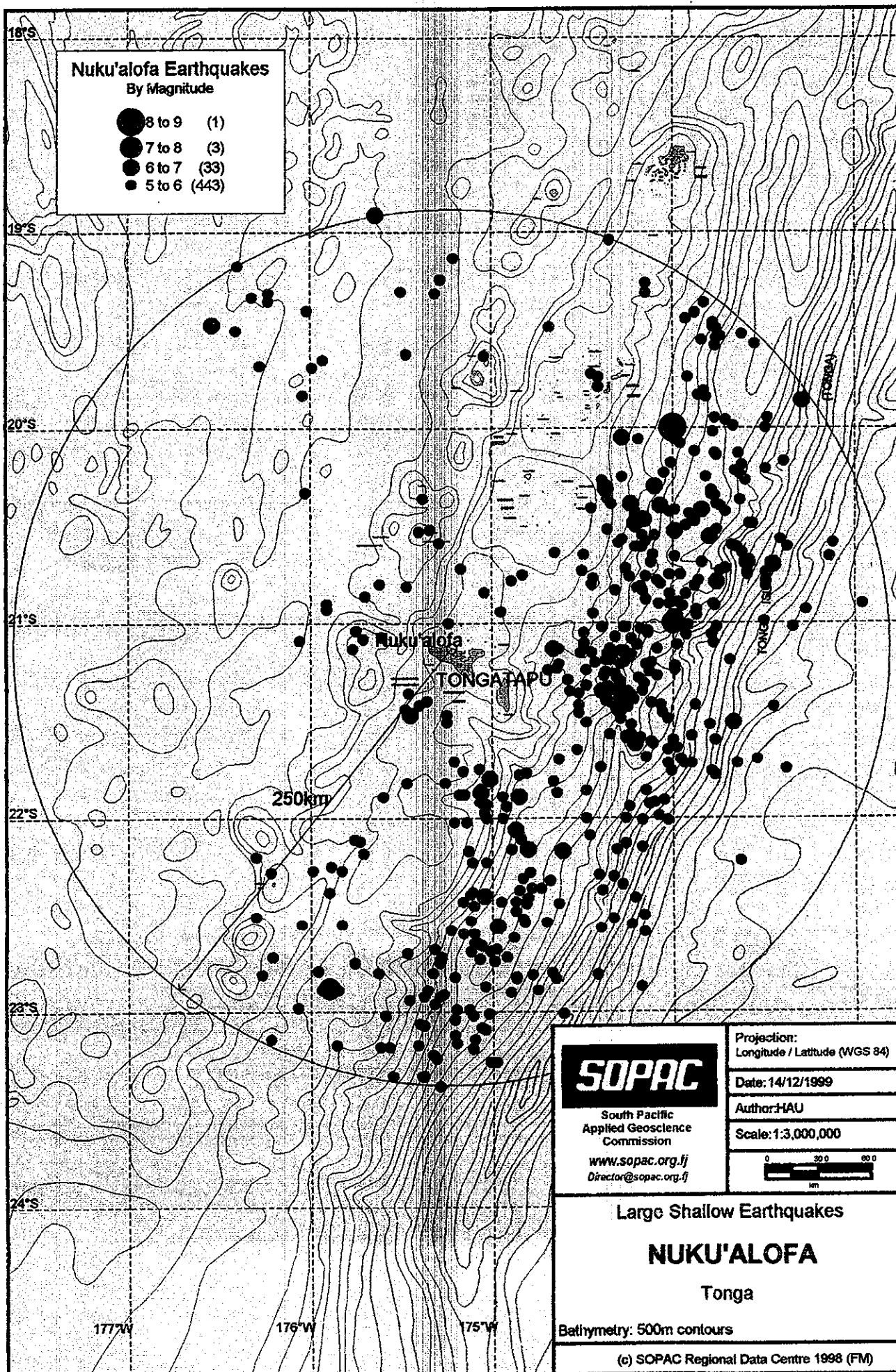
Despite its location close to the Tonga Trench, Nuku'alofa has experienced relatively little damage from earthquakes during its history of settlement.

1853: Nunn & Finau (1995) quoted Sawkins (1856) regarding the effects of an earthquake in Tongatapu on Christmas eve 1853. Sawkins noted that the northeast part of the island was "...tilted down to an inclination sufficient to produce an encroachment of the sea for nearly two miles inland, while the south and west coasts were elevated some feet".

1977: Extensive damage was caused in Nuku'alofa and other parts of Tongatapu, as well as in the islands Ha'apai, Vava'u and 'Eua where the effects were most severe, by a magnitude 7.2 earthquake on 23rd June 1977 (Campbell et al. 1977). The tremor, lasting almost three minutes, caused damage that equated to MM 6-8 effects. Electricity and water supplies were cut throughout Nuku'alofa, while the Queen Salote and Vuna wharves and the Custom's Shed on the city waterfront were all severely damaged. Several church bell towers were extensively damaged and many concrete buildings experienced cracking in the walls, while a number of houses and bungalow-style buildings were completely destroyed.

(over page: p.122)

Figure 37: Large Shallow Earthquakes around Nuku'alofa



(over page: p.124-131)

Table 18: Catalogue of Large Shallow Earthquakes, Nuku'alofa

Circle Search: Earthquakes for Nuku'alofa	
Circle Centre Point:	Latitude: 21.1290 S Longitude: 175.2217 W
Radius:	250 km
Magnitude Range:	5.0-9.0
Depth Range:	0-70 km

Date	Origin Time (UTC)	Latitude	Longitude	Depth (km)	Magnitude	Solution	Recorder	Epicentral Distance from Nukualofa (km)
9-Feb-02	073500.00	-20.00	-174.00	60	7.8	Ms		178
26-Jun-13	045700.00	-20.00	-174.00	60	8.2	Ms		178
8-Sep-48	150900.00	-21.00	-174.00	25	7.9	Ms		127
5-Jan-65	180558.60	-20.30	-174.10	33	6.8	Ms		
10-Sep-71	062851.10	-20.43	-174.21	33	5.8	Ms		
29-Sep-72	063735.30	-21.13	-174.63	33	5.7	Ms		
29-Jan-73	142615.70	-21.89	-174.94	33	5.1	mb	GS	89
8-Mar-73	143518.40	-23.02	-175.59	33	5.6	Ms	GS	212
10-Mar-73	180756.20	-23.06	-175.40	33	5.2	Ms	GS	214
1-May-73	095331.70	-19.81	-173.83	33	5.0	mb	GS	206
22-May-73	170525.70	-20.85	-174.02	33	5.2	Ms	GS	128
22-Jun-73	195140.50	-21.17	-174.26	33	5.5	mb	GS	99
1-Sep-73	180708.80	-22.81	-176.27	33	5.2	mb	GS	214
6-Jan-74	041952.70	-21.85	-175.06	33	5.3	Ms	GS	80
29-Jan-74	143915.00	-20.35	-173.77	33	5.0	Ms	GS	173
20-Feb-74	003637.70	-20.78	-174.89	60	5.0	mb	GS	51
17-Mar-74	171442.60	-22.68	-174.98	33	5.0	mb	GS	172
23-Mar-74	214612.00	-20.72	-175.17	33	5.2	Ms	GS	45
25-Mar-74	040811.00	-19.35	-176.23	33	5.2	Ms	GS	222
29-Mar-74	164546.60	-21.89	-175.60	68	5.0	mb	GS	92
22-Jun-74	095953.00	-20.80	-174.45	33	5.1	mb	GS	88
23-Jul-74	002813.30	-20.72	-174.26	33	5.0	mb	GS	110
6-Aug-74	183813.10	-21.76	-175.16	48	5.8	UK	BRK	69
11-Aug-74	021828.50	-21.47	-175.25	33	5.0	mb	GS	37
4-Sep-74	075822.10	-22.58	-175.23	58	5.1	mb	GS	159
20-Oct-74	041735.30	-20.27	-174.39	44	5.0	mb	GS	128
31-Oct-74	064635.20	-22.36	-174.78	33	5.3	Ms	GS	143
4-Nov-74	144700.10	-22.37	-174.85	33	5.0	mb	GS	142
9-Dec-74	094632.10	-20.25	-174.28	33	5.4	mb	GS	137
17-Dec-74	230152.60	-20.52	-175.34	31	5.4	mb	GS	67
18-Jan-75	085117.80	-20.52	-173.76	33	5.6	mb	GS	165
20-Jan-75	185744.00	-21.76	-173.79	33	5.2	mb	GS	163
7-Mar-75	023026.90	-20.42	-173.99	37	5.4	Ms	GS	150
31-Mar-75	104220.40	-23.08	-175.06	46	5.2	Ms	GS	216
2-Apr-75	103132.00	-23.02	-175.11	33	5.6	mb	GS	209
16-Apr-75	140759.50	-22.80	-175.33	38	5.3	mb	GS	184
17-Apr-75	011550.60	-22.82	-175.21	33	5.1	Ms	GS	186
23-Apr-75	144108.50	-20.81	-173.88	40	5.1	mb	GS	143
13-May-75	093400.70	-21.43	-174.25	25	5.1	Ms	GS	106
18-May-75	235353.80	-20.97	-173.99	43	6.0	Ms	GS	129
24-May-75	015338.00	-20.91	-173.77	19	5.5	Ms	GS	152
24-May-75	055416.10	-20.78	-173.86	33	5.1	mb	GS	146
14-Jun-75	035936.90	-20.39	-174.34	39	5.0	mb	GS	122
14-Jun-75	040516.80	-20.66	-173.99	33	5.1	mb	GS	137
19-Jun-75	085038.00	-21.39	-174.22	33	5.0	mb	GS	107
24-Jun-75	211519.00	-20.61	-174.17	23	5.4	mb	GS	123
4-Jul-75	112824.50	-21.25	-174.13	15	5.7	mb	GS	113
8-Jul-75	104531.20	-19.95	-173.48	12	5.0	mb	GS	223
15-Sep-75	164732.90	-21.29	-174.58	31	5.4	mb	GS	69
24-Sep-75	014749.70	-20.53	-173.99	33	6.5	Ms	GS	143
27-Dec-75	115345.80	-21.49	-174.03	37	5.1	mb	GS	129
3-Jan-76	233715.90	-21.70	-174.63	53	5.3	mb	GS	88
20-Jan-76	191612.00	-21.92	-174.10	33	5.4	mb	GS	144
2-Feb-76	163226.90	-21.04	-175.75	53	5.2	mb	GS	56
4-Apr-76	174105.40	-20.12	-173.88	57	5.0	mb	GS	178
7-Apr-76	120612.40	-19.95	-173.77	33	5.1	mb	GS	199
3-May-76	135125.90	-21.04	-174.14	33	5.1	mb	GS	112
4-May-76	083007.10	-21.93	-175.03	54	5.6	UK	BRK	90
28-May-76	074413.00	-20.61	-173.65	33	5.1	mb	GS	173
11-Jun-76	195651.10	-20.06	-173.99	34	5.0	mb	GS	174

Date	Origin Time (UTC)	Latitude	Longitude	Depth (km)	Magnitude	Solution	Recorder	Epicentral Distance from Nuku'alofa (km)
12-Jun-76	052706.50	-21.38	-174.30	34	5.4	mb	GS	99
9-Aug-76	053237.10	-20.84	-175.04	33	5.6	mb	GS	36
29-Sep-76	153901.00	-22.98	-176.07	33	5.4	mb	GS	221
6-Feb-77	030914.00	-21.82	-175.26	33	5.7	Ms	GS	76
17-Apr-77	023443.00	-21.01	-173.92	33	5.0	mb	GS	135
8-May-77	043731.50	-19.65	-175.93	33	5.0	mb	GS	179
1-Jun-77	085730.90	-21.19	-174.37	33	5.2	mb	GS	88
22-Jun-77	120833.40	-22.88	-175.90	65	7.2	UK	BRK	205
24-Jun-77	003020.90	-22.89	-175.94	33	5.5	mb	GS	208
26-Jun-77	055921.20	-22.70	-175.47	51	5.4	mb	GS	175
26-Jun-77	235257.20	-22.27	-175.83	33	5.0	mb	GS	141
28-Jun-77	012339.70	-21.00	-175.24	68	5.2	mb	GS	14
29-Jun-77	031139.80	-23.16	-175.20	38	5.2	mb	GS	224
9-Jul-77	164409.40	-22.45	-175.10	33	5.5	mb	GS	147
11-Jul-77	044450.50	-23.18	-175.62	42	5.1	Ms	GS	230
13-Jul-77	001406.00	-23.24	-175.31	63	5.0	mb	GS	233
7-Aug-77	164624.70	-23.01	-175.02	33	5.0	mb	GS	209
15-Aug-77	054112.10	-23.33	-175.38	33	5.3	mb	GS	243
27-Sep-77	172205.80	-21.49	-174.29	33	5.0	mb	GS	104
28-Sep-77	121210.30	-21.52	-174.23	33	5.6	mb	GS	111
19-Oct-77	022140.40	-20.75	-173.96	33	5.5	Ms	GS	137
23-Oct-77	111911.40	-20.43	-174.02	33	5.0	mb	GS	146
1-Nov-77	082522.10	-22.83	-174.65	33	5.0	Ms	GS	196
3-Dec-77	175931.30	-22.00	-174.94	33	5.3	mb	GS	100
15-Jan-78	074110.30	-22.28	-176.22	33	5.0	mb	GS	163
9-Feb-78	042430.00	-22.38	-175.11	33	5.2	mb	GS	139
2-Mar-78	182306.10	-22.99	-175.13	33	5.1	mb	GS	206
3-Mar-78	073459.80	-23.26	-175.00	33	5.2	mb	GS	236
3-Mar-78	074208.60	-23.26	-174.98	33	5.2	mb	GS	237
4-Mar-78	044636.10	-21.89	-174.85	33	6.3	Ms	GS	92
17-Mar-78	110039.50	-22.89	-175.36	33	5.7	mb	GS	195
26-Mar-78	104628.60	-22.09	-174.46	45	5.1	mb	GS	132
26-Mar-78	212442.60	-22.13	-174.26	33	5.2	Ms	GS	148
29-Mar-78	140821.70	-21.57	-174.35	33	5.0	mb	GS	102
29-Mar-78	220026.70	-21.76	-174.01	33	5.7	Ms	GS	143
1-Apr-78	013136.60	-22.01	-174.03	33	5.2	mb	GS	156
11-Apr-78	234207.60	-19.49	-173.76	33	5.7	UK	BRK	237
14-Apr-78	044945.30	-21.02	-174.26	33	5.2	mb	GS	101
24-Apr-78	154418.90	-21.27	-174.38	33	5.8	Ms	GS	88
9-May-78	175548.50	-22.00	-174.48	33	5.4	mb	GS	122
13-May-78	223813.90	-22.41	-174.21	33	5.0	mb	GS	175
27-May-78	171655.10	-21.49	-174.29	33	5.0	mb	GS	104
18-Jul-78	115053.70	-20.80	-175.62	33	5.1	mb	GS	55
25-Jul-78	105330.40	-21.20	-174.43	33	5.0	mb	GS	82
17-Aug-78	085151.30	-21.07	-174.32	20	5.7	mb	GS	93
9-Nov-78	151853.10	-21.07	-175.61	33	5.4	Ms	GS	41
29-Dec-78	054914.40	-21.36	-174.52	45	5.3	mb	GS	76
5-Jan-79	053127.80	-20.83	-174.17	33	5.3	mb	GS	114
7-Jan-79	002523.50	-22.94	-175.46	33	5.5	mb	GS	202
4-Feb-79	164758.90	-21.06	-173.93	33	5.4	Ms	GS	133
18-Feb-79	105146.20	-21.28	-174.31	58	5.1	mb	GS	95
27-Mar-79	224020.90	-21.22	-173.99	33	5.1	mb	GS	128
26-Jun-79	034920.00	-22.39	-175.12	33	5.4	UK	BRK	139
26-Jun-79	081946.10	-19.40	-176.02	33	5.4	mb	GS	208
1-Jul-79	090733.00	-19.26	-174.15	33	5.4	mb	GS	235
24-Jul-79	005357.90	-20.49	-174.21	33	6.1	UK	PAS	126
24-Jul-79	073450.10	-20.41	-174.45	33	5.2	mb	GS	112
2-Aug-79	104610.30	-20.25	-173.82	33	5.0	mb	GS	175
1-Oct-79	122348.60	-21.08	-175.71	33	5.6	Ms	GS	50
12-Oct-79	050357.20	-20.75	-173.59	33	5.0	mb	GS	174

Site-Specific Earthquake Hazard Determinations in Capital Cities in the South Pacific

Date	Origin Time (UTC)	Latitude	Longitude	Depth (km)	Magnitude	Solution	Recorder	Epicentral Distance from Nuku'alofa (km)
27-Oct-79	074622.60	-21.35	-174.57	33	5.2	mb	GS	71
30-Nov-79	224706.40	-23.09	-175.04	47	5.0	mb	GS	217
5-Dec-79	190100.70	-19.63	-175.04	33	5.3	mb	GS	166
16-Dec-79	212756.60	-20.40	-173.74	39	5.5	Ms	GS	173
14-Jan-80	121940.20	-22.40	-175.04	33	6.0	Ms	GS	141
14-Feb-80	231152.10	-22.57	-174.40	33	5.3	mb	GS	180
31-Mar-80	130431.10	-20.56	-173.80	33	6.2	Ms	GS	160
31-Mar-80	132602.80	-20.55	-173.79	33	5.2	mb	GS	162
31-Mar-80	184237.70	-20.73	-173.74	34	5.7	Ms	GS	160
1-Apr-80	111154.90	-20.69	-173.59	37	6.3	UK	BRK	176
1-Apr-80	111509.70	-20.06	-174.19	33	5.2	mb	GS	159
1-Apr-80	154552.50	-20.48	-173.89	33	5.0	mb	GS	156
6-Apr-80	035152.20	-20.13	-173.77	33	5.0	mb	GS	186
22-Apr-80	081026.10	-20.57	-173.41	33	5.1	mb	GS	198
28-Apr-80	164352.90	-20.08	-173.96	33	5.5	mb	GS	175
28-Apr-80	171005.00	-19.44	-173.93	33	5.1	Ms	GS	230
30-Apr-80	113704.90	-19.48	-173.78	22	5.5	mb	GS	236
28-May-80	222428.90	-20.00	-173.49	36	5.2	mb	GS	219
28-Jul-80	201323.50	-22.12	-175.73	65	5.6	UK	BRK	121
20-Oct-80	115104.70	-21.65	-174.03	33	5.3	mb	GS	136
28-Oct-80	201926.80	-19.13	-175.21	33	5.3	mb	GS	220
10-Nov-80	102707.00	-21.20	-174.27	33	5.0	mb	GS	98
18-Nov-80	070159.00	-21.75	-175.07	33	5.3	mb	GS	70
18-Nov-80	072242.80	-21.78	-174.85	33	5.3	mb	GS	82
1-Dec-80	120149.00	-22.16	-174.89	33	5.4	mb	GS	118
9-Dec-80	014027.40	-20.90	-172.96	33	5.2	mb	GS	236
19-Dec-80	025757.40	-21.34	-174.36	33	6.2	UK	PAS	92
19-Dec-80	102357.60	-20.69	-173.84	33	5.0	mb	GS	151
20-Dec-80	145216.50	-20.14	-173.76	33	5.2	Ms	GS	187
25-Dec-80	075336.50	-21.42	-174.07	33	5.1	mb	GS	123
26-Dec-80	135604.20	-21.13	-174.35	33	5.5	mb	GS	90
28-Dec-80	010528.90	-20.90	-173.78	33	5.1	mb	GS	151
14-Jan-81	113418.70	-21.16	-174.23	41	5.2	Ms	GS	102
28-Jan-81	035504.80	-22.55	-174.23	33	5.0	mb	GS	187
20-Feb-81	003709.50	-23.14	-175.10	33	5.2	mb	GS	222
28-Feb-81	130944.70	-21.20	-174.12	33	5.2	mb	GS	113
11-Mar-81	071707.20	-23.38	-175.29	33	5.5	Ms	GS	248
11-Mar-81	092835.20	-23.33	-175.39	33	5.4	mb	GS	243
26-Mar-81	031950.60	-19.79	-174.41	33	5.3	mb	GS	169
26-Mar-81	101611.90	-21.59	-174.26	43	5.7	mb	GS	111
2-Apr-81	065535.50	-20.61	-174.21	33	5.1	Ms	GS	119
25-Aug-81	071658.40	-22.89	-175.85	33	5.9	mb	GS	205
25-Aug-81	072245.67	-22.90	-175.90	33	5.7	mb	GS	208
6-Oct-81	184809.33	-21.32	-174.48	33	5.1	mb	GS	79
4-Nov-81	143810.73	-20.05	-174.28	33	6.3	mb	GS	154
2-Dec-81	233304.38	-20.81	-174.18	33	5.2	Ms	GS	113
9-Dec-81	120121.74	-21.31	-174.29	33	5.2	mb	GS	98
28-Feb-82	170024.18	-21.70	-173.54	37	5.6	mb	GS	185
4-Mar-82	084527.73	-22.79	-175.96	68	5.0	mb	GS	198
24-Mar-82	005017.07	-19.31	-174.15	33	5.3	mb	GS	230
24-Mar-82	223435.59	-22.81	-174.42	33	5.4	mb	GS	203
8-Apr-82	114030.58	-20.61	-174.18	41	5.5	mb	GS	122
12-Jun-82	033847.91	-22.72	-176.21	33	5.0	mb	GS	203
9-Jul-82	170148.16	-21.24	-173.99	55	5.3	mb	GS	128
26-Jul-82	043713.51	-19.99	-173.67	33	5.3	mb	GS	204
27-Sep-82	191700.08	-19.48	-174.68	33	5.2	mb	GS	191
30-Sep-82	132037.17	-20.22	-173.66	33	5.1	mb	GS	191
5-Oct-82	044614.63	-22.69	-175.01	33	5.0	mb	GS	173
19-Dec-82	191952.64	-23.14	-176.22	33	5.2	mb	GS	245
23-Dec-82	055758.90	-22.80	-175.63	33	5.1	mb	GS	189

Date	Origin Time (UTC)	Latitude	Longitude	Depth (km)	Magnitude	Solution	Recorder	Epicentral Distance from Nuku'alofa (km)
2-Feb-83	143611.83	-20.75	-174.02	33	5.1	mb	GS	131
17-Feb-83	161039.13	-21.59	-174.18	32	5.8	mb	GS	119
17-Mar-83	224744.05	-21.46	-174.52	33	5.2	mb	GS	81
18-Mar-83	083702.65	-22.50	-174.16	38	5.4	mb	GS	186
21-Mar-83	074417.79	-21.47	-175.45	68	6.4	Ms	BRK	44
21-Mar-83	154952.01	-21.51	-175.25	63	5.5	mb	GS	42
7-Apr-83	153836.06	-22.53	-175.12	33	5.5	mb	GS	155
14-Apr-83	102414.22	-21.42	-175.40	33	5.2	mb	GS	37
15-Apr-83	210022.23	-21.86	-174.15	33	5.2	mb	GS	137
27-Apr-83	172035.21	-21.14	-174.27	21	5.6	Ms	GS	98
30-Apr-83	025143.32	-21.35	-174.25	23	5.8	mb	GS	103
6-May-83	115941.84	-21.28	-174.19	33	5.3	mb	GS	108
11-May-83	214815.42	-21.43	-173.45	33	5.7	mb	GS	186
15-May-83	002400.68	-18.91	-175.64	33	6.5	Ms	GS	249
17-May-83	135950.01	-21.06	-173.79	33	5.1	Ms	GS	149
3-Jun-83	145957.31	-19.48	-176.54	33	5.0	mb	GS	228
28-Jun-83	215547.53	-22.44	-174.81	33	5.1	mb	GS	151
6-Jul-83	045438.14	-21.46	-174.06	40	5.3	mb	GS	125
8-Jul-83	100500.43	-21.75	-173.38	33	5.5	mb	GS	202
17-Aug-83	125910.51	-22.52	-174.33	33	5.0	mb	GS	179
16-Sep-83	074331.57	-21.40	-175.36	46	5.4	mb	GS	32
17-Oct-83	132521.13	-20.79	-173.76	30	6.3	Ms	GS	156
20-Oct-83	020541.26	-20.91	-173.95	69	5.3	mb	GS	134
3-Dec-83	032205.75	-20.44	-173.91	33	5.2	Ms	GS	156
4-Dec-83	193040.84	-20.74	-173.59	33	5.4	Ms	GS	174
15-Dec-83	083939.80	-21.44	-175.48	33	5.0	mb	GS	43
23-Dec-83	143554.89	-20.90	-175.91	33	5.6	Ms	GS	76
28-Dec-83	112139.27	-20.96	-173.87	49	5.3	mb	GS	141
22-Jan-84	135151.35	-21.37	-174.23	50	5.3	mb	GS	106
4-Mar-84	155501.25	-21.91	-174.05	33	5.1	mb	GS	148
8-May-84	065940.02	-20.17	-173.39	33	5.2	mb	GS	217
29-May-84	191242.28	-21.19	-173.69	33	5.4	Ms	GS	158
2-Jun-84	141538.24	-20.76	-174.24	33	5.0	mb	GS	110
29-Jun-84	042852.38	-20.93	-173.27	42	5.4	mb	GS	203
17-Jul-84	012549.75	-19.46	-173.78	59	5.2	mb	GS	237
25-Jul-84	230655.62	-20.33	-176.03	33	5.3	mb	GS	122
31-Aug-84	001818.47	-20.58	-174.15	33	5.1	mb	GS	126
31-Dec-84	100819.57	-19.55	-173.84	33	5.5	Ms	GS	226
3-Jan-85	235834.17	-21.62	-174.11	33	5.6	Ms	GS	127
3-Feb-85	045055.24	-20.55	-174.10	56	5.8	mb	GS	133
9-Feb-85	203328.44	-23.07	-175.38	33	5.4	Ms	GS	215
16-Feb-85	134846.46	-23.26	-175.01	42	5.3	Ms	GS	236
16-Feb-85	191642.81	-23.04	-175.21	42	5.0	Ms	GS	211
17-Feb-85	030000.21	-23.19	-175.11	42	5.5	Ms	GS	228
24-Feb-85	045433.81	-22.02	-175.21	33	5.3	mb	GS	98
21-Apr-85	175427.33	-22.81	-174.78	33	5.3	mb	GS	190
21-Aug-85	161544.73	-22.90	-174.90	33	5.0	mb	GS	198
22-Aug-85	192958.01	-22.36	-174.73	33	5.5	mb	GS	145
16-Sep-85	070824.31	-20.81	-173.49	33	5.1	mb	GS	182
27-Sep-85	101018.90	-22.17	-174.61	33	6.4	Ms	BRK	131
28-Sep-85	055041.03	-20.90	-174.08	33	5.2	mb	GS	121
9-Oct-85	034655.10	-21.08	-174.23	65	5.1	mb	GS	102
9-Oct-85	172338.38	-21.11	-174.20	65	5.2	mb	GS	106
10-Oct-85	151116.87	-22.37	-174.39	33	5.2	mb	GS	161
8-Nov-85	093755.09	-22.80	-174.67	33	5.1	mb	GS	193
26-Nov-85	061859.39	-21.98	-175.04	43	5.4	mb	GS	96
21-Jan-86	052422.27	-21.58	-174.26	40	5.6	mb	GS	111
27-Jan-86	154559.83	-21.64	-173.98	33	5.1	mb	GS	139
11-Feb-86	130026.05	-20.32	-173.79	35	5.0	mb	GS	174
17-Feb-86	020514.14	-20.49	-173.58	33	5.3	Ms	GS	184

Date	Origin Time (UTC)	Latitude	Longitude	Depth (km)	Magnitude	Solution	Recorder	Epicentral Distance from Nuku'alofa (km)
2-Apr-86	120716.56	-19.57	-173.55	40	5.0	mb	GS	245
13-May-86	095636.72	-20.65	-174.11	33	5.5	Ms	GS	126
17-Jun-86	214456.49	-20.95	-174.44	33	5.2	mb	GS	83
21-Jul-86	121115.85	-20.57	-174.28	36	5.5	mb	GS	115
18-Aug-86	015954.50	-20.49	-174.21	19	5.9	mb	GS	126
5-Sep-86	031110.98	-20.86	-175.70	62	5.1	mb	GS	57
15-Sep-86	084811.44	-22.75	-175.29	33	5.8	Ms	GS	179
25-Sep-86	001407.41	-21.99	-174.08	33	5.1	mb	GS	151
5-Dec-86	223100.37	-21.72	-173.65	33	5.6	mb	GS	175
24-Dec-86	103206.35	-19.96	-173.71	33	5.2	Ms	GS	203
30-Dec-86	153213.57	-20.40	-174.07	23	6.1	mb	GS	144
9-Jan-87	080135.95	-19.47	-176.54	33	6.8	Ms	BRK	229
10-Jan-87	025315.76	-19.50	-176.41	33	5.2	mb	GS	218
16-Jan-87	131808.51	-22.22	-173.63	33	5.1	mb	GS	204
26-Mar-87	064710.64	-21.52	-173.80	20	5.4	mb	GS	153
27-Mar-87	091528.13	-21.24	-174.69	33	5.0	mb	GS	56
30-Mar-87	202726.45	-21.31	-174.16	32	5.0	mb	GS	111
21-Apr-87	040102.46	-19.30	-175.50	33	5.3	mb	GS	204
19-May-87	165818.70	-21.18	-174.25	33	5.5	mb	GS	100
20-May-87	234047.50	-19.36	-173.83	33	5.2	mb	GS	243
23-Jun-87	180237.66	-22.54	-174.82	33	5.3	mb	GS	160
27-Jun-87	143340.43	-21.30	-174.29	36	5.3	mb	GS	98
11-Jul-87	174557.16	-22.20	-176.30	33	5.2	mb	GS	162
15-Jul-87	004453.24	-21.86	-174.48	33	5.1	mb	GS	111
17-Jul-87	134201.91	-22.27	-175.99	33	5.1	mb	GS	148
6-Aug-87	183902.65	-22.29	-174.41	33	5.1	mb	GS	153
7-Aug-87	043918.25	-22.00	-174.26	33	5.3	mb	GS	138
16-Aug-87	004403.43	-20.36	-174.36	33	5.0	Ms	GS	123
22-Oct-87	131033.52	-20.13	-173.64	33	5.2	mb	GS	198
11-Dec-87	020309.68	-22.16	-174.80	36	6.0	Ms	BRK	121
1-Feb-88	122303.32	-21.19	-174.35	33	5.4	mb	GS	90
27-Feb-88	134615.89	-21.02	-173.76	33	5.3	Ms	GS	151
17-Mar-88	153623.86	-21.42	-173.88	39	5.9	Ms	GS	142
6-Apr-88	210611.02	-23.18	-175.57	33	5.2	mb	GS	230
6-May-88	054746.96	-21.11	-173.98	33	5.2	mb	GS	128
13-May-88	032258.59	-22.82	-174.87	33	5.2	Ms	GS	190
19-May-88	032232.17	-20.59	-173.12	33	5.5	mb	GS	225
21-May-88	151622.59	-20.37	-173.63	46	5.7	Ms	GS	185
30-May-88	191837.61	-21.87	-174.64	33	5.4	mb	GS	101
31-May-88	185138.00	-20.53	-175.40	33	5.1	mb	GS	68
6-Jun-88	104352.32	-20.34	-173.79	38	5.1	mb	GS	172
22-Aug-88	163706.62	-19.69	-175.99	33	5.0	mb	GS	178
27-Aug-88	101502.38	-19.68	-176.28	35	5.6	Ms	BRK	193
5-Nov-88	030441.43	-21.57	-174.23	33	5.9	Ms	GS	113
22-Nov-88	100507.67	-22.74	-174.99	33	5.0	mb	GS	179
23-Jan-89	141335.98	-22.51	-176.30	33	5.3	mb	GS	188
16-Feb-89	051729.13	-21.70	-173.96	33	5.0	mb	GS	144
7-May-89	165345.37	-21.82	-175.47	33	5.0	mb	GS	80
30-May-89	135250.18	-21.27	-174.09	33	5.1	mb	GS	118
8-Jun-89	095156.84	-19.53	-173.74	22	5.5	mb	GS	234
12-Jun-89	182103.30	-22.55	-175.83	70	5.5	mb	GS	169
29-Jun-89	001839.81	-22.96	-175.32	34	5.2	mb	GS	202
29-Jul-89	054814.38	-20.72	-173.71	35	5.1	mb	GS	162
31-Jul-89	134035.15	-20.82	-174.20	33	5.0	mb	GS	111
9-Aug-89	004036.16	-20.64	-173.62	37	5.3	mb	GS	175
9-Aug-89	030351.35	-20.60	-173.68	36	5.0	mb	GS	171
12-Aug-89	204640.68	-20.50	-173.93	37	5.3	mb	GS	151
14-Aug-89	172243.71	-19.83	-176.04	33	5.0	mb	GS	167
15-Aug-89	004622.45	-21.88	-175.15	38	5.1	Ms	GS	83
15-Aug-89	075357.90	-21.97	-175.04	33	5.1	mb	GS	95

Date	Origin Time (UTC)	Latitude	Longitude	Depth (km)	Magnitude	Solution	Recorder	Epicentral Distance from Nuku'alofa (km)
7-Sep-89	102545.76	-23.17	-175.86	33	5.1	mb	GS	234
19-Sep-89	085602.21	-19.24	-175.28	33	5.1	mb	GS	208
27-Oct-89	043930.60	-20.89	-173.97	33	5.3	Ms	GS	132
23-Nov-89	012327.62	-22.31	-174.83	33	5.4	mb	GS	137
21-Jan-90	164344.67	-21.10	-173.78	33	5.1	mb	GS	149
22-Jan-90	023204.47	-20.93	-173.87	37	5.4	mb	GS	141
22-Jan-90	051612.31	-20.90	-174.02	33	5.2	Ms	GS	127
16-Feb-90	062209.81	-22.30	-174.33	33	5.1	mb	GS	158
2-Mar-90	220625.25	-21.93	-174.13	33	5.4	mb	GS	143
3-Mar-90	212625.03	-22.15	-174.17	33	5.1	mb	GS	157
21-Mar-90	021226.17	-19.62	-175.47	33	5.2	Ms	GS	168
29-Mar-90	014224.35	-20.93	-175.91	33	5.0	mb	GS	74
4-Apr-90	054009.16	-21.58	-173.90	36	5.2	mb	GS	145
6-Apr-90	143146.14	-21.62	-174.21	28	6.4	Ms	GS	117
15-Jul-90	100106.69	-23.12	-175.21	38	5.6	mb	GS	220
26-Jul-90	233449.03	-20.23	-174.05	70	5.0	mb	GS	156
2-Sep-90	095242.97	-23.01	-174.61	40	5.2	Ms	GS	217
8-Sep-90	203157.75	-20.55	-174.17	33	5.7	Ms	GS	126
2-Nov-90	072235.65	-21.25	-174.37	28	5.7	Ms	BRK	89
3-Dec-90	074036.33	-20.21	-173.49	10	5.2	mb	GS	206
11-Dec-90	011103.84	-22.16	-174.31	38	5.2	Ms	GS	148
21-Dec-90	052928.72	-20.47	-174.16	13	6.4	Ms	BRK	132
30-Dec-90	143143.86	-20.74	-173.49	33	5.1	mb	GS	184
1-Jan-91	172802.49	-21.21	-174.15	29	5.7	mb	GS	111
2-Mar-91	224110.04	-21.94	-174.92	33	5.1	mb	GS	94
2-Mar-91	230603.76	-22.00	-175.03	43	5.6	mb	GS	97
3-Mar-91	060016.20	-22.54	-174.70	33	5.0	mb	GS	164
3-Mar-91	152024.73	-21.87	-175.06	16	6.1	Ms	GS	83
30-Mar-91	144025.50	-21.02	-173.34	33	5.1	mb	GS	195
29-Apr-91	065454.26	-20.76	-174.15	39	5.2	mb	GS	118
2-May-91	022339.28	-21.72	-173.90	33	5.3	Ms	GS	151
12-May-91	122755.30	-21.72	-174.03	34	5.6	mb	GS	139
5-Aug-91	060547.28	-21.36	-174.40	30	5.8	Ms	GS	89
8-Aug-91	135810.35	-21.61	-174.12	34	5.2	mb	GS	125
25-Aug-91	064005.96	-21.35	-174.17	33	5.5	mb	GS	111
4-Sep-91	085706.03	-21.60	-174.00	38	5.0	mb	GS	137
7-Sep-91	220736.76	-21.14	-174.29	58	5.2	mb	GS	96
25-Sep-91	111630.22	-20.75	-174.83	33	5.2	mb	GS	58
27-Sep-91	121123.03	-21.41	-174.12	34	5.2	mb	GS	118
11-Dec-91	062941.86	-22.69	-175.12	42	5.7	mb	GS	173
27-Dec-91	023243.11	-19.17	-176.40	25	5.7	Ms	GS	248
28-Jan-92	152905.64	-21.36	-174.27	36	5.3	mb	GS	101
3-Mar-92	114803.70	-20.02	-173.78	55	5.0	mb	GS	194
27-Apr-92	051315.44	-22.34	-174.28	33	5.0	mb	GS	166
10-Jun-92	094335.96	-22.83	-174.87	39	5.1	mb	GS	191
16-Jul-92	223307.24	-20.61	-173.37	33	5.1	mb	GS	200
18-Jul-92	153141.22	-22.72	-175.28	25	5.5	Ms	GS	176
21-Jul-92	065751.90	-22.87	-175.04	33	5.4	mb	GS	193
16-Aug-92	063703.54	-22.32	-174.68	33	5.1	mb	GS	142
18-Aug-92	061558.08	-22.28	-174.79	44	5.2	mb	GS	134
25-Aug-92	082412.96	-20.94	-174.95	66	5.5	mb	GS	35
10-Sep-92	104320.38	-22.56	-174.97	37	6.3	Ms	BRK	160
10-Sep-92	220947.60	-22.60	-175.10	38	5.5	mb	GS	163
10-Sep-92	231339.27	-22.62	-174.88	33	5.1	mb	GS	168
10-Sep-92	232029.31	-22.43	-174.87	33	5.5	mb	GS	148
11-Sep-92	213310.77	-22.43	-174.95	30	5.2	Ms	GS	146
14-Sep-92	171500.39	-22.73	-175.07	49	5.0	mb	GS	178
17-Sep-92	083959.06	-22.72	-174.92	33	5.0	mb	GS	178
19-Sep-92	223434.61	-22.89	-174.75	33	5.2	mb	GS	200
24-Sep-92	201851.61	-21.13	-175.77	33	5.5	Ms	GS	56

Date	Origin Time (UTC)	Latitude	Longitude	Depth (km)	Magnitude	Solution	Recorder	Epicentral Distance from Nuku'alofa (km)
10-Oct-92	095011.63	-20.66	-173.14	37	5.2	mb	GS	222
16-Oct-92	000135.92	-19.72	-174.45	70	5.1	mb	GS	175
9-Nov-92	012713.84	-21.05	-174.14	33	5.1	mb	GS	112
22-Nov-92	173520.39	-19.58	-173.77	20	5.5	mb	GS	228
4-Dec-92	194805.85	-19.52	-173.62	33	5.3	mb	GS	244
4-Jan-93	204111.20	-22.06	-174.87	33	6.3	Ms	BRK	108
20-Feb-93	071152.12	-22.11	-174.84	43	5.6	mb	GS	115
20-Feb-93	231855.28	-22.87	-174.18	33	5.0	mb	GS	220
6-Apr-93	190901.33	-20.19	-173.62	31	5.2	mb	GS	196
18-Apr-93	103144.35	-22.41	-174.80	42	5.0	mb	GS	148
16-Jun-93	065920.57	-21.78	-173.77	34	5.6	mb	GS	166
31-Jul-93	091334.73	-20.18	-174.01	33	5.2	Mw	HRV	163
27-Sep-93	005204.43	-19.83	-173.86	33	5.0	mb	GS	202
4-Oct-93	205438.34	-21.44	-174.30	34	6.0	Mw	GS	101
15-Oct-93	004354.61	-22.23	-175.11	33	5.0	mb	GS	122
30-Oct-93	140443.49	-19.31	-176.23	17	5.7	Mw	HRV	227
24-Nov-93	112720.27	-21.41	-174.27	33	5.4	Mw	HRV	103
29-Nov-93	063524.46	-20.78	-174.09	32	5.3	mb	GS	123
12-Dec-93	042803.50	-19.74	-174.41	33	5.2	mb	GS	174
13-Dec-93	114344.23	-20.42	-173.84	33	6.0	Ms	BRK	163
14-Dec-93	063119.33	-20.70	-173.45	30	6.1	Ms	GS	189
14-Dec-93	064745.40	-20.78	-173.49	36	5.7	Ms	GS	183
16-Dec-93	041819.23	-20.47	-173.88	24	5.1	mb	GS	156
18-Dec-93	224420.04	-20.48	-173.88	33	5.7	mb	GS	156
22-Dec-93	134656.63	-20.43	-173.71	33	5.2	Ms	GS	175
27-Dec-93	070011.69	-20.49	-173.56	33	5.2	mb	GS	186
15-Jan-94	170331.00	-20.85	-173.93	36	5.7	Ms	BRK	137
16-Jan-94	101840.06	-20.36	-175.38	33	5.4	Mw	HRV	85
27-Jan-94	001805.45	-21.72	-173.94	33	5.4	mb	GS	147
4-Feb-94	184851.12	-21.69	-174.15	33	5.6	Mw	HRV	127
9-Feb-94	192708.82	-21.13	-174.09	25	5.7	mb	GS	117
12-Apr-94	144248.90	-21.03	-174.18	30	5.5	Mw	HRV	109
22-Apr-94	093639.93	-20.59	-175.29	16	5.3	mb	GS	59
27-Apr-94	092326.27	-21.51	-173.67	28	6.3	Mw	GS	166
28-Jun-94	161018.03	-21.74	-174.40	33	5.0	mb	GS	108
14-Jul-94	153841.87	-22.59	-174.16	33	5.4	mb	GS	195
11-Aug-94	204208.99	-21.60	-173.77	31	5.9	mb	GS	159
28-Aug-94	074203.64	-20.27	-173.60	33	5.6	mb	GS	193
29-Aug-94	083144.45	-22.65	-175.10	33	5.4	mb	GS	168
29-Aug-94	092455.23	-22.66	-175.06	33	5.1	Ms	GS	169
29-Aug-94	093109.20	-22.65	-175.08	33	5.4	Mw	HRV	169
29-Aug-94	105107.88	-22.60	-175.16	33	5.0	mb	GS	162
30-Aug-94	212105.95	-22.52	-174.83	33	5.1	mb	GS	158
2-Sep-94	054856.78	-22.75	-175.76	59	5.2	mb	GS	187
20-Oct-94	040533.26	-21.92	-175.06	33	5.5	Mw	HRV	88
14-Nov-94	152438.90	-21.23	-174.64	54	5.3	Mw	HRV	61
17-Nov-94	001310.74	-21.81	-174.66	33	5.1	mb	GS	95
9-Jan-95	214911.45	-19.74	-173.92	47	5.1	mb	GS	204
31-Mar-95	163957.32	-22.43	-175.16	66	5.7	Mw	HRV	143
16-Apr-95	203609.02	-21.02	-174.39	31	5.2	Mw	HRV	87
28-Apr-95	095916.08	-21.41	-174.34	9	5.7	mb	GS	96
30-Apr-95	115013.78	-21.51	-174.48	33	5.2	Mw	HRV	87
29-Aug-95	085130.73	-21.16	-174.35	18	6.1	Mw	HRV	89
31-Aug-95	203944.78	-21.21	-174.29	33	5.6	Mw	HRV	97
1-Sep-95	182548.32	-21.21	-174.63	30	5.2	Mw	HRV	62
20-Sep-95	064934.32	-21.26	-174.32	33	5.1	mb	GS	94
25-Sep-95	011007.05	-19.54	-173.76	33	5.7	Mw	HRV	232
29-Sep-95	040923.61	-20.88	-174.15	33	5.5	Mw	HRV	114
9-Nov-95	182842.26	-20.99	-173.50	44	5.0	mb	GS	179
26-Dec-95	122550.00	-21.94	-174.24	33	5.2	mb	GS	135

Date	Origin Time (UTC)	Latitude	Longitude	Depth (km)	Magnitude	Solution	Recorder	Epicentral Distance from Nuku'alofa (km)
26-Dec-95	165515.83	-21.65	-174.53	10	5.9	Mw	GS	91
1-Jan-96	013416.00	-20.39	-174.23	33	6.0	Mw	HRV	131
25-Feb-96	041711.31	-22.25	-175.89	33	5.7	mb	GS	142
16-Mar-96	114943.61	-21.15	-174.51	33	5.2	Mw	HRV	73
23-Mar-96	062734.74	-21.77	-174.81	34	5.5	Mw	HRV	82
7-May-96	121302.32	-22.99	-175.20	33	5.1	Ms	GS	205
27-Jun-96	172708.37	-22.55	-176.05	35	5.4	Mw	HRV	179
28-Jun-96	024113.36	-21.71	-175.21	35	5.6	Mw	HRV	64
28-Jun-96	093442.52	-21.88	-175.18	33	5.6	Mw	HRV	83
6-Aug-96	101314.30	-21.36	-175.46	33	5.6	Mw	HRV	35
25-Aug-96	203326.43	-19.04	-174.35	60	5.2	Mw	HRV	248
7-Sep-96	025530.35	-20.52	-174.36	35	5.3	Mw	HRV	111
25-Oct-96	071457.34	-22.01	-174.17	33	5.3	mb	GS	146
23-Dec-96	002844.91	-22.68	-175.32	10	5.8	Mw	HRV	172
19-Jan-97	065754.84	-19.31	-175.31	64	5.0	mb	GS	201
22-Jan-97	042401.58	-22.18	-175.71	33	5.0	mb	GS	126
1-Feb-97	183437.12	-19.84	-173.82	33	5.6	Mw	HRV	204
7-Feb-97	084113.41	-19.86	-173.29	28	6.4	Mw	GS	245
9-Feb-97	231104.67	-20.24	-173.63	39	5.0	mb	GS	192
27-Feb-97	125111.08	-22.48	-174.87	33	5.5	Mw	HRV	153
28-Feb-97	082319.17	-23.22	-175.33	33	5.4	Mw	HRV	231
7-Mar-97	000140.03	-23.17	-175.41	33	5.2	Mw	HRV	226
7-Mar-97	030400.08	-22.38	-175.90	33	5.9	Mw	GS	154
15-Mar-97	005059.93	-23.33	-175.55	33	5.3	Ms	GS	245
4-May-97	035821.11	-22.11	-175.76	33	5.2	mb	GS	122
18-May-97	070832.62	-20.64	-174.65	62	5.1	mb	GS	80
21-May-97	000846.48	-20.81	-175.47	69	5.4	mb	GS	43
17-Jul-97	070134.46	-22.92	-175.29	33	5.1	Mw	HRV	198
22-Jul-97	142814.59	-22.91	-175.27	33	5.2	Mw	HRV	197
5-Aug-97	204527.21	-21.31	-174.29	33	5.4	Mw	HRV	98
8-Sep-97	234932.52	-20.73	-174.50	33	5.4	Mw	HRV	87
10-Sep-97	125707.07	-21.35	-174.39	10	6.2	ME	GS	89
24-Sep-97	151628.34	-21.02	-174.27	33	5.1	Mw	HRV	99
20-Oct-98	115240.60	-20.58	-174.28	33	5.1	mb	GS	114
9-Nov-98	045741.02	-21.23	-174.39	52	5.2	mb	GS	86
15-Nov-98	025255.94	-20.69	-174.12	33	5.1	mb	GS	123
24-Jan-99	070158.40	-21.13	-174.66	33	6.1	Mw	GS	58
26-Jan-99	070420.90	-21.10	-174.49	33	5.2	Mw	HRV	76
26-Jan-99	123049.16	-20.51	-174.21	41	5.8	Mw	GS	125
3-Feb-99	011357.58	-20.31	-174.37	33	6.3	Mw	GS	127
12-Feb-99	134750.04	-21.40	-174.37	33	5.1	mb	GS	93
23-Feb-99	185656.16	-20.80	-174.07	36	5.3	mb	GS	124
7-Aug-99	061728.85	-21.09	-176.06	33	5.3	Ms	GS	87
20-Aug-99	201901.07	-21.42	-174.52	33	5.1	Ms	GS	78
21-Aug-99	025805.32	-20.39	-173.76	33	5.7	Ms	GS	172
25-Sep-99	155935.74	-22.02	-175.14	33	5.0	mb	GS	98
8-Oct-99	050948.92	-21.05	-174.49	33	5.9	Mw	HRV	75
12-Oct-99	132745.62	-21.12	-174.49	33	5.6	Mw	HRV	75
25-Oct-99	000120.24	-19.41	-173.88	33	5.8	Mw	HRV	236
7-Nov-99	115723.64	-20.77	-174.44	33	5.0	mb	GS	90
25-Nov-99	085019.69	-21.24	-174.48	33	5.1	mb	GS	77
30-Nov-99	044024.76	-21.33	-174.30	33	5.0	mb	GS	97

8.5 Microtremor Recordings - Site-Response Measurements, Nuku'alofa

The first phase of recordings in Nuku'alofa was invalidated due to operator error in varying the gain on the three channels on which seismic components were being measured. The method fundamentally relies on comparing horizontal and vertical signals measured with the same gain.

A second set of data was obtained by the Department of Lands, Survey & Natural Resource with the assistance of Marc Regnier of IRD (ORSTOM), Noumea. A total of 26 sites were measured by Kelepi Mafi and Marc Regnier at sites spread widely over Nuku'alofa. These sites were selected as representative of the full range of geological conditions in the city.

Stacked groups of site-response spectra are shown together with the appropriate spectral models in Figure 38, and the site characteristics are summarised in Table 19.

The locations of recording sites are shown at the end of the Nuku'alofa chapter (see Figure 41).

Field recordings were made for 3 minutes every 10 minutes during a one-hour period using the equipment and procedures described in Section 4.1.

The uniform geology across Nuku'alofa and the lack of significant changes in topography provided little guidance for the choice of sites to characterise structural units. Based as they are on a small number of site measurements, the zone boundaries in this study are therefore not well constrained and should be more precisely ascertained in the case of a new building project distant from any actual site measurements.

The zones were defined according to the resonant frequency obtained at each site and the geomorphology of Nuku'alofa area. All sites have a frequency of resonance between 1.5 and 2 Hz. This small variation in the fundamental-mode frequency suggests quite a homogeneous superficial structure with slight variations of the upper-layer thickness. The amplification factors were usually quite low, between 1 and 2, and could not be used to further constrain the zonation process. Only the two sites near Queen Salote wharf (sites 1 and 2) have amplification factors close to 3, but at high frequencies between 5 and 10 Hz.

(over page: p.133)

Table 19: Microtremor Site-Response Recordings, Nuku'alofa

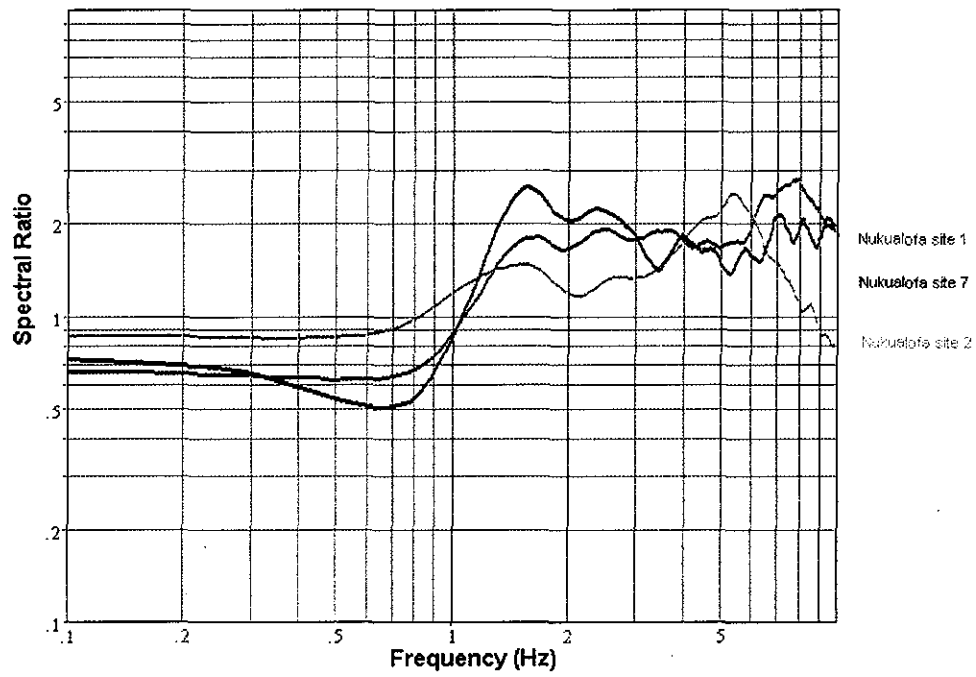
Site Response Table, Nuku'alofa

NUKU'ALOFA Site No.	Amplified Frequency Hz	Amplification Factor	Site Response Class	UTC Date	UTC Time	WGS84 UTM Easting	WGS84 UTM Northing	Locality
1	1.5	1.7	A	240598	2319	689,250	7,661,050	Apifo'ou
2	1.6	1.5	A	250598	0049	688,550	7,661,250	Fa'ua
3	2	1.7	B	250598	0159	687,350	7,661,850	Fa'onelua
4	2	1.3	B	250598	2259	686,750	7,662,300	British High Commission
5	1.3	1.3	B	260598	0009	686,150	7,662,500	Tevita Tio
6	2.2	1.5	B	260598	0119	685,550	7,662,100	Halaano
7	2.6	1.6	A	260598	0229	685,750	7,660,950	Vaololoa Sand
8	1.6	1.5	B	270598	2239	688,800	7,660,150	Sia'atevolo
9	2	1.2	B	280598	0009	687,500	7,660,200	Mata'ika
10	1.8	1.5	B	280598	0109	687,700	7,660,650	Pili
11	2	1.8	B	280598	0209	687,550	7,661,700	Dateline Hotel
12	-	-	B			687,050	7,661,600	Kolofo'ou
13	-	-	A	010698	2259	686,550	7,660,850	Pahu
14	1.7	1.1	B	020698	0035	686,200	7,661,350	TTC
15	-	-	B	040698	2109	685,250	7,660,600	Vaololoa playground
16	1.8	1.2	B	040698	2129	685,000	7,661,000	Longolongo
17	2	1.3	B	040698	2229	685,600	7,661,300	FWS Longolongo
18	1.6	1.5	B	070698	2209	684,950	7,661,300	Tu'atakilangi
19	1.7	1.5	B	080698	0019	688,200	7,661,000	Maufanga
20	2.5	1.2	B	080698	0129	688,300	7,660,150	Takaetupa
21	2	1.2	B	140698	2129	687,500	7,661,050	Fasimoeafi
22	1.8	1.5	B	150698	2139	689,450	7,659,650	Mosimosi
23	2	1.3	B	150698	2252	685,400	7,660,250	Havelutokelau
24	-	-	B	200798	1449	684,400	7,660,000	Apimataka
25	-	-	B	200798	1349	685,050	7,659,800	Tailulu
26	2.5	1.4	B	160698	0019	685,200	7,662,150	Halaano

(over page: p.135-136)

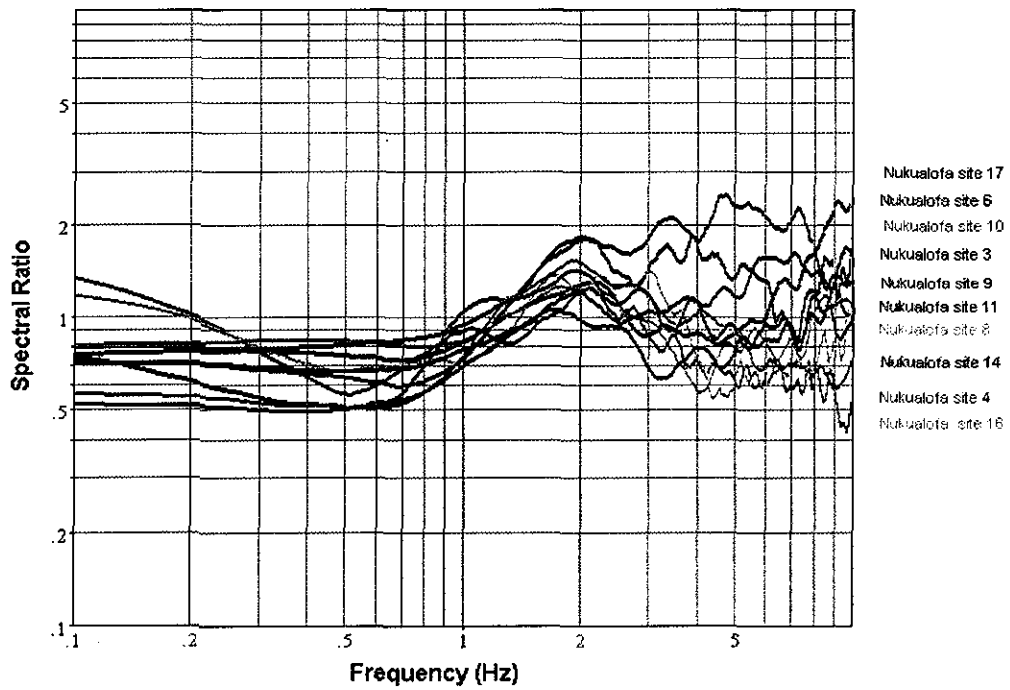
Figure 38: Site-Response Spectra, Nuku'alofa

NUKUALOFA SITE RESPONSE SPECTRA ZONE A



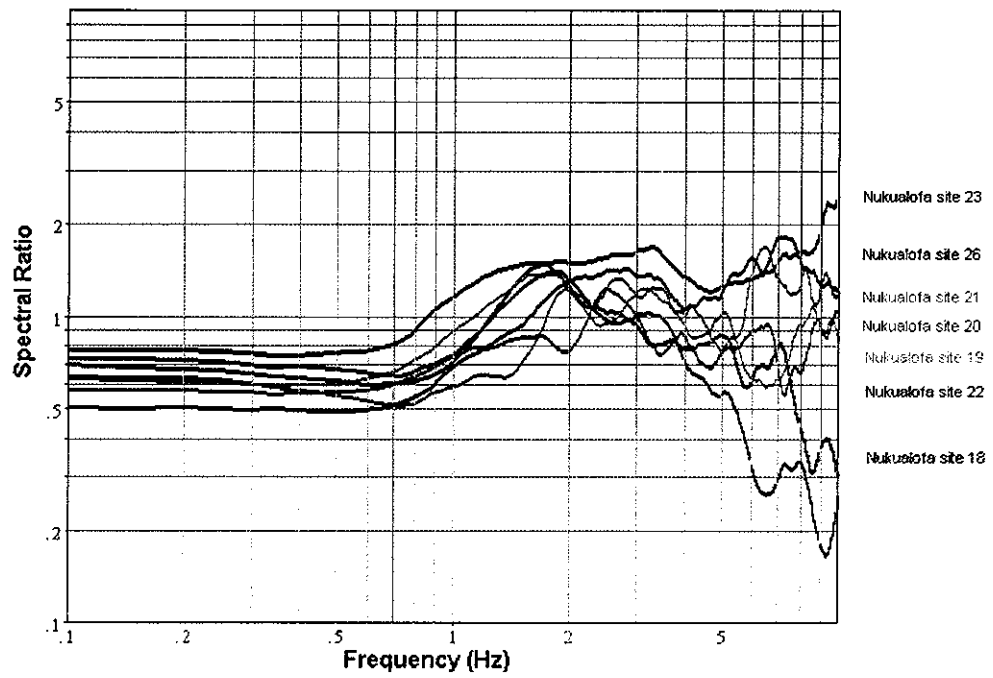
a

NUKUALOFA SITE RESPONSE SPECTRA ZONE B - STACK 1



b

NUKUALOFA SITE RESPONSE SPECTRA ZONE B - STACK 2



C

8.6 Analysis of Site-Response Measurements and Zonation of Nuku'alofa

Based on the analysis of the observed site responses, the Nuku'alofa area has been divided into two zones, each zone characterised by a predominant resonant frequency.

The characteristic resonant frequencies of the spectral models and corresponding zone names are shown in Table 20, and the critical parameters defining the spectral models are shown in Table 21.

A diagrammatic, generalised cross-section of subsurface conditions and their relationship to the adopted subsurface models is shown in Figure 39.

The spectral models are compared in Figure 40a, and the acceleration-response functions for each zone are shown in Figure 40b.

Several sites have no amplification at all and are difficult to include in either zone. They are probably located on massive limestone terraces with a thin, flat sedimentary layer on top or, alternatively, no soil layer at all. This type of structure is known to produce very little resonance, and then only in a high-frequency band (around 10 Hz); well beyond the resonant frequency range of most buildings.

According to the published information on the geology and the geomorphology of the island, most of the shallow bedrock of Tongatapu is composed of terraced and uplifted limestone. The sites that exhibit some resonance can then be interpreted as lying on topographic variations, such as sinkholes or block collapses of the island-scale shallow limestone structure.

The depth, wavelength and the smoothness of the topographic variations of the limestone platform can control both amplitudes and frequency bands of resonance in the spectral ratio function. Convincing examples of resonance have been observed only along the northern shore (sites 1 and 2), although site 7 near the southern shoreline also produced a similar response (Figure 38a). The response is probably related to either a thin, very low-velocity layer of carbonate sand and gravel, or topographic effects at the edge of the limestone platform. Elsewhere, a peak frequency between 1.5 and 2 Hz could suggest fill with low-velocity material down to shallow depths between 10 to 20 m. Alternatively, a weathered limestone layer 40-50 m thick could be invoked to produce similar spectral responses, and this assertion is supported by the results obtained at site 8 located in a limestone quarry (Figure 38b).

Zone A is characterised by a two-layer model consisting of low-velocity material overlying the island limestone platform. This zone is found in two different locations though in each case close to a lagoon shoreline. The top layer is composed of non-lithified Holocene carbonate deposits. Both the amplitude and the frequency suggest that the depth of fill and the basement morphology are different in each case. Nevertheless these two areas have the highest amplifications recorded during the survey and therefore were included in the same class.

Table 20: Map Zones vs. Site-Response Models, Nuku'alofa

Map Zones - Nuku'alofa	Characteristic Resonant Frequency (Hz)	Applicable Models
A	1.6	Nuku a
B	2.0	Nuku b

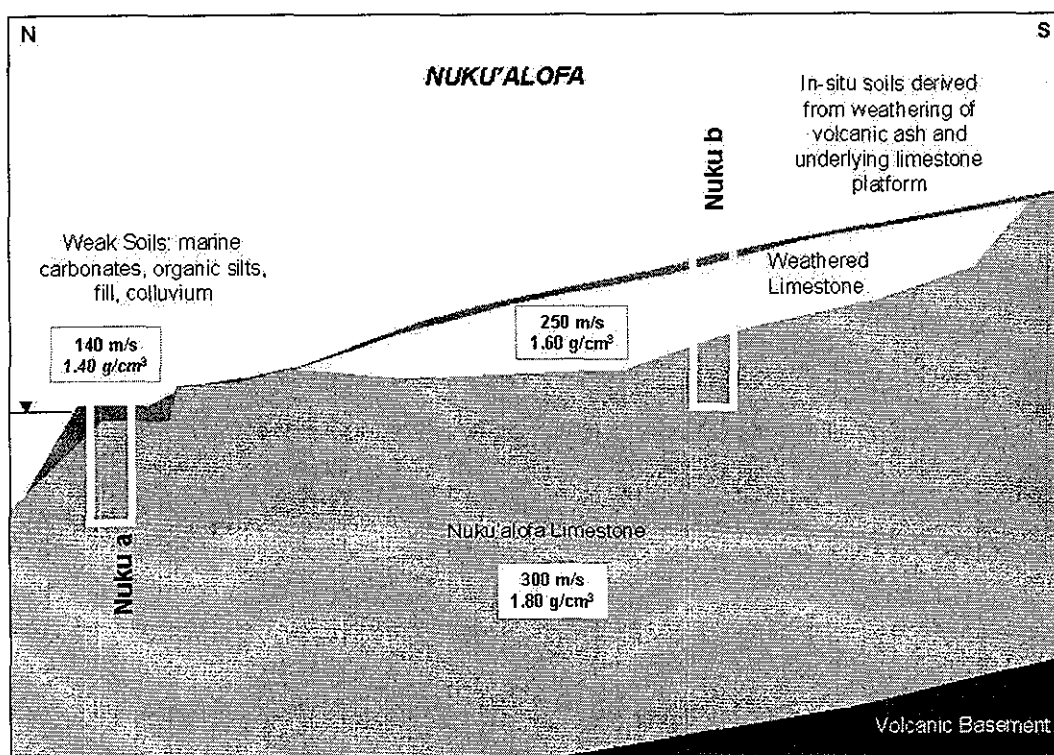
Table 21: Definition of Site-Response Models, Nuku'alofa

Model	Layer	Thickness (m)	Shear Velocity (m/s)	Density (g/cm ³)	Geotechnical Description
Nuku a	1	25	140	1.40	weak sediments, reclaimed areas
	2	Half-space	300	1.80	Nuku'alofa limestone basement
Nuku b	1	40	250	1.60	weathered limestone
	2	Half-space	300	1.80	Nuku'alofa limestone basement

Zone B is also characterised by a two-layer model. In this zone, no frequency peaks with amplitude higher than 2 were observed. The weak amplitudes observed in the spectral ratios do not allow an

unambiguous resolution of the shallow structure beneath the seismometer. However, they do suggest a velocity in the top layer higher than the one inferred for Zone A. The most likely structure to account for the observed spectral functions would be a thick layer (up to 50 m at least) of weathered limestone in the top section of the regionally uplifted and recrystallised limestone platform. Very localised, shallow fill and variations of the thickness of the weathered zone can explain lateral variations of the observed response in Zone B.

Figure 39: Diagrammatic Summary Cross-Section, Nuku'alofa



8.7 SvE Results and Interpretation, Nuku'alofa

For a prescribed probability of exceedance of 10% in 50 years, our estimates for Nuku'alofa yield a peak ground acceleration (PGA) of 0.7 g and the acceleration-response functions for each zone are shown in Figure 40b and Figure 41.

The mapped distribution of seismic microzones in Nuku'alofa is shown in Figure 41.

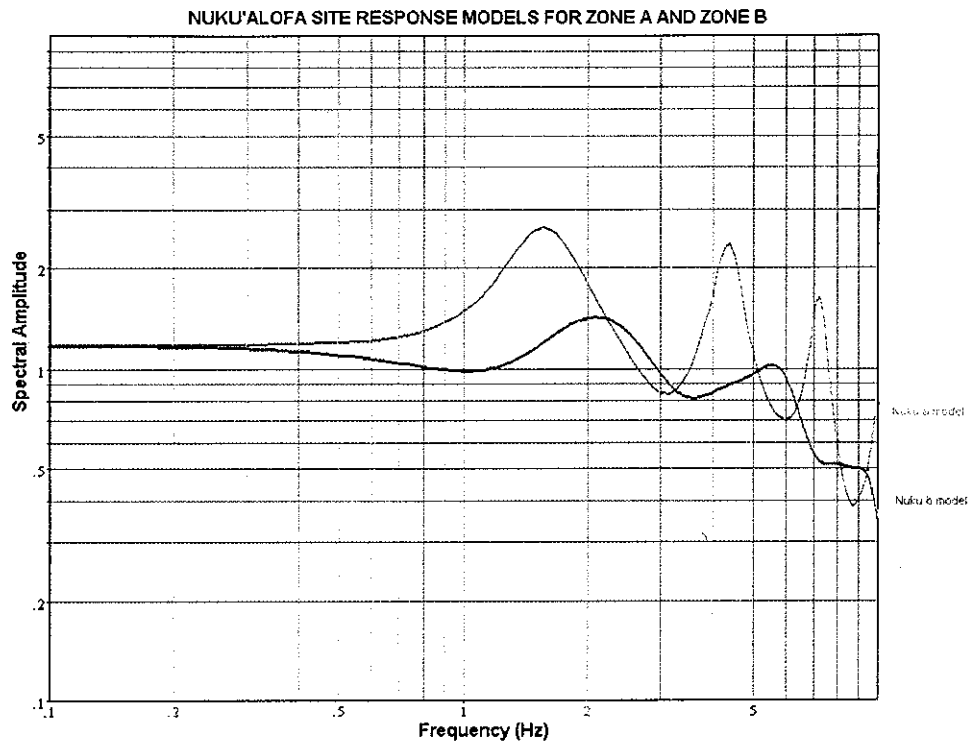
Nuku'alofa is divided into two zones based on the local geology. The response functions in Figure 40b are computed under the assumption (as in the other cases) that the dynamic shear strength of the surface layers is in the order of 20×10^5 dyne/cm (200 kPa). This strength is low enough to warrant non-linear behaviour of the soil under high stresses. However, in the opinion of several engineers, it is higher than anticipated for the types of soil in the city. According to the procedure developed by Joyner (1977), we obtain a strong non-linear effect in both zones. The non-linear effects in Zone B, for periods lower than 1.0 second, suggest that the soil would not be able to transmit elastic energy, and seismic energy may be transformed into plastic deformation. The fact that the function for Zone B falls below that of Zone A does not mean that the hazard is lower. In other words, although it is expected that vibratory motions of strong earthquakes will be less intense, the possibility of ground deformations is likely to present much more of a hazard.

(over page: p.140)

Figure 40: Site-Response Models and Acceleration-Response Functions, Nuku'alofa

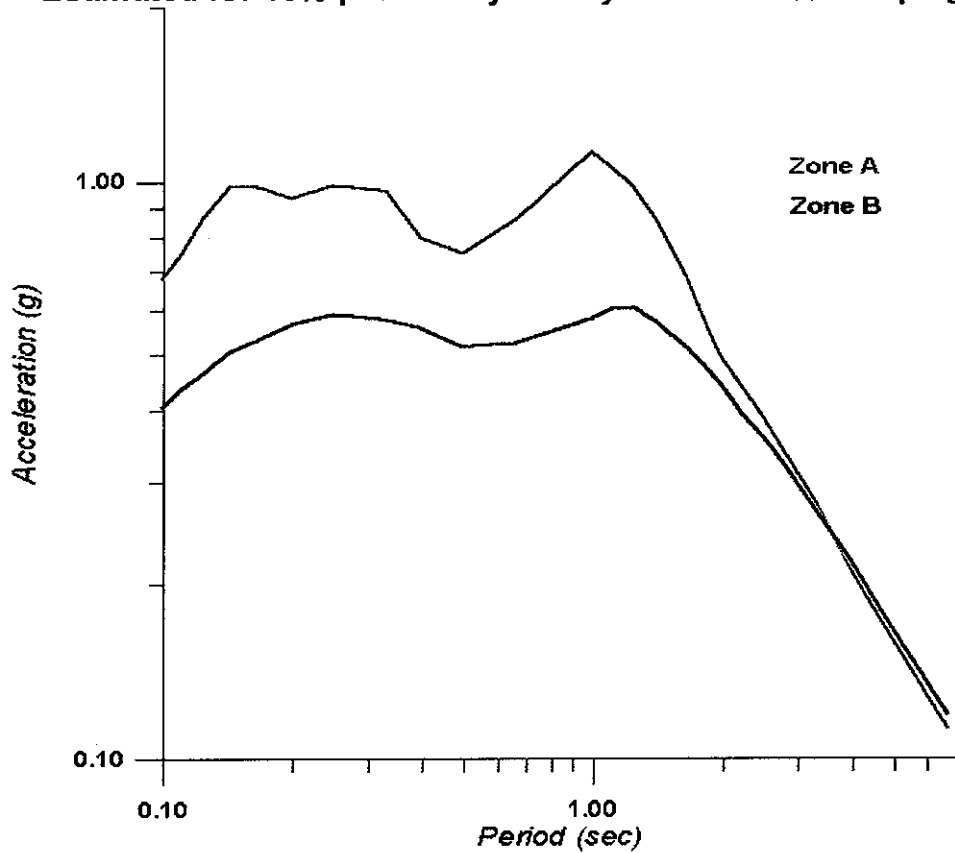
(over page: p.141)

Figure 41: Seismic Microzonation Site-Response Map, Nuku'alofa



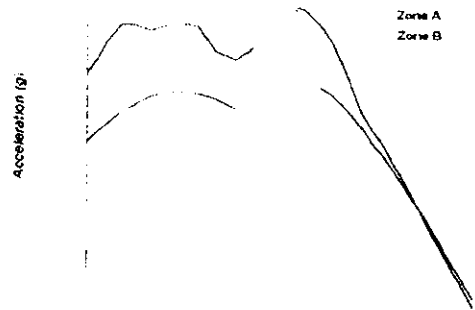
a

**Acceleration Response for Seismic Zones in NUKU'ALOFA
Estimated for 10% probability in 50 years with 5% damping**



b

Acceleration Response for Seismic Zones in NUKU'ALOFA
Estimated for 10% probability in 50 years with 5% damping



SOUTH PACIFIC OCEAN



South Pacific
Applied Geosciences
Commission
www.sopac.org.fj
Director@sopac.org.fj

Projection:
UTM Zone 1 S (WGS 84)

Date: 20/2/2004

Author: HAU

Scale: 1:20,000



Seismic Microzonation
Site Response Map
NUKU'ALOFA
Tongatapu
Tonga

(c) SOPAC Regional Data Centre 1999 (FM)

7,662,000mN

7,661,000mN

7,660,000mN

7,659,000mN

683,000mE

684,000mE

685,000mE

686,000mE

687,000mE

688,000mE

689,000mE

690,000mE

FANGA UTA
LAGOON

Legend

24

Microtremor Recording Site

Site Response Zone



A



B

BEST AVAILABLE COPY

141

9 Summary of Microzonation Results Across All Cities

As mentioned in the body of the report, data acquisition in each city in this study was undertaken primarily by in-country personnel trained by GII and SOPAC. This system of acquisition was adopted for the purpose of capacity building in each country, and with a view to the use of the information in-country for hazard management and planning. One drawback to this approach was a lack of consistency in data acquisition and, consequently, some loss of repeatability of data processing and analysis across the region. Although operators in each country were trained together in the same methodology, circumstances required that the microtremor acquisition for each city be undertaken independently.

In order to provide some universal appreciation of the effects of earthquake hazard and microzonation across the whole region under discussion, the outcomes from each city are summarised and compared here. General conclusions are drawn on seismic microzonation in the Pacific, and simplified relationships are extracted which lead to broad generalisations on seismic hazard in areas where data is lacking.

It should be stated at the outset that many of the parameters used in the study were either adopted from research elsewhere or estimated theoretically through trial-and-error variations to result in a sustainable model that fitted with the observed geological sub-surface conditions. In some cases these geological/geotechnical conditions have been well described, but a general lack of data in most of the cities makes the geological models somewhat speculative in nature. The following discussion should not be taken to indicate that all parameters have been systematically and directly measured. Consequently, any relationships developed below should be viewed only as indicators of the variability amongst the four studied cities of the region for the purpose of contrast and comparison, indicating broad trends that might be expected in similar areas of the Pacific region.

9.1 Generalised Geotechnical Results

The geology of each of the Pacific cities studied is unique and the geotechnical characteristics of each zone vary across the region. However, in a general sense, all four cities have a similar geological history, and are founded in comparable physical and geographic situations, *viz*:

1. The fundamental basement for the islands in all cases consists of high-strength (hard) andesitic and basaltic volcanics with, in some cases, recrystallised limestones overlying the volcanics. Because they occur at considerable depth below overlying weaker rocks and do not form an interface with the surface soil layers, these hard rocks generally play no part in the Joyner models which were developed to examine resonance close to the surface.
2. The material considered as the half-space of the Joyner models is in nearly all cases an uplifted, younger (<2 million years old) and weaker rock formation, generally pure carbonate or carbonate-cemented terrigenous material having high void ratios (porosity) and with considerably reduced seismic velocities compared with the volcanic basement.
3. The predominant soft surface layer in most cases is young sediment (< 10,000 years old) with the engineering properties of soil. This layer generally consists of sediment deposited in a marine environment, containing varying amounts of terrigenous and carbonate-derived silt, sand and gravel-sized material. These soils usually have very high void ratios, are mostly fully saturated, and generally have a matrix containing high proportions of fine carbonate and organic matter which tend to dominate the bulk behaviour of the soil mass. Deposits of this material are generally lenticular, being deposited in structural or erosional embayments and channels and coastal plains developed on the carbonate rock basement.

A global perspective of the city-zones in this project can be achieved by comparing these Pacific geotechnical zones with the ones developed by Borchardt (1991, 1994) specifically for central and southern California, and later redefined by Crouse & McGuire (1996) in the NEHRP Seismic Provisions.

The comparisons given in Table 22 indicate that the basement half-space of the Pacific city models coincides with the lower part of the range of the NEHRP Site Class B. The soft surface layer generally approximates to NEHRP Site Class D and, in some cases, the special soils of NEHRP Site Class E.

The geotechnical materials found in the Pacific to date vary little between cities and represent only a restricted part of the range of materials considered in the NEHRP studies.

Table 22: NEHRP Site Classifications

NEHRP Site Class	NEHRP Description	NEHRP Shear-Wave Velocity	Suva	Port Vila	Honiara	Nuku'alofa
Ao	Hard Rock	>1,400 m/s				
A	Rock	700 - 1,400 m/s				
B	Soft rock; Very stiff-hard clays; Very dense gravels	375 - 700 m/s	Zone A basement Zone B basement Zone C basement Zone D basement	Zone A basement Zone B basement Zone C basement Zone D basement Site 50 basement	Zone A basement Zone B basement Zone C basement	Zone A basement Zone B basement
C	Stiff-very stiff clays; Loose dense sands, silts, some gravels	200 - 375 m/s		Zone B surface	Zone A mid	Zone B surface
D	Soft-firm clays (d=3-40m) in profile (PI >20%)	100 - 200 m/s	Zone D surface	Site 50 surface Zone C surface Zone D surface	Zone B surface Zone C surface	Zone A surface
E ₁	Soils vulnerable to potential failure or collapse under seismic loading (Liquefiable soils, quick and highly sensitive clays, collapsible weakly-cemented soils)			Zone A surface	Zone A surface	
E ₂	Peats, highly organic clays (d >3m)		Zone A surface Zone B surface Zone C surface			
E ₃	Very high plasticity clays (d >8m; PI >75%)					
E ₄	Soft-firm clays, very thick (d >40m)					

9.2 Generalised Nakamura Results and Interpretation

Shear-wave Velocities

Since the definitions or models describing the microzonation vary from one city to another, a comparison among the cities is required to understand the variations and similarities found across the region. The Joyner model is most sensitive to changes in the parameters of formation-layer thickness and shear-wave velocity. Figure 42 demonstrates the similarity among the values of the shear-wave velocity adopted independently in each case by trial-and-error for the weak, uppermost soil layer for each zone in each city (100-200 m/s). Likewise, the similarity among the values of shear velocity adopted for the Joyner-modelled rock basement (300-400 m/s, but generally greater than 350 m/s) is also demonstrated. The parameters for Nuku'alofa Zone B have been omitted from this comparison as they represent a simple contrast in basement velocity rather than the interface between soil and rock which is the case in the other cities in the study.

Due to technical and resource constraints, it was never intended to make direct, in-situ measurements of shear-wave velocity within this microzonation study. In addition, it must be stressed that there are no known records of such measurements in the region.

In all cases, the values of shear-wave velocity are inferred from knowledge of other parameters, and by comparison with values for similar materials in published literature elsewhere. Best-fit values for the parameter were determined through an iterative trial-and-error fashion for each city (mainly constrained by known layer thickness). The test of the suitability of the adopted value was the fit of the Joyner models to the recorded Nakamura responses in each city and the match between the models and the geological situation which they represent in each of the cities.

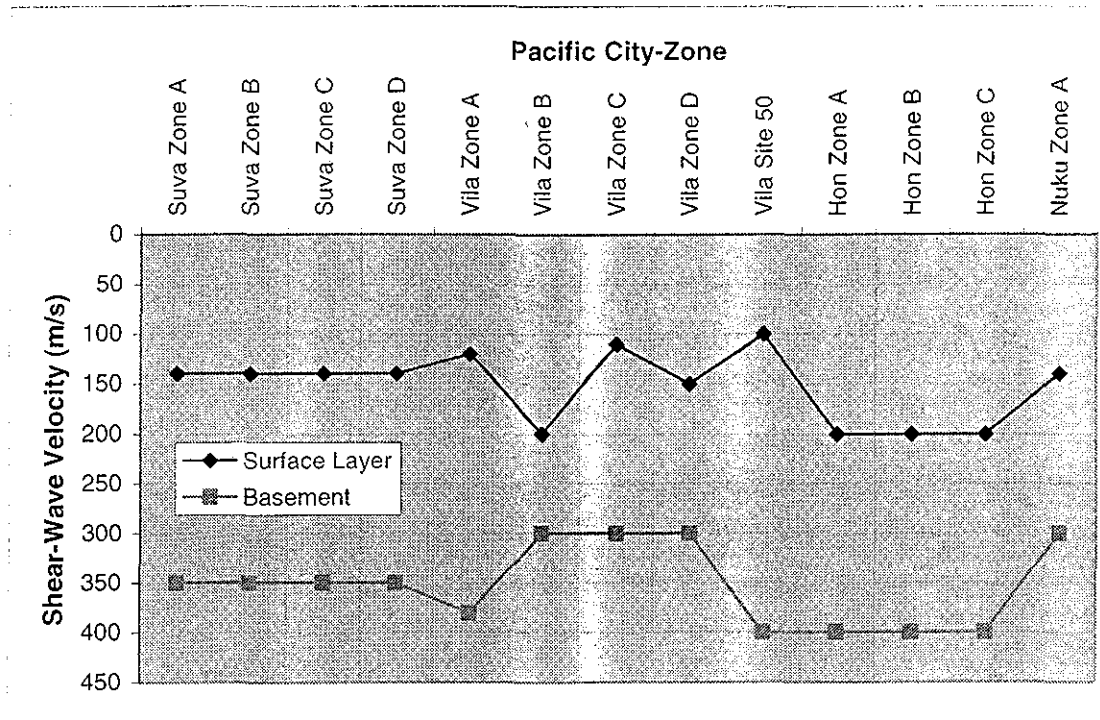


Figure 42: Seismic shear-wave velocities for the surface layer (upper) and basement half-space (lower) in the four Pacific Cities

To fully utilise the Nakamura test results and more closely constrain the microzonation boundaries, it is highly recommended that shear-wave velocity profiles be made, preferably using SCPT (Seismic Cone Penetration Test) equipment at significant sites across the cities (see recommendations in Chapter 10).

Meanwhile, in order at least to gain some confidence that the estimated shear-wave velocities lie within a reasonable range, comparisons can be made with theory and with experience in similar soils elsewhere.

A match between the soil types of the upper layers in the four cities and the generalised descriptions from the NEHRP Site Classification (Table 22) suggest that upper-layer shear velocities should lie, as they do, between 100 and 200 m/s.

Resonance theory predicts that, for the simplest case of primary-mode resonance for a model involving a single surface layer over a half-space, the resonant frequency of the shear wave is given by:

$$T = 4H/V_s$$

where:

T is the period in seconds

H is the thickness of the layer in metres

V_s is the s-wave velocity in m/s.

The measured period T of natural resonance observed in practice for various city-zones is plotted against the grouped parameters $4H/V_s$ in Figure 43. The thickness H of each layer at these particular sites is known from borehole records.

The reader should bear in mind that the shear-wave velocities V_s were effectively estimated by trial-and-error fitting to the same form of equation within the SRD method. As a result, the best-fit line and the R^2 value for the resulting plot in Figure 43 serve only to demonstrate that the velocities adopted through that procedure at least show a good fit to the theoretical prediction.

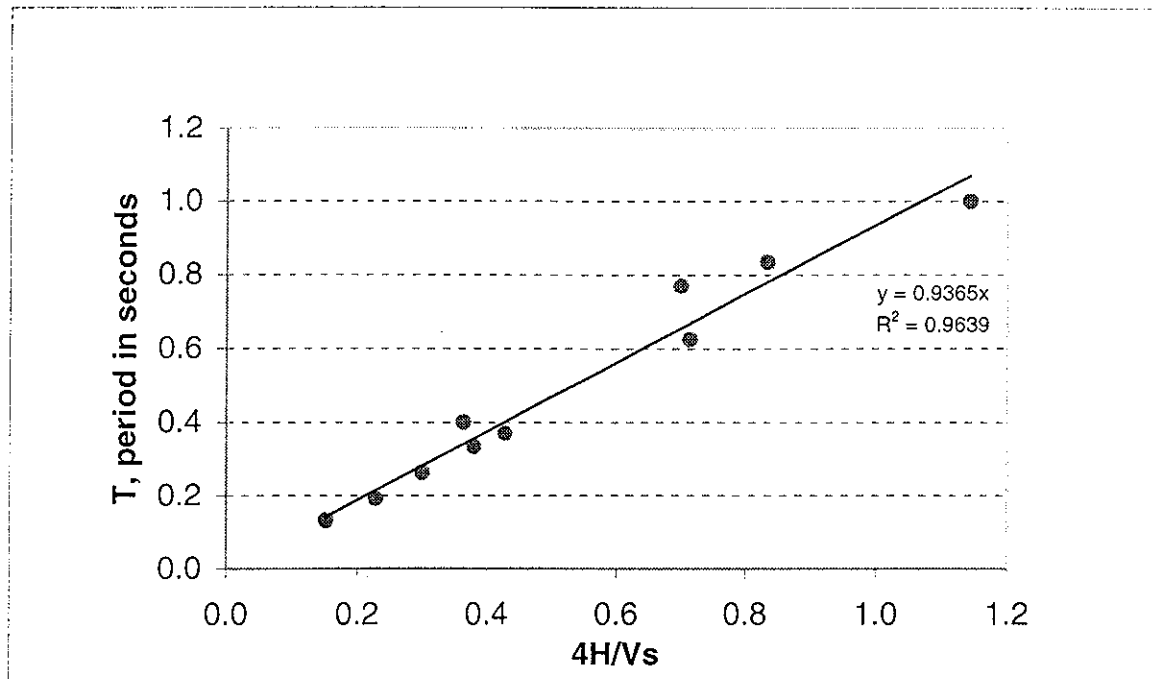


Figure 43: Relationship between observed period of resonance (T), known thickness (H) and adopted shear-wave velocity (V_s) of the surface layer in the Pacific cities.

On the other hand, comparisons with experience in similar situations suggest that the velocities adopted in this study may be too high.

The geotechnical properties of the harbour muds (organic silts) of Suva, for example, have previously been judged to be similar to the San Francisco Bay muds, with comparable values of thickness, bulk wet density, penetration resistance and seismic p-wave velocity (Shorten 1993a, b). Measured shear-wave velocities quoted by Tiedemann (1992) of 55-115 m/s for the San Francisco Bay muds fall significantly below the 140 m/s adopted for Suva in the present study.

The void ratio values (a significant index for shear velocity) for the Suva organic silts ($e = 1.3-3.0$) have been compared by W. R. Stephenson (pers. comm.) to similar soils in Porirua, New Zealand ($e = 1.5$) where the shear-wave velocity was measured as 110 m/s. This agrees with the evidence from San Francisco, although, in their own assessment of the Porirua value, Stephenson et al. (1990) declared the figure to be extraordinarily low. Stephenson also compared the Suva values with Mexico City ($e = 7$), where the shear-wave velocity was measured as 60 m/s. However, we believe the physical microstructure of the Mexico City soils to be so vastly different, and the void ratios so extremely high, as to preclude comparison with the Suva muds (see Shorten 1993a).

One independent, though indirect, means of estimating the shear-wave velocity for fine-grained sediments comes from the findings of Maruyama (1986) and Taniguchi (1989) who developed an empirical relationship linking Standard Penetration Test (SPT) N-values, the depth of the surface layer and shear-wave velocity of Japanese soils as follows:

$$V_s = 64.964 N^{0.193} H_m^{0.228} E.F$$

V_s is the shear-wave velocity

N is the SPT N-value (blows per 300 mm)

H_m is the mean depth at which the layer is located

E is a constant related to soil type (1.00 for silt, 1.134 for sand, 1.221 for sandy gravel)

F is a constant related to depositional mode (1.00 for alluvium)

Adopting typical values for the Suva Zone A surface layer of 'alluvial' silt ($N = 1$, $H_m = 20$ m), and for Nuku'alofa Zone A surface layer of 'alluvial' sandy gravel ($N = 3$, $H_m = 5$ m), based on geotechnical site investigations, gives values of V_s for Suva of 129 m/s, and for Nuku'alofa of 142 m/s. Although this is close to the adopted value for Nuku'alofa, 140 m/s, it is lower than theory predicts for Suva.

It has been suggested (W. R. Stephenson, pers. comm.) that the influence of steep and irregular basement topography and lenticular shape of sediment deposits - conditions known to exist in the subsurface of all the Pacific cities studied here - may be in part responsible for the departure from the theoretical values. At least for Suva, situations of true resonance might be less common than assumed in this report.

The subsurface model adopted for Suva supposes constant velocities for the surface layer (140 m/s) and the half-space (350 m/s). Seismic microzonation in Suva is predicated mainly on the assumption of a change in the thickness of a soft soil layer with consistent properties, and assumes a sharp boundary between the soft soil layer and the basement. The situation of a horizontal layer of soft soil over the infinite half-space (bedrock) is the most desirable aspect for true representation of the spectral ratio obtained through the Nakamura method (Nakamura 1989).

The body of available evidence suggests that true shear-wave velocities for the Suva muds could be as low as 100-120 m/s, and that the 140 m/s value adopted in this study to fit theoretical models is influenced by the presence of irregular and steep basement topography.

Microzone characterisation at depth by shear-wave profiling in all the cities studied would constrain the results more closely by addressing the adopted model which assumes this consistent formation, and enable these issues to be assessed more rigorously.

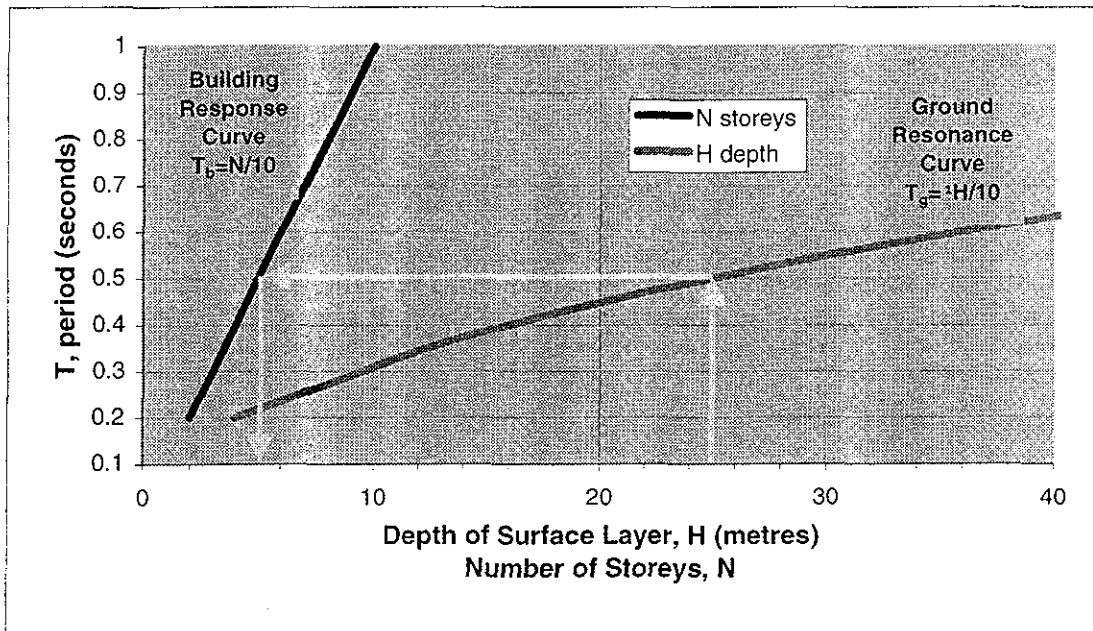


Figure 44: Nomogram for estimating the relationship between the depth of the surface layer and the possibility of resonance effects in buildings of a given height in Pacific cities

Layer Thickness

In the absence of extreme changes in sediment properties (and hence shear velocity) within the upper layer of each city zone, variations in the thickness (or depth) of the surface layer appear to have the greatest influence on the characteristic resonant frequency. Tiedemann (1992) presented an approximate relationship between the measured period of ground resonance T_g and known upper-layer thickness H based on work in Mexico City:

$$T_g = \sqrt{H/10}$$

As the scatter of values adopted for the four Pacific cities overlaps the measured values presented by Tiedemann up to depths of about 50 m, his approximation is seen as being broadly representative of the Pacific situation.

Adopting the widely used approximation for the period of natural resonance of a building T_b relative to the number of storeys N as:

$$T_b = N/10$$

and plotting this in Figure 44 on the same chart as Tiedemann's period-depth relationship given above, essentially provides a nomogram for comparing the surface layer thickness with the height of a building coupled to this layer in which it might be expected that structural resonance would be induced (the case where $T_b = T_g$). Use of the nomogram is meant to provide a first estimate, and is only appropriate for the regions for which it has been developed. The details of the nomogram method are demonstrated in Box 7 below.

For a situation where resonance is controlled by layer thickness alone with other factors held constant, this implies that the numerical relationship which approximates the simplest case where resonance is induced in a building of N storeys coupled to a resonating surface soil layer of thickness H is given by:

$$N = \sqrt{H}$$

Box 7: Nomogram method for estimating the relationship between ground resonance and building response

To estimate building response from known ground conditions (i.e. when $T_b = T_g$):

1. Determine the surface-layer thickness (in the example shown above, $H = 25$ m)
2. Read off the fundamental resonance period T , from the Ground Resonance Curve (e.g. $T = 0.5$ s)
3. Transfer the corresponding period to the Building Response Curve
4. Read off the corresponding building height likely to be affected by resonance (e.g. $N = 5$)

It should be stressed that, in general, only poor geotechnical records and borehole details currently exist in the four cities, with the exception of Suva where the situation is somewhat better.

9.3 Summary of SvE Results

It was shown in Section 3 how the Joyner method was used to provide an overall best fit to the site-specific Nakamura site-response spectral ratios that had previously been stacked and sorted according to similarity of response. The parameters from the Joyner model were then used in the SvE calculations. The SvE method was used to generate a range of discrete values of acceleration in terms of g (where $g = 9.8 \text{ m/s}^2$) as a function of the period of resonance (in seconds), taking into account the levels of regional seismicity.

In absolute values, the acceleration levels obtained are very high. This is especially true for Port Vila, Nuku'alofa and Honiara. It is likely that there will be severe difficulties in designing buildings to sustain such strong motions. One practical solution is to allow for this higher risk; that is, to compute the seismic-hazard functions and design the buildings for a higher probability of exceedance. However the acceptance of higher risk is ultimately a political, not a scientific or engineering decision.

In this study the results are presented for the case of a 5% damped response spectrum with the commonly applied risk criterion of 10% probability of exceedance in any given 50-year period. This probability level corresponds approximately to an event occurring at least once in any given period of approximately 450-500 years.

As described earlier, the SvE results show non-linear behaviour in the soft soil layers, which results in information gaps at certain periods or frequencies in some of the zones. The physical interpretation is that the surface-layer material is too weak to sustain an elastic response in the face of the higher stresses predicted in the cities, and deforms in a plastic, non-linear manner instead which usually incorporates volume change. Although it is not possible to determine amplification due to resonance in these gaps, it is, however, possible to conclude that soil failure, in the foundations of the affected buildings, may create as significant a threat as resonance to a given structure.

Amplification

The acceleration-response curves for each city zone show peaks of amplification, which coincide with the characteristic resonance period determined by the Nakamura method for that zone, modified by the influence of regional seismicity. Amplification at any point is calculated by considering the ratio of the acceleration value on the particular response function with the value at the corresponding period on the function describing the basement (non-amplified) behaviour.

In the case of Suva, for example, although the acceleration-response functions determined for Suva Zones A, B and C (Figure 45) appear to show peaks of acceleration at discrete periods (or frequencies),

this is probably an artefact of the original, somewhat arbitrary, choice of the four broad zones. In view of the fact that the thickness of sediment in Suva is known to vary continuously between 0 and 50 m, it should probably be considered that there is also a continuous envelope of peaks, from which amplifications can be derived, at discrete frequencies depending on discrete values of depth.

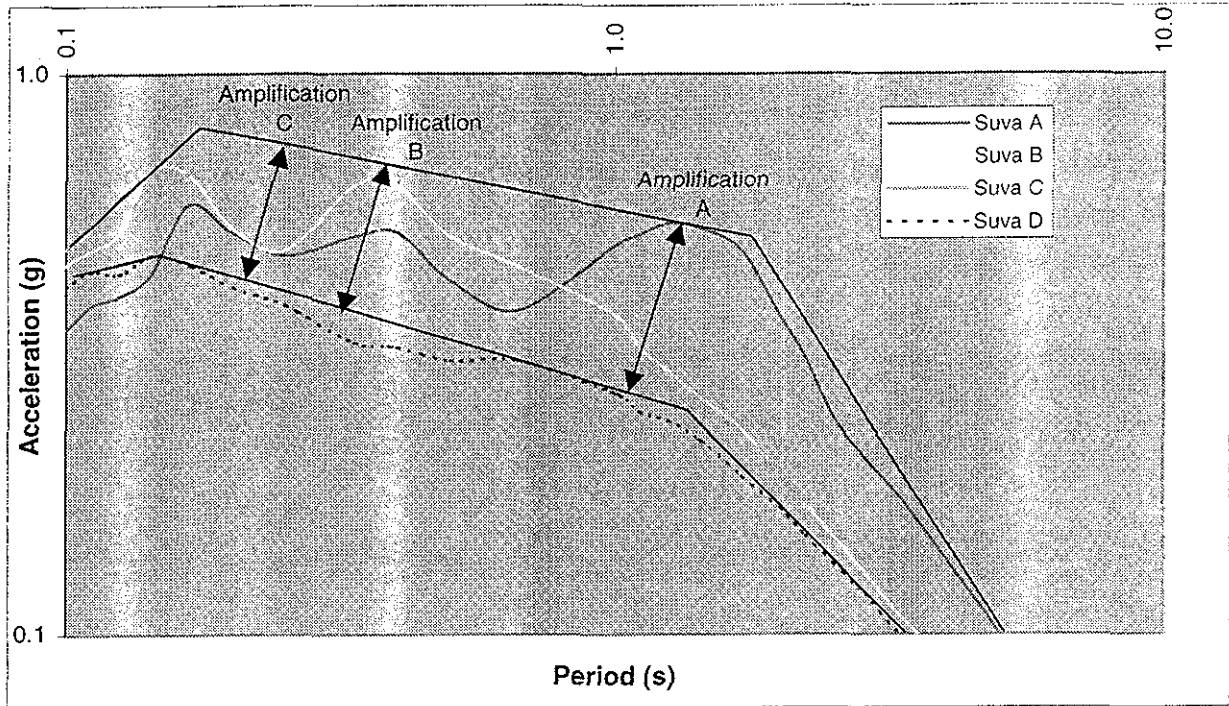


Figure 45: Acceleration-response curve for Suva with theoretical envelope of amplification: lower bound marks smoothed rock basement and upper bound joins peaks of resonance from layers of different thickness

Therefore, the amplification for any thickness of the upper layer could ideally be calculated from the graph, as the ratio of the acceleration derived from the smoothed line joining the crests of the peaks in the functions for Suva Zones A, B, and C (upper bound of envelope), and the corresponding acceleration derived from a smoothed basement function line for Suva Zone D (lower bound of envelope).

The amplifications across the zones of the four cities, determined at the maximum difference (or peak amplification) between the response function of the particular zone and the basement response function, range from 1.2 to 5 (see Table 23). These values, however, should be regarded as preliminary, until the recommended activities (see Chapter 10) are undertaken to provide more-robust modelling of the results obtained through the Nakamura method.

Table 23: Maximum amplification, period of resonance and probable heights of buildings susceptible to resonance for all Pacific city-zones

Pacific City Zone	Amplification at Resonant Period A	Period of Natural Resonance T (seconds)	Adopted Resonant Building Height N (storeys)
Suva A	2.5	1.0-1.2	10-12
Suva B	2.0	0.4	4
Suva C	1.9	0.2-0.3	2-3
Port Vila A	2.0	0.8-1.1	8-11
Port Vila B	1.5	0.3	3
Port Vila C	1.4	0.1	1
Vila Site 50	1.7	0.4-0.5	4-5
Honiara A	1.2	0.8-1.3	8-13
Honiara B	1.2	0.3	3
Nuku'alofa A	1.8	0.6-0.1	6-10

Assessments of non-linear response effects and the probability of ground deformation are heavily dependent on our estimates of the shear-wave velocities and dynamic shear strengths of the soft soil layers. The values of these parameters ideally need to be verified by direct geotechnical and geophysical measurements.

Values of the adopted resonant building height N , and the maximum expected amplification A , are represented graphically in Figure 46. The chart should be interpreted in a qualitative, rule-of-thumb way only.

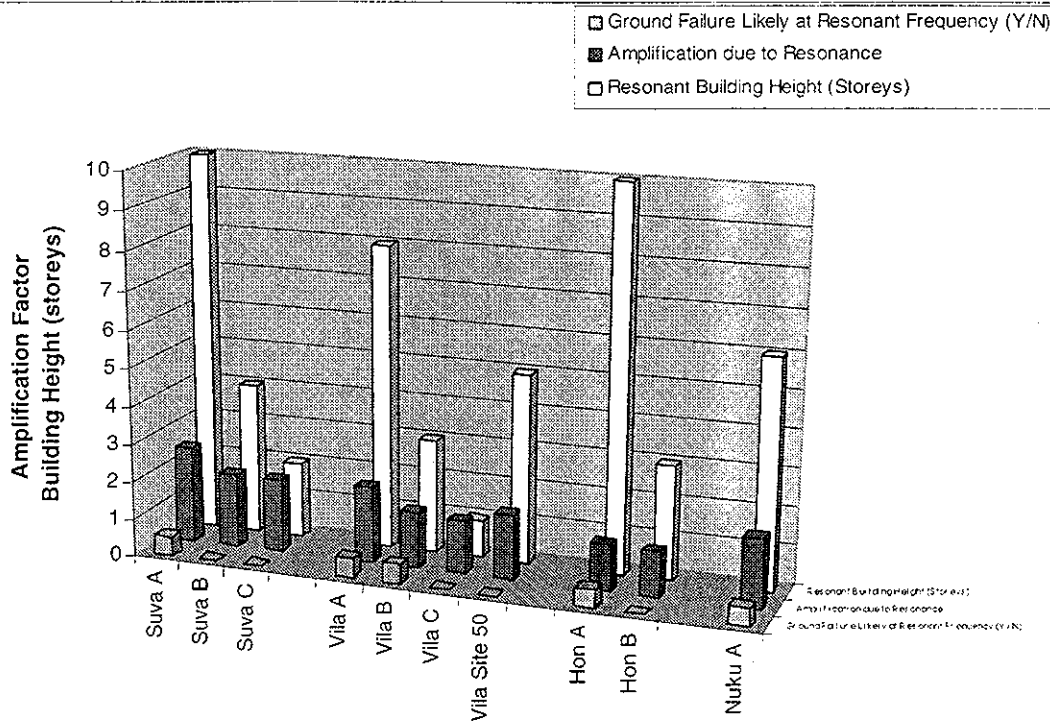


Figure 46: Seismic-response zones: Predicted amplifications due to resonance, and probable heights of buildings affected, shown together with the likelihood of ground failure at the resonant frequency

The number of stories N of a building can be used as a crude estimate of the period of natural resonance T in seconds of the building through the relationship $N = 10/T$, which is a simplified form of a more complex relationship determined through laboratory studies. For example, a 10-storey building would be predicted to have a natural resonant period of 1 second (or frequency of 1 Hz). In considering the risk to buildings in each city-zone the following assumptions have been made:

1. The building has no special structural features that significantly modify response;
2. Good coupling exists between a building and the ground during an earthquake; and
3. Amplification of ground shaking occurs at the site where the building stands.

As a first approximation, the building heights represented in Figure 46 will be at most risk of resonance-induced damage or collapse. The heights are estimated from the characteristic resonant frequency of the ground determined through the Nakamura microtremor process.

Notwithstanding the above, attempts to predict amplifications in specific situations should be made with caution for two reasons:

1. In general, the Nakamura method, on which these figures are ultimately based, is not considered to provide a good estimate of earthquake amplification, although the SvE analysis has been used to refine this result; and
2. Specifically, ground deformation under high earthquake accelerations may preclude any further consideration of resonance. Non-linear effects across significant parts of the frequency range of the

response functions for each city suggest that ground failure will occur through liquefaction, collapse or shear failure in many instances.

The last point is particularly exemplified by the relatively low soil shear strength of the Port Vila A zone in the face of the high predicted resonant amplification in that zone. Premature ground failure is indicated in a number of other city-zones as well.

It is strongly recommended that before specific buildings are identified as being at high risk, the natural responses of characteristic buildings in each city zone should be determined directly, through either SDA and SRD or another method, and the foundation strength conditions assessed in parallel.

10 Conclusions and Recommendations

It must be stressed again that this study is of a regional nature and there is generally a paucity of data in each country from which conclusions are drawn. Field observations are only at a reconnaissance level and zone boundaries may change with further work. For site-specific assessments, any observations and broad conclusions in this report should be checked by geotechnical specialists.

The predictive models used in this study demonstrate that each of the cities may be statistically at a much higher risk from strong earthquakes than hitherto inferred from the very brief period of historical recordings available. Port Vila and Nuku'alofa have been singled out as likely to experience particularly high-intensity events. Specific foundation conditions, particularly in Suva, and in some inner and outlying areas of Port Vila and Honiara, are expected to lead to doubly-intensified earthquake effects or, perhaps worse, liquefaction and settlement of structural foundations.

It can generally be concluded that Suva, Port Vila, Honiara, and Nuku'alofa all face a significant hazard from amplification of earthquake shaking due to resonance. Depending on the situation and style of buildings involved, the amplification of earthquake effects could range up to more than twice that experienced in the basement rocks, and perhaps higher in the Mele and Bauerfield areas north of Port Vila.

The division of each city into discrete zones of weak surface cover with discrete earthquake effects is largely an artificial one. The more likely situation is that a continuous gradation of resonance effects exists, and that buildings ranging anywhere from 2 to 12 storeys may be susceptible to resonant amplification of earthquake shaking, depending, of course, on the particular foundation setting for each building. This assessment is further complicated by the prevalence of many inverted-pendulum style buildings, particularly in Suva which, while only one or two storeys high, may behave in a dramatically worse manner than a rigid structure of the same height. This area will be the subject of further study.

Modelling in this study and independent investigations further indicate that the material in some of the surface layers is not strong enough to sustain the high accelerations predicted on the basis of the seismological setting of the cities involved. In these cases ground failure can be expected to occur, resulting in destruction of foundation integrity, and hence damage to or collapse of superstructures, without even considering the possibility of the damaging effects of resonance.

The following recommendations are made to overcome shortcomings in this study and the general lack of information in the region:

Recommendation 1:

Much delay was experienced in gathering existing background information that would, under ideal circumstances, be readily available to such a project in each participating country:

- Member countries be encouraged to continue to build on the kernel of the Pacific Cities Hazards GIS database to provide the essential basis for further hazard, risk and disaster studies in the Pacific.

Recommendation 2:

In the current study, optimal, rigorously controlled microtremor recording and analysis was not achieved for all cities. However, the initial goal to augment country capacity was. Due to poor and inconsistent data acquisition in Honiara, more than half of the microtremor sites had to be abandoned at the data analysis stage, leaving just 16 spectral ratios remaining for analysis and interpretation. It is recommended that:

- A follow-up microtremor survey be conducted in Honiara to gain a better understanding of resonant frequency and amplification information across that city.

Recommendation 3:

To assist with robust interpretation of Nakamura results and delineation of seismic microzones, it is recommended that:

- In each city, characterisation of the areas to be zoned be made through shear-wave velocity profiling, using the SCPT (Seismic Cone Penetration Test) method.

Recommendation 4:

To provide a control on resonant-frequency information and provide better estimates of site amplification it is recommended that:

- On-site recordings be made of actual earthquake ratios at representative sites in each city zone.

Recommendation 5:

To provide a robust database for use by managers and planners to identify specific buildings in specific zones as having high risk it is recommended that:

- The natural building responses of a range of characteristic buildings in each city zone be determined, either through SDA and SRD, or another method.

Recommendation 6:

Much was achieved to characterise the seismic hazard of the four cities with the available human resources and international scientific collaboration. However, for future work in this area, it is recommended that:

- The uniform hazard spectra be recalculated once the preceding recommendations have been fulfilled.

Recommendation 7:

In the long term, meaningful assessment of earthquake risk in the Pacific cities requires a detailed database of seismicity (including relatively low-level activity) that is not presently available:

- A Pacific Regional Seismology Centre should be established without delay to encourage research on essential seismicity data, and to accumulate and distribute the results within the region.

Until the activities mentioned in the recommendations above are undertaken, thorough investigation of the socio-economic seismic risk assessment of the four Pacific Cities cannot be completed. However, preliminary studies in SOPAC have commenced in order to address the issues. These include:

- Assessment of the number of occupants in each building in the four cities
- Identification of number and monetary value of buildings at risk in the four cities utilising the Pacific Cities GIS assets database
- Earmarking of the specific buildings and occupants threatened, and the likelihood of suffering from damaging earthquakes in a given 50-year period
- Incorporation of the results of site-specific earthquake-hazard determinations of the four cities into building codes for each country

It should be emphasised that the zonation within each city is a result of empirical site-response investigations as well as a generalisation of surface and subsurface geotechnical conditions. There are, however, significant variations in site responses within each zone. Owing to the high seismic activity around the investigated cities, it is highly advisable that detailed site investigations be conducted for new developments, and the appropriate building codes adopted. This should take place particularly for special engineering projects such as hospitals, schools and critical facilities, as well as other public and residential buildings used to accommodate many people. It can be expected that building codes will evolve and be adapted to incorporate new knowledge, including the current study. This experience should also be incorporated into building development even where final building codes have not yet been developed or legislated.

11 Acknowledgments

The compilers of this report wish to acknowledge the permission of the four respective Governments of Fiji Islands, Vanuatu, Solomon Islands and Tonga to publish the data. We also acknowledge the important contributions of the National Representatives and project counterparts. We have relied heavily on the provision of existing information available in-country by the project counterparts in those respective countries, especially for historical, geological, geotechnical and borehole data, in order to ensure an accurate report. In this regard, we especially mention the project counterparts Gajendra Prasad, Arvin Singh and Lasarus Vuetibau of the Mineral Resources Department of Fiji; Christopher Ioan and Morris Stephen of the Geology, Mines and Water Resources Department, Vanuatu; Kenneth Bulehite and Alison Papabatu of the Department of Energy, Mines and Water Resources, Solomon Islands; and Kelepi Mafi of the Department of Lands, Survey & Natural Resources, Tonga. The invaluable input of many staff of the Geophysical Institute of Israel and SOPAC, and the advice and involvement of Trevor Jones of the Australian Geological Survey Organisation are also gratefully acknowledged. Trevor Jones took a major role in the initiation of the project while seconded to the Mineral Resources Department of Fiji. We are deeply grateful for the thorough reviews undertaken by Bill Stephenson, Tam Larkin and John Taber through the offices of Hugh Cowan of Geohazards Services (NZ) Ltd and the Institute of Geological and Nuclear Sciences Ltd, and by Peter Rodda of the Mineral Resources Department of Fiji. USAID is gratefully acknowledged as the major source of funding for the project.

12 References

- Aggarwal, T. Y., Barazangi, M., and Isacks, B. 1972. P and S travel times in the Tonga-Fiji region: a zone of low velocity in the uppermost mantle behind the Tonga island arc. *Journal of Geophysical Research*, 77: 6427-6434.
- Baker, R. C. 1950. The occurrence of saline groundwater on Guadalcanal. *Transactions of the American Geophysical Union*, 31: 58-60.
- Berkman, D. A. (compiler) 1976. Field Geologist's Manual. Berkman, D. A. and Ryall, W. R. editors, *The Australasian Institute of Mining and Metallurgy Monograph Series*, 9.
- Biukoto, L., Swamy, M., Shorten, G. G., Schmall, S., and Teakle, G. 2001a. Pacific Cities CD, Nuku'alofa. GIS Hazards Dataset, Version 1.0. *SOPAC Data Release Report*, 3.
- Biukoto, L., Swamy, M., Shorten, G. G., Schmall, S., and Teakle, G. 2001b. Pacific Cities CD, Port Vila. GIS Hazards Dataset, Version 1.0. *SOPAC Data Release Report*, 4.
- Biukoto, L., Swamy, M., Shorten, G. G., Schmall, S., and Teakle, G. 2001c. Pacific Cities CD, Suva. GIS Hazards Dataset, Version 1.0. *SOPAC Data Release Report*, 5.
- Boore, D. M. 1983. Stochastic simulation of high-frequency ground motions based on seismological models of the radiated spectra. *Bulletin of the Seismological Society of America*, 73: 1865-1894.
- Borcherdt, R. D. 1991. On the observation, characterisation, and predictive GIS mapping of strong ground shaking for seismic zonation. A case study in the San Francisco Bay region, California. *Proceedings, Pacific Conference on Earthquake Engineering*, Vol. 1, pp. 1-24.
- Borcherdt, R. D. 1994. Estimates of site-dependent response spectra for design (Methodology and justification). *Earthquake Spectra*, 10(4): 617-653.
- Brune, J. N. 1970. Tectonic stress and spectra of seismic shear waves from earthquakes. *Journal of Geophysical Research*, 75: 4997-5009.
- Campbell, M. D., McKay, G. R., and Williams, R. D. 1977. The Tonga earthquake of 23 June 1977. Some initial observation. *Bulletin of the New Zealand Society for Earthquake Engineering*, 10(4): 208-218.
- Cooper, P., and Kroenke, L.W. 1993. Deep Seismicity in the North Fiji Basin. In Kroenke L.W., and Eade, J.V., editors, 1993, *Basin Formation, Ridge Crest Processes, and Metallogenesis in the North Fiji*

- Basin. Houston, Texas, Circum-Pacific Council for Energy and Mineral Resources, Earth Science Series, Vol. 15, Springer-Verlag, New York.
- Cowie, J. D., and Orbell, G. E. 1991. Soil Map of Tongatapu Island, Tonga. Scale 1:60,000. DSIR Land Resources Map 313. Part of *DSIR Land Resources Scientific Report*, 21. Department of Scientific and Industrial Research, Land Resources, Lincoln, Christchurch, New Zealand.
- Crouse, C. B., and McGuire, J. W. 1996. Site response studies for purpose of revising NEHRP seismic provisions. *Earthquake Spectra*, 12(3): 407-439.
- Cunningham, J. K., and Anscombe, K. J. 1985. Geology of 'Eua and other islands, Kingdom of Tonga. In Scholl, D. W. and Vallier, T. L. editors. *Geology and offshore resources of Pacific island arcs: Tonga region*. Circum-Pacific Council for Energy and Mineral Resources Earth Science Series 2. Circum-Pacific Council for Energy and Mineral Resources, Houston, pp. 221-257.
- Davis, W. M. 1928. The coral reef problem. *American Geographical Society Special Publication*, 9.
- Directorate of Overseas Surveys 1973. *Geology of Efate and offshore islands*. Scale 1:100,000. New Hebrides Geological Survey Sheet 9. Reprinted by Ordnance Survey, Government of Vanuatu, 1990.
- Everingham, I. B. 1983. Focal mechanisms for 1982 earthquakes in Fiji. *Fiji Mineral Resources Department Note*, BP33/4 (Unpublished).
- Everingham, I. B. 1984. Provisional list of felt earthquakes reported in Fiji, 1941-1981. *Fiji Mineral Resources Department Note*, BP33/8 (Unpublished).
- Everingham, I. B. 1987. Catalogue of felt earthquake reports in Fiji, 1940-1981. *Fiji Mineral Resources Department Report*, 64.
- Fah, D., Ruttener, E., Noack, T., and Kruspan, P. 1997. Microzonation of the city of Basel. *Journal of Seismology*, 1: 87-102.
- Granger K., Jones, T., Leiba, M., and Scott, G. 1999. *Community Risk in Cairns: A Multi-Hazard Risk Assessment*. AGSO, Canberra.
- Hackman, B. D. 1979. Geology of the Honiara area. *Solomon Islands Geological Survey Bulletin*, 3.
- Hamburger, M.W and Isacks, B. L. 1993. Shallow Seismicity in the North Fiji Basin. In Kroenke L.W., and Eade, J.V., editors, 1993, *Basin Formation, Ridge Crest Processes, and Metallogenesis in the North Fiji Basin*. Houston, Texas, Circum-Pacific Council for Energy and Mineral resources, Earth Science Series, Vol. 15, Springer-Verlag, New York.
- Harrison, D. J. 1993. The limestone resources of Tongatapu and Vava'u, Kingdom of Tonga. *British Geological Survey Technical Report*, wc/93/23.
- Hofstetter, A., Shapira, A., Bulehite, K., Jones, T., Mafi, K., Malitzky, A., Papabatu, A., Prasad, G., Regnier, M., Shorten, G., Singh, A., Stephen, M., and Vuetibau, L. 2000. Frequency-magnitude relationships for seismic areas around the capital cities of Solomon, Vanuatu, Tonga and Fiji Islands. *Journal of Seismology*, 4: 285-296.
- Houtz, R. E. 1962a. The 1953 Suva earthquake and tsunamis. *Bulletin of the Seismological Society of America*, 52(1): 1-12.
- Houtz, R. E. 1962b. Note on minor damage caused by the Suva earthquake of June 1961. *Bulletin of the Seismological Society of America*, 52(1): 13-16.
- Howorth, R. 1983. Baseline coastal studies, Port Vila, Vanuatu. Geology and stability. *CCOP/SOPAC Technical Report*, 29.
- Howorth, R. 1985. Baseline coastal studies, Port Vila, Vanuatu. Holocene uplift record and evidence for recurrence of large earthquakes. *CCOP/SOPAC Technical Report*, 51.

- Hull, A. G., Hengesh, J., Heron, D., and Rynn, J. 1997. Earthquake ground shaking in Suva: Notes to accompany maps, Suva Earthquake Risk Management Scenario Pilot Project. *Institute of Geological and Nuclear Sciences Client Report*, 43698D.
- Jones, T. 1998. Probabilistic earthquake hazard assessment for Fiji. *Australian Geological Survey Organisation Record*, 1997/46.
- Joyner, W. B. 1977. A Fortran program for calculating nonlinear seismic response. *USGS Open File Report*, 77-671. (Unpublished).
- Joyner, W. B., and Chen, A. T. F. 1975. Calculation of nonlinear ground response in earthquakes. *Bulletin of the Seismological Society of America*, 65: 1315-1356.
- Kroenke, L. W. 1984. The Solomon Islands: San Cristobel to Bougainville and Buka. In Kroenke, L. W. editor. *Cenozoic tectonic development of the Southwest Pacific*. CCOP/SOPAC Technical Bulletin, 6: 47-61.
- Lachet, C., and Bard, P. Y. 1994. Numerical and theoretical investigations on the possibilities and limitations of Nakamura's technique. *Journal of Physique of the Earth*, 42: 377-397.
- Lermo, J., and Chávez-García, F. J. 1994. Are microtremors useful in site response evaluation? *Bulletin of the Seismological Society of America*, 84(5): 1350-1364.
- Lister, J. J. 1891. Notes on the geology of the Tonga islands. *Quarterly Journal of the Geological Society of London*, 47: 590-617.
- Louat, R., and Baldassari, C. 1989. Chronologie des seismes et des tsunamis ressentis dans la région Vanuatu-Nouvelle Calédonie / Chronology of felt earthquakes and tsunamis in the region Vanuatu-New Caledonia. *ORSTOM Report*, 1-89.
- Mafi, K. S., and Shapira, A. 2000. On Local Magnitude determination in the South Pacific region. *Bulletin of the Seismological Association of the Far East*, 4 (1): 32-40.
- Malitsky, A., and Shapira, A. 1996. PC-SDP PC-based seismic data processing software package, Version 2.0. *IPRG Document*, Z1/567/79 (111).
- Maruyama, M. 1986. *Ground amplification of Muroran and of Noboribetsu region, Hokkaido*. Unpublished PhD thesis, Japan.
- Nakamura, Y. 1989. A method for dynamic characteristics estimation of subsurface using microtremor on the ground surface. *Quarterly Report of Railways Technical Research Institute*, 30(1): 25-33.
- Nunn, P. D., and Finau, F. T. 1995. Holocene emergence history of Tongatapu island, *South Pacific Z Geomorph NF*, 39(1): 69-95.
- Orbell, G. E., Rijkse, W. C., Laffen, M. D., and Blakemore, L. C. 1985. Soils of part Vava'u Group, Kingdom of Tonga. *New Zealand Soil Survey Report*, 66.
- Prevot, R., and Chatelain, J. L. 1984. Seismicity and earthquake risk in Vanuatu (Text), and 1983. Seismicity and seismic hazard in Vanuatu (Figures). *ORSTOM Report*, 5-83.
- Quantin, P. 1980. *Atlas des sols, Archipel des Nouvelles Hebrides*. ORSTOM, Noumea.
- Regnier, M., Morris, S., Shapira, A., Malitsky, A., and Shorten, G. 2000. Microzonation of the expected seismic site effects across Port Vila, Vanuatu. *Journal of Earthquake Engineering*, 4(2): 215-231.
- Roy, P. S. 1990. The morphology and surface geology of the islands of Tongatapu and Vava'u, Kingdom of Tonga. *CCOP/SOPAC Technical Report*, 62.
- Sawkins, J. G. 1856. On the movement of land in the South Sea islands. *Quarterly Journal of the Geological Society of London*, 12: 383-384.

- Seismology Research Centre, 1990. *The Kelunji Digital Seismograph*. Seismology Research Centre, Phillip Institute of Technology, Bundoora, Victoria.
- Shapira, A. 1999. *Seismic Microzoning in Capital Cities in the South Pacific*. The Geophysical Institute of Israel, Final report, submitted to the US Agency for International Cooperation - CDR Program, USAID Grant No.: TA-MOU-95-C13-024.
- Shapira, A., and van Eck, T. 1990. Using synthetic acceleration spectra to obtain statistical estimates of characteristic response spectra. Abstracts of the Meeting of the European Seismological Commission, Barcelona, Spain, September 1990.
- Shapira, A., and van Eck, T. 1993. Synthetic uniform-hazard site specific response spectrum. *Natural Hazards*, 8: 201-215.
- Shapira, A., and Avirav, T. 1991. Synthetic site specific response spectrum. Abstracts of the Meeting of the International Union for Geodesy and Geophysics, Abstracts, Vienna, Austria, August 1991.
- Shapira, A., and Avirav, T. 1996. PC-SDA operation manual, Version 2.2. IPRG Document Z1/567/79 (110C).
- Shapira, A., and Hofstetter, A. 1993. Source parameters and scaling relationships of earthquakes in Israel. *Tectonophysics*, 217: 217-226.
- Shorten, G. G. 1990. Structural geology of Suva peninsula and harbour and its implications for the Neogene tectonics of Fiji. *New Zealand Journal of Geology and Geophysics*, 33: 495-506.
- Shorten, G. G. 1993a. Stratigraphy, sedimentology and engineering aspects of Holocene organo-calcareous silts, Suva Harbour, Fiji. *Marine Geology*, 110: 275-302.
- Shorten, G. G. 1993b. The geological and tectonic setting for ground failure hazards in Suva Harbour and environs. *Fiji Mineral Resources Department Memoir*, 3.
- Shorten, G. G. 1995. Quasi-overconsolidation and creep phenomena in shallow marine and estuarine organo-calcareous silts, Fiji. *Canadian Geotechnical Journal*, 32: 89-105.
- Shorten, G., Shapira, A., Regnier, M., Teakle, G., Biukoto, L., Swamy, M., and Vuetibau, L. 1999. Applications of the uniform-hazard site-specific acceleration response spectrum in Pacific Cities. *Proceedings, Australian Disaster Conference, Canberra, 1-3 November 1999*, pp. 69-74.
- Singh, A., and Prasad, G. 1997. Suva microtremor studies. *Fiji Mineral Resources Department Note*, BP 70/4. (Unpublished).
- Singh, A., Stephenson, B., and Hull, A. 1998. assessment for amplification of earthquake shaking by soft soils in Suva. *Fiji Mineral Resources Department Report*, 71.
- SOLMAP, 1988. *Honiara Sheets XK0457, XK0657, XK0256 and XK0656, Solomon Islands 1:2,500*. SOLMAP, Survey and Mapping Division, Ministry of Lands, Honiara.
- Somerville, M., McCue, K. F., and Sinadinovski, C. 1998. Response spectra recommended for Australia. *Proceedings, Australian Structural Engineering Conference, Auckland, 30th September - 2nd October, 1998*, pp. 439-494.
- Standards Australia 1993. *Minimum design loads on structures Part 4: Earthquake loads*. AS 1170.4-1993. Standards Australia, Homebush.
- Standards Australia 1998. *Strengthening existing buildings for earthquake*. Australian Standard AS3826-1998. Standards Australia, Homebush.
- Stephenson, W.R., Barker, P.R., and Mew, G. 1990. Report on Resonant Alluvium Conditions for Part of Porirua Basin. Wellington Regional Council: Regional Natural Disaster Reduction Plan - Seismic Hazard.

Contract 90/5, Division of Land and Soil Sciences, Department of Scientific and Industrial Research, New Zealand.

Stephenson, W.R., and Baguley, D.E. 1996. Assessment for amplification of earthquake shaking by soft soils in Wanganui. *Institute of Geological and Nuclear Sciences Client Report, 1996/43662B.10*, prepared for Wanganui District Council (Confidential).

Swamy, M., Biukoto, L., Shorten, G. G., Schmall, S., and Teakle, G. 2001. Pacific Cities CD, Honiara. GIS Hazards Dataset, Version 1.0. *SOPAC Data Release Report, 2*.

Taniguchi, H. 1989. *A study on urban earthquake risk assessment and mitigation*. Unpublished PhD thesis, Japan.

Taylor, F. W. 1978. *Quaternary tectonic and sea level history, Tonga and Fiji, Southwest Pacific*. Unpublished PhD thesis, Cornell University, Ithaca.

Thompson, R. B., and Tunj, D. 1977. *Guadalcanal earthquakes 1977*. Solomon Islands Geological Survey, Honiara.

Tickell, S. J. 1985. Geology of the Honiara urban area. *Solomon Islands Geological Survey Report, R1/85*.

Tiedemann, H. 1992. *Earthquakes and Volcanic Eruptions: A Handbook on Risk Assessment*. Swiss Reinsurance Company, Zurich.

Tunj, D. 1981. The regional distribution of earthquakes greater than magnitude 5.5 in the Solomon Islands from 1960 to 1980. *Geological Survey Division, Solomon Islands Government Report, 81/14*.

Tunj, D. 1986. *The Guadalcanal earthquake 1984*. Solomon Islands Geological Survey, Honiara.

United States Bureau of Reclamation 1973. *Earth Manual*. Denver, Colorado, Federal Center.

Wilde, R. H., and Hewitt, A. E. 1983. Soils of 'Eua island, Kingdom of Tonga. *New Zealand Soil Survey Report, 68*.

Wong, F. L., and Greene, H. G. 1988. Geological hazard in the central Basin region, Vanuatu. In Greene, H. G., and Wong, F. L., *editors*. Geology and offshore resources of Pacific island arcs - Vanuatu region, Circum-Pacific Council for Energy and Mineral resources Earth Sciences Series, Houston, Texas, Vol. 8, pp. 225-251.

13 Appendices


APPENDIX 1: Explanation of Borehole Legend

APPENDIX 2: The Unified Soil Classification System

APPENDIX 3: Relationship between Soil Strength Number and SPT N-value

APPENDIX 1: Explanation of Borehole Legend

Colour/Symbol Code	Corresponding Material Classification (USCS system) (For details of soil material classifications, see Appendix 2 Unified Soil Classification System)
---------------------------	--

	<p>F Fill</p> <p>GP Gravel, poorly graded</p> <p>GW Gravel, well graded</p> <p>GM Gravel, excess silt</p> <p>GC Gravel, excess clay</p> <p>SP Sand, poorly graded</p> <p>SW Sand, well graded</p> <p>SM Sand, excess silt</p> <p>SC Sand, excess clay</p> <p>ML Silt soil, low plasticity</p> <p>CL Clay soil, low plasticity</p> <p>OL Organic soil, low plasticity</p> <p>MH Silt soil, high plasticity</p> <p>CH Clay soil, high plasticity</p> <p>OH Organic soil, high plasticity</p> <p>Pt Peat</p> <p>I Weathered in-situ soil or colluvium</p> <p>R Rock</p> <p>N/A Classification not available</p>
--	--

(Bedrock level taken as top of R, or I, if present)

Engineering classification of soils - The Unified Soil Classification System.

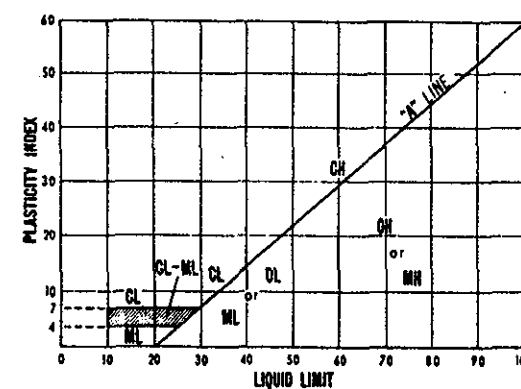
		FIELD INVESTIGATION PROCEDURES						GROUP SYMBOL	GROUP NAME and typical materials	LABORATORY CLASSIFICATION CRITERIA	
		Excluding particles larger than 7.5cm and basing fractions on estimated weights								GRAVELS	
COARSE-GRAINED SOILS More than 50% of material is larger than 0.06 mm	GRAVELS More than 50% of the coarse fraction is larger than 2mm. (retained on B.S.7 sieve)	CLEAN GRAVELS Little or no fines	Wide range in grain sizes, and substantial amounts of all intermediate particle sizes				GW	GRAVEL, well graded; gravel sand mixtures, little or no fines	Coarse-grained soil classified on basis of percentage of fines, as follows: PERCENT OF FINES GRAVELS SANDS Less than 5 SW SP More than 12 GM GC 5 to 12 Borderline cases, use 2 symbols	$C_u = \frac{D_{60}}{D_{10}}$ Greater than 4 $C_c = \frac{(D_{30})^3}{D_{10} \cdot D_{60}}$ Between 1 and 3	
			Predominantly one size or a range of sizes, with some intermediate sizes missing				GP	GRAVEL, poorly graded; gravel sand mixtures, little or no fines		Not meeting all gradation requirements for GW	
	DIRTY GRAVELS Appreciable amount of fines $\geq 12\%$	Non-plastic fines—for identification see ML below				GM	GRAVEL, excess silty fines; poorly graded gravel-sand-silt mixtures	Atterberg limits below "A" line or PI less than 4 Above "A" line with PI between 4 and 7 are borderline cases requiring use of dual symbols			
		Plastic fines—for identification see CL below				GC	GRAVEL, excess clayey fines; poorly graded gravel-sand-clay mixtures	Atterberg limits above "A" line or PI greater than 7 $C_u = \frac{D_{60}}{D_{10}}$ Greater than 6 $C_c = \frac{(D_{30})^3}{D_{10} \cdot D_{60}}$ Between 1 and 3			
	SANDS More than 50% of the coarse fraction is smaller than 2mm. (passing B.S.7 sieve)	CLEAN SANDS Little or no fines	Wide range in grain sizes, and substantial amounts of all intermediate particle sizes				SW	SAND, well graded; well graded sands, gravelly sands, little or no fines		Not meeting all gradation requirements for SW	
			Predominantly one size or a range of sizes, with some intermediate sizes missing				SP	SAND, poorly graded; poorly graded sands, gravelly sands, little or no fines		Atterberg limits below "A" line or PI less than 4 Above "A" line with PI between 4 and 7 are borderline cases requiring use of dual symbols	
DIRTY SANDS Appreciable amount of fines $\geq 12\%$		Non-plastic fines—for identification see ML below				SM	SAND, excess silty fines; poorly graded sand-silt mixtures	Atterberg limits above "A" line or PI greater than 7 Above "A" line with PI between 4 and 7 are borderline cases requiring use of dual symbols			
		Plastic fines—for identification see CL below				SC	SAND, excess clayey fines; poorly graded sand-clay mixtures				
		FIELD INVESTIGATION PROCEDURES on fraction smaller than 0.4mm. (passing B.S.36 sieve)						GROUP SYMBOL	GROUP NAME and typical materials	<div>GRAIN SIZE CURVES to be used to identify soil fractions</div> <div>PLASTICITY INDEX</div> <div>PLASTICITY CHART FOR LABORATORY CLASSIFICATION OF FINE-GRAINED SOILS</div>	
SILTS AND CLAYS Liquid limit less than 50	SOIL CAST (soil wet)	SOIL THREAD	SHINE	DILATANCY	ODOUR	DRY STRENGTH	ML	SILT SOIL, low plasticity; inorganic silts and very fine silty or clayey sands, rock flour			
	Forms fragile cast. Cracks form when handled while moist	Thick crumbly thread; easily broken	None to very dull	Distinct	Not significant	None to slight	CL	CLAY SOIL, low plasticity; inorganic clays of low to medium plasticity, gravelly clay, sand, clays, silty clays, lean clays			
	Cast maybe handled freely without breaking. Can be handled moist without cracking. Material adheres to the hand	Thread can be pointed as fine as a lead pencil but is fragile	Moderate	None to slight	Not significant	Moderate	OL	ORGANIC SOIL, low plasticity; organic silts and silt clays of low plasticity			
SILTS AND CLAYS Liquid limit more than 50	Cast fragile to cohesive material will adhere somewhat to the hand	Soft, weak thread	None to very dull	Slight to distinct	Decayed organic matter	Low	MH	SILT SOIL, high plasticity; inorganic silts, micaceous or diatomaceous fine sandy or silty soils, elastic silts			
	Moderately plastic and cohesive. Material adheres somewhat to the hand	Weak to medium thread. May be crumbly	Dull	None to slight	Not significant	Moderate. Powdered soil feels flowy	CH	CLAY SOIL, high plasticity; inorganic clays of high plasticity, fat clays			
	Very plastic and cohesive. Material very sticky to the hand. Greasy to touch	Very tough thread, can be rolled to a pin point	Very glossy	None	Strong earthy	High to very high. Cannot be powdered by finger pressure	OH	ORGANIC SOIL, high plasticity; organic clays of medium to high plasticity			
		Plastic and cohesive. Feels slightly spongy. Greasy to touch	Weak to medium thread. Often soft and fibrous	Moderate to very glossy	None	Decayed organic matter	Moderate to high. Powdered soil may be fibrous	PI	PEATY SOIL; Peat and other highly organic soils		
		Readily identified by colour, odour, spongy feel and frequently by fibrous texture									
NOTE: BOUNDARY CLASSIFICATIONS: Soil possessing characteristics of two groups are shown as a combination of two group symbols, eg. GW-GC, well graded gravel with clay binder.											

Based on "The Unified Soil Classification System" United States Department of the Interior, Bureau of Reclamation "Earth Manual" First Edition, Denver COLORADO 1960.

S.A. Dept. of Min

GRAIN SIZE CURVES to be used to identify soil fractions

PERCENT OF FINES GRAVELS SANDS	GRAVELS		SANDS	
	GW	GP	SW	SP
Less than 5	SW	GP	SW	GP
More than 12	SM	SC	SM	SC
5 to 12	Borderline cases, use 2 symbols			



PLASTICITY CHART FOR LABORATORY CLASSIFICATION OF FINE-GRAINED SOILS

NOTE: BOUNDARY CLASSIFICATIONS: Soil possessing characteristics of two groups are shown as a combination of two group symbols, eg. GW-GC, well graded gravel with clay binder.

Based on "The Unified Soil Classification System" United States Department of the Interior, Bureau of Reclamation "Earth Manual" First Edition, Denver COLORADO 1960. S.A. Dept. of Mines

APPENDIX 3: Relationship between Soil Strength Number and SPT N-Value

Table 1: Relationship between Soil Strength Number and SPT N-Value

Soil Strength Number	Equivalent SPT N-Value	Soil Strength Class
1	0 to 2	A
2	3 to 4	B
3	5 to 8	C
4	9 to 10	D
5	11 to 15	E
6	16 to 30	F
7	31 to 50	G

Table 2: Relationship between relative density, penetration resistance, static resistance, and angle of internal friction

SPT N-Value	Relative Density (δ_r)	Description of Compactness	Static Cone Resistance (q_c)	Angle of internal friction (ϕ)
4	0.2	Very loose	Under 2.0	Under 30°
4 to 10	0.2 to 0.4	Loose	2.0 to 4.0	30° to 35°
10 to 30	0.4 to 0.6	Medium dense	4.0 to 12	35° to 40°
30 to 50	0.6 to 0.8	Dense	12 to 20	40° to 45°
50	0.8 to 1	Very dense	Over 20	Over 45°

Adapted from: Berkman, D. A. (compiler) 1976. Field Geologists Manual. The Australasian Institute of Mining and Metallurgy Monograph 9.

Table 3: Relationship between consistency, penetration resistance, and unconfined compressive strength

SPT N-Value	Consistency	Unconfined compressive strength (kPa)
Under 2	Very soft	Under 40
2 to 4	Soft	40 to 75
4 to 8	Firm	75 to 150
8 to 15	Stiff	150 to 300
15 to 30	Very stiff	300 to 450
Over 30	Hard	Over 450

Adapted from: Berkman, D. A. (compiler) 1976. Field Geologists Manual. The Australasian Institute of Mining and Metallurgy Monograph 9.

To determine consistency or compactness of soils from Soil Strength Number:

Refer to individual borehole logs for Soil Strength Number and determine the equivalent range of SPT N-values from Table 1. Check from borehole logs whether soil is cohesive or non-cohesive. Using the range of SPT N-values, assess the degree of compactness of sands and gravels from Table 2, or consistency of clays and silts from Table 3.